
INAUGURAL-DISSERTATION

**zur
Erlangung der Doktorwürde
der
Naturwissenschaftlich-Mathematischen Gesamtfakultät
der Ruprecht-Karls-Universität
Heidelberg**

vorgelegt von

Christina Raupp geb. Stegelmann, MSc Biomedical Sciences

aus Jülich, Nordrhein-Westfalen

Tag der mündlichen Prüfung

18.06.2010

**Analysis of Infection Relevant Protein Domains of the
Adeno-Associated Virus Serotype 8 in Comparison to
Serotype 2**

Gutachter:

apl. Prof. Dr. Jürgen Kleinschmidt
Prof. Dr. Lutz Gissmann

The experimental work described in this thesis was started December 2005 and finished September 2009. C. Raupp was chosen to be a PhD student of the International PhD Program July 2005. The study was supervised by apl. Prof. Dr. Jürgen A. Kleinschmidt in the Department Infection and Cancer of the German Cancer Research Center (DKFZ), Heidelberg.

Parts of the presented study have been published:

Characterization of a Recombinant Adeno-Associated Virus Type 2 Reference Standard Material, Martin Lock, Susan McGorray, Alberto Auricchio, Eduard Ayuso, E. Jeffrey Beecham, Véronique Blouin-Tavel, Maria Fátima Bosch-Tubert, Mahuya Bose, Barry Byrne, Tina Caton, Jay Chiorini, Abdelwahed Chtarto, K. Reed Clark, Thomas Conlon, Christophe Darmon, Monica Doria, Anne Douar, Terry Flotte, Joyce, D. Francis, Mauro Giacca, Michael T. Korn, Irina Korytov, Xavier Leon, Barbara Leuchs, Gabrielle Kroener-Lux, Catherine Melas, Hiroaki Mizukami, Philippe Moullier, Marcus Müller, Keiya Ozawa, Tina Philipsberg, Karine Poulard, **Christina Raupp**, Christel Rivière, Sigrid D. Roosendaal, R. Jude Samulski, Steven M. Soltys, Richard Surosky, Liliane Tenenbaum, Darby L. Thomas, Bart van Montfort, Gabor Veres, J. Fraser Wright, Yili Xu, Olga Zeleniaia, Lorena Zentilin and Richard O Snyder (submitted)

Stegelmann C., Poster Presentation, Analysis of infection relevant protein domains of AAV8 in comparison to AAV2, Retreat in Weil der Stadt, 2008, 2nd Poster Prize.

Stegelmann C., Mueller O., Kleinschmidt J. A., ANALYSIS OF INFECTION RELEVANT PROTEIN DOMAINS OF ADENO-ASSOCIATED VIRUS SEROTYPE 8 IN COMPARISON TO SEROTYPE 2, XII Parvovirus Workshop

Index

Zusammenfassung	I
Summary	II
Abbreviations	III
1. Introduction	1
1.1 <i>Biology of Adeno-Associated Viruses</i>	1
1.1.2 Virus Classification	1
1.1.3 AAV2 Genome	3
1.1.4 AAV2 Proteins	6
1.1.4.1 Non-structural Proteins	6
1.1.4.2. Structural Proteins	7
1.1.5 AAV2 Capsid Structure	9
1.1.6 AAV2 Capsid Assembly and Genome Encapsidation	10
1.1.7 AAV Life Cycle	11
1.1.8 AAV Infection	12
1.2 <i>AAV as a Gene Therapy Vector</i>	15
1.2.1 Immune Response to AAV	16
1.2.2 AAV Vectorology	17
1.2.2.1 Improvements in Packaging Capacity and Transgene Expression	18
1.2.2.2 Natural Diversity as a Source for Transcapsidation	19
1.2.2.3 Mosaic and Chimeric Vectors	21
1.2.2.4 Ligand Conjugation and Peptide Insertion	23
1.2.2.5 DNA Family Shuffling and Peptide Display Libraries	24
1.3 <i>AAV8, a New Primate AAV as a Gene Therapy Vector</i>	27
1.3.1. Capsid Structure and other Characteristics of AAV8	28
1.3.2 Evaluation of AAV8 in Animal Models for Gene Therapy	30
1.4 <i>AAV Clinical Trials</i>	31
1.5 <i>Aim of the Study</i>	32
2. Materials and Methods	34
2.1 <i>Materials</i>	34
2.1.1 Animals	34
2.1.2 Cell Lines and Primary Cells	34
2.1.3 Bacteria	35

2.1.4	Viruses and AAV Vector Mutants	36	
2.1.5	Antibodies and Antisera	40	
2.1.6	Oligonucleotides	41	
	2.1.6.1 Mutagenesis Primer		41
	2.1.6.2 Primer for Insertion		42
	2.1.6.3 Primers for Semi-Quantitative PCR		43
	2.1.6.4 Primer/Probe Sets for Quantitative Real-Time PCR		43
	2.1.6.5 Oligonucleotide Library Primers		44
2.1.7	Plasmids	44	
2.1.8	DNA Probes	47	
2.1.9	Nucleotides	47	
2.1.10	Standard Marker	48	
2.1.11	Enzymes	48	
2.1.12	Kits	48	
2.1.13	Cell Culture Media and Additives	49	
2.1.14	Constituents for Bacterial Cultures	50	
2.1.15	Chemicals	50	
	2.1.15.1 Special Chemicals		51
2.1.16	Buffers and Reagents	52	
2.1.17	Equipment	53	
2.1.18	Materials	55	
2.1.19	Software	56	
	<i>2.2 Methods</i>		57
2.2.1	Microbiological Methods	57	
	2.2.1.1 Cultivation of Bacteria		57
	2.2.1.2 Production of CaCl ₂ Competent Bacteria		57
	2.2.1.3 Production of Electrocompetent Bacteria		57
	2.2.1.4 Transformation of CaCl ₂ Competent Bacteria		58
	2.2.1.5 Transformation of Electrocompetent Bacteria		58
2.2.2	Preparation, Modification and Analysis of Plasmid DNA	59	
	2.2.2.1 DNA Mini-Preparation		59
	2.2.2.2 DNA Maxi-, Mega- and Giga- Preparation		59
	2.2.2.3 Precipitation and Purification of Plasmid DNA		60
	2.2.2.4 DNA Isolation from Cultured Cells or Animal Tissue		60
	2.2.2.5 Spectrophotometric Analysis		61
	2.2.2.6 Restriction Digest of DNA		61
	2.2.2.7 DNA Agarose-Gel-Electrophoresis		61
	2.2.2.8 Preparative Agarose Gel Extraction and Purification of DNA		62
	2.2.2.9 Purification of DNA Fragments after a Restriction Digest		62
	2.2.2.10 Dephosphorylation of DNA Fragments		62
	2.2.2.11 Ligation of DNA Fragments		63
	2.2.2.12 Polymerase Chain Reaction (PCR)		63

2.2.2.13 PCR-based Mutagenesis	64
2.2.2.14 TOPO Cloning	65
2.2.2.15 DNA Immobilization on a Nylon Membrane	65
2.2.2.16 Radioactive DNA Labeling	66
2.2.3 Cell Biology Methods	67
2.2.3.1 Cultivation of Cells	67
2.2.3.2 Determination of Number of Viable Cells	67
2.2.3.3 Cell Cryo-Conservation	67
2.2.3.4 Cultivation of Hybridoma Cells	68
2.2.3.5 Isolation of Primary Hepatocytes	68
2.2.3.6 Primary Neonatal Rat Cardiomyocyte Isolation	69
2.2.3.7 Organotypic Culture of Mouse Liver Tissue Slices	71
2.2.3.8 Transfection of Cells	73
2.2.3.8.1 Calcium Phosphoate (CaPO ₄) Transfection	73
2.2.3.8.2 PolyFect Transfection	73
2.2.4 Virological Methods	73
2.2.4.1 Infection and Transduction of Cultured Cells	73
2.2.4.2 AAV Harvest after Transfection	74
2.2.4.3 Large-Scale Production and Purification of AAV Particles	74
2.2.4.4 Titration of AAV Vector Stocks	75
2.2.4.4.1 Electron Microscopy of AAV Vector Productions (Negative Staining)	75
2.2.4.4.2 AAV2 Capsid ELISA	75
2.2.4.4.3 DNA Dot-Blot Assay	76
2.2.4.4.4 Quantitative Real-Time PCR	77
2.2.4.4.5 Replicative Titer Determination	77
2.2.4.5 Heparin Binding Analysis of rAAV Vectors	78
2.2.4.6 AAV Cell Binding and Entry	79
2.2.4.7 Luciferase Transgene Expression	79
2.2.4.8. AAV <i>In Vivo</i> Application and Analysis	80
2.2.5 Protein Biochemical Methods	81
2.2.5.1 Bradford Method	81
2.2.5.2 NanoOrange [®] Method	81
2.2.5.3 SDS-Page Gel Electrophoresis	81
2.2.5.4 Coomassie-Blue Staining	82
2.2.5.5 Western-Blot-Transfer of Proteins	82
2.2.6 Antibody Purification and Analysis	83
2.2.6.1 Immunological Detection after Protein Transfer	83
2.2.6.2 Antibody Purification	83
2.2.6.3 Immunofluorescences of Recombinant AAV Vectors	84
2.2.6.4 Antibody Isotyping	84
2.2.6.5 Antibody Conjugation	85
2.2.6.6 AAV8 ELISA Establishment	85
2.2.6.7 Monoclonal Antibody for AAV Vector Characterization	86
2.2.6.7.1 AAV Cell Binding and Entry	86
2.2.6.7.2 AAV N-terminal Externalization	87
2.2.6.7.3 Endosomal Cleavage Analysis	87
2.2.6.7.4 Neutralization Analysis	88
2.2.7 AAV8 Library Generation and Screening	88
2.2.7.1 Generation of AAV8 Library Backbone Plasmids	88
2.2.7.2 Preparation of a Random Insert Sequence	89
2.2.7.3 Ligation of Library Backbone Plasmid and Insert	90
2.2.7.3.1 Test Ligation	90
2.2.7.3.2 Large Scale Ligation	90

2.2.7.4 Production of the AAV8 Transfer Shuttle Library	92
2.2.7.5 Generation of the AAV8 Random Peptide Display Library	92
2.2.7.6 <i>In Vitro</i> Selection by the AAV8 Peptide Display Library	93
2.2.7.7 PCR Amplification and Sequencing of Selected Clones	93
2.2.7.9 Generation of Selected AAV8 Vector Mutants	94
2.2.8 Statistical Data Analysis	94
3. RESULTS	95
3.1 <i>In Vitro</i> Analysis of rAAV8 in Comparison to rAAV2	95
3.1.1 Homology between AAV8 and AAV2 Capsids	95
3.1.2 Transduction Efficiencies of rAAV8 and rAAV2 in Different Cell Lines or Primary Cells	98
3.1.3 Heparan Sulphate Proteoglycan Binding of rAAV2 and rAAV8	99
3.1.4 Differences in Infection Pathways between AAV2 and AAV8	100
3.1.4 Investigating Poor <i>In Vitro</i> Performance of AAV8	101
3.2 <i>In Vivo</i> Performance of rAAV Vectors and rAAV derived Capsid Mutants	103
3.2.1 <i>In Vivo</i> Analysis of rAAV2 and rAAV8	103
3.3.2 Vector Analysis of Mutants Comprising Large AAV2 Domains in AAV8 Capsids	106
3.3.3 Seven Regions of Non-conserved AA between AAV2 and AAV8	108
3.3.4 Single AA Exchanges of Non-Conserved Residues from AAV2 into AAV8	110
3.3.5 Adequate Substitutions of Non-Conserved Residues of AAV2 by those of AAV8	112
3.3.6 Validation of a Peptide Insertion Site within the AAV8 Scaffold	115
3.4 Development of a Random AAV8 Peptide Display Library	117
3.4.1 Generation and Characterization of the Plasmid Library	118
3.4.2 Analysis of the AA Frequency Distribution in the Generated Plasmid Library	119
3.4.3 Transfer Shuttle Library Generation	120
3.4.4 <i>In Vitro</i> Selection and Identification of Liver Targeting Vectors from the AAV8 Display Peptide Library	121
3.4.4.1 Characterization of Targeting Peptides Recovered from the <i>In Vitro</i> Selections	123
3.4.5 Generation of Vectors Displaying AAV8 Library Selected Peptides	125
3.4.6 Hepatotropic Peptide Identification by Gene Transduction Analysis	126
3.5 AAV8 dependent Cell Binding and Post-Entry Processing	128

3.5.1 Comparison of Genome Transfer and Transgene Expression in Different Tissues	128
3.5.2 Characterization of an AAV8 Capsid Specific Monoclonal Antibody ADK8	130
3.5.3 Monoclonal Antibody ADK8 Neutralization of AAV8 Capsids	134
3.5.4 Analysis of ADK8 Neutralization	137
4. Discussion	143
4.1 Comparison of rAAV8 and rAAV2 Vectors In Vitro	143
4.2 In Vivo Analysis of Domain and Single Residue Exchanges between AAV2 and AAV8	147
4.3 Selection of Targeted rAAV8 Vectors from the AAV8 Peptide Display Library	150
4.4 Uncoating – A Critical Step of Post Entry-Processing	152
4.5 Monoclonal Antibody ADK8 Uncovers New AAV8 Capsid Features	153
4.6 Final Conclusion	155
5. References	156
Acknowledgement	172

Zusammenfassung

Ausgangspunkt für die in dieser Arbeit durchgeführten Untersuchungen war die außergewöhnlich hohe Gentransduktionseffizienz von AAV8 Vektoren. Ein Vergleich zwischen AAV2 und AAV8 konnte zeigen, dass sich grundlegende Unterschiede auf den Kapsid Oberflächen befinden, trotz einer 83 % Homologie auf der Proteinsequenzebene zwischen beiden Serotypen. Ziel dieser Studie war es, die Rolle verschiedener Kapsidabschnitte beim Gentransfer zu charakterisieren. In Mutanten waren entweder große Sequenzabschnitte zwischen AAV2 und AAV8 oder einzelne Aminosäuren von AAV2 nach AAV8 oder von AAV8 nach AAV2 ausgetauscht worden. Das Ersetzen von großen AAV2 Kapsidomänen im AAV8 Kapsid zeigte, dass insbesondere ein Sequenzabschnitt, der in die Bildung der Kapsidoberfläche involviert ist, einen großen Einfluss auf die Gentransduktion von AAV8 hatte. Der Austausch von einzelnen Aminosäuren in dieser Region des Kapsids verursachte für AAV8, sowie auch für AAV2 Partikel, einen starken Einfluss auf die Genexpression *in vivo*. Im Vergleich zum Wildtyp AAV8 Kapsid konnten Kapsidoberflächenmutanten eine Transduktionssteigerung, aber auch eine Transduktionsenkung induzieren. Eine Substitution, die sich im Inneren des Kapsidmantels befand, verursachte einen vollständigen Verlust der Gentransduktion mittels AAV8 Vektoren. Hingegen konnte eine weitere Substitution, die an der inneren Schulter der "Kapsid-Spikes" generiert worden war und Heparinbindung für das AAV8 Kapsid erzeugt hatte, die Transduktionseffizienz von AAV8 noch steigern. Überraschenderweise konnte eine reverse Substitution von AAV2 Aminosäuren durch Aminosäuren von AAV8 im Bereich der inneren Schulter der "Spikes" ebenfalls zu einer Steigerung der Gentransduktion von AAV2 - teilweise sogar auf das Niveau von AAV8 - bewirken.

Nach der Analyse von Domänen, die die Gentransduktion von AAV8 beeinflussen, wurde in das AAV8 Kapsid eine Insertionsstelle eingefügt, um zu testen, ob das Kapsid aufgrund von insertierten Peptidsequenzen sein "Targetingprofil" verändert. Bekannte Peptidsequenzen, die in AAV2 Vektoren ein "Retargeting" bewirkt hatten, konnten auch im AAV8 Kapsid ein verändertes "Targeting" verursachen. Eine AAV8 Bibliothek mit zufälligen Peptidsequenzen in dieser Insertionsstelle wurde für die Selektion von Leber-spezifischen Vektoren verwendet. Es wurden Peptidmotive isoliert, die den unerwünschten Gentransfer von AAV8 Vektoren auf andere Organe als Lebergewebe drastisch reduzierten.

Studien mit einem monoklonalen Antikörper gegen AAV8 Kapside zeigten, dass dieser an dieselbe Stelle im AAV8 Kapsid bindet, in welche die Peptide insertiert wurden und welche nach Austausch gegen AAV2 Aminosäuren zu einer Transduktionssteigerung führte. Die Bindung der Antikörper an das Kapsid neutralisierte die Infektion, verhinderte aber nicht die Virusaufnahme in die Zelle. Der Mechanismus der Neutralisierung konnte jedoch nicht vollständig aufgeklärt werden.

Summary

The starting point of this work was the analysis of the unusually high gene transduction efficiency of AAV8 vectors. A comparison between AAV8 and AAV2 revealed fundamental differences of the capsids even though an 83 % homology is shared in the VP protein sequences. The aim of this thesis was to characterize the involvement of different capsid sequence domains in gene transfer. Therefore, AAV8 and AAV2 capsid mutants were generated which contained either large capsid domain exchanges between AAV2 and AAV8 or single amino acid residue swaps from AAV2 into the AAV8 capsid and vice versa. The exchange of large AAV2 domains into the AAV8 capsid showed that especially one domain which is involved in the capsid surface formation had also a strong impact on gene transduction of AAV8. The exchange of single amino acids in that domain induced for AAV8 as well as AAV2 particles a strong impact on gene transduction *in vivo*. In comparison to the wild type AAV8 capsid, capsid surface mutants could induce increased transduction efficiency as well as decreased transduction efficiency. One substitution which was located within the capsid shell caused a complete loss of gene transduction for AAV8 vectors, whereas another substitution situated at the inner shoulder of the spike region reconstituted heparin binding and strongly increased transduction efficiency of AAV8. Surprisingly, one reverse substitution of AAV2 amino acids exchanged with AAV8 amino acids which was also present on the inner shoulder of the spike region, could also increase gene transduction of AAV2 capsids, even close to the level of AAV8 gene transduction in some cases.

Having determined domains which influence gene transduction of AAV8, a random peptide insertion site was inserted into the AAV8 capsid at the inner shoulder of the 3-fold spike region to test whether the capsid could change its targeting profile due to peptide insertions. Known peptide sequences which had been described to retarget AAV2 vectors could also induce targeting displayed on the AAV8 capsid. At that insertion site, an AAV8 random peptide display library was also inserted and used to select for hepatotropic vectors. Peptide motifs were recovered which reduced undesired gene transfer of rAAV8 vectors to other organs than liver tissue.

Monoclonal antibody studies against the AAV8 capsid showed that binding occurs at the same site of the AAV8 capsid in which peptides had been inserted and amino acids had been exchanged to AAV2 amino acids and induced increased transduction efficiency. Antibody binding to the capsid could neutralize the infection, but did not inhibit viral uptake of the cell. The mechanism of neutralisation could not be enlightened completely.

Abbreviations

AAV(s)	adeno-associated virus(es)
AAV1-11	adeno-associated virus type 1-11
Ad	adenovirus
Ad5	adenovirus type 5
aa	amino acids
BSA	bovine serum albumin
cap	capsid gene of AAV
CF	cystic fibrosis
cFIX	canine factor IX
CMV	human cytomegalovirus promoter
°C	degree centigrade
Δ	deletion
DMEM	Dulbecco's modified Eagle medium
DMSO	dimethyl sulfoxide
DNA	desoxyribo nucleic acid
DNase	desoxyribonuclease
dH₂O	sterile deionized H ₂ O
dNTP_s	deoxyribonucleoside triphosphates
<i>E.coli</i>	<i>Escherichia coli</i>
EDTA	ethylene-diamine-tetra-acetate
EE	early endosome(s)
EGFP	enhanced green fluorescent protein
ELISA	enzyme-linked immunoabsorbent assay
FCS	fetal calf serum
FGFR	fibroblast growth factor receptor
FVIII	factor VIII
FIX	factor IX
Fig.	figure
g / x g	gram / gravity
GFP	green fluorescent protein
gp	genome-containing particles
HBSS	Hepes buffered saline solution
H₂O	water
HSPG(s)	heparan sulfate proteoglycan(s)
HSV	herpes simplex virus
hFIX	human factor IX
IgG(s)	immunoglobulinG(s)
INF	interferon
ip	intraperitoneal injection
ITS(s)	inverted terminal repeat(s)
IU	infectious unit(s)
iv	intravenous injection
IVIS	<i>In vivo</i> imaging software
kDa	kilo dalton
LamR	laminin receptor
LB	"luria broth" medium
LE	late endosome(s)
luc	luciferase gene
μ (g,l,m)	micro – (gram, litre, metre)

m (g,l,m)	milli – (gram, litre, metre)
MLC	myosin light chain
MNase	micrococcus nuclease
MOI	multiplicity of infection
mRNA	messenger RNA
N-	amino-
NCS	newborn calf serum
NHP	non-human primate
NHS	normal horse serum
ng	nanogram
nm	nanometer
O/N	over night
ORF(s)	open reading frame(s)
OTC	organotypic culture
p	plasmid
p5/19/40	map unit position 5/19/40 promoter
PBS	phosphate buffered saline
PCR	polymerase chain reaction
PET	polyethylene terephthalate
PLA2	phospholipase A2
pfu	plaque-forming unit
pH	“pons hydrogenium“
p.i.	post infection
pg	picogram
qRT-PCR	quantitative real-time PCR
r	recombinant
rAAV	recombinant AAV
rep	non-structural gene of AAV
RLB	reporter lysis buffer
RLU	relative light unit
RNA	ribonucleic acid
RT	room temperature
scAAV	self-complementary AAV
SDS	sodium dodecyl sulfate
sec	second(s)
sel.	deletion
s.	see
ss	single-stranded
TAE	Tris-Acetate-EDTA
TE	Tris-EDTA
trs	terminal resolution site
U	unit(s)
UV	ultraviolet light
VMD	visual molecular dynamics
VP	structural proteins of AAV
vg	viral genomes
wt	wild-type

Size Units and Physical Scales

A	Ampere
A_(x)	Absorption at (x) nanometers
bp	Basepairs
Bq	Bequerel
C°	Degree Celsius
cpm	Counts per minute
D	Dalton
g	Gram
(n) x g	n times gravitational acceleration
h	Hour
kb	Thausand basepairs
l	Liter
M	Molar, mol/l
m	Meter
min	Minute
Nt	Nucleotide
OD	Optical density
rpm	Rounds per minute
S	Svedberg unit
s	Second
t	Time
T	Temperature
U	Units
V	Volt
Vol.	Volume
W	Watt

Prefix of Scale Units

M	Mega	10^6
k	Kilo	10^3
c	Zenti	10^2
m	Milli	10^{-3}
μ	Micro	10^{-6}
n	Nano	10^{-9}
p	Pico	10^{-12}

One and Three Letter Code of the Amino Acids

A	Ala	Alanine	M	Met	Methionine
C	Cys	Cysteine	N	Asp	Asparagine
D	Asp	Aspartate	P	Pro	Proline
E	Glu	Glutamate	Q	Gln	Glutamine
F	Phe	Phenylalanine	R	Arg	Arginine
G	Gly	Glycine	S	Ser	Serine
H	His	Histidine	T	Thr	Threonine
I	Ile	Isoleucine	V	Val	Valine
K	Lys	Lysine	W	Trp	Tryptophan
L	Leu	Leucine	Y	Tyr	Tyrosine

The Genetic Code

		Second Letter								
		T	C	A	G					
First Letter	T	TTT } Phe TTC } TTA } Leu TTG }	TCT } TCC } Ser TCA } TCG }	TAT } Tyr TAC } TAA } Stop TAG } Stop	TGT } Cys TGC } TGA } Stop TGG } Trp	T	C	A	G	
	C	CTT } Leu CTC } CTA } CTG }	CCT } CCC } Pro CCA } CCG }	CAT } His CAC } CAA } Gln CAG }	CGT } Arg CGC } CGA } CGG }	C	A	G		
	A	ATT } Ile ATC } ATA } ATG } Met	ACT } ACC } Thr ACA } ACG }	AAT } Asn AAC } AAA } Lys AAG }	AGT } Ser AGC } AGA } Arg AGG }	A	T	C	A	G
	G	GTT } Val GTC } GTA } GTG }	GCT } GCC } Ala GCA } GCG }	GAT } Asp GAC } GAA } Glu GAG }	GGT } Gly GGC } GGA } GGG }	G	T	C	A	G

1. Introduction

Adeno-associated virus (AAV) vectors belong to the most frequently used viral vectors currently used in gene therapy. Most AAVs were originally reported as contaminants of laboratory stocks of adenoviruses (Kilham *et al.* 1959; Atchison *et al.* 1965; Hoggan *et al.* 1966) which contributed to its given nomenclature. AAV was not of medical interest for decades, as it was not identified as a pathogen, but the consistency of viral persistence, the multiple serotypes, and the lack of pathogenicity has increased the AAV's potential as a delivery vehicle for gene therapy applications.

1.1 Biology of Adeno-Associated Viruses

1.1.2 Virus Classification

The wild type AAV particle is a small (25 nm), non-enveloped virus that packages a linear, single-stranded DNA genome. It belongs to the family *Parvoviridae* (Mayor *et al.* 1966; Siegl *et al.* 1985) and is a member of the genus *Dependovirus*. AAV serotypes share the general requirement for an unrelated DNA virus to complete their life cycle. Host cell co-infection with the helper virus adenovirus (Myers *et al.* 1980; Richardson *et al.* 1981) accounts for AAV replication but helper functions are also accomplished by other viruses such as herpes simplex virus types 1 and 2 (Buller *et al.* 1981), the human cytomegalovirus (McPherson *et al.* 1985), vaccinia virus (Schlehofer *et al.* 1986), human herpesvirus type 6 (Thomson *et al.* 1994) or by human papillomavirus type 16 (Ogston *et al.* 2000). In the absence of a helper virus, AAV can become latent through site-specific chromosomal integration or by remaining episomal.

Among the primate AAVs, thirteen AAV-serotypes were isolated whose genomes have been cloned and mostly sequenced (Srivastava *et al.* 1983; Chiorini *et al.* 1997; Rutledge *et al.* 1998; Bantel-Schaal *et al.* 1999; Chiorini *et al.* 1999; Xiao *et al.* 1999; Gao *et al.* 2002; Mori *et al.* 2004; Schmidt *et al.* 2008). Serotypes 2, 3, 3a, 5 and 9 have been derived from human tissue samples, and the natural hosts of serotypes 4, 7, 8, 10, 11 and 12 are non-human-primates (NHP). Whether AAV1 originated from human or NHP, remains inconclusive (Gao *et al.* 2005). Six amino acid (aa) differences are found between AAV1 and

AAV6, which suggests that AAV6 is an AAV1 variant (Rutledge *et al.* 1998). AAV2 is, among all naturally discovered serotypes, the best characterized serotype and is considered the prototype for AAV research. A PCR based method led to the additional identification and cloning of more than 100 new AAV capsid DNA sequences from human, as well as NHP tissue (Gao *et al.* 2002; Gao *et al.* 2003; Gao *et al.* 2004). The increasing amount of new AAV capsid variants makes a classification system difficult. Isolates have been subdivided by three different classification systems based on capsid differences:

- Serology
- Subgroups via capsid subunit mixing compatibility
- Clades based on genetic relatedness

A classical method to group viruses is serology. Isolates can be found in serologically distinct clusters, but if newly identified capsids differ from each other only in a few amino acids, unique antigenic sites are difficult to obtain. An alternative classification system is the 'transcapsidation' method that allows determining the relatedness of different capsids based on their ability to form mixed shells from different isolate subunits (Rabinowitz *et al.* 2004). It is a complex method, but it helps to gain insight into the structural relatedness of the serotypes.

Computational analysis, such as PhyloDraw (Morgenstern *et al.* 1998) has been used to construct phylogenetic trees of different AAV serotypes (Fig. 1-1 A). Six clades have been identified (Grimm *et al.* 2008), prototypical members of Clade A, B, D, E and F are AAV1 (AAV6), AAV2, AAV7, AAV8 (AAV10) and AAV9, respectively. AAV2/3 hybrids belong to Clade C, and other AAVs, such as AAV3a, AAV3b, AAV4, AAV5, AAV11 and AAV12, do not fit into any clade and are thus defined as clonal isolates (Fig. 1-1 B).

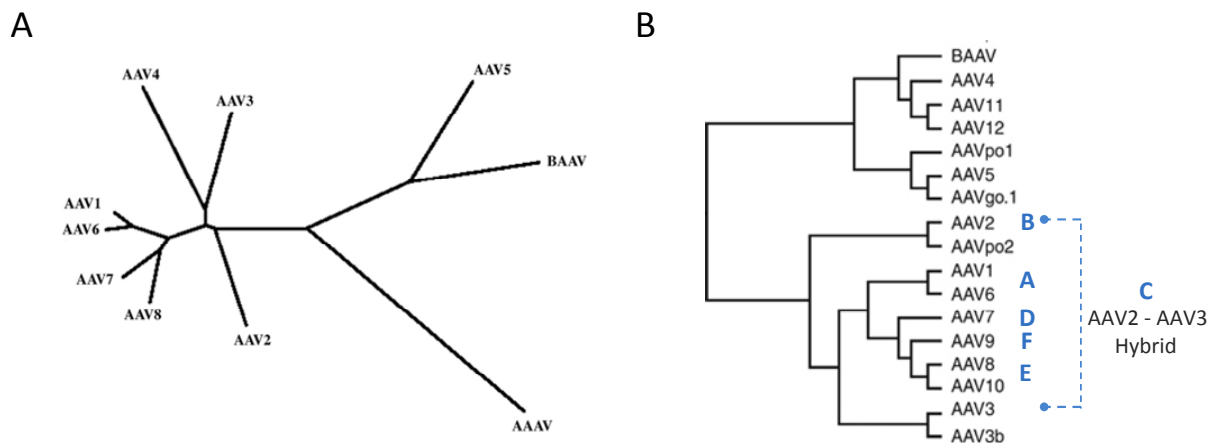


Figure 1-1 Evolutionary relationship among human and nonhuman primate AAVs. A) The unrooted phylogenetic tree was constituted by a merged ClustalW alignment of partial genome sequences. It demonstrates the relatedness of different AAVs by lengths of branches, proportional to evolutionary distances between isolates (Schmidt *et al.* 2008). B) A branched phylogenetic tree of the truncated 1.4 kb 'end-of-cap' region for published AAV serotypes aligned with AAVpo1, -po2 and -go.1 was constructed by TreeViewer (Bello *et al.* 2009). Clades are additionally indicated by capital letters, clade C has been identified to have originated from one recombination event, the unrooted neighbour-joining phylogeny is indicated by a dashed line with round heads.

1.1.3 AAV2 Genome

The AAV2 capsid harbours a single-stranded (ss), linear DNA genome with a length of 4679 nucleotides (Srivastava *et al.* 1983; Cassinotti *et al.* 1988; Ruffing *et al.* 1994). Two open reading frames, *rep* and *cap*, have been identified and are known to encode for the synthesis of non-structural (Rep proteins) (Hermonat *et al.* 1984; Tratschin *et al.* 1984) and structural proteins (Cap proteins) (Johnson *et al.* 1971; Rose *et al.* 1971) (Fig. 1.2 A). Four non-structural proteins are encoded by the *rep* gene and are named according to their molecular weights; Rep78, Rep68, Rep52 and Rep4. These share overlapping amino acid sequences (Mendelson *et al.* 1986; Trempe *et al.* 1987). The synthesis of the two larger Rep proteins is driven by the p5 promoter. In the case of Rep68, the intron is removed from the splice-donor-site (nucleotide 1907) to the splice-acceptor-site (nucleotide 2201). The mRNAs for the translation of Rep52 and Rep40 is initiated by the p19 promoter. Like Rep68, Rep40 has to undergo the same splicing event (Laughlin *et al.* 1979; Green *et al.* 1980). The p40 promoter controls the synthesis of the amino acid overlapping structural proteins VP1 (87 kD), VP2 (72 kD) and VP3 (62 kD). The capsid proteins share the same C-terminal 533 amino acids, but differ in N-terminal sequence. Alternative splicing induces the generation

of two mRNA transcripts. Instead of the splice-acceptor-site at nucleotide 2201, the site at nucleotide 2228 of the shorter mRNA transcript is predominantly used (Johnson *et al.* 1971; Rose *et al.* 1971; Laughlin *et al.* 1979; Becerra *et al.* 1988). Two different start codons initiate translation in VP2 and VP3 in the shorter mRNA sequence. ACG, a non-canonical start codon, is used to generate VP2, a 65 aa shorter version of VP1. The conventional start codon, AUG, is located 202 aa downstream, directing VP3 synthesis. Inverted terminal repeats (ITRs) flank both sides of the viral genome. The ITR-sequence comprises many important functions in the viral life-cycle. Under non-permissive conditions, it is responsible for viral integration (Nahreini *et al.* 1992; Balague *et al.* 1997; Wang *et al.* 1997), whereas under permissive conditions it monitors excision, gene expression, replication and packaging (Lusby *et al.* 1980; McLaughlin *et al.* 1988; Samulski *et al.* 1989; Pereira *et al.* 1997). ITRs are cis-acting elements, able to independently guide DNA packaging, the termini are identified as 145 bases in length, of which the outer 125 bases were capable of self-basepairing (Lusby *et al.* 1980; Lusby *et al.* 1981). This 125 base region could self-anneal to form a T-shaped structure, the stem (A-A') (Fig. 1.2 B). The central 44 bases contain two small palindromes (B-B' and C-C'), forming the arms of the T. The internal palindromes occur in two forms in which the internal palindromic sequences are switched from one arm to the other arm (designated as flip and flop; (Ryan *et al.* 1996).

Both orientations exist independent from each other in similar quantities (Lusby *et al.* 1981). Only seven bases are left unpaired in the complete T-shaped form; three bases at the end of each palindromic arm and the central base of the entire palindrome. Located on the stem palindrome is the Rep binding site (RBS), as well as the replication dependent terminal resolution site (*trs*) (Snyder *et al.* 1990). The remaining 20 nucleotides at the end of the ITR, the D-sequence, remain single-stranded.

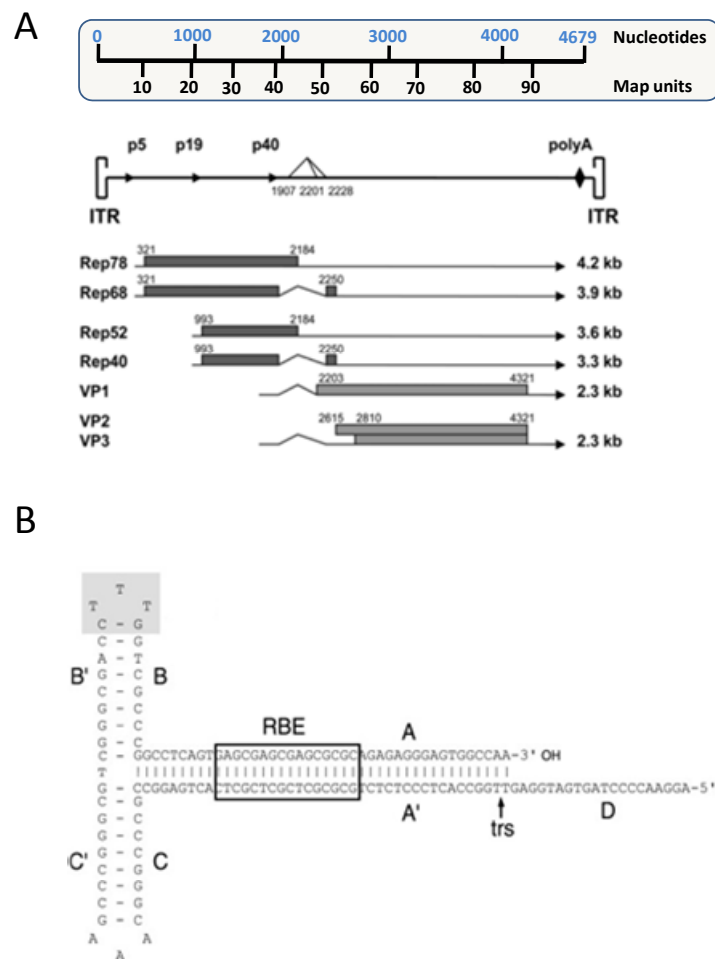


Figure 1-2 AAV2 genome organization and the secondary structure of the AAV2 ITR. (A) General organization of the genome and genetic elements of AAV type 2. A bar indicates the amount of nucleotides present in the AAV2 genome, the scale of 100 map units is also depicted; 1 map unit being equivalent to 47 nucleotides. Round structures on either side indicate the ITRs. Vertical arrows display the three transcriptional start sites of the promoters at map unit 5, 19 and 40. Polyadenylation sites (poly A) are present at map unit 96 (indicated with rhombi). Three additional positions are also presented, splice-donor (Nt 1907) and splice-acceptor sites (Nt 2201, Nt 2228). Solid lines present the transcripts. Two open reading frames (orf) are marked with dark grey or light grey. The first open reading frame encodes the four regulatory proteins (dark grey) arising from promoters p5, p19 and alternative splicing. The second orf (promoter p40) encodes the three capsid proteins (light grey). Transcribed mRNA lengths of the structural and non-structural proteins are pointed out on the right hand side. (B) The AAV2 ITR is composed of two arm palindromes (B-B' and C-C') embedded into one large stem palindromic (A-A'). The schematic overview is shown in the flip orientation. D is present once at the genome end, remaining single-stranded. The Rep-binding element (RBE) is framed by a black box, indicating the position where the Rep78 and Rep68 proteins bind. An arrow shows the terminal resolution site (trs), the position where the hairpin is nicked. Shaded nucleotides at the apex of the T-shaped structure correspond to the additional binding element (RBE') which stabilizes the two large Rep proteins and the ITR (Goncalves 2005).

1.1.4 AAV2 Proteins

1.1.4.1 Non-structural Proteins

All four Rep proteins are multifunctional regulators of the viral life cycle and they play a key role in viral replication, gene expression as well as excision (Hermonat *et al.* 1984; Tratschin *et al.* 1984). Three different functional domains have been identified (Fig. 1-3 A). Only Rep78 contains the complete set of domains. The central domain, which contains ATPase and Helicase activity, a nuclear localization signal (NLS), and the N-terminal located endonuclease domain of Rep78/68, controls the interaction between the viral genome, the ITRs, and the C-terminal linked Zinc finger domain. Rep78/52 induces interactions with many cellular factors (Mendelson *et al.* 1986; Hunter *et al.* 1992; Bevington *et al.* 2007). Each of the Rep proteins features a central domain of to the viral life cycle critical ATPase and Helicase activity (Im *et al.* 1992; Wonderling *et al.* 1995; Zhou *et al.* 1999; Collaco *et al.* 2003; James *et al.* 2003). All Rep helicases exhibit a 3'-5'polarity, however, Rep40 does not necessarily need a free 3'-single strand end to unwind. Contrary to Rep40, Rep68 and Rep52 activity strictly depend on the presence of a free 3'-single strand end. Moreover, Rep40 ATPase is actively stimulated by a single stranded DNA genome (Smith *et al.* 1998; Collaco *et al.* 2003). During the infection process, Rep proteins are synthesized from the DNA genomes at first. Rep78/68 proteins initiate viral genome replication by binding to the Rep binding site (RBS) (Snyder *et al.* 1990; Owens *et al.* 1991; Im *et al.* 1992; Smith *et al.* 1998). The hairpin is nicked at the terminal-resolution-site (trs) at nucleotide 124 (McCarty *et al.* 1994; Zhou *et al.* 1999) by Rep78/68. The hairpin end is unwound and the Rep78 molecule is left attached to the new 5'end. The 3' end formed by Rep cleavage is extended to the end of the template strand. The ends then refold into their self-base pairing hairpin structures, producing a single-stranded and a duplex genome upon a new round of strand displacement and replication. Helicase-activity of Rep78/68 induces genomic displacement so that newly synthesized genomes can either serve as a substrate for additional replication, or are prepared for genome packaging (Chejanovsky *et al.* 1989; Im *et al.* 1992). The Helicase activity of Rep52/40 is important to the encapsidation of viral genomes into pre-assembled empty capsids (Chejanovsky *et al.* 1989; King *et al.* 2001).

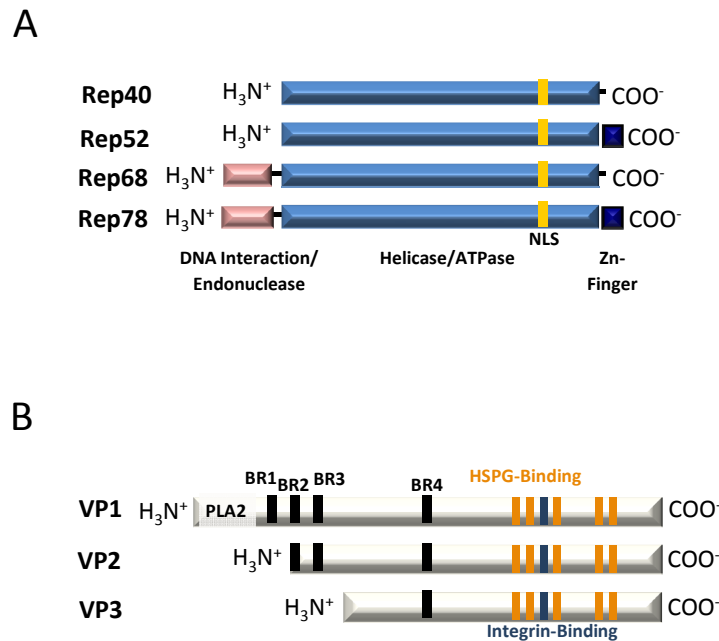


Figure 1-3 Schematic illustration of AAV2 proteins and their functional domains. A) AAV2 Rep proteins with the N-terminal located DNA interaction and endonuclease domain (light blue bars), the domain of helicase and ATPase activity (blue bars) including the NLS (yellow) and the C-terminal Zinc finger domain (dark blue bars). B) Identified functional domains of AAV2 VP proteins: the receptor binding domains of AAV2 are heparansulfate-proteoglycan (HSPG) and integrin ($\alpha 5\beta 1$). Identified amino acids involved in receptor binding are indicated for HSPG by five orange boxes and for integrin –binding by one blue box. Basic regions are marked in black (BR1-4, short motifs containing positively charged aa R and K) and the phospholipase A2 domain (PLA2) located at the N-terminus of VP1 is also illustrated.

1.1.4.2. Structural Proteins

As described previously (Section 1.1.3), the capsid is comprised of three viral capsid proteins VP1 (87 kD), VP2 (72 kD) and VP3 (60 kD). The majority of its T=1 icosahedral architecture is made up by the 60 kDa VP3 proteins. Alternative splicing causes a less frequent production of the VP1 mRNA (Becerra *et al.* 1988; Cassinotti *et al.* 1988; Trempe *et al.* 1988). VP2 and VP3 are translated from the commonly synthesized mRNA transcript, but the unconventional start codon ACG of VP2 cause the presence of capsid proteins in a 1:1:10 molar ratio. For 10 VP3 molecules, one VP1 and one VP2 capsid monomer is anchored in the particle structure by the C terminus that is structurally identical to the VP3 monomer (Rose *et al.* 1971).

Functional domains have also been identified for the VP proteins (Fig. 1-3 B). Heparan sulphate proteoglycan (HSPG) was identified as a primary receptor (Summerford *et al.*

1998) of AAV2, and binding was specified to two aa regions (AA 509-522 and AA 561-591) of the VP3 protein (Rabinowitz *et al.* 1999; Wu *et al.* 2000). Later studies determined that five basic aa, specifically R484, R487, K532, R588 and R588, are responsible for HSPG binding (Kern *et al.* 2003; Opie *et al.* 2003). Together, they make up a domain located on the capsid outer surface (Xie *et al.* 2002). Located close to the HSPG binding domain of the VP proteins, is the aa sequence NGR (AA511-513) of the $\alpha 5\beta 1$ integrin (Fig. 1-3 A) (Asokan *et al.* 2006). This motif is partially exposed on the capsid outer surface and functions as a co-receptor of AAV2 internalization. Other integrin-receptors, like $\alpha V\beta 5$, may also interact with NGR (Summerford *et al.* 1999).

Like in most parvoviruses, the phospholipase A2 domain (PLA2) has been determined in AAV2 within the N-terminal region of VP1 (Figure 1-3B). The exact function of the viral PLA2 domain has not been identified, however introduced mutations into the PLA2 catalytic center or Ca-binding site drastically reduced enzymatic activity and resulted in a reduced infectivity (Girod *et al.* 2002). It has been estimated that parvoviral PLA2 activity is required between viral perinuclear accumulation and early gene expression (Zadori *et al.* 2001; Girod *et al.* 2002). Interestingly, PLA2 activity could not be demonstrated in intact capsids suggesting that the N-terminus is located within native capsids (Kronenberg *et al.* 2005). N-terminal externalization or capsid dissociation during infection is inevitable to achieve PLA2 activity. It was initially demonstrated in autonomous parvoviruses (Cotmore *et al.* 1999) that pH or heat treatment can induce externalization of the PLA2 catalytic domain of AAV2. Electron microscopy and molecular modelling of the VP1 N-terminal region even suggested a partial defolding of the VP1 terminus, allowing exposure through a channel at a 5-fold symmetry (Kronenberg *et al.* 2005). Furthermore, the VP1/VP2 termini, with its PLA2 domain, are also exposed *in vivo*, presumably in the endosomal compartment (Sonntag *et al.* 2006).

Basic regions (BR) have also been identified in the N-terminal region of the VP proteins (Figure 1-3B), representing possible nuclear localization sequence (NLS) motifs. The domain contains four short motifs which are conserved in all AAV serotypes and consist of positively charged aa : BR1 (KKR, AA122-124) is only present in the N-terminus of VP1 ; BR2 (KKR, AA 142-144) and BR3 (RKR, AA 168-170) are located in VP1 and VP2; BR4 (RPKR, AA 307-310) is part of all VP proteins (Grieger *et al.* 2006). BRs may play a role in the nuclear transport of newly synthesized VP proteins, in fact, nuclear transport signals were determined for VP1

and VP2 as well as nuclear entry dependence of VP3 on VP1/2 interaction (Ruffing *et al.* 1992). But these basic clusters (BC) have also been suggested to permit nuclear uptake of viral particles. In fact, mutations of the basic elements did not reduce viral production but its infectivity (Wu *et al.* 2000; Sonntag *et al.* 2006). Especially BC3 seems to play a key role in nuclear transport of AAV genomes, in situ hybridization revealed that recombinant AAV genomes packaged into wt or BC3 mutant capsids showed differences in the perinuclear accumulation, furthermore, BC4 seems to be critical for the virion assembly (Grieger *et al.* 2006). A direct attempt to assay BC elements involvement in nuclear transport of AAV capsids failed mostly due the general inefficiency of the nuclear transport. Endosomal release, proteosomal degradation as well as the relatively large particle size compared to the nuclear pore size contribute to a low amount of viral capsids within the nucleus, below immunofluorescent detection levels (Sonntag *et al.* 2006).

1.1.5 AAV2 Capsid Structure

The AAV2 particle is comprised of a non-enveloped, icosahedral capsid with a diameter of 25 nm, and a three-dimensional structure of 60 protein subunits that share identical interaction sites. A symmetry with the triangulation number (T) = 1 is therefore obtained in this structure (Caspar *et al.* 1962). VP1, VP2 and VP3 are present in a 1:1:10 stoichiometry, contributing to the 5 VP1, 5 VP2 and 50 VP3 molecules (Rose *et al.* 1971). A capsid features twelve 5-fold, twenty 3-fold and thirty 2-fold symmetry axes (Fig. 1-4 A).

The AAV2 structure has been determined to a 3-Å resolution in X-ray crystallography (Xie *et al.* 2002). All 60 protein subunits have a conserved eight-stranded antiparallel β -barrel motif. These β -strands (A-I) are interspersed with long loops. The GH loop situated between β -strand G and H, is mainly responsible for the formation of proximal peaks at the three-fold symmetry axis. This loop contributes significantly to the unique AAV2 surface topology and cell tropism. Proximal peaks consist of 3 spike-like extrusions (Fig. 1-4 B) (Kronenberg *et al.* 2001; Xie *et al.* 2002). Other capsid features are the pore at the 5-fold symmetry axis (Fig. 1-4 B) (Bleker *et al.* 2005) and the depression at the 2-fold axis (Fig. 1-4 B). Additionally, the flexible HI loop, which extends from each viral subunit, overlapping the neighboring five-fold VP on the capsid surface, could be of importance to the viral particle (Fig. 1-4 C) (DiPrimio *et al.* 2008). Within the capsid, Cryo-EM assists in identifying globular

structures, which might represent the folded VP1/VP2 N-termini (Fig. 1-4 A) (Kronenberg *et al.* 2005).

Capsid structure analysis has been further advanced by Cryo-EM single particle analysis (SPA). The procedure confirmed previous findings and resolved structural features at near atomic resolution. The native AAV2 capsids can be complexed with a fragment of the primary cellular receptor heparin (Fig. 1-4 D) and the extra density becomes located directly over amino acids, which were previously implicated in mutagenic binding studies (O'Donnell *et al.* 2009; Ward *et al.* 2009).

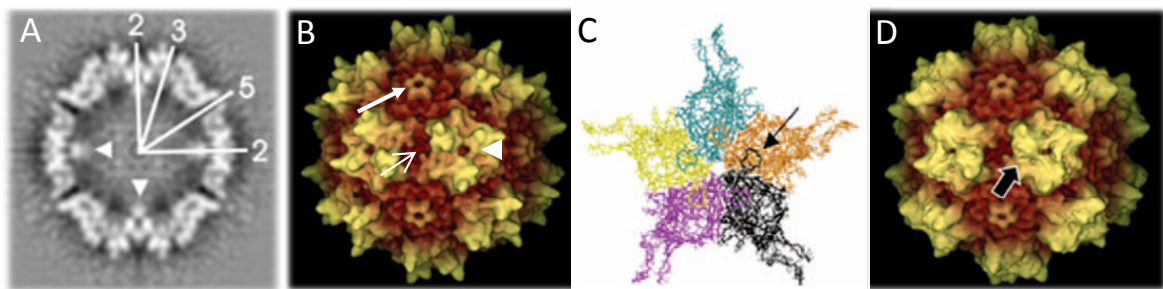


Figure 1-4 AAV2 capsid structure. A) The equatorial slice of the AAV2 capsid reconstructed by Cryo-EM is shown, all symmetry axes are indicated. White arrow heads point out the globular structures at the 2-fold depression (figure from Kronenberg *et al.* 2005). B) Surface topology of a native AAV2 capsid in garnet and yellow at 7.8Å. Symmetry axes are indicated by a solid arrow (5-fold axis), an arrow head (3-fold axis) and a thin-lined arrow (2-fold axis). C) AAV2 pentamer of the 5 VP subunits. The black arrow indicates the HI loop which extends from one VP subunit to overlapping the neighbouring VP (from DiPrimio *et al.* 2008). D) AAV2 capsid surface topology with an extra density located near the shoulder of each three-fold related peak due to bound heparin (O'Donnell *et al.* 2009).

1.1.6 AAV2 Capsid Assembly and Genome Encapsidation

After mRNA translation, VP proteins are guided into the nucleus to assemble into an icosahedral protein shell. Due to their NLS motifs, VP1/2 proteins are primarily detected in the nucleus. VP3 proteins can mainly get into the cell by interacting with the other 2 VP proteins. Consequently, VP3 proteins are evenly distributed throughout nucleus and cytoplasm during capsid formation (Ruffing *et al.* 1992; Wistuba *et al.* 1997). VP3 proteins alone can assemble to an intact capsid (Warrington *et al.* 2004), however, a newly identified AAV protein has to be coexpressed to promote the assembly reaction (Sonntag *et al.* 2010). Assembled AAV capsids are detected in the nucleoli at the first instance, but are

instantly redirected towards the nucleoplasm (Hunter *et al.* 1992; Wistuba *et al.* 1997). In the nucleoplasm, empty capsids co-localize with Rep proteins and viral DNA in a Rep-dependent manner. Helicase activity of Rep78/68 and the Rep78 molecule, still attached to the new 5' end, initiate encapsidation by protein-protein interaction. But Rep52/40 still needs to unwind the newly synthesized single stranded DNA genome (Chejanovsky *et al.* 1989; King *et al.* 2001). At this stage, the viral genome is able to load into the capsid, with the passage through the pore at the five-fold axis suggested as the capsid entry site (Bleker *et al.* 2005; Bleker *et al.* 2006).

1.1.7 AAV Life Cycle

After successful infection, an AAV particle enters either a lytic or a latent stage. In the presence of a helper virus, such as an adenovirus, the lytic stage ensues, and a productive infection takes place. The adenoviral helper functions have been identified and include the genes E1a, E1b, E2a, E4 and VA RNA (Richardson *et al.* 1981; Laughlin *et al.* 1982). These genes regulate cellular gene expression and provide a permissive intracellular milieu for an AAV productive infection (Laughlin *et al.* 1982; Clark *et al.* 1996). Without helper viral co-infection, a productive AAV life cycle is normally impeded. However, if carcinogenic, cell-synchronising substances or β - or UV- irradiation induce cellular stress, a permissive state is also presented to AAV particles and AAV replication is initiated without any helper viruses present (Yakobson *et al.* 1987; Yalkinoglu *et al.* 1988; Yakobson *et al.* 1989).

In the absence of helper viruses or cell induced stress, the AAV genome establishes latency and integrates into a 4-kb region on chromosome 19, termed AAVS1 (Berns *et al.* 1975; Laughlin *et al.* 1986; Kotin *et al.* 1990; Samulski *et al.* 1991). A latent AAV genome can be rescued and replicated upon superinfection. The AAVS1 locus is located within the gene MBS85, which is involved in actin organization (Tan *et al.* 2001). Besides ITRs (in *cis*), Rep 78/68 proteins (in *trans*), the 15-bp RBE in P5 needs to be present in *cis* (Feng *et al.* 2006). AAVS1 targeted integration is only possible due to its RBE-like and TRS-like sequence, which come in close proximity to each other during integration (Samulski *et al.* 1991). However, integration into AAVS1 is not completely specific, with only 60% of all integrants detected within the locus. Many debates on non-specific integration of AAV2 particles contributing to

malignancy have been presented, but the experimental designs and animal models did not allow any serious considerations (Donsante *et al.* 2007; Kay 2007).

1.1.8 AAV Infection

AAV2 enters target cells by using its primary receptor heparin sulphate proteoglycan (Summerford *et al.* 1998). Internalization is enhanced by interactions with at least one of the identified co-receptors, including the $\alpha V\beta 5$ and $\alpha 5\beta 1$ integrins, the fibroblast growth receptor 1 (FGFR1), the hepatocyte growth factor receptor (c-Met) and the laminin receptor (LamR) (Qing *et al.* 1999; Summerford *et al.* 1999; Kashiwakura *et al.* 2005; Akache *et al.* 2006; Asokan *et al.* 2006). Co-receptors not only trigger endocytosis directly, but also stimulate intracellular signalling pathways for factors crucial to cellular uptake as well as post-entry trafficking. A Rac1 protein appears to be required for the initiation of AAV2 particle endocytosis (Sanlioglu *et al.* 2000). Moreover, the activation of the Rac1 protein and the phosphatidylinositol 3-kinase (PI3K) pathway are critical for intracellular trafficking of AAV particles using microtubules (Sanlioglu *et al.* 2000; Harbison *et al.* 2008). However, it was also shown that virions released into the cytoplasm soon after endocytosis can also be transported by diffusion (Seisenberger *et al.* 2001). Not all factors mediating AAV trafficking post-entry have been elucidated. But it is known that cells which are defective for dynamin hinder AAV2 infection. Therefore, it has been suggested that particles are mostly endocytosed via clatherin-coated vesicles in a dynamin dependent manner (Duan *et al.* 1999). By fixing cells at different times after viral uptake, AAV can be co-localized with markers of early endosome (EE), late endosome (LE), perinuclear recycling endosome and lysosome (Bartlett *et al.* 2000; Ding *et al.* 2005; Ding *et al.* 2006). For a successful infection, AAV2 needs to escape from any of these endocytic vesicles (Fig. 1-5). Many potential escape routes have been demonstrated and described (Duan *et al.* 1999; Bartlett *et al.* 2000; Douar *et al.* 2001; Hansen *et al.* 2001; Xiao *et al.* 2002). All the escape routes have commonly a low pH in the endosome, which seems to contribute to viral escape. It has been described that particles are either directly released from EE or they are further transported into LE or PNRE. At that stage, particles have to be released into the cytoplasm. Otherwise, lysosomal degradation is an inevitable consequence. A drop in pH, from 7.5 to 5.5, in addition to another not yet identified physiological trigger (Sonntag *et al.* 2006), contributes to a

conformational change of AAV2. The VP1/2 N terminus, with its conserved PLA2 motif, is exposed and assists the virus to escape the late endosome (Girod *et al.* 2002; Suikkanen *et al.* 2003; Bleker *et al.* 2005; Farr *et al.* 2005). Endosomal cysteine proteases, cathepsins B and L, showed specific endosomal cleavage pattern of different serotypes and have been identified to contribute to intracellular processing and capsid disassembly (Akache *et al.* 2007). Exactly how AAV2 enters the nucleus is not known, but as previously described (see section 1.1.4.2.), BRs are externalized together with VP1/2 N-termini when particles are released into the cytoplasm. Inheriting possible nuclear localization sequence (NLS) motifs, BRs have been suggested to support particle nuclear targeting from the cytoplasm (Grieger *et al.* 2006; Sonntag *et al.* 2006). It has been hypothesized that AAV is theoretically small enough to enter the nucleus via a nuclear pore complex for the final capsid disassembly. However, an earlier study suggests a nuclear core complex independent pathway (Hansen *et al.* 2001).

In general, it needs to be considered that many different serotypes of AAV exhibit diverse intracellular trafficking patterns. As an example, AAV2 and AAV5 can accumulate in the Golgi compartment (Bantel-Schaal *et al.* 2002; Pajusola *et al.* 2002) but whether particles are released into the cytoplasm to traffick towards the nucleus or rather out of the cell has not demonstrated yet. Moreover, cell type/tissue and capsid concentration affect the distribution of AAV particles post-entry, AAV ubiquitin-dependent degradation, as well as transduction efficiency (Duan *et al.* 2000; Duan *et al.* 2000; Douar *et al.* 2001; Yan *et al.* 2002).

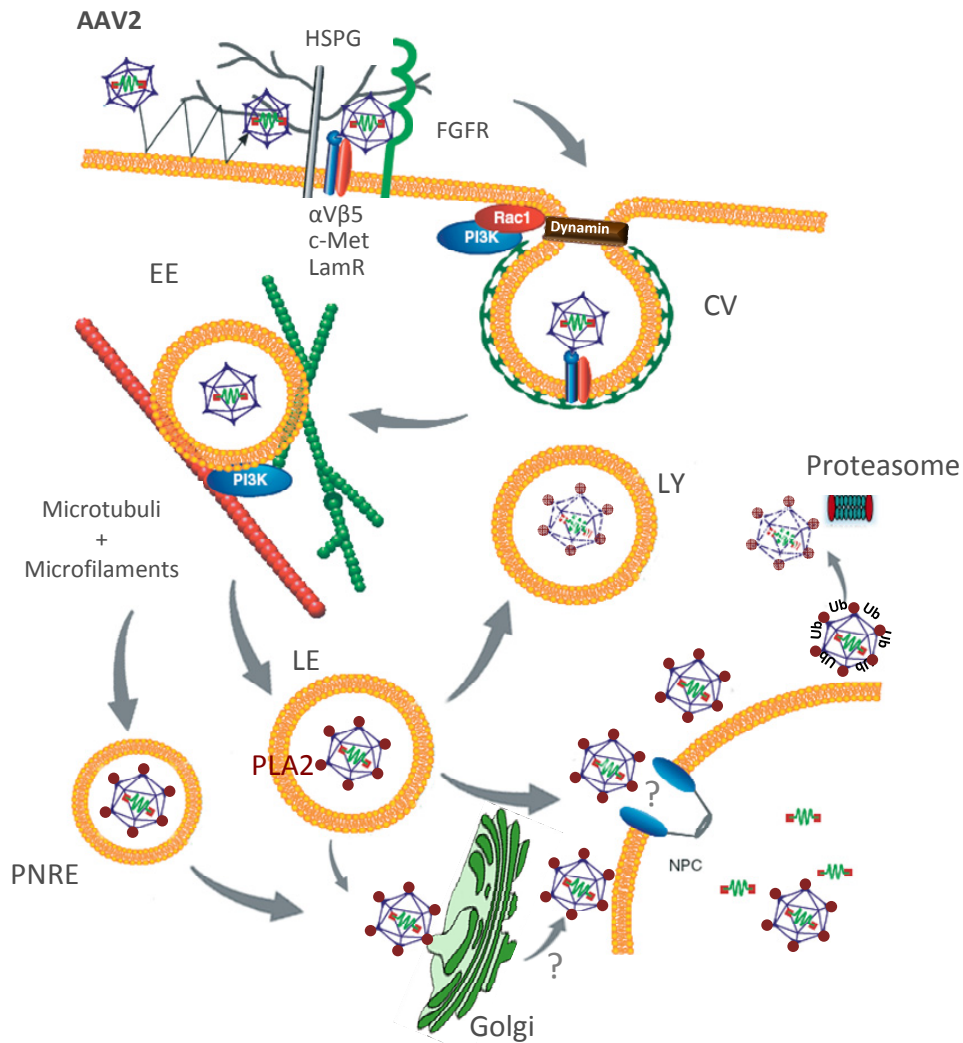


Figure 1-5 Model of the intracellular trafficking pathway of AAV2. After binding to its primary receptor (HSPG) and its co-receptors (FGFR1, c-Met, $\alpha\text{V}\beta 5$ -integrin, LamR), AAV2 is endocytosed in a dynamin dependent manner into clathrin-coated vesicles (CV). After activation of the Rac1 protein and phosphatidylinositol 3-kinase (PI3K) pathway, AAV2 is transported into early endosomes (EE). Post-entry trafficking most likely takes place along microtubuli and microfilaments due to the PI3K towards the late endosome (LE) or the perinuclear recycling endosome (PNRE). Particles undergo capsid conformational changes (PLA2 domain presentation due to VP1/2 N-termini externalization) which is partially due to a pH drop and plus a not yet identified trigger in the endosomes. PLA2 domain assists virions to escape the endosomes and to release particles into the cytoplasm. If the capsids circumvent ubiquitination and subsequent degradation in the proteasome or degradation in lysosomes (LY), released capsids accumulate in the Golgi compartment (? – whether AAV5 particle are released from the golgi to cell surface or for nuclear transport has not been demonstrated yet) or directly perinuclear. Translocation of complete capsids into the nucleus (in presence of the NLS motifs of the externalised BR domains) through a nuclear pore complex (NPC) has been indirectly demonstrated in several attempts (Grieger *et al.* 2006; Sonntag *et al.* 2006) but an NPC independent process has also been hypothesized, nuclear membrane disruption by the particle might also induce a nuclear entry. (Modified figure (Buning *et al.* 2003).

1.2 AAV as a Gene Therapy Vector

More than 40 years ago, AAV was discovered (Atchison *et al.* 1965; Hoggan *et al.* 1966), nearly 20 years later, basic elements of AAV such as genome structure, growth cycle and latency had been described permitting the isolation of infectious molecular clones of AAV2 and the determination of its DNA sequence (Samulski *et al.* 1983; Daya *et al.* 2008). Subsequently, the first AAV vector was described (Hermonat *et al.* 1984; Tratschin *et al.* 1984; Tratschin *et al.* 1985), which was the initiation step to AAV vectorology and contributing directly to the first human clinical trial of AAV vectors in cystic fibrosis patients (Flotte *et al.* 1996). The interest in AAV vector development gave rise to important vector improvements. Genetic studies had shown that only ITR sequences were required *in cis* and that Rep and Cap could both be provided *in trans* (Tratschin *et al.* 1986), trans-complementation transfection systems optimized AAV vector production processes. Helper-free recombinant virus stocks became an option (Samulski *et al.* 1989; Flotte *et al.* 1995). Recombinant AAV vectors could be produced which harboured transgene cassettes enclosed in ITRs but were devoid of *rep* and *cap* genes. Deletion of AAV rep and RBE sites showed that AAV vectors would not specifically integrate into the host genome, but mainly persist in host cells *in vivo* as duplex, circular episomes (Afione *et al.* 1996; Duan *et al.* 1998; Schnepf *et al.* 2005). AAV2 based vectors demonstrated a sustained transgene expression in a large variety of target tissues. No vector related toxicity or host immune response was detected in muscle, CNS or retinal tissue of the animal models used (Kotin 1994; Rabinowitz *et al.* 1998; Grimm *et al.* 2003). In fact, rAAV2 are less likely to cause a destructive cellular immune response against its transgene than adenoviral vectors (Zaiss *et al.* 2002). Long term expression of the AAV2 gene has been reported beyond one year in mice (Xiao *et al.* 1996), for more than three years in dogs (Arruda *et al.* 2005), and even five years in NHP (Rivera *et al.* 2005). AAV2 infection is believed to be non-pathogenic and has not been associated with any kind of disease, which adds up to the AAV2 safety profile for clinical trials (Berns *et al.* 1995). Therefore, AAV became a promising gene delivery vector for long term intervention of many inherited diseases. Studies in animal models have also suggested therapeutic benefits for tumor treatments using AAV vectors. Therapeutic genes within an AAV shell could be delivered for immune regulation, e.g. synthetic type I interferon (INF) inhibited tumor cell proliferation in nude mice (Zhang *et al.* 1996). Antiangiogenesis has

been employed by e.g. an AAV2/angiostatin vector injected into human gliomas of an animal model (Ma *et al.* 2002; Ma *et al.* 2002). Transfer of wt p53 cDNA into cancer cells suppressed tumor phenotype *in vitro* and *in vivo* (Qazilbash *et al.* 1997). More recently, rAAV2 derived vectors showed a high transduction of ovarian and hepatocarcinoma cells, also implicating its functionality for directed cancer gene therapy (Malecki *et al.* 2009). However, uproar was caused when insertional mutagenesis by rAAV vectors was associated with the development of hepatocellular carcinoma in a mouse model, a fraction of AAV vector genomes appeared to have integrated into the host cell chromosomes at sites of double strand break repairs (Donsante *et al.* 2007). In response, it was suggested that oncogenicity was rather due to the neonatal mouse model which is susceptible to tumor formation, but not due to the rAAV (Kay 2007). No other group demonstrated any cancer development in their mice models (Bell *et al.* 2005; Nakai *et al.* 2005; Kay 2007; Inagaki *et al.* 2008). Nonetheless, this study was important to stimulate further studies elucidating the mechanisms of tumor formation. It also increased the attention of safety aspects of rAAV vectors.

1.2.1 Immune Response to AAV

Host immune response is perhaps the most challenging field to AAV gene delivery. It has been estimated that independent of the ethnic group or the continent, 50% to 96% of all adults in the human population are seropositive for AAV2. Serum analysis revealed a high prevalence of neutralizing antibodies against the AAV2 capsid (up to 60%) which could significantly hamper AAV mediated gene transfer (Erles *et al.* 1999; Moskalenko *et al.* 2000; Vandenberghe *et al.* 2007; Calcedo *et al.* 2009). In fact, it was determined that pre-existing neutralizing antibodies (Nabs) in patients, due to a prior infection, accounted for the humoral response against AAV. In a cystic fibrosis (CF) study, 96% of all subjects were seropositive and 32% showed a neutralizing ability, strongly reducing the efficacy of the clinical trial (Chirmule *et al.* 1999). Nabs inhibit transduction to liver and lung (Halbert *et al.* 1998; Murphy *et al.* 2008b), but not to muscle, brain or retina (Fisher *et al.* 1997; Anand *et al.* 2002; Mastakov *et al.* 2002). Furthermore, patients who did not have any Nabs initially could elicit a neutralizing antibody response after a first vector administration. Additional vector application to the same patient could become difficult (Halbert *et al.* 2000). Inhibiting T-cell formation using anti CD4 antibodies prevents Nabs generation and allows

vector re-administration (Halbert *et al.* 1998; Manning *et al.* 1998; Chirmule *et al.* 2000). Cytotoxic-T-lymphocytes are also generated in response to an AAV2 infection, liver toxicity was observed in a clinical trial and was attributed to a CTL response to AAV2 transduced liver cells (Manno *et al.* 2006). It was discovered that the AAV2 heparin binding motif is mainly responsible for T-cell activation (Vandenberghe *et al.* 2006). The corollary was that other AAV serotypes, which did not inherit heparin binding, were investigated for their T cell activation. Whereas CD8(+) T cells specific to AAV2 capsids demonstrate cytolytic activity, no response was observed with the AAV7 and AAV8 vectors (Wang *et al.* 2007). Furthermore, they could determine that liver toxicity present in patients of a clinical trial was not due to targeted killing of vector-transduced hepatocytes by capsid-specific T cells (Li *et al.* 2007). Luckily other serotypes such as AAV8 show a much better liver transduction than AAV2 (Gao *et al.* 2002; Nakai *et al.* 2005; Gao *et al.* 2006; Jiang *et al.* 2006). AAV8 not only transduces murine hepatocytes more efficiently than AAV2, but they do not bind to heparin and escape anti-AAV2 neutralizing antibodies (Scallan *et al.* 2006). Nonetheless, tissue types exist which are resistant to any other AAV serotype. Screening for new natural variants would be a time consuming method, so another possible solution might be the identification and mutation of capsid epitopes that are recognized by Nabs. Educated guesses and 'evolutionary' strategies have been used to tackle this situation. *In silico* modelling identified possible antibody binding sites, analysed by the AAV2-neutralizing murine monoclonal antibody A20 and human polyclonal serum (Lochrie *et al.* 2006). One mutant was identified which completely escaped antibody neutralization. An error prone PCR was also used to produce a mutant library, which was used to infect permissive cells in the presence of antibodies. Two types of mutants were not neutralized in the experiment (Perabo *et al.* 2003).

Taken together, a great deal of progress has been made in understanding the AAV derived immune response. A deeper understanding on the AAV-host interaction is still needed and required for the efficient use of AAV vectors in clinical trials.

1.2.2 AAV Vectorology

The limiting packaging capacity, inefficient AAV trafficking, second-strand synthesis (Ferrari *et al.* 1996; Hauck *et al.* 2004), and high prevalence of pre-existing immunity in human populations (Gao *et al.* 2004; Vandenberghe *et al.* 2007; Calcedo *et al.* 2009) have

influenced the successful clinical development of AAV2 based vectors for gene therapy application. Consequently, an enormous variety of vector modifications have been applied to further enhance AAV vector utility in gene therapy.

1.2.2.1 Improvements in Packaging Capacity and Transgene Expression

Novel AAV vector technologies have been assayed to either increase genome packaging capacity for AAV or enhance gene expression. AAV2 vectors can normally package genes between 4.1 and 4.9 kb (Dong *et al.* 1996). This limiting packaging capacity hindered AAV2 vector treatment of some diseases, which depended on transgenes too large in size. The *trans*-splicing approach has the possibility of increasing the AAV vector capacity (Duan *et al.* 2000; Flotte 2000; Sun *et al.* 2000; Yan *et al.* 2000). *Trans*-splicing takes advantage of the AAV's ability to form head-to-tail concatamers via recombination in the ITRs (Fig.1-6 A).

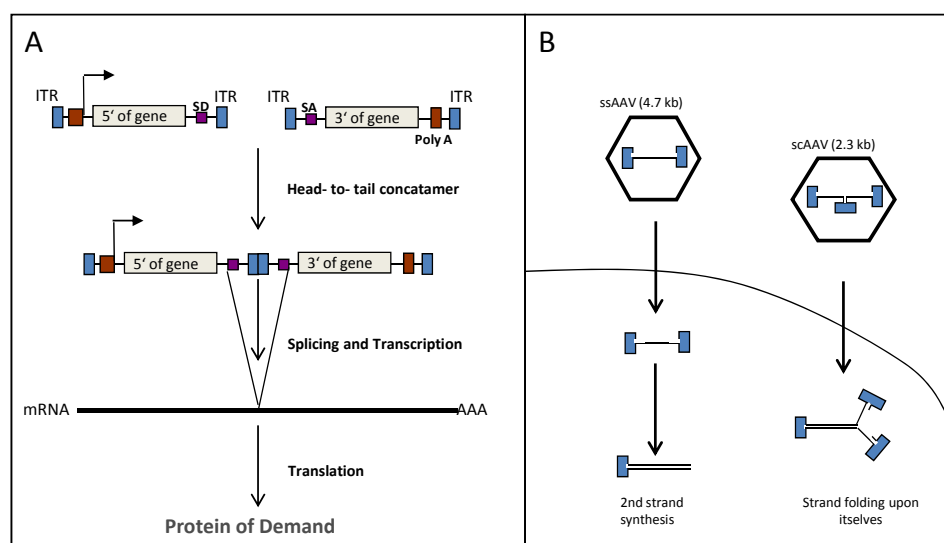


Figure 1-6 Rational of improved vector design. A) In a *trans*-splicing model, the head-to-tail concatamer formation of two different vectors results in a functional protein after transcription, splicing and translation. B) Compared to a ssAAV vector, the scAAV vector bypasses second strand synthesis folding upon itself.

The oversized transgene cassette is split into two independent vectors containing adequately placed splice donor and acceptor sites. After cell transfection, the recombined AAV molecules are transcribed, spliced and translated into the functional gene product. This application is used to package therapeutic transgenes up to 9 kb in size and has been successfully applied for gene expression of oversized transgenes in the retina (Reich *et al.*

2003), the lung (Liu *et al.* 2005) and muscle tissue (Ghosh *et al.* 2006). Even though the dual-vector system has been improved and can be used to achieve therapeutic levels of dystrophin in Duchenne muscular dystrophy gene therapy (Lai *et al.* 2008), the *trans*-splicing of vectors is still less efficient than gene expression from single rAAV vectors.

To bypass the limiting aspects of delayed onset in transgene expression, a self-complementary AAV (scAAV) was designed by D-sequence deletion or mutagenesis in the trs sequence in a stem palindrome (McCarty *et al.* 2003; Wang *et al.* 2003). Recently, it was demonstrated that scAAV vectors are less functional as substrates than single-stranded AAV vectors for site-specific integration (Daya *et al.* 2009). ScAAV vectors significantly shorten the lag time before transgene expression, increasing the biological efficiency of AAV vectors (McCarty *et al.* 2003; Ren *et al.* 2005). The vectors can fold upon themselves, leading to the direct formation of a transcription competent double-stranded DNA (Fig. 1-6 B). One drawback to the use of scAAV vectors is a decreased packaging capacity by approximately 50 %. The usage of scAAV vectors was mainly restricted to small transgenes, such as ribozymes (Zhong *et al.* 2004) and siRNA (Xu *et al.* 2005), until scAAV vectors were optimized and designed to encapsidate up to 3.3 kb of DNA (Wu *et al.* 2007; Wu *et al.* 2008).

1.2.2.2 Natural Diversity as a Source for Transcapsidation

AAV2 efficiently transduces many cell types *in vitro*, but *in vivo* transduction efficiency is limited in a number of clinical relevant tissues and cell types. Less than 5 % of hepatocytes are stably transduced by AAV2 (Nakai *et al.* 2002), with other tissues such as apical surfaces of airway epithelia being completely refractory to AAV2 transduction (Zabner *et al.* 2000). Transcapsided with capsid proteins from alternative serotypes, the very same AAV2 recombinant genome could overcome rate limiting barriers in entry and post-entry. An ideal model system was developed to evaluate the impact of a serotype specific capsid on AAV transduction without changing its transgenic content (Rabinowitz *et al.* 2002; Rabinowitz *et al.* 2004; Wu *et al.* 2006a). Improved gene transfer to different target tissues by pseudotyping has potential (Fig. 1-7 I). For instance, the AAV1 capsid led to a 10-100 fold higher gene transfer in muscles, as well as gene transfer to arthritic joints and neurons (Xiao *et al.* 1999; Passini *et al.* 2003; Ghosh *et al.* 2006; Sandalon *et al.* 2007), whereas vectors with an AAV3 based capsid transduction has been identified in cochlear inner hair cells (Liu

et al. 2005). In contrast to AAV2, AAV2/1 and AAV2/5 vectors mediate a rapid onset of gene expression in photoreceptors and retinal pigment epithelium (RPE) cells after subretinal vector delivery to murine eyes (Auricchio *et al.* 2001; Yang *et al.* 2002; Auricchio 2003). Novel pseudotypes AAV2/8 and AAV2/9 vectors transduce photoreceptor and RPE, as does AAV2/5, but a better transduction to cone cells. AAV2/8 driven gene transduction onset even was significantly faster than for AAV2/5 (Allocca *et al.* 2007; Natkunarajah *et al.* 2008). Instead, AAV2/4 vectors showed a unique and exclusive-long transduction of RPE cells in a murine, rat and dog models (Weber *et al.* 2003). The AAV5 capsid significantly increased gene transfer to lung and central nervous system (CNS) (Davidson *et al.* 2000; Zabner *et al.* 2000; Auricchio *et al.* 2001; Chao *et al.* 2001) and AAV6 based gene transfer could be directed to organs such as heart, muscle and airway epithelium (Halbert *et al.* 2001; Blankinship *et al.* 2004; Kawamoto *et al.* 2005). As mentioned in chapter 1.1.2, Gao and his colleagues developed a PCR based method to search for other AAV serotypes. After the characterization by sequence analysis of more than 100 non-redundant novel AAVs, potent AAV vectors with broader tissue tropism and higher gene transfer efficiency were detected (Gao *et al.* 2002; Gao *et al.* 2003; Grimm *et al.* 2003; Gao *et al.* 2004). The derived serotype AAV8 transduced liver and muscle tissue with efficiencies of several logs higher than AAV2. AAV7 achieved muscle transduction similar to AAV1 and AAV9, out-performing most AAVs in varied tissues, especially in cardiac muscle (Gao *et al.* 2003; Grimm *et al.* 2003; Gao *et al.* 2004; Conlon *et al.* 2005; Louboutin *et al.* 2005; Wang *et al.* 2005).

Table 1-1 Capsid homology among AAV serotype 1 to 9

AAV Serotype	% Homology to AAV:								
	AAV 1	AAV 2	AAV 3	AAV 4	AAV 5	AAV 6	AAV 7	AAV 8	AAV 9
AAV 1	100								
AAV 2	83	100							
AAV 3	87	88	100						
AAV 4	63	60	63	100					
AAV 5	58	57	58	53	100				
AAV 6	99	83	87	63	58	100			
AAV 7	85	82	85	63	58	85	100		
AAV 8	84	83	86	63	58	84	88	100	
AAV 9	82	82	84	62	57	82	82	85	100

(Daya *et al.* 2008)

To date, most of the studies have involved vectors based on serotype 1 to 9, because homology studies of the AAV capsids revealed large differences between all the serotypes, excepting AAV1 and AAV6 (Table 1-1). Different tissue types are being successfully transduced, but some tissue types remain non-transducible or are transduced, though not targeted. This not only enforces the development of new and more potent vectors, but also encourages further investigation into the AAV capsid surface to determine new routes of capsid optimization.

1.2.2.3 Mosaic and Chimeric Vectors

A better understanding of the AAV capsid properties has become important for the design of AAV vectors displaying specific tissue targets. Cell surface primary receptors have been identified for only some of the many AAV serotypes, specifically AAV2 and AAV3 (heparan sulphate proteoglycan), AAV4 (O-linked sialic acid), AAV5 (N-linked sialic acid), and AAV6 (sialic acid and heparin sulphate proteoglycan) (Summerford *et al.* 1998; Handa *et al.* 2000; Kaludov *et al.* 2001; Blackburn *et al.* 2006; Seiler *et al.* 2006). Co-receptors, contributing to viral entry, have been described especially for AAV2 (see Chapter 1.1.8) and a yeast two-hybrid screen has revealed that the 37 kDa/67 kDa laminin receptor (LamR) is also a co-receptor for AAV serotypes 2, 3, 8 and 9 (Akache *et al.* 2006). Receptor binding properties of different AAVs helped to further dissect the foundation of AAV based cell transduction. Through capsid modifications, AAV tropism could be expanded to a cell type of interest or AAV transduction was further enhanced.

One interesting asset was the approach to produce mosaic virions. They were constructed by a mixture of capsid subunits from different serotypes (Wu *et al.* 2006a) (Fig. 1-7 II). Correspondingly, AAV1/AAV2 mosaic vectors could transduce two cell types: liver and muscle cells (Hauck *et al.* 2003). Resulting mosaic particles were able to bind heparin in an affinity column purification and target muscle and liver tissue *in vivo*. A combination of different modifications resulted in a mosaic AAV1 vector particle with inserted biotin acceptor peptides that could be purified by avidin affinity chromatography and demonstrated increased vascular gene transfer after an RGD4c peptide (targets $\alpha V\beta 5$ and $\alpha V\beta 3$ integrin) insertion (Stachler *et al.* 2006). Similar to the classical approach of pseudotyping, mosaic vectors could not be specifically targeted to a single cell type.

Additionally, immunogenicity could be possibly increased by VP proteins of different serotypes. Lastly, the reproducibility of mosaic capsid protein stoichiometry was a difficult venture (Hauck *et al.* 2003).

The generation of an optimized vector has to be reproducible to make a gene therapy approach feasible. Therefore, chimeric capsids were developed (Fig. 1-7 III) and complete amino acid stretches of VP proteins were exchanged between different serotypes. For example, for a chimeric vector, a domain of amino acids 350-430 of AAV2 was exchanged with the corresponding amino acid stretch of AAV1. Subsequently, vector purification was performed by heparin affinity chromatography.

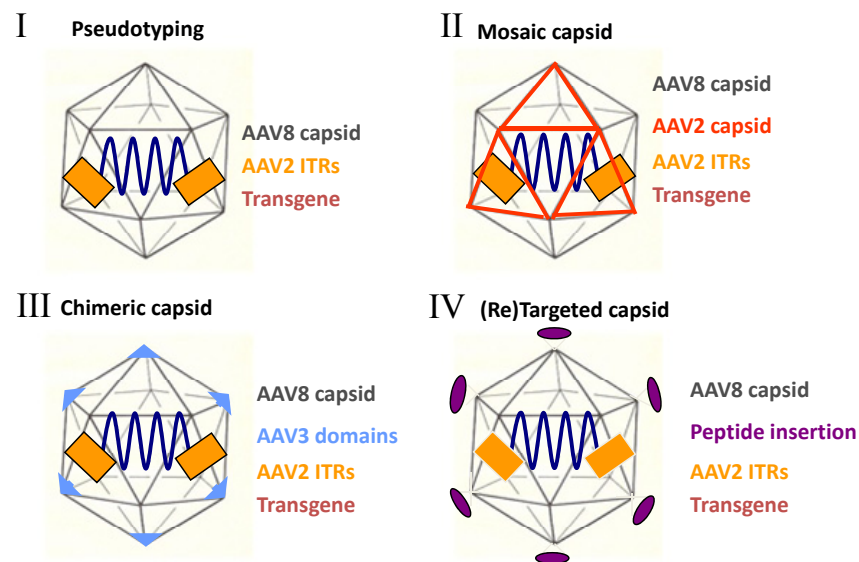


Figure 1-7 AAV vector optimization. I Pseudotyping, vector transgene packaged by AAV2 Rep proteins and flanked by AAV2 ITRs into a capsid shell of AAV8. II Mosaic capsid, a mixture of VP protein subunits from two different parental serotypes. III Chimeric capsid, certain amino acid domains are exchanged between different AAV serotypes. IV Retargeted capsid, at defined positions on the capsid surface ligands or peptide motifs are inserted.

Muscle transduction was increased, whereas reduced recognition by anti-AAV2 neutralizing serum could be determined (Hauck *et al.* 2006). Large domain swaps between AAV2 and AAV8 revealed that a more efficient liver tropism of AAV8 was caused by a small region on loop IV of its secondary structure (Shen *et al.* 2007). Domain exchanges can help to elucidate the infectious biology of AAV serotypes, even though a broad tissue tropism can be a drawback to safety, as a non-target tissue may be transduced following vector application.

1.2.2.4 Ligand Conjugation and Peptide Insertion

Indirect targeting is mediated by the conjugation of receptor ligands to the capsid surface. A receptor ligand can either be a bi-specific antibody or protein, complexed to the capsid surface and interacting with a specific cell surface receptor. Therefore, the AAV2 vector can be redirected to a cell type of interest. Non-permissive cells, $\alpha\text{IIb}\beta\text{3}$ integrin expressing megakaryocytes were successfully targeted by a bispecific F(ab' γ)₂ antibody (Bartlett *et al.* 1999). In another report conjugation of a bispecific targeting protein to the vector was achieved by biotinylating purified rAAV2 without abolishing the capsid structure, internalization, and subsequent transgene expression. Targeting via epidermal growth factor receptor (EGFR) or fibroblast growth factor 1alpha receptor (FGFR1alpha), resulted in a significant increase in transduction efficiency of EGFR-positive SKOV3.ip1 cells and FGFR1alpha-positive M07e cells, respectively (Ponnazhagan *et al.* 2002; Arnold *et al.* 2006). The advantage of this approach is that ligand conjugation is performed without direct changes to the capsid surface. One disadvantage of using ligands for targeting may involve the stability of the capsid-adaptor complex *in vivo*. Additionally, a complex vector-ligand conjugate could hamper viral uptake or induce ligand derived immunogenicity (Buning *et al.* 2003).

In contrast to indirect targeting, direct targeting requires an extensive knowledge of the capsid structure. Peptides or ligands are directly inserted into the capsid and must be exposed at the capsid outer surface (Girod *et al.* 1999). Natural tropism has to be ablated to maximize newly directed targeting without significantly affecting capsid structure or assembly (Fig. 1-7 IV). Choice of peptide insertion sites and type of targeting peptides are the two most critical parameters to be considered. At first, peptide sequences were primarily inserted into the N-terminus of VP1/VP2 capsid genes, fusing a single-chain antibody to the N-terminus of VP2, to direct AAV vectors towards CD34⁺ cells (Yang *et al.* 1998), but resulting titres were too low to achieve noteworthy results. Later, many successful attempts demonstrated that peptides can be fused to the N-terminus of VP1 or VP2 to generate additional tropism (Wu *et al.* 2000; Shi *et al.* 2001; Loiler *et al.* 2003). Fusion of GFP to the VP2 N-terminus helped to visualize the infectious pathway of AAV (Warrington *et al.* 2004; Lux *et al.* 2005), but N-terminal fusion neither allows an early presentation of a peptide, as the VP1/VP2 N-terminus is located inside native capsids (Bleker *et al.* 2005; Kronenberg *et al.* 2005), nor does it hinder HSPG binding. Girod *et al.*

successfully demonstrated that HSPG binding can be ablated and the AAV2 capsid can even be retargeted (Girod *et al.* 1999). The RGD motif was inserted into several putative insertion sites with aa position 587 appearing to be the most promising insertion site. R585 and R588 were identified to be responsible for heparin binding and a peptide insertion at either aa 587 or 588 inhibited AAV2 from HSPG binding (Kern *et al.* 2003; Opie *et al.* 2003), allowing gene transfer into resistant tumor cell lines such as K562, Raji or SKOV-3 via binding to RGD driven integrin receptors (Shi *et al.* 2003). Other sites have been exploited as peptide insertion sites within the AAV *cap* gene. Amino acid position 34 and position 520 in combination with 584 could be used to generate AAV targeting vectors (Girod *et al.* 1999; Wu *et al.* 2000; Shi *et al.* 2006), but insertions are most frequently performed at aa 587 and 588. Recently, it has been demonstrated that an insertion at position 453 also becomes an option, but only if the arginines at position 585 and 588 are substituted to alanines. Thus, the position 453 mutants emerges as prominent insertion site, superior to those with a ligand in position 587 (Boucas *et al.* 2009).

Insertion peptides were primarily selected from targeting motifs identified by phage display libraries. A CD13 specific peptide sequence was inserted at aa position 587 resulting in the targeting of kaposi and rhabdomyosarcoma cell lines (Grifman *et al.* 2001). Other inserted motifs, such as MTP, VNT or QPE, showed re-targeting to distinct vascular beds (White *et al.* 2004; Work *et al.* 2006). However, not all selected motifs were successful in retargeting AAV2 vectors. Phage display has a physiological and structural context difference, and selected peptides could display a non-functional conformation in AAV trafficking. Alternatively, phage display selected peptide motifs are only chosen according to cell binding, but stability of viral particles and the impact on the infection cannot be estimated. New technologies, such as peptide display libraries and multispecies interbreeding, are tools modified for AAV based vector production.

1.2.2.5 DNA Family Shuffling and Peptide Display Libraries

DNA family shuffling and peptide display library technology have proven to be of enormous potential to select peptide motifs or capsid surface subunits according to conformation, cell binding, vector producibility, internalization and post-entry processing.

DNA family shuffling was developed to evolve and improve many types of proteins, but its potential for viral gene therapy was discovered and successfully used to create retro- and lentiviral vectors of improved stability and efficacy (Powell *et al.* 2000; Soong *et al.* 2000; Pekrun *et al.* 2002). Recently, DNA family shuffling has been applied for a highly efficient interbreeding of several multispecies AAVs to produce chimeric capsids, which are able to transduce cells that are resistant to any wt AAV infection (Fig. 1-8 A). AAV-DJ, a recombinant vector derived from a DNA shuffling library, was selected and mediated superior *in vitro* transduction. *In vivo*, it yielded robust gene expression in the mouse liver (Grimm *et al.* 2008). A myocardium tropic AAV vector was isolated from an *in vivo* selection after DNA family shuffling (Yang *et al.* 2009). High transduction of the myocardium and de-targeting from other organs was primarily observed in this approach. However, in both cases it is claimed that DNA family shuffling should be combined with a peptide insertion library. In fact, Grimm *et al.* showed that the vector AAV DJ could be used as the backbone for a random peptide library. An *in vivo* biopanning on mouse lung tissue was performed and two vectors with distinct peptide insertion were re-targeted to distinct alveolar cells (Grimm *et al.* 2008).

A peptide display library is an elegant technique to combine capsid engineering with a high-throughput screen to obtain a mutant with the desired phenotype. It allows the selection of retargeted AAV vectors from a library of approximately 10^7 vector mutants. The generation of a random AAV2 display library has been successful using two different methods. In both approaches, randomized oligonucleotide sequences encoding seven aa peptides were inserted either into the aa position N587 (Perabo *et al.* 2003) or position R588 (Muller *et al.* 2003) of the AAV2 *cap* gene (Fig. 1-8 B). Whereas Perabo *et al.* produced a library by direct transfection of the library plasmids into AAV producer cells (Perabo *et al.* 2003), Müller *et al.* generated a transfer shuttle library of chimeric capsids composed of wild type and library-derived subunits first (Fig. 1-8 C). In a last step, the AAV2 random display library was produced by infecting 293T cell at a MOI 1 (Muller *et al.* 2003). MOI 1 is necessary to ensure that produced library clones consist of capsids containing the corresponding *cap* gene. For the second approach, a major limitation was AAV2 wt contamination, but optimized plasmids were developed that inhibited non-homologous recombination and ensured wt free library production (Waterkamp *et al.* 2006). In both cases, targeted vectors from display libraries have been isolated from a number of different

cell types. Several rounds of selection improved the selection of a permissive clone for a wt AAV2 non-transducible cell line. In Mec1 cells, a targeted vector with an inserted peptide was isolated which transduced B-cell chronic lymphocytic leukemia (B-CLL) cells up to 54%. Mec1 cells are normally refractory to AAV2 infection (Perabo *et al.* 2003). Vectors selected with a viral display peptide library on an AML (Acute myeloid leukemia) cell line, Kasum 1, confirmed a selective killing, as the targeted vector harboured a suicide gene (Michelfelder *et al.* 2007). Targeted vectors were also be isolated from AAV2 display libraries applied on Calu6, (a mouse carcinoma cell line), PC3, (a human prostate cell line), H9C2 (rat cardiomyoblasts), as well as rat primary cardiomyocytes and human venous endothelial cells (Waterkamp *et al.* 2006; Ying *et al.* 2010). Targeted vectors were also be isolated from AAV2 display libraries applied on Calu6, (a mouse carcinoma cell line), PC3, (a human prostate cell line), H9C2 (rat cardiomyoblasts), as well as rat primary cardiomyocytes and human venous endothelial cells (Waterkamp, Müller *et al.* 2006, Ying *et al.*, under revision). Isolated vectors containing the peptide sequence NSSRDLG remarkably increased transduction to heart cells when compared to AAV2 with an unmodified capsid.

Selected vectors by *in vivo* biopanning of random virus display peptide libraries on mouse heart tissue demonstrated a strong heart targeting and detargeting from other tissues (Ying *et al.* 2010). Michelfelder *et al.* also observed that *in vivo* selected clones could target tumor tissue, but the additional transduction of heart tissue could not be prevented (Michelfelder *et al.* 2009). It was suggested that the modification of the heparin binding motif by target-binding peptide insertion was necessary, but not sufficient, to achieve tissue specific transgene expression.

Concluding, DNA shuffling and peptide insertion libraries are novel strategies which are fundamental to molecular evolution of synthetic AAV vectors. Combination of DNA shuffling with peptide insertion libraries could help to engineer designer AAVs that are tailored for the therapeutic transduction of clinically relevant organs. Above all, library approaches should be based upon more promising serotypes, such as AAV8, to yield a specific and efficient transgene expression in one target organ.

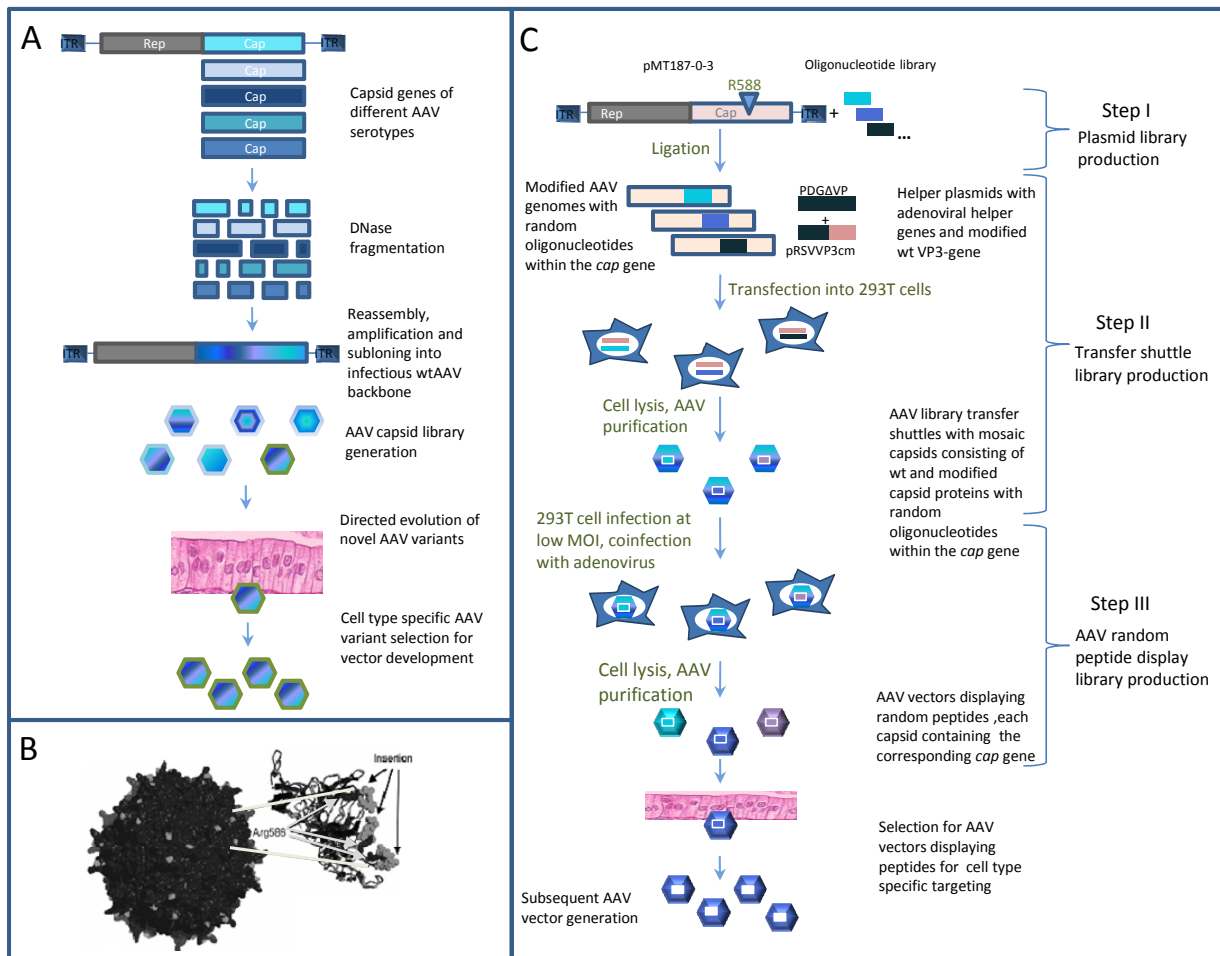


Figure 1-8 Generation of AAV Libraries. A) Combinatorial AAV library generation which is subjected to directed evolution to isolate cell type specific mutants. *Cap* genes are randomly fragmented and reassembled by PCR. Generated full length chimeric plasmids are cloned into wt AAV2 backbone to generate a shuffled plasmid library. The AAV chimeric particle library is generated using a standard transfection protocol. The non-transducible cell line is infected with the library to isolate a permissive clone. The selected vector is then subjected to vector development and *in vivo* targeting B) Capsid topology of an AAV2 modified capsid (grey) with the peptide insertion sites (grey lines). Magnification shows a cross-section through the spikes with the insertion site at R588 (light grey arrows) and the inserted seven aa (black arrows). C) The three-step-system to produce a wt-free random AAV2 display peptide library. In step I, the AAV2 plasmid library is produced by the library plasmid pMT-0-3 into which a random oligonucleotide library was inserted at position R588. A transfer shuttle library was generated by transfection of library vector plasmid, the adenoviral helper plasmid pDGΔVP and the wtVP3 modified plasmid pRSVVP3cm in step II. In the final step these chimeric vectors infected 293T cells at MOI 1 to achieve uptake of only one vector per cell and to ensure the production of capsids containing the corresponding *cap* gene.

1.3 AAV8, a New Primate AAV as a Gene Therapy Vector

In an attempt to identify potent AAV vector candidates, Gao *et al.* developed a PCR based method to rescue proviral sequences of endogenous AAVs from primate tissue (Gao *et al.* 2002; Gao *et al.* 2003; Gao *et al.* 2004). Characterization by sequence analysis, followed by a

thorough functional screen of novel AAVs, revealed several candidates with potential in gene therapy applications (Gao *et al.* 2002). It was found that AAV8 based vectors transduced liver several logs higher than AAV2. Transcapsided AAV vectors consisting of AAV8 capsid harbouring recombinant AAV2 genomes can, therefore, possibly be produced in a large scale format by transfection. Standard sedimentation methods, such as CsCl gradient or Iodixanol-step gradient, yield approximately 5×10^{13} total viral genomes (Gao *et al.* 2002; Rabinowitz *et al.* 2002; Davidoff *et al.* 2005). An Ion exchange chromatography method has been developed to generate clinical grade vectors derived from AAV8 (Davidoff *et al.* 2004) and this technique has been used to achieve a recovery rate of 41 % with purity greater than 90 %.

1.3.1. Capsid Structure and other Characteristics of AAV8

The reported crystal structure of the AAV8 viral capsid was identified at 2.6 Å. It revealed that the VPs are structurally similar to the VPs of the previously published AAV2 crystal structure (Xie *et al.* 2002; Nam *et al.* 2007). Coordinates for the AAV8 VP3 structure were deposited at the Protein Data Bank (Accession number 2QA0) and allowed the calculation of a complete capsid surface topology (Fig. 1-9 A). Significant differences between AAV8 and AAV2 lie within the loops between the β -strands. The most prominent differences occur in variable regions I and IV (Fig. 1-9 B), which play a crucial role to AAV2 transduction and antibody recognition (Wobus *et al.* 2000; Wu *et al.* 2000; Kern *et al.* 2003; Opie *et al.* 2003; Lochrie *et al.* 2006). A reduced amount of basic residues have been observed for AAV8 in this region reflecting the non-heparin-binding phenotype of AAV8 (Nam *et al.* 2007). The primary receptor of AAV8 has not yet been identified, even though yeast two-hybrid screens recovered several plasma membrane proteins which are possible receptor candidates (Akache *et al.* 2007). The 37/67-kilodalton laminin receptor was the first identified co-receptor of AAV8 (Fig. 1-9 C), its binding site was mapped down to two protein subdomains (aa 491-547 and 593-623) on the AAV capsid exterior (Akache *et al.* 2006).

LamR is present on many cell surfaces and is even overexpressed in numerous cancers, explaining the AAV8's broad tissue tropism. Another yeast two-hybrid screen was performed to screen a mouse liver complementary DNA library for cellular proteins capable of interacting with the viral capsid proteins.

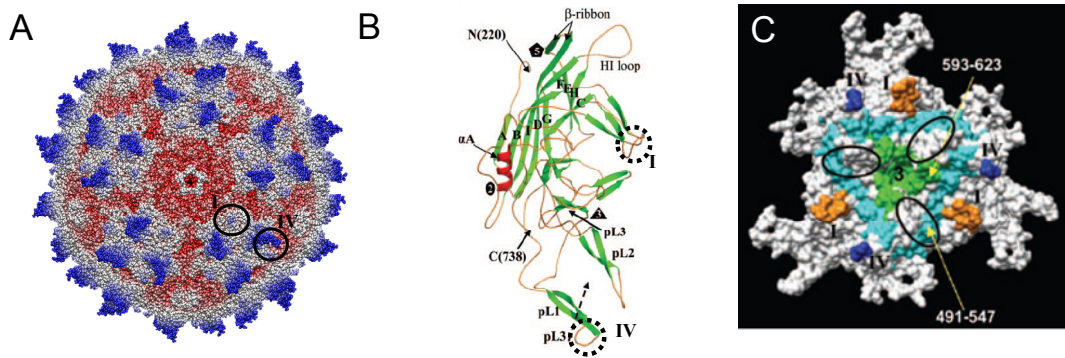


Figure 1-9 Structural analysis of AAV8. A) AAV8 capsid topology based on the AAV8 VP3 coordinates from the Protein Data Bank. The colour shift indicates the mode of protrusion from the outer surface dimple (red) to the spikes (blue). Variable regions I and IV, regions which differ strongly between AAV2 and AAV8 are encircled in black. B) Ribbon diagram of AAV8 VP3 showing the core eight-stranded β -barrel strands (green), stretches of small antiparallel β - strands (green), loops (orange), N- and C-terminal residue (220, 738), a conserved α -helix (red), the HI-loop and the loop region (L1-L3) which make up the protrusions surrounding the 3-fold axis. Black polygons indicate 2-, 3- and 5-fold axes. Variable regions I and IV are encircled in dashed lines (modified from Nam *et al.* 2007). C) AAV8 laminin receptor binding site. The 3-fold region is depicted to show aa residues involved in LamR binding by AAV8 (cyan 491-547, green 593-623). Variable loops are indicated in blue and orange. Theoretical heparin sulphate binding region is indicated with an oval (Nam *et al.* 2007).

Multiple hits for over 100 genes were revealed, including two encoding the endosomal cysteine proteases cathepsins B and L. *In vitro* experiments revealed that these endosomal cleavage factors bind and cleave AAV8 and AAV2 in a serotype-specific pattern to prime AAV capsids for subsequent nuclear uncoating (Akache *et al.* 2006). The AAV8 capsid protein is cleaved at a single site in the VP3 protein, whereas two cleavage sites of the VP3 are present in AAV2. AAV8 capsids appear to be cleaved more efficiently and quickly than AAV2 capsids, a finding which is consistent with another study demonstrating a faster uncoating rate of AAV8. Thomas *et al.* showed that AAV8 vectors could uncoat faster in hepatocytes and that their genomes become quicker biologically active compared to AAV2 (Thomas *et al.* 2004). Therefore, the rate of uncoating vector genomes must be a limiting step to AAV2 transduction. It was the first attempt to explain molecular mechanisms of a hepatotropic AAV serotype. Nonetheless, other post-entry effects cannot be ruled out. Structural changes during the entry process of AAV8 may also contribute to a different endosomal processing and a faster uncoating (Murphy *et al.* 2008a; Murphy *et al.* 2008b). It is crucial to improve the analysis of all facets of trafficking *in vivo*, as an *in vitro* transduction cannot accurately reflect the *in vivo* pathway. *In vitro* evaluation has proven to be difficult. In fact, *in vitro* transduction efficiency of AAV8 is lower than of AAV2 in all kind of cell lines which cannot be correlated with the AAV8 superior *in vivo* performance. AAV8 has already

been shown to have an enormous potential in different animal models. Moreover, the faster processing and uncoating of AAV8 could be the key to reduced immunological response and influence the longevity of gene expression in clinical investigations (Lowenstein 2004).

1.3.2 Evaluation of AAV8 in Animal Models for Gene Therapy

Since the first isolation of novel primate AAVs, many laboratories started evaluating these vectors, particularly AAV8, in their model systems. Encouraging data was generated with rodent and canine models, with the phenotypic correction of liver diseases after liver directed gene therapy was achieved, and the efficient whole-body muscle gene delivery observed Duchenne muscular dystrophy (DMD). The study of primate derived AAV vectors in NHP models is more challenging due to pre-existing immunity against AAV capsids and an adaptive immunity to the transgene product.

The first reported application of AAV8 vector to deliver factor VIII (FVIII) gene to the liver of Hemophilia A mice was reported 2004 (Sarkar *et al.* 2004). The vector genomes were transcapsidated into AAV2, AAV5, AAV7 and AAV8 capsids and administered either intravenously or intraportally. No matter the route of administration, AAV8 performed best and achieved a long term 100 % phenotypic correction of FVIII deficient mice. A phenotypic correction of a monogenetic defect involving a metabolic pathway was identified as a potential treatment for use with the novel AAVs. Lebherz *et al.* compared the therapeutic effects of several AAVs in a mouse model of familial hypercholesterolemia (FH) and revealed that AAV8 nearly normalized serum lipids and diminished the development of atherosclerosis. AAV2 only achieved a modest improvement in atherosclerosis (Lebherz *et al.* 2004). Additionally, a Hemophilia B study described that human FIX could be delivered by AAV8 to achieve therapeutic levels of gene expression. Assays identified AAV8 producing 10 times more factor IX (FIX) protein to liver by rapid uncoating (Thomas *et al.* 2004). Data from another FIX study showed that gene expression levels of canine FIX protein to Hemophilia B mice from AAV7, AAV8 and AAV9 were 10-50 fold higher than of AAV2 (Wang *et al.* 2005). For systematic muscle gene transfer, transcapsidated AAV8 vectors expressing EGFP were the most efficient vectors to transduce both skeletal and cardiac muscle (Wang *et al.* 2005). Even though AAV9 showed to be a better candidate for cardiac gene transfer (Bish *et al.* 2008), AAV8 gene transfer

demonstrated a long persistence of AAV vector genomes in whole-body muscle tissues (Louboutin *et al.* 2005; Wang *et al.* 2005) and was successfully used to treat δ -sarcoglycan deficient hamsters. Profound cardiac and functional muscle recovery was also demonstrated in treated animals (Zhu *et al.* 2005).

In a canine hemophilia model, Wang *et al.* could also test the performance of AAVs (Wang *et al.* 2005). In fact, even at low doses, 5-30 % of normal canine factor IX (cFIX) expression was achieved. Serum cFIX concentrations revealed that animals treated with AAV7 or AAV8 vectors rendered a 5-10 fold higher cFIX expression than other AAV vectors. Studies on NHP animals face a major obstacle to AAV vector application; high sero-positive frequencies of newly isolated primate AAVs throughout different species causes a blockage or reduced efficiency of gene transfer. Pre-screening and pre-evaluation of AAV vectors is expensive and time consuming. To minimize immunogenic responses against transgenes, Rhesus Epo derived from NHP animals was selected to evaluate viral vectors first (Zoltick *et al.* 2000), but studies revealed that 50 % of Rhesus and Cynomolgus Macaques developed a polycythemia and a considerable autoimmune response (Gao *et al.* 2003; Chenuaud *et al.* 2004). In 2006, a scAAV8 and AAV7 vector containing a Macaque-derived choriogonadotropic hormone based transgene was developed, which finally achieved a 20 % gene transfer improvement with AAV8 to the liver of NHP animals after portal vein application without an autoimmune response (Gao *et al.* 2006; Nathwani *et al.* 2006).

Consequently, novel AAVs like AAV8 show a lot of potential, but in respect of safety, the transduction efficiency of AAV vectors have to be carefully estimated in several animal models. The NHP animal model is the translational step to human clinical trials for gene therapy, and AAV variants must be evaluated, not only for specificity and efficiency, but also to determine a useful dosage and the most optimal administration route.

1.4 AAV Clinical Trials

In November 1995, the first AAV vector was administered to a human subject (Flotte *et al.* 2003). AAV has become increasingly common in *human* clinical trials. Long term gene expression in animal models and a relative lack of immune response and other toxicities ensures a strong appreciation for AAV in human clinical trials. Additionally, isolation of new serotypes with different tissue targets allows matching of a tissue specific serotype with

the presumptive target tissue to further advance an effective gene therapy approach. Approximately 5 gene transfer protocols have been submitted per year to the NIH Recombinant DNA Advisory Committee (RAC) and the Food and Drug Administration (FDA), in years where about 65 protocols are reviewed in total. So far, 38 protocols have been approved and more than 400 research participants have been dosed. Earlier clinical trials have been conducted with AAV2 vectors for obvious reasons, but vectors from other serotypes are more prevalent in newer submitted protocols (Carter 2005). AAV trials have been less focused on cancer, but more on monogenic disorders, such as cystic fibrosis, hemophilia B and Canavan's disease. Administration routes for AAV vectors are mostly respiratory or intracerebral. The majority of AAV protocols are in Phase I (31 Protocols), whereas five protocols are in Phase II and two protocols are in Phase III (Office of Biotechnology Activities Protocol, 2007) (Daya *et al.* 2008).

One of the latest studies is currently recruiting participants for a dose-escalation study of a scAAV8 vector with the transgene human factor IX (hFIX) for gene transfer in hemophilia B patients (Nathwani *et al.* 2006). Three major aspects have been considered in the submitted protocol. A self complementary AAV vector mediates a higher and quicker transgene expression. Lower vector doses might achieve therapeutic hFIX levels in patients. Secondly, pseudotyped with the AAV 8 capsid would serve as an advantage to the vector to evade the host immunity and at last, the efficient liver tropism of AAV8 based vector could allow a peripheral venous route administration, which is favoured by patients with a bleeding diathesis. This new approach is promising indeed, but it still needs to be considered that AAV8 also targets other tissues. It can only be assumed that a non-target site, expressing the transgene, has not a deleterious effect on the entire system (Manno *et al.* 2003; Jiang *et al.* 2006; Manno *et al.* 2006). An ideal AAV vector with a singular, specific tissue target and no immunogenicity is still to be developed and must be the focus for gene therapy clinical trials in the near future.

1.5 Aim of the Study

The primate derived serotype AAV8 demonstrated in animal models potential as an effective gene transfer vehicle to liver and muscle tissue. To develop a beneficial AAV8 vector for clinical trials, many structural and functional characteristics of the protein need

to be elucidated. This study was performed to investigate the molecular basis of AAV8s outstanding gene transfer ability and to further advance its functionality as a transgene delivery vector. Main focus of this study was to characterize capsid domains exposed to the outer surface in comparison to the structural similar but functionally different AAV2 capsid. Hence, an AAV8 library could be produced to screen hepatocyte cell lines for peptide motifs with liver tropism but reduced targeting to other tissue types. Detargeting from other tissues with gene transfer effectively to one target tissue should be one of the major goals for AAV8 vector based human clinical trials in the near future.

2. Materials and Methods

2.1 Materials

2.1.1 Animals

Female immunocompetent NMRI mice (6-8 weeks of age) were purchased from the Charles River Laboratories (German Headquarters, Sulzfeld). Animal experiments were part of an application handed in May 2006 (request number is 35-9185.81/G-90/07).

2.1.2 Cell Lines and Primary Cells

Cell Type	Details	Source
293T	Derivative of the 293 cell line, contains the large T-antigen of SV40	Laboratory stock ATCC-No.CRL-11268
C2C12	Murine muscle myoblast cell line, it differentiates rapidly to form contractile myotubes	S. Herzig, A170 DKFZ
Caco-2	Human colorectal adenocarcinoma derived cell line	Laboratory stocks ATCC-No. HTB-37
H9C2	Cardiomyoblast cell line of an embryonic BD1X rat	R. Blaschke, Human Genetics, University of Heidelberg
Hep G2	Human derived hepatoma cell line carrying wt p53	U. Bantel-Schaal F030 DKFZ
Huh7	Human derived hepatoma cell line which contains a mutated form of p53	U. Bantel-Schaal F030 DKFZ
HeLa	Human epithelioid cervical carcinoma cell line	Laboratory stock ATCC-No.CCL-2
K-562	Human derived ovary adeno- carcinoma tumor cell line	Tumor Bank of the National Cancer Institute, Frederick No.0507281
LOX IMVI	Human derived tumor cell line from a lymph node metastasis	Tumor Bank of the National Cancer Institute, Frederick No.0507286
MDCK	Epithelial-like cell line derived from a healthy adult female cocker spaniel	Laboratory stock ATCC-No.CCL-34
OVCAR-4	Human derived ovary adeno-carcinoma cell line	Tumor Bank of the National Cancer Institute,

SK-MEL-28	Human derived malignant melanoma cell line	Frederick No.0502528 Tumor Bank of the National Cancer Institute, Frederick No.0507300
SNB-19	Human derived glioblastoma tumor cell line	Tumor Bank of the National Cancer Institute, Frederick No.0502595
Primary mouse hepatocytes	Primary endothelial cells, derived from liver tissue after perfusion	L.D'Alessandro A150 DKFZ
Neonatal rat cardiomyocytes	Primary cells, directly isolated from Sprague-Dawley rats (1-3-day-old)	Y.Ying F010 DKFZ

2.1.3 Bacteria

Clade	Description	Source
<i>E.coli</i> Dh5 α	For plasmid amplification, dam- and dcm-positive (restriction sites which can be methylated by the enzymes, will be methylated after plasmid amplification in these bacteria), transformation by heat-shock treatment	Gibco BRL, Eggenstein
<i>E.coli</i> Sure	For plasmid amplification, dam- and dcm-positive (restriction sites which can be methylated by the enzymes, will be methylated after plasmid amplification in these bacteria), transformation by heat-shock treatment	ATCC-No.55695 Stratagene Amsterdam
ElectroMaX <i>E.coli</i> DH5 α	For plasmid amplification, dam- and dcm-positive (restriction sites which can be methylated by the enzymes, will be methylated after plasmid amplification in these bacteria), transformation by electroporation	Invitrogen, Karlsruhe
<i>E.coli</i> TOPO 10	Used to amplify pCR2.1-plasmids (hsdR-, mcrA-, lacZ Δ M15-, endA1-, recA1-positive)	Invitrogen, Karlsruhe
MegaX DH10B TM T1 ^R Electrocomp TM Cells	For electroporation of AAV plasmid libraries to improve transformation efficiency (F ⁻ mcrA Δ (mrr-hsdRMS-mcrBC) Φ 80lacZ Δ lacX74 recA1 endA1 araD139 Δ (ara,leu)7697 galU galK λ ⁻ rpsL nupG tonA)	Invitrogen, Karlsruhe

2.1.4 Viruses and AAV Vector Mutants

Virus Type	Description	Source
rAAV2 [ss, CMV-Luc]	Recombinant adeno-associated virus type 2 vector with a transgene (single stranded vector genome, CMV Promoter, <i>luciferase</i> gene)	This study
rAAV8 [ss,CMV-Luc]	Recombinant adeno-associated virus type 8 vector with a transgene (single stranded vector genome, CMV Promoter, <i>luciferase</i> gene)	This study
Ad5	wild-type adenovirus type 5	Laboratoire de Thérapie Génique, Nantes

AAV Vector Mutant with peptide insertions	Description	Source
AAV2-VNSTRLP [ss,CMV-Luc]	Targeted AAV2 mutants displaying peptide VNSTRLP (single stranded vector genome, CMV Promoter, <i>luciferase</i> gene)	Y.Ying F010 DKFZ
AAV2-PSVSPRP [ss,CMV-Luc]	Targeted AAV2 mutants displaying peptide PSVSPRP (single stranded vector genome, CMV Promoter, <i>luciferase</i> gene)	Y.Ying F010 DKFZ
AAV2-TEWPQPF [ss,CMV-Luc]	AAV2 mutants displaying a random peptide TEWPQPF (single stranded vector genome, CMV Promoter, <i>luciferase</i> gene)	Y.Ying F010 DKFZ
AAV8-VNSTRLP [ss,CMV-Luc]	Targeted AAV8 capsid mutants displaying peptide VNSTRLP (single stranded vector genome, CMV Promoter, <i>luciferase</i> gene)	This study
AAV8-PSVSPRP [ss,CMV-Luc]	Targeted AAV8 mutants displaying peptide PSVSPRP (single stranded vector genome, CMV Promoter, <i>luciferase</i> gene)	This study
AAV8-ASSLNIA [ss,CMV-Luc]	Targeted AAV8 capsid mutants displaying peptide ASSLNIA (single stranded vector genome, CMV Promoter, <i>luciferase</i> gene)	This study
AAV8-GQHPRPG [ss,CMV-Luc]	Targeted AAV8 capsid mutants displaying peptide ASSLNIA (single stranded vector genome, CMV Promoter, <i>luciferase</i> gene)	This study
AAV8-SSRGLGK [ss,CMV-Luc]	Targeted AAV8 mutants displaying peptide SSRGLGK (single stranded	This study

AAV8-SEVARCR [ss,CMV-Luc]	vector genome, CMV Promoter, <i>luciferase</i> gene) Targeted AAV8 capsid mutants displaying peptide ASSLNIA (single stranded vector genome, CMV Promoter, <i>luciferase</i> gene)	This study
AAV8-VGLVLR [ss,CMV-Luc]	Targeted AAV8 capsid mutants displaying peptide VGLVLR (single stranded vector genome, CMV Promoter, <i>luciferase</i> gene)	This study
AAV8-SEGLKNL [ss,CMV-Luc]	Targeted AAV8 capsid mutants displaying peptide SEGLKNL (single stranded vector genome, CMV Promoter, <i>luciferase</i> gene)	This study
AAV Vector Mutant Capsid Mutants	Description	Source
Domain Swap I [ss,CMV-Luc]	Before vector production, AAV8 capsid encoding helper plasmid p5E18-VD-2/8 has the domain of nucleotide 1900 to 3269 swapped to AAV2 encoding <i>cap</i> nucleotide sequence (single stranded vector genome, CMV Promoter, <i>luciferase</i> gene)	This study
Domain Swap II [ss,CMV-Luc]	Before vector production, AAV8 capsid encoding helper plasmid p5E18-VD-2/8 has the domain of nucleotide 1900 to 3671 swapped to AAV2 encoding <i>cap</i> nucleotide sequence (single stranded vector genome, CMV Promoter, <i>luciferase</i> gene)	This study
Domain Swap III [ss,CMV-Luc]	Before vector production, AAV8 capsid encoding helper plasmid p5E18-VD-2/8 has the domain of nucleotide 3265 to 3671 swapped to AAV2 encoding <i>cap</i> nucleotide sequence (single stranded vector genome, CMV Promoter, <i>luciferase</i> gene)	This study
Domain Swap IV [ss,CMV-Luc]	Before vector production, AAV8 capsid encoding helper plasmid p5E18-VD-2/8 has the domain of nucleotide 3265 to 4300 swapped to AAV2 encoding <i>cap</i> nucleotide sequence (single stranded vector genome, CMV Promoter, <i>luciferase</i> gene)	This study
Domain Swap V [ss,CMV-Luc]	Before vector production, AAV8 capsid encoding helper plasmid p5E18-VD-2/8 has the domain of nucleotide 3265 to 4300 swapped to AAV2 encoding <i>cap</i>	This study

	nucleotide sequence (single stranded vector genome, CMV Promoter, <i>luciferase</i> gene)	
8→2 Mutant 1 TQTLG → QQRLG [ss,CMV-Luc]	Before vector production, AAV8 capsid encoding helper plasmid p5E18-VD-2/8 undergoes AA substitutions from AAV8 to AAV2 TQTLG → QQRLG (AAV8, AA 460-464) (single stranded vector genome, CMV Promoter, <i>luciferase</i> gene)	This study
8→2 Mutant 2 TMAN → DMRN [ss,CMV-Luc]	Before vector production, AAV8 capsid encoding helper plasmid p5E18-VD-2/8 undergoes AA substitutions from AAV8 to AAV2 TMAN → DMRN (AAV8, AA 472-475) (single stranded vector genome, CMV Promoter, <i>luciferase</i> gene)	This study
8→2 Mutant 3 AARD → AERT [ss,CMV-Luc]	Before vector production, AAV8 capsid encoding helper plasmid p5E18-VD-2/8 undergoes AA substitutions from AAV8 to AAV2 AARD → AERT (AAV8, AA 550-553) (single stranded vector genome, CMV Promoter, <i>luciferase</i> gene)	This study
8→2 Mutant 4 DYSDV → DISDV [ss,CMV-Luc]	Before vector production, AAV8 capsid encoding helper plasmid p5E18-VD-2/8 undergoes AA substitutions from AAV8 to AAV2 DYSDV → DISDV (AAV8, AA 556-560) (single stranded vector genome, CMV Promoter, <i>luciferase</i> gene)	This study
8→2 Mutant 5 GIVAD → GSVAT [ss,CMV-Luc]	Before vector production, AAV8 capsid encoding helper plasmid p5E18-VD-2/8 undergoes AA substitutions from AAV8 to AAV2 GIVAD → GSVAT (AAV8, AA 580-584) (single stranded vector genome, CMV Promoter, <i>luciferase</i> gene)	This study
8→2 Mutant 6 QNTA → GNRQ [ss,CMV-Luc]	Before vector production, AAV8 capsid encoding helper plasmid p5E18-VD-2/8 undergoes AA substitutions from AAV8 to AAV2 QNTA → GNRQ (AAV8, AA 589-592) (single stranded vector genome, CMV Promoter, <i>luciferase</i> gene)	This study
8→2 Mutant 7 QIGTV → ATGDV [ss,CMV-Luc]	Before vector production, AAV8 capsid encoding helper plasmid p5E18-VD-2/8 undergoes AA substitutions from AAV8 to AAV2 QIGTV → ATGDV (AAV8, AA 594-598) (single stranded vector genome, CMV Promoter, <i>luciferase</i> gene)	This study
2→8 Mutant Rev1 TQ SRLQ → TTQTLG [ss,CMV-Luc]	Before vector production, AAV8 capsid encoding helper plasmid BSΔTR18 undergoes AA substitutions from AAV2 to	This study

2→8 Mutant Rev2 SDIRD→NTMAN [ss,CMV-Luc]	AAV8 TQSRLQ→TTQTLG (AAV2,AA456-461) (single stranded vector genome, CMV Promoter, <i>luciferase</i> gene) Before vector production, AAV8 capsid encoding helper plasmid BSΔTR18 undergoes AA substitutions from AAV2 to AAV8 SDIRD→NTMAN(AAV2, AA 468-472) (single stranded vector genome, CMV Promoter, <i>luciferase</i> gene)	This study
2→8 Mutant Rev4 DIEKV→DYSDV [ss,CMV-Luc]	Before vector production, AAV8 capsid encoding helper plasmid BSΔTR18 undergoes AA substitutions from AAV2 to AAV8 DIEKV→DYSDV (AAV2, AA 553-557) (single stranded vector genome, CMV Promoter, <i>luciferase</i> gene)	This study
2→8 Mutant Rev5 SVSTNL→IVADNL [ss,CMV-Luc]	Before vector production, AAV8 capsid encoding helper plasmid BSΔTR18 undergoes AA substitutions from AAV2 to AAV8 SVSTNL→IVADNL (AAV2, AA 578-581) (single stranded vector genome, CMV Promoter, <i>luciferase</i> gene)	This study
2→8 Mutant Rev6 QRGNRQ→QQQNTA [ss,CMV-Luc]	Before vector production, AAV8 capsid encoding helper plasmid BSΔTR18 undergoes AA substitutions from AAV2 to AAV8 QRGNRQ→QQQNTA (AAV2, AA 585-589)(single stranded vector genome, CMV Promoter, <i>luciferase</i> gene)	This study
2→8 Mutant Rev7 ATADV→QIGTV [ss,CMV-Luc]	Before vector production, AAV8 capsid encoding helper plasmid BSΔTR18 undergoes AA substitutions from AAV2 to AAV8 ATADV→QIGTV (AAV2, AA 591-594)(single stranded vector genome, CMV Promoter, <i>luciferase</i> gene)	This study
ADK8_Mutant8→2 455-GTTTQS-460 [ss,CMV-Luc]	Before vector production, AAV8 capsid encoding helper plasmid p5E18-VD-2/8 undergoes AA substitutions from AAV8 to AAV2 (single stranded vector genome, CMV Promoter, <i>luciferase</i> gene)	This study
ADK8_Mutant8→2 493-KTSAD-497 [ss,CMV-Luc]	Before vector production, AAV8 capsid encoding helper plasmid p5E18-VD-2/8 undergoes AA substitutions from AAV8 to AAV2 (single stranded vector genome, CMV Promoter, <i>luciferase</i> gene)	This study
ADK8_Mutant8→2 586-LQRGNR-591 [ss,CMV-Luc]	Before vector production, AAV8 capsid encoding helper plasmid p5E18-VD-2/8 undergoes AA substitutions from AAV8 to AAV2 (single stranded vector genome, CMV Promoter, <i>luciferase</i> gene)	This study

2.1.5 Antibodies and Antisera

Primary Antibody	Binding Site/Description	Source/Reference
A1	Monoclonal, Hybridoma Culture and purified, against VP1 N-terminus of AAV2	Laboratory Stocks (Wobus <i>et al.</i> 2000)
A20	Monoclonal, Hybridoma Culture and purified, against assembled capsids of AAV2	Laboratory Stocks (Wistuba <i>et al.</i> 1997)
A69	Monoclonal, Hybridoma Culture and purified, against VP1 and 2 N-terminus of AAV2	Laboratory Stocks (Wobus <i>et al.</i> 2000)
ADK4	Monoclonal, Hybridoma Culture and purified, against assembled capsids of AAV4	Laboratory Stocks (Kuck <i>et al.</i> 2007)
ADK8	Monoclonal, Hybridoma Culture and purified, against assembled capsids of AAV8	Laboratory Stocks
B1	Monoclonal, Hybridoma Culture, against VP1, VP2 and VP3 of AAVs	Laboratory Stocks (Wistuba <i>et al.</i> 1997)
C37B	Monoclonal, purified, against AAV2 assembled capsid	Laboratory Stocks (Wobus <i>et al.</i> 2000)
IVA7	Monoclonal, purified, against a 33 kD Protein of <i>Onchocera volvulus</i> (Nematode)	
Anti-VP51	Polyclonal rabbit serum against VP proteins of AAVs	Laboratory Stocks

Secondary Antibody	Source/Reference
Secondary biotinylated goat anti-rabbit IgG	Vector Laboratories, Burlingame
Fluorescein/streptavidin conjugate	Vector Laboratories, Burlingame
Goat-anti-Mouse IgG, Alexa 488	Dianova, Hamburg
Goat-anti-Mouse IgG, Peroxidase	Dianova, Hamburg

2.1.6 Oligonucleotides

The listed oligonucleotides were synthesized from the company MWG Biotech (Ebersberg) and were synthesized either for mutagenesis or for sequencing. Oligonucleotide-pairs (forward and reverse primer) were designed according to the protocol (QuikChange[®] Site-Directed Mutagenesis Kit, Stratagene) and served as the basis for mutagenesis. Substitutions within the primers are indicated in bold. Additionally, oligonucleotides were designed according to peptides selected *in vivo* and *in vitro* from random AAV2 and AAV8 display peptide libraries. To produce recombinant AAV2 and AAV8 vectors displaying a selected peptide motif, forward (F) and reverse (R) oligonucleotides were synthesized with a *Sfi*I linker (underlined).

2.1.6.1 Mutagenesis Primer

Name	Oligonucleotide Sequence 5'→3'	Template
I-f-AAG	5'-GGAAAACAGCA AAG CGCTGGAATCCCG-3'	BSΔTR
I-r-CTT (<i>Eco</i> 47III Insertion)	5'-CGGGATTCCAGCG CTT GCTGTTTTCC-3'	18
II-f-CGA	5'-CGATAT CGAG CTTATCGATACCG-3'	BSΔTR
II-r-TCG (<i>Hind</i> III Excision)	5'-CGGTATCGAGCTTAT CG ATACCG-3'	18
III-f-ACGC	5'-GCCAGCA ACGC GTATCAAAGACATCTGC-3'	BSΔTR
III-r-GCGT (<i>Mlu</i> I Insertion)	5'-GCAGATGTCTTTGATAC GCGT TGCTGGC-3'	18
QQR-f	5'-GGCACGGCAAAT CAGCAGCGT CTGGGCTTCAGCC-3'	P5E18-
QQR-r	5'-GGCTGAAGCCCAGAC CGT GCTGATTTGCCGTGCC-3'	VD2/8
DMR-f	5'-GGTGGGCCTAAT GATATGAGAAAT CAGGCAAAGAAC-3'	P5E18-
DMR-r	5'-GTTCTTTGCCTGATTT TCTCATATC ATTAGGCCACC-3'	VD2/8
ERT-f	5'-GGCAAACAAATGCT GAGAGA ACCAATGCGGATTACAGC-3'	P5E18-
ERT-r	5'-GCTGTAATCCGCATTG GTTCTCTC AGCATTTTGTGGCC-3'	VD2/8
I-f	5'-CAGAGACAATGCGGAT ATCAGCGAT GTCTGCTC-3'	P5E18-
I-r	5'-GAGCATGACATCGCTG ATATCCGC ATTGTCTCTG-3'	VD2/8
DIEK-f	5'-CTGCCAGAGACAATGCGGAT ATCGAAAAGG TCTGCTCACC AG-3'	P5E18-
DIEK-r	5'-GCTGGTGAGCATGAC TTTCGATATCCGC ATTGTCTCTGGCAG-3'	VD2/8

SVAT-f	5'-GAGGAATACGGT TCCGTGGCAACT AACTGCAGCAGC-3'	P5E18-
SVAT-r	5'-GCTGCTGCAAGTTAG TTGCCACGGA ACCGTATTCTC-3'	VD2/8
GNRQ-f	5'-GATAACTGCAGCAG GGAAACCGGCAAC CTCAAATTGG-3'	P5E18-
GNRQ-r	5'-CCAATTTGAGG TTGCCG TTTTCCCTGCTGCAAGTTATC-3'	VD2/8
ATGD-f	5'-CACGGCTCCT GCAACTGGAGAT GTCAACAGCCAGGGG-3'	P5E18-
ATGD-r	5'-CCCCTGGCTGTTGACAT CTCCAGTTGC AGGAGCCGTG-3'	VD2/8
TQTL-f	5'-CCAAGTGGAAACCACCA ATACGCAAACT CTTGGGTTTTCTCAGGC-3'	BSΔTR
TQTL-r	5'-GCCTGAGAAAAC CCAAGAGTCTGCGTATT GGTGGTTCCAATTGG-3'	18
NTMAN-f	5'-CTCAGGCCGGAGCGA ATACAATGGCCAAT CAGTCTAGGAACTG-3'	BSΔTR
NTMAN-r	5'-CCAGTTCTAGACT GATTGGCCATTGTATT CGCTCCGGCCTGAG-3'	18
DYSD-f	5'-CTCAGAGAAAACAAATGTGGACT ACAGCGAT GTTCATGATTACAG-3'	BSΔTR
DYSD-r	5'-CTGTAATGAT GATCGCTGTAGT CCACATTTGTTTTCTCTGAGC-3'	18
IVAD-f	5'-GGAGCAGTATGGT ATTGTAGCTGACAAC CTCCAGAGAGG-3'	BSΔTR
IVAD-r	5'-CCTCTCTGGAGGTT GTCAGCTACAAT ACCATACTGCTCC-3'	18
QQNTA-f	5'-CCAACCTCCAG CAACAAAACACAGCGG CAGCTACCGC-3'	BSΔTR
QQNTA-r	5'-GCGGTAGCTGCC GCTGTGTTTTGTG TCTGGAGGTTGG-3'	18
RQNTA-f	5'-CCAACCTCCAGAG CAAAAACACAGCGG CAGCTACCGC-3'	BSΔTR
RQNTA-r	5'-GCGGTAGCTGCC GCTGTGTTTTGT TCTCTGGAGGTTGG-3'	18
QIGTV-f	5'-GGCAACAGACAAGC ACAGATCGGAACT GTCAACACACAAGGC-3'	BSΔTR
QIGTV-r	5'-GCCTTGTGTGTTAC AGTTCCGATCTGTG CTTGTCTGTTGCC-3'	18
TTQS-f	5'-GGAGGCACG ACAACCTCAGT CGACTCTGGGC-3'	P5E18-
TTQS-r	5'-GCCCAGAGTC GACTGAGTTGTC GTGCCTCC-3'	VD2/8
KTSAD-f	5'-GCTATTGTTGTT GTCCGCGCTTGT CTTTGAGACGCG-3'	P5E18-
KTSAD-r	5'-CGCGTCTCAA AGACAAGCGCGGACA ACAACAATAGC-3'	VD2/8
RGNR-f	5'-GCAGATAACTGCAGCG GGGAAACAG GGCTCCTC-3'	P5E18-
RGNR-r	5'-GAGGAGCC CTGTTTCCCCG CTGCAAGTTATCTGC-3'	VD2/8

2.1.6.2 Primer for Insertion

Peptide Motif	Oligonucleotide Sequence 5'→3'	Backbone for Insertion
2PSVSPRP-f	<u>AGGCCTTCGGT</u> GAGTCCGCGTCT <u>GCCCAGG</u>	pMT187XX2
2PSVSPRP-r	<u>GGGCAGGACGCGG</u> ACTCACCGAAG <u>GGCCTCTC</u>	

2VNSTRLP-f	<u>AGGCGTTAATTCGACTCGTTTGCCTGCCCAGG</u>	pMT187XX2
2VNSTRLP-r	<u>GGGCAGGCAAACGAGTCGAATTAACGCCTCTC</u>	
8ASSLNIA-f	<u>AGGCGCCAGCAGCCTGAACATCGCCGCCCAGG</u>	P5E18-VD2/8 + <i>Sfi</i> I Sites
8ASSLNIA-r	<u>GGGCGGCGATGTTTCAGGCTGCTGGCGCCTCTC</u>	
8GQHPRPG-f	<u>AGGCGGTCAGCATCCGCGGCCGGGTGCCCAGG</u>	P5E18-VD2/8 + <i>Sfi</i> I Sites
8GQHPRPG-r	<u>GGGCACCCGGCCGCGGATGCTGACCGCCTCTC</u>	
8PSVSPRP-f	<u>AGGCCCTTCGGTGAGTCCGCGTCCTGCCCAGG</u>	P5E18-VD2/8 + <i>Sfi</i> I Sites
8PSVSPRP-r	<u>GGGCAGGACGCGGACTCACCGAAGGCCTCTC</u>	
8VNSTRLP-f	<u>AGGCGTTAATTCGACTCGTTTGCCTGCCCAGG</u>	P5E18-VD2/8 + <i>Sfi</i> I Sites
8VNSTRLP-r	<u>GGGCAGGCAAACGAGTCGAATTAACGCCTCTC</u>	

2.1.6.3 Primers for Semi-Quantitative PCR

Name	Sequence 5'→3'
3+ -f (AAV2 library)	GGTTCTCATCTTTGGGAAGCAAG
3- - r (AAV2 library)	TGATGAGAATCTGTGGAGGAG
Lib8ctrl	CTCGTCGGCCGCCTGG
AAV8lib-f	CCAGAGACAATGCGGATTACAG
TopoLib8-f	CTGGCATCGCTATGGCAACACAC
TopoLib8-r	GGATCTGAGGCGGAGGATGTTTC
TOPO+ -f (AAV2)	ACCTCCAGAGAGGCCAGAGAG
2-TOPO-r (AAV2)	CTGAAGGTACACATCTCTGTC
wt-	GGTAGCTGCTTGTCTGTTGCC
Luciferase+	GACGCCAAAAACATAAAGAAAG
Luciferase -	CCAAAAATAGGATCTCTGGC
M13R	AGGAAACAGCTATGACCATG
RQA	ATCTGCGGTGGCCGCCTGGGC
β-actin +	ATGTTTGAGACCTTCAACAC
β-actin -	AACGTCACATTTTCATGATGG

2.1.6.4 Primer/Probe Sets for Quantitative Real-Time PCR

Name	Sequence 5'→3'
Rep+	AAGTCCTCGGCCAGATAGAC
Rep-	CAATCACGGCGCACATGT
Rep-Probe	6-fam-TGATCGTCACCTCCAACA-MGB
CMV+	TGCCCAGTACATGACCTTATGG
CMV-	GAAATCCCCGTGAGTCAAACC
Probe	6-fam-AGTCATCGCTATTACCATGG-MGB

Details on functionality of different primers are described in appropriate sections of methods and results.

2.1.6.5 Oligonucleotide Library Primers

The oligonucleotides encode random peptide inserts (seven amino acids in length) and are designed according to their *SfiI* insertion sites in the AAV2 and the AAV8 plasmid backbone. The sequences of the primers with seven random oligonucleotide amino acids are described for AAV8 and AAV2 as indicated:

5' -CAGTCGGCCAGAGAGGC(NNK)₇GCCCAGGCGGCCGACGAG-3'(AAV8 Library)

5' -CAGTCGGCCAGAGAGGC(NNK)₇GCCCAGGCGGCTGACGAG-3' (AAV2 Library)

(N=A, T, C, or G; K= G or T)

2.1.7 Plasmids

Plasmid	Description	Source/Reference
P5E18-VD2/8	AAV8 helper plasmid providing AAV2 <i>rep</i> and AAV8 <i>cap</i> gene	Gao <i>et al.</i> 2003 Received from Julie Johnston, Vector Core, Philadelphia
pBSΔTR18	AAV2 helper plasmid providing wt <i>rep</i> and <i>cap</i> gene without ITRs	Weger <i>et al.</i> 1997
pCR2.1	TOPO cloning plasmid vector, supplied as linearized form with single 3'-thymidine overhangs for TA cloning of PCR products	TOPO TA Cloning Kit, Stratagene
pDP2	AAV2/Ad-helper plasmid	Grimm <i>et al.</i> , 2003
pDGΔVP	AAV2/Ad-helper plasmid without <i>cap</i> gene	Grimm <i>et al.</i> , 1998
pDG	AAV2/Ad-helper plasmid	Grimm <i>et al.</i> , 1998
pMT187-0-3	Library backbone plasmid developed from pSub201 for cloning of the oligo nucleotide insert, containing wt AAV2 genome with modification at nucleotide position 3967 of the <i>cap</i> gene, where two incompatible <i>SfiI</i> restriction sites were generated and separated by a 'stuffer' oligonucleotide	Müller <i>et al.</i> , 2003
pMT187XX2	ITR-deleted library backbone plasmid	Y.Ying F010

pRSVVP3cm	Codon-modified wt-VP3 helper plasmid	DKFZ Waterkamp <i>et al.</i> 2006
pSSV9	AAV2 helper plasmid providing wt <i>rep</i> and <i>cap</i> genes and ITRs	J.Samulski, Chapel Hill, North Carolina
pTAV2.0	Bluescript-plasmid containing the entire wt AAV2 sequence	Heilbronn <i>et al.</i> , 1990
pUF2CMV-EGFP	Recombinant AAV2 vector plasmid containing an EGFP reporter gene under control of CMV promoter, flanked by ITRs	Laboratory stock
pUF2CMV-Luc	Recombinant AAV2 vector plasmid containing a luciferase reporter gene under control of CMV promoter, flanked by ITRs	Zolotukhin <i>et al.</i> , 1996
pXX2	AAV2 helper plasmid providing wt <i>rep</i> and <i>cap</i> genes lacking the ITRs	J.Samulski, Chapel Hill, North Carolina
Modified Plasmid	Description	Source/ Reference
pM187XX2+V NSTRLP	AAV2 Library backbone plasmid with inserted motif	Supplied by Y.Ying
pM187XX2+P SVSPRP	AAV2 Library backbone plasmid with inserted motif	Supplied by Y.Ying
pLib588-92+itr	AAV8 Library backbone plasmid + ITRs	This Study
P5E18-VD2/8Δlib +VNSTRLP	AAV8 Library backbone plasmid with inserted motif	This Study
P5E18-VD2/8Δlib +PSVSPRP	AAV8 Library backbone plasmid with inserted motif	This Study
P5E18-VD2/8Δlib +ASSLNIA	AAV8 Library backbone plasmid with inserted motif	This Study
P5E18-VD2/8Δlib +GQHPRPG	AAV8 Library backbone plasmid with inserted motif	This Study
P5E18-VD2/8Δlib +SSRGLGK	AAV8 Library backbone plasmid with inserted motif	This Study
P5E18-VD2/8Δlib +SEVARCR	AAV8 Library backbone plasmid with inserted motif	This Study
P5E18-VD2/8Δlib +VGLVLR	AAV8 Library backbone plasmid with inserted motif	This Study

P5E18- VD2/8Δlib +SEGLKNL	AAV8 Library backbone plasmid with inserted motif	This Study
DS I	AAV8 capsid encoding helper plasmid p5E18-VD-2/8 has the domain of nucleotide 1900 to 3269 swapped to AAV2 encoding <i>cap</i> nucleotide sequence	This Study
DS II	AAV8 capsid encoding helper plasmid p5E18-VD-2/8 has the domain of nucleotide 1900 to 3671 swapped to AAV2 encoding <i>cap</i> nucleotide sequence	This Study
DS III	AAV8 capsid encoding helper plasmid p5E18-VD-2/8 has the domain of nucleotide 3265 to 3671 swapped to AAV2 encoding <i>cap</i> nucleotide sequence	This Study
DS IV	AAV8 capsid encoding helper plasmid p5E18-VD-2/8 has the domain of nucleotide 3265 to 4300 swapped to AAV2 encoding <i>cap</i> nucleotide sequence	This Study
DS V	AAV8 capsid encoding helper plasmid p5E18-VD-2/8 has the domain of nucleotide 3265 to 4300 swapped to AAV2 encoding <i>cap</i> nucleotide sequence	This Study
8-2Mut1 [8→2QqR]	AAV8 capsid encoding helper plasmid p5E18-VD-2/8 undergoes AA substitutions from AAV8 to AAV2 TQTLG → QQRLG (AAV8, AA 460-464)	This Study
8-2Mut2 [8→2DmR]	AAV8 capsid encoding helper plasmid p5E18-VD-2/8 undergoes AA substitutions from AAV8 to AAV2 TMAN → DMRN (AAV8, AA 472-475)	This Study
8-2Mut3 [8→2ErT]	AAV8 capsid encoding helper plasmid p5E18-VD-2/8 undergoes AA substitutions from AAV8 to AAV2 AARD → AERT (AAV8, AA 550-553)	This Study
8-2Mut4 [8→2I]	AAV8 capsid encoding helper plasmid p5E18-VD-2/8 undergoes AA substitutions from AAV8 to AAV2 DYSDV → DISDV (AAV8, AA 556-560)	This Study
8-2Mut5 [8→2SvaT]	AAV8 capsid encoding helper plasmid p5E18-VD-2/8 undergoes AA substitutions from AAV8 to AAV2 GIVAD → GSVAT (AAV8, AA 580-584)	This Study
8-2Mut6 [8→2GnRQ]	AAV8 capsid encoding helper plasmid p5E18-VD-2/8 undergoes AA substitutions from AAV8 to AAV2 QNTA → GNRQ (AAV8, AA 589-592)	This Study
8-2Mut7 [8→2ATgD]	AAV8 capsid encoding helper plasmid p5E18-VD-2/8 undergoes AA substitutions from	This Study

2-8Rev1 [2→8TQTLG]	AAV8 to AAV2 QIGTV → ATGDV (AAV8, AA 594-598) AAV8 capsid encoding helper plasmid BSΔTR18 undergoes AA substitutions from AAV2 to AAV8 TQSRLQ→TTQTLG (AAV2,AA456-461)	This Study
2-8Rev2 [2→8NTMAN]	AAV8 capsid encoding helper plasmid BSΔTR18 undergoes AA substitutions from AAV2 to AAV8 SDIRD→NTMAN(AAV2, AA 468-472)	This Study
2-8Rev4 [2→8dYSDv]	AAV8 capsid encoding helper plasmid BSΔTR18 undergoes AA substitutions from AAV2 to AAV8 DIEKV→DYS DV (AAV2, AA 553-557)	This Study
2-8Rev5 [2→8IvAD]	AAV8 capsid encoding helper plasmid BSΔTR18 undergoes AA substitutions from AAV2 to AAV8 SVSTNL→IVADNL (AAV2, AA 578-583)	This Study
2-8Rev6 [2→8QQnTA]	AAV8 capsid encoding helper plasmid BSΔTR18 undergoes AA substitutions from AAV2 to AAV8	This Study
2-8Rev7 [2→8QIGTv]	AAV8 capsid encoding helper plasmid BSΔTR18 undergoes AA substitutions from AAV2 to AAV8 QRGNRQ→QQQNTA (AAV2, AA 585-590)	This Study
GTTTQS	AAV8 capsid encoding helper plasmid p5E18- VD-2/8 undergoes AA substitutions from AAV8 to AAV2	This Study
LQRGNR	AAV8 capsid encoding helper plasmid p5E18- VD-2/8 undergoes AA substitutions from AAV8 to AAV2	This Study
KTSAD	AAV8 capsid encoding helper plasmid p5E18- VD-2/8 undergoes AA substitutions from AAV8 to AAV2	This Study

2.1.8 DNA Probes

Name	Length in bp	Fragment
AAV2 <i>rep</i> probe	1477	<i>Sall</i> from pTAV2.0
CMV probe	620	<i>XhoI-EcoRI</i> from pUF2CMV-Luc

2.1.9 Nucleotides

Name	Company
³² P-dCTP (radioactive)	GE Healthcare, Freiburg
dNTPs (dATP, dTTP, dCTP, dGTP)	Roche, Mannheim

2.1.10 Standard Marker

Marker	Size	Company
Smart Ladder (DNA Marker)	10.000, 8000, 6000, 5000, 4000, 3000, 2500, 2000, 1500, 1000, 800, 600, 400, 200 bp	Eurogentec Seraing Belgium
100 bp DNA Ladder (DNA Marker)	1517, 1200, 1000, 900, 800, 700, 600, 517, 500, 400, 300, 200, 100 bp	New England Biolabs Frankfurt
Novex [®] Sharp Pre-Stained	260, 160, 110, 80, 60, 50, 40, 30, 20, 15, 10, 3.5 kDA	Invitrogen Karlsruhe
SeeBlue [®] Plus2 (Protein Marker)	198, 98, 62, 49, 38, 28, 17, 14, 6, 3 kDA	Invitrogen Karlsruhe
Rainbow Marker (Protein Marker)	225, 150, 102, 76, 52, 38, 31, 24, 17, 12 kDA	GE Healthcare Freiburg

2.1.11 Enzymes

Enzyme	Company
Benzonase	Sigma-Aldrich, Deisenhofen
Calf Intestine Phosphatase (CIP)	Roche, Mannheim
DNase I	Roche, Mannheim
Klenow Enzyme	Roche, Mannheim
MNase (Nuclease S7)	Roche, Mannheim
Proteinase K	Roche, Mannheim
Sequenase	GE Healthcare, Freiburg
Shrimp Alkaline Phosphatase (SAP)	Roche, Mannheim
T4-DNA-Ligase	Roche, Mannheim
Taq-DNA-Polymerase	Invitrogen, Karlsruhe

Restriction enzymes and buffers used during this study were either supplied from Roche (Boehringer Mannheim) or New England Biolabs (NEB, Frankfurt).

2.1.12 Kits

Kit	Company
AAV2 Titration ELISA	Progen, Heidelberg
ECL [™] Chemiluminescence Kit	GE Healthcare, Freiburg
Lynx Rapid Conjugation Kit	AbD Serotech, Munich

Maxi and Giga Kit	Qiagen, Hilden
Mouse Monoclonal Antibody Isotyping Kit	Roche, Mannheim
NanoOrange [®] Protein Quantitation Kit	Invitrogen, Karlsruhe
Nexttec [™] Genomic DNA Isolation Kit	Bio and Sell, Nuremberg
peqGOLD Plasmid DNA Mini Kit	PEQLAB, Erlangen
peqGOLD Tissue DNA Mini Kit	PEQLAB, Erlangen
QIAquick Nucleotide Removal Kit	Qiagen, Hilden
QuikChange [®] Site-Directed Mutagenesis Kit	Stratagene, Amsterdam
Random Primed Labeling Kit	Roche, Mannheim
Sequenase 2.0 Kit	GE Healthcare, Freiburg
TOPO TA Cloning Kit	Invitrogen, Karlsruhe
SilverXpress [®] Silver Staining Kit	Invitrogen, Karlsruhe

2.1.13 Cell Culture Media and Additives

Product	Company
Dulbecco's modified eagle medium (DMEM)	Sigma – Aldrich, Deisenhofen
DMEM high glucose	Sigma – Aldrich, Deisenhofen
Fetal calf serum (FCS)	Gibco BRL, Eggenstein
Glucose	Braun, Eschweiler
Human FIX	Innovative Research, Novi
Insulin	Sigma – Adrich, Deisenhofen
ITS	Sigma – Aldrich, Deisenhofen
L-Glutamine	Gibco BRL, Eggenstein
Minimum essential medium (MEM)	Invitrogen, Karlsruhe
Newborn calf serum (NCS)	Gibco BRL, Eggenstein
Normal goat serum (NGS)	Promocell,

Normal horse serum (NHS)	Heidelberg
Penicillin/Streptomycin	Gibco BRL, Eggenstein
RPMI 1640 Medium	Gibco BRL, Eggenstein
Trypsin-EDTA 0.025 %	Sigma – Aldrich, Deisenhofen
Trypsin-EDTA 0.005 %	Sigma – Aldrich , Deisenhofen

2.1.14 Constituents for Bacterial Cultures

Name	Company
Ampicillin	Sigma-Aldrich, Deisenhofen
Bacto-agar	Difco, Hamburg
Bacto-yeast extract	Difco, Hamburg
Bacto-tryptone	Difco, Hamburg

2.1.15 Chemicals

All commonly used chemicals as well as chemicals not described in this thesis have been purchased in the highest purities from the listed companies:

- Biomol Feinchemikalien, Ilvesheim
- BioRad, Richmond (USA)
- Carl Roth GmbH & Co.KG, Karlsruhe
- GE Healthcare, Freiburg
- Gibco BRL, Eggenstein
- Merck, Darmstadt
- Pharmacia, Freiburg
- Roche, Mannheim
- Roth, Karlsruhe
- Serva Feinbiochemika GmbH & Co. KG, Heidelberg
- Sigma-Aldrich, Deisenhofen

2.1.15.1 Special Chemicals

Reagent	Company
Acetic acid	GE Healthcare, Freiburg
β - Mercaptoethanol	Roth, Karlsruhe
Bovine serum albumin (BSA)	GE Healthcare, Freiburg
Cathepsin B from human liver	Merck KGaA, Darmstadt
Collagen	GE Healthcare, Freiburg
Collagenase type II	Gibco BRL, Eggenstein
D-luciferin	Synchem, Illinois, USA
Dimethyl sulfoxide (DMSO)	Merck, Darmstadt
Ethidium bromide	Serva, Heidelberg
Ethylendiamintetraacetate (EDTA)	Serva, Heidelberg
Gentamicin	GE Healthcare, Freiburg
2-[4-(2-Hydroxyethyl)-1-piperazine]ethanesulfonic acid (HEPES)	GE Healthcare, Freiburg
N-2-Hydroxyethylpiperazine-N'-2-ethanesulfonic acid buffered saline solution (HepesBSS)	Promocell, Heideberg
Formaldehyde 37 %	Merck, Darmstadt
Iodixanol (OptiPrep™)	Romega, Heidelberg
Isopropanol	Riedel-de-Haen, Seelze
NuPage® Sample Buffer (20x)	Invitrogen, Karlsruhe
Luciferin	Promega, Heidelberg
Natriumbicarbonat	Gibco BRL, Eggenstein
Pancreatin	GE Healthcare, Freiburg
Percoll™	Sigma-Aldrich, Deisenhofen
Permafluor	Immunotech, Cary, USA
Protease Inhibitors (Complete Mini, EDTA free)	Roche, Mannheim
Protein-A or G-Sepharose	GE Healthcare, Freiburg
Phenol-chloroform-isoamylalcohol (25:24:1)	Roth, Karlsruhe
Polyfect transfection reagent	Qiagen, Hilden
Reporter lysis buffer (5x)	Promega, Heidelberg
TaqMan Universal PCR Master Mix	Applied Biosystems, Frankfurt
Trishydroxymethylaminomethane (Tris)	Gibco BRL, Eggenstein
4-(1,1,3,3-tetramethylbutyl) phenyl polyethylene glycol (Triton X-100)	Sigma-Aldrich, Deisenhofen
Polyoxyethylene sorbitan monolaurate (Tween-20)	Sigma-Aldrich, Deisenhofen
5-bromo-4-chloro-3-indolyl- β -D-galactopyranosid (X-gal)	Appligene, Watford, UK

2.1.16 Buffers and Reagents

The listed solutions are frequently used for several methods. Specific solutions only used for a single method will be described in the method section.

Name	Composition
20x SSC	3 M NaCl, 0.3M Tri-Sodium-Citrate (Dihydrate), pH 7
2x HBSS	280 mM NaCl, 50 mM Hepes, 1.5 mM Na ₂ HPO ₄ , 10 mM KCL, 12 mM glucose, pH 7.05
Denaturation buffer	1.5 M NaCl, 0.5 M NaOH
DNA loading buffer (10x)	50 mM EDTA pH 8.0, 30 % Ficoll, 2 % SDS, 0,25 % bromophenol-blue, 0,25 % xylene cyanol
Hybridisation buffer	125 mM Na ₂ HPO ₄ , 250 mM NaCl, 1 mM EDTA, 45 % formamide, 7 % SDS
LB medium	1 % bacto-tryptone, 0.5 % bacto-yeast extract, 0.5 % NaCl
Lysis buffer	150 mM NaCl, 50 mM Tris-HCl, pH 8.5
MNase buffer	10 mM Tris pH 8.0, 1 mM CaCl ₂
Neutralisation buffer	0.5 M Tris-HCL pH 7.0, 0.3 M Tri-Sodium-Citrate, 3 M NaCl
PBS (1x)	18.4 mM Na ₂ HPO ₄ , 10,9 mM KH ₂ PO ₄ , 125 mM NaCl, pH7.2
PBS-MK	1 x PBS, 1 mM MgCl ₂ , 2.5 mM KCL, pH 7.2
Proteinase buffer (2x)	20 mM Tris HCl pH 8.0, 20 mM EDTA, 1 % (v/v) SDS
SOC medium	2 % trypton, 0.5 % bacto-yeast extract, 10 mM NaCl, 2.5 mM KCl, 10 mM MgCl ₂ , 10 mM MgSO ₄ , 20 mM glucose
TAE (1x)	40 mM Tris-Acetate, 1 mM EDTA, pH 8.0
TE (1x)	10 mM Tris-HCl pH 8.0; 1 mM EDTA
Trypsin/EDTA	0.125 % Trypsin, 0.125 % EDTA pH 8.0, 0.115 % Na ₂ HPO ₄ , 0.8 % NaCl, 0.02% KCl, 0.01 % CaCl ₂ , 0.01 % MgSO ₄
Wash buffer I	2 x SSC, 0.1 % SDS
Wash buffer II	0.2 x SSC, 0.1 % SDS

2.1.17 Equipment

Device	Details	Company
CCD camera system	IVIS 100	Xenogen
Centrifuge for Eppendorf tubes	5415C (rotor F45-18-11) 2K15 (rotor 12145)	Eppendorf Sigma
Centrifuge for Falcon tubes	Varifuge F (rotor BS4402A) ZK 380	Heraeus
Classic E.O.S. processor		AGFA
Freezing container	Cryo 1°C freezing container	NALGENE
Electrophoresis chamber, horizontal (DNA)	Mini-,Midi- gel	Renner
ELISA reader	Thermo Multiscan EX	MWG Biotech
Fluorescence microscope	DM RBE	Leica
Fluorescence microscope (invert)	DM IL	Leica
Gas anesthesia system	XGI-8	Xenogen
Hybridization Oven	Typ 400 HY-E	Bachofer
HybriDot apparatus	HybriDot Manifold	BRL
Incubator	B5061 EC-CO2	Heraeus
IVIS imaging system	IVIS 100	Xenogen
Laminar flow chamber	UVF 6.158	BDK
Light microscope	CK2	Olympus
Luminometer	Lumat LB 9501	Berthold Technologies
Microwave oven	600 W	Bosch
Microplate fluorometer	Fluoroskan Ascent FL	Thermo Labsystems
PCR cycler	DNA thermal cycler	Perkin Elmer
Peristaltic pump	P-1	Pharmacia
pH-meter	Calimatic with electrode 81-02	Knick
Phosphor-Imager	Storm 860	Molecular
Pipetboy	Classid Line	Integra Biosciences
Protein Gel Chamber	Mini-Gel Apparatus Page® Novex®	Invitrogen
Power supplies	EPS500/400 and 600	Pharmacia
QRT-PCR sequence detection system	ABI PRISM 7900	Perkin Elmer
Shaker	Rockomat Labdancer	Tecnorama VWR
Sliding vibratome	VT1000 S – Microtome	Leica
Sonifier	Type 250	Branson
Sorvall centrifuges	RC-5C (rotor SS34, SA600, GS3, SLA1500)	DuPont Instruments
Speed-Vac	Vacuum Concentrator	Bachofer
NanoDrop Spectrophotometer	ND-1000	NanoDrop
Spectrophotometer	Ultrospec 3100 pro	Biochrom
Ultracentrifuge	Sorvall Combi Plus (rotor	Beckman

UV Cross-Linker	SW41, 50.2Ti, 70.1Ti)	Stratagene
UV transilluminator	UV-Stratalinker 1800	Konrad Benda
Vortex mixer	N90 LW 254 nm or 366 nm	Neolab
Water bath	7-2020	Benderund Hobein
	Julabo UC/JulaboSW 20C	

2.1.18 Materials

Before the materials could be used for the study, glass products were sterilized and plastic containers were autoclaved. To ensure sterility and RNase free materials, gloves were worn during handling of the different materials. Cell culture material was treated with 70% ethanol and Incidin[®] sprays to prevent cell culture contamination.

Material	Detail	Company
Cell culture dishes	Ø 3/6/10/15 cm	Greiner/Nunc/Costar
Cell culture flasks	75/175 cm ²	Greiner/Nunc
Cell culture plates	6/12/24/48/96 well	Greiner/Nunc/Costar
Cell scraper		Costar
Collagen coated sterile dishes	Collagen I coated Ø 6/10 cm	Nunc
Concentrator	F96-well plate	
Cover slides	Vivaspin 10kDa	Sartorius
Cryo tube	Ø 1.5 cm	Langenbrinck
Electroporation cuvettes	1.8 ml	Nunc
Eppendorf tubes	0.2 cm gap	Pharmacia
Falcon tubes	0.5/1/2 ml	Eppendorf
Falcon [™] cell culture insert	15/50 ml	BectonDickinson (BD)
Falcon [™] cell culture insert companion plates	Pore size 0.4 µm	BectonDickinson (BD)
Filter paper	6 wells	BectonDickinson (BD)
Flexible assay plate	Ø 125 mm	Schleicher & Schuell
Histoacryl-blue tissue adhesive	96-well	BectonDickinson (BD)
Microtitre plates	1 x 0.5 ml	Braun
Mini quick spin oligo columns	167008	Nunc
Neubauer counting chamber	Sephadex G-50	Pharmacia
Nitrocellulose membrane	HBG	Neubauer
Nylon membrane	PROTRAN BA 85	Schleicher & Schuell
Pasteur pipette	Gene Screen [™]	DuPont
Petridishes	230 mm	WU Mainz
Pipette tips	10 cm	Greiner
Polysorb microtiter plates	2/20/100/200/1000 µl	Eppendorf/Biozym
Quartz cuvette	96 well	Nunc
Roller bottles	500 µl	Pharmacia
Sephadex G25 Column	1L , 2.5 L	Integra Biosciences
Scalpel		Biorad, Richmond
Sterile filter	disposable	Feather
Ultracentrifuge tubes	Pore size 0.2 µm	Schleicher & Schuell
Whatman paper	Quick-Seal	Beckman
X-ray film	Whatman 3 mm	Schleicher & Schuell
	BioMax MS	Kodak

2.1.19 Software

Software	Company / Reference
Adobe Photoshop™ 7.0	Adobe
Clone Manager 9	Sci-Ed Software
Phylodraw	(Morgenstern <i>et al.</i> 1998)
Rasmol 2.7.5	(Sayle <i>et al.</i> 1995)
VMD 1.8.7	(Humphrey <i>et al.</i> 1996)
(Molecular visualization program)	Theoretical and Computational Biophysics Groups, University of Illinois
Image J	(Bearer 2003)
(Image processing and analysis)	

2.2 Methods

2.2.1 Microbiological Methods

2.2.1.1 Cultivation of Bacteria

All used *E.coli* bacteria strains were cultivated in suspension in LB medium with gentle agitation at 160-180 rpm or grown on agar plates (1.5 % Bacto agar in LB medium) at 37°C. Incubation time of bacteria for plasmid amplification was 12-16 h, to produce competent bacteria, only 3-4 h were needed. According to antibiotic resistance on the plasmid to be amplified and to select only transformed bacteria, the appropriate antibiotic (end concentration 100 µg/ml) was added to the culture medium or agar plates.

2.2.1.2 Production of CaCl₂ Competent Bacteria

Non-transformed bacteria were inoculated to a 100 ml LB medium O/N culture (without antibiotics). Next day, 2 ml bacterial culture were transferred to 250 ml fresh LB medium and grown under gentle agitation until an OD₍₆₀₀₎ of 0.5-0.6. The bacterial culture was stored on ice for 10 min, centrifuged at 5000 x g at 4°C for 10 min and resuspended in 50 ml ice-cold 100 mM MgCl₂. After an additional centrifugation time, bacteria were resuspended in 50 ml ice-cold CaCl₂ and incubated on ice for 30 min. Once again, the bacteria were centrifuged down and resuspended in 10 ml ice-cold CaCl₂ (plus 14 % glycerol), aliquoted, flashly frozen in liquid nitrogen and stored directly at -80°C.

2.2.1.3 Production of Electrocompetent Bacteria

To prepare competent cells for electroporation, a single colony of *E.coli* DH5α from a fresh agar plate (without selection antibiotics) was inoculated to 25 ml LB medium and incubated O/N at 37°C under agitation at 200 rpm on a rotary shaker. From the O/N culture, 5 ml were transferred to 400 ml fresh LB medium (without antibiotics) and grown under gentle agitation at 37°C until the bacterial culture had an OD₆₀₀ of 0.5 – 0.55. The culture was then transferred into large centrifuge tubes and cooled down on ice for 15 – 20 min. After a centrifugation time of 15 min at 5000 x g and 4°C, the bacterial cell pellet was resuspended

in 30 ml ice-cold sterile deionized H₂O (dH₂O). Then, resuspended cells were transferred into a dialysis tube and dialyzed against 4 L ice-cold H₂O O/N. Next, bacterial culture was transferred into 50 ml Falcon tubes and centrifuged for 15 min at 4000 x g and 4°C. The bacterial cell pellet was resuspended in 600 µl ice cold H₂O containing 10 % glycerine and the OD₍₆₀₀₎ was measured. The OD₍₆₀₀₎ should be 1 (2.5E+10 cells) to ensure the correct amount of added glycerine, if higher values were measured, the bacterial culture had to be diluted accordingly in more ice cold H₂O containing 10 % glycerine. For storage, 95 µl aliquots of the bacterial cell suspension were dispensed into sterile, ice-cold eppendorf tubes, flashly frozen in liquid nitrogen and stored at -80 °C.

2.2.1.4 Transformation of CaCl₂ Competent Bacteria

To amplify a bacterial plasmid, 100 ng plasmid DNA was incubated for 30 min on ice with 50 µl *E.coli* DH5α (thawed on ice). The mixture was heated at 42°C for 90 sec and cooled down on ice for additional 2 min. Then, the reaction mixture was diluted in 500 µl LB medium without antibiotics and incubated for 45 min at 37°C under gentle shaking at 200 rpm. Transformed bacterial culture (100-200 µl) was plated onto LB-agar-plates containing the appropriate antibiotics and incubated O/N at 37°C.

2.2.1.5 Transformation of Electrocompetent Bacteria

For each electroporation, 100 ng plasmid DNA was incubated on ice for 30 – 60 sec with 50 µl electrocompetent cells (thawed on ice). The DNA/bacteria mixture was then pipetted into an electroporation cuvette (0.2 cm gap) precooled on ice. The cuvette was gently tapped to ensure that the DNA/bacteria suspension is at the bottom of the cuvette without any air bubbles. Fluid was removed from the metal contacts before the cuvette was placed into the Biorad electroporation apparatus. An electrical pulse was set to 25 µF capacitance, 2.5 kV and 200 Ω. The electrical discharge was applied to the bacterial cell mixture and transferred quickly to 2 ml pre-warmed (37°C) SOC medium. After 1 h at 37°C under gentle rotation, 200 µl transformed bacteria was spread out on the LB-agar-plate with the appropriate antibiotics and incubated O/N at 37°C.

2.2.2 Preparation, Modification and Analysis of Plasmid DNA

2.2.2.1 DNA Mini-Preparation

Plasmid DNA preparation was developed according to the principle of alkaline lysis developed 1979 (Birnboim et al. 1979). Plasmid DNA purification is assayed in small-scale by the usage of membrane absorbtion and in large-scale by the adsorption to a matrix bed.

To confirm ligation or to send plasmid DNA for sequencing, a small-scale purification by the peqGOLD Plasmid DNA Mini Kit (PeqLab, Erlangen) was performed. A single colony carrying the desired plasmid was picked from the LB-agar-plate after O/N incubation and inoculated into 3 ml LB medium with the appropriate antibiotic. An O/N bacterial culture (1 ml) was pelleted by centrifugation for 1 min at 10,000 x g, further proceedings for plasmid DNA preparation was implemented according to the manufacturer's instructions.

2.2.2.2 DNA Maxi-, Mega- and Giga- Preparation

For cloning and cell transfection, large amounts of plasmid DNA had to be prepared. Large-scale plasmid DNA preparations are purified by gravity-flow columns (Tip500, Tip2500, Tip10000) as part of the **Maxi-**, **Mega-**, or **Giga-** plasmid DNA preparation kits (Qiagen, Hilden). A single colony picked from a selective LB-agar-plate was inoculated into a starter culture (3 ml, 10 ml, 10 ml) LB medium containing the corresponding antibiotics (ampicillin: 100 µg/ml) and incubated for 8 h at 37°C under vigorous shaking (approximately 300 rpm). The starter culture was diluted 1:500 into fresh LB medium (300 ml, 1 L, 3 L) with antibiotics and grown o/n at 37°C once again under vigorous shaking conditions. The bacterial culture was centrifuged for 15 min at 5000 x g and 4°C. The bacterial pellet was handled according to the manufacturer's instructions for large-scale DNA preparation. The resulting plasmid DNA was dissolved in (250 µl, 600 µl or 1500 µl) dH₂O. The concentration and purity of the plasmid DNA was determined by a NanoDrop ND-1000 spectrophotometer.

Buffers :

P1	50 mM Tris-HCl pH 8.0, 10 mM EDTA pH 8.0, 100 µg/ml RNaseA
P2	200 mM NaOH, 1 % SDS
P3	3 M calium-acetate (Ka-Ac) pH 5.5
QBT	750 mM NaCl, 50 mM MOPS pH 7.0, 15 % ethanol, 0.15 % Triton X-100

QC	1 M NaCl, 50 mM MOPS pH 7.0, 15 % ethanol
QF	1.25 M NaCl, 50 mM Tris-HCL pH 8.5, 15 % ethanol

2.2.2.3 Precipitation and Purification of Plasmid DNA

For DNA precipitation, the sample was mixed with 0.1 vol. 3 M sodium acetate and 2.5 vol. 100 % ethanol. After 1 h at -80°C, the sample was centrifuged 30 min at 16500 x g and 4°C, the supernatant was decanted and the pellet was washed once with 70 % ethanol. After repeated centrifugation, the DNA pellet was resuspended in the appropriate Vol. ddH₂O.

To remove protein contamination from DNA plasmid samples, the same vol. of phenol (50 %)-chloroform (50 %) was added, thoroughly mixed, and left for 5 min at room temperature. After centrifugation for 10 min at 16500 x g, the aqueous phase containing pure, low molecular DNA, was taken off and transferred to a new tube for further analysis.

2.2.2.4 DNA Isolation from Cultured Cells or Animal Tissue

The peqGOLD Tissue DNA Mini Kit provides a rapid method to isolate up to 30 µg genomic DNA from cultured cells or mice tissue. Reversible binding properties of a HiBind® matrix are combined with the speed of mini-column spin technology. Tissue samples were cut up into small pieces (30 mg in total) and placed into a 1.5 ml tube with 200 µl tissue lysis buffer (TL). OP™ Protease was added according to standard protocol, mixed thoroughly and incubated at 55°C O/N in a rotary shaker. In case of isolating DNA from culture cells, up to 10⁷ cells were pelleted by centrifugation for 5 min at 400 x g and resuspended cells in 400 µl TL. After pipetting the lysis sample up and down, 25 µl OB™ Protease was added, mixed thoroughly and incubated at 55°C for 1 h in a rotary shaker. For cell and tissue lysis samples, 220 µl BL Buffer per 200 µl TL Buffer were added and mixed thoroughly. After 10 min incubation at 70°C, 220 µl of absolute ethanol was added per 200 µl TL Buffer. The samples were loaded onto HiBind® columns and centrifuged for 1 min at maximal force. Twice, 700 µl of a Wash Buffer was applied followed by a maximal speed centrifugation step. At next, binding columns were placed into new tubes and dried completely by centrifugation for 2 min at maximum speed before applying 100 µl of the Elution Buffer onto the membrane. After a final incubation time of 3 min at room temperature, samples were centrifuged for 1 min at 8000 x g. Concentration of the extracted DNA was determined by a NanoDrop ND-1000 spectrophotometer.

2.2.2.5 Spectrophotometric Analysis

DNA samples were diluted 1:50 to 1:500 in H₂O and measured at a wavelength of 260 nm in an Ultrospec 3100 pro spectrophotometer. Alternatively, 1 µl DNA sample was measured in a NanoDrop ND-1000 spectrophotometer. An absorption of 1 corresponded to a concentration of 33 µg/ml for ssDNA and 50 µg/ml for dsDNA. The purity of each preparation was determined by measuring the ratio of 260 nm and 280 nm with an optimal value for pure DNA between 1.8 and 1.95.

2.2.2.6 Restriction Digest of DNA

It is of extreme importance to use restriction enzymes in terms of cloning strategies according to manufacturer's protocol. Star-activity and reduced restriction activity can strongly hamper proper cloning results. To test whether specific restriction sites are present in a plasmid of interest, an analytical restriction digest is performed. Digestion of 1 µg DNA with 5 to 10 units of the appropriate enzyme was recommended by the supplier. Together with the instructed reaction buffer and other conditions (temperature, BSA), the total reaction volume should be around 20 µl and after 1 h incubation time, the plasmid should be completely digested. To isolate DNA fragments, a preparative restriction digest is inevitable. About 20 µg plasmid DNA was digested for 4 to 12 h, the total volume of the restriction was 100 µl containing the reaction buffer and up to 80 units of the correct enzyme. To stop a restriction reaction, the digested sample was heat inactivated for 20 min at high temperatures as indicated in the manufacturer's protocols. If the cleavage of the plasmid DNA required a double digest of two restriction enzymes with different reaction buffers or temperature optima, the reactions were performed sequentially. After the first restriction reaction, the DNA was purified by a QIAquick PCR Purification Kit (Qiagen, Hilden) before the second restriction reaction was set up.

2.2.2.7 DNA Agarose-Gel-Electrophoresis

The separation of DNA fragments was carried out according to the fragment sizes in 1 % to 2 % (w/v) agarose gels. Therefore, the adequate amount of agarose was dissolved in 1x TAE buffer by cooking. Cooled down to 60°C, the DNA interjacent agent ethidium bromide (1µg/ml) was added to the solution before it was poured into a gel chamber with an inserted

gel comb to solidify. A 1 % agarose gel was used to separate DNA fragments from 250 bp to 12 kb, for smaller DNA fragments of 100 – 200 bp, 2 % agarose gels were used. A DNA marker was loaded for size determination and quantification of DNA fragments. DNA samples were mixed with 10 x DNA loading buffer before loading. Electrophoresis was carried out at constant 85 V (Minigel) or 100 V (Midigel), 10 V/cm. For analytic gels, separated DNA fragments were visualized under 254 nm UV light and photographed. To extract DNA fragments from a preparative gel, DNA fragments were visualized under 366 nm UV light, avoiding damage of DNA molecules by too intense UV radiation.

2.2.2.8 Preparative Agarose Gel Extraction and Purification of DNA

To extract separated DNA fragments from agarose gels, separated DNA fragments were visualized under 366 nm UV light and gel slices containing desired DNA fragments were excised from the agarose gel with a scalpel. After extraction, DNA fragments were purified by the QIAquick Gel Extraction Kit according to the manufacturer's instructions.

2.2.2.9 Purification of DNA Fragments after a Restriction Digest

DNA fragments ranging from 100 bp to 10 kb were purified from enzyme and its buffer by QIAquick PCR Purification Kit (Qiagen, Hilden) according to the manufacturer's instructions. Alternatively, DNA fragments could also be purified from restriction enzymes by ethanol precipitation. About 0.1 vol. of 3M sodium acetate (pH 5.2) and 2 vol. of ice-cold 100 % ethanol were added to the reaction. To precipitate low concentration of DNA or small DNA fragments, 20 µg glycogen was applied in addition. The mixture was incubated at -20 °C for 2 h or O/N and centrifuged at 16,500 x g for 30 min and 4°C. DNA pellet was washed with 500 µl 70 % ethanol by centrifugation at 10,000 x g for 10 min. Precipitated DNA was air-dried and dissolved in ddH₂O or 10 mM Tris-HCl (pH 8.5).

2.2.2.10 Dephosphorylation of DNA Fragments

To prevent re-ligation or self-ligation of isolated DNA fragments such as linearized vector plasmids in a cloning procedure, calf intestine alkaline phosphatase (CIP) was used to remove 5' phosphates before DNA fragments were used in a ligation reaction. To dephosphorylate DNA fragments, 0.5 µg of purified vector DNA was incubated with 1 U CIP

and 0.1 vol. of 10x CIP buffer at 37°C for 1h. Subsequently, the enzyme was heat-inactivated at 65°C for 20 min. Dephosphorylated DNA fragments were purified by a QIAquick PCR Purification Kit (Qiagen, Hilden) and instantly used in a ligation reaction.

2.2.2.11 Ligation of DNA Fragments

Linearized plasmid DNA was mixed with a double-stranded DNA fragment at a molar ratio of 1:5 to 1:15 (vector: inserted fragment) for a ligation reaction. Between 50 - 100 µg DNA in 20 µl vol. was used for a single ligation reaction. The DNA mixture was incubated with 1 – 2 U of T4-DNA-Ligase plus 0.1 vol. of 10 x T4-DNA-Ligase-buffer added up to its final volume with dH₂O. A negative control lacking insert DNA was additionally set up. The ligation mixture was incubated at 12°C O/N for optimized plasmid-insert interaction. Ligated plasmids were transformed into CaCl₂ competent *E.coli* DH5α (s. 2.2.1.4), colonies were picked, followed by amplification for DNA mini-preparation (s. 2.2.2.1). To assay positive ligation products, DNA restriction digests and sequencing analysis were carried out.

2.2.2.12 Polymerase Chain Reaction (PCR)

PCR is a standard technique which was described first in 1987 and showed to be useful for *in vitro* enzymatic amplification of a specific segment of DNA (Mullis *et al.* 1987). Per 50 µl PCR reaction, template DNA (≤1 µg/reaction) was added to a master mix consisting of 5 µl of MgCl₂-free 10 x PCR buffer (Invitrogen, Karlsruhe), 4 µl of deoxyribonucleoside-triphosphates (dNTPs, 2.5 mM each), 3 µl of 50 mM MgCl₂, 1 µl of each forward and reverse primer (10 pmol each) and was added up with dH₂O to a final volume of 50 µl. The PCR reaction mix was completed with 1 µl Taq-DNA-Polymerase containing a polymerization dependent 5'-3' exonuclease activity (10 units). A negative control without template DNA was also included. The amplification was performed in a PCR thermal cycler using cycling programs optimized for each target and primer pair. In most cases, the amplification reaction was started by an initial denaturation at 95 °C for 1 min, followed by 25 to 35 cycles of denaturation at 95°C for 1 min, annealing from 60°C to 64°C for 1 min and extension at 72°C for 1 min, with a final extension step at 72 °C for 7 min. PCR products were separated by DNA gel electrophoresis on 1 – 2 % agarose gels stained with ethidium bromide. The annealing temperature is a critical step in a PCR. Its temperature depends on the melting temperature (T_m) of the primers.

For sequences less than 14 nucleotides the formula is:

$$T_m [^{\circ}\text{C}] = (wA + xT) \times 2 + (yG + zC) \times 4;$$

For sequences longer than 14 nucleotides, the used equation is:

$$T_m [^{\circ}\text{C}] = 64.9 + 41 \times (yG + zC - 6.4) / (wA + xT + yG + zC)$$

Where w, x, y, z are the number of the bases A, T, G, C in the sequence, respectively.

2.2.2.13 PCR-based Mutagenesis

Amino acid substitutions were performed by a manufacturer's protocol of the QuikChange[®] Site-Directed Mutagenesis Kit (Stratagene, Amsterdam). It is based on the PCR technology but uses the *PfuTurbo* DNA-Polymerase with proof reading activity. A double-stranded DNA plasmid with the sequence of interest was used as a DNA template. Complementary oligonucleotide primer (s. 2.1.1.6) containing the appropriate substitutions were used to be elongated and produced mutant plasmids.

PCR-based Reaction Mix:	Plasmid DNA	1 μl (25 ng)
	Primer	1 μl (each 125 ng)
	dNTP-Mix	1 μl (each 2.5 mM)
	10 x Buffer	5 μl
	100 % DMSO	4 μl
	ddH ₂ O	37 μl

Cycler-Conditions:	Initial Denaturation	95°C, 3 min	
	30 Cycles {	Denaturation	95°C, 2 min
		Annealing	60°C, 2 min
		Elongation	68°C, 12 min
	Terminal Elongation	68°C, 15 min	

To verify the DNA plasmid amplification, 10 μl of the PCR reaction were analysed on a 1 % - agarose gel. Next, 40 μl of the PCR product were digested with *DpnI* at 37°C for 1 h, to remove the methylated, parental DNA plasmid from the product. Of the *DpnI* digested PCR product, 5 μl were mixed with XL1-Blue super-competent bacteria, left on ice for 30 min, heat-shocked for 45 s at 42°C and left on ice for another 2 min. After 500 μl SOC medium

was added, the reaction was left on a rotary shaker for 1 h at 37°C. About 200 µl of each bacteria-mix were plated onto agar plates (containing the appropriate antibiotics) and incubated at 37°C o/n. Colonies were picked, DNA was amplified and send for sequencing to assure inserted mutations.

2.2.2.14 TOPO Cloning

TOPO TA Cloning Kit was used for fast and effective cloning of *Taq* polymerase - amplified PCR products. About 3 µl of the PCR product was incubated with 1 µl pCR2.1-TOPO vector and 1 µl salt solution for 15 min at RT. Then, 2 µl of this ligation reaction was added to a vial of thawed One Shot TOPO10 chemically competent *E. coli*, and incubated on ice for 10 min. The bacteria were heated at 42°C for 30 sec and 250 µl of pre-warmed SOC medium were added. The mixture was incubated at 37°C for 1 h under gentle agitating. Then, 100 µl of the bacterial culture was plated on a LB-agar-plate containing 50 µg/ml kanamycin and 160 µg X-Gal. After an incubation time of 12 h, a blue/white screening could be performed. White colonies, vector plus ligated PCR product, should appear, whereas blue colonies should contain the vector-only plasmids. Therefore, only white colonies were picked for DNA preparation and sequencing.

2.2.2.15 DNA Immobilization on a Nylon Membrane

To immobilize DNA, a nylon membrane (GeneScreenTM, DuPont, Mannheim) and Whatman paper (3 mm) was cut for the measures of a HybriDot apparatus and moistened with 1 x PBS. The Whatman paper was placed into the apparatus with the membrane placed on top of it. The apparatus top was set onto the membrane and sealed tightly to it. Each purified DNA sample was diluted in 300 µl 0.4 M NaOH/10 mM EDTA and spotted onto the nylon membrane. By applying a vacuum to the HybriDot apparatus the DNA samples were transferred to the membrane. Removed from the Dot-Blot apparatus, the membrane was placed into a denaturation buffer (1.5 M NaCl, 0.5 M NaOH) for 10 min to obtain only ssDNA. Subsequently, a treatment with neutralization buffer (0.5 M Tris-HCl pH 7.0, 0.3 M Tris-Sodium-Citrate, 3 M NaCl) was carried out for 10 min. DNA was fixed on the nylon membrane by UV-crosslinking at 1200 Joule in a UV cross-linker. The membrane was stored at RT until DNA labeling was performed.

2.2.2.16 Radioactive DNA Labeling

A DNA fragment used as a DNA probe (s. 2.1.8) was digested and then purified from a 1 % agarose gel. To label the DNA fragment, a Random Primed DNA Labeling Kit was used (Roche, Mannheim). About 100 ng DNA fragment was added up to 9 µl with dH₂O. The DNA was denatured by 10 min at 99°C, followed by a rapid transfer to ice afterwards. The denatured DNA was mixed with 2 µl hexanucleotide mix (containing 10 x reaction buffer) and 1 µl of each unlabeled dATP, dGTP, and dTTP. In a control area, 5 µl [α -³²P] dCTP (50 µCi) was added and completed with 1 µl Klenow enzyme. The mix was incubated for 2 h at 37°C, placed on ice and the reaction was stopped by adding 150 µl TE (pH 8.0). DNA probe purification from unincorporated dNTPs was achieved by mini quick spin column (Sephadex G-50, Roche, Mannheim). The mini column was centrifuged for 1 min at 3000 rpm and the flow-through was discarded. Afterwards, the labelling mixture was applied onto the center of the column matrix and the column was centrifuged for 3 min at 3000 rpm. The flow-through containing the labeled probe was saved and the cpm value was measured. Then, the labeled DNA probe was denatured by heating at 95°C for 10 min and a rapid transfer to ice. After the addition of 450 µl hybridization buffer (125 mM Na₂HPO₄, 250 mM NaCl, 1 mM EDTA, 45 % formamide, 7 % SDS), the probe was used for O/N DNA labeling.

Before labeling, the nylon membrane with immobilized template DNA had to be pre-hybridized in 15 – 20 ml hybridization buffer in a glass tube for 1 h with rotation at 42°C in a hybridization oven. Then, the denatured, radioactively labeled DNA probe was added directly to the membrane, and incubated O/N with rotation at 42°C. The next day, the membrane was washed 6 x 5 min with wash buffer I (2 x SSC, 0.1 % SDS) at 42°C and 3 x 20 min with wash buffer II (0.1 x SSC, 0.1 % SDS) at 68 °C, air dried, and exposed to an X-ray film in a radiographic cassette for one to several hours at RT. At last, the film was developed in a Classic E.O.S. processor.

2.2.2.17 DNA Sequencing and Sequence Analysis

DNA sequencing was performed by the company MWG (Ebersberg). About 1 µg purified DNA per sample was sent. Sequencing was assayed according to the developed principal of Sanger *et al.* (Sanger *et al.* 1977) by high-throughput sequencing machines. However, the

used technology changed from using radioactive-labeled nucleotides to fluorochrome-labeled dideoxynucleotides. Sequence analysis was performed by Clone-Manager software.

2.2.3 Cell Biology Methods

2.2.3.1 Cultivation of Cells

Adherent cell lines were maintained in monolayer cultures in DMEM supplemented with 10 % FCS, 2 mM L-glutamin, 100 µg/ml penicillin/streptomycin. Cells were cultured in cell culture flasks at 37°C, 5 % CO₂ and 95 % humidity. For passaging, cell medium was removed and cells, they were washed with PBS before 2 ml 0.025 % trypsin-EDTA solution was added. As soon as the cells completely lost their adherence to the plastic surface, cells were resuspended in fresh growth medium and according to their dilution factor (1:2 until 1:10), the correct amount of cells was added to new culture flasks or dishes, incubated at 37°C, 5 % CO₂ and 95 % humidity until the next passaging.

2.2.3.2 Determination of Number of Viable Cells

To determine the exact cell number, cells were washed, trypsinized (s. 2.2.3.1) and medium was added to transfer cells to a 50 ml Falcon tube. To count the cells, a 10 µl aliquot of the cell suspension was mixed with 10 µl of Trypan Blue which permeates into dead cells and stains them blue. Next, 10 µl were transferred on a Neubauer-counting-chamber and cells were counted in the four squares consisting of 16 small squares. The mean value of the four squares, multiplied by the dilution factor 2 and the chamber factor 1×10^4 , the cell number per ml was calculated. Total cell number depends on the amount of medium the cells were suspended in.

2.2.3.3 Cell Cryo-Conservation

To conserve a cell lines, cryo-conservation is used. About 1×10^7 cells were pelleted by centrifuging for 10 min at 220 x g, were resuspended in 1 ml of an ice cold solution containing 90 % FCS and 10 % DMSO and transferred into a cryo-tube. Cells were slowly

cooled down in an isopropanol isolated container at -80°C (temperature is reduced 1°C per minute) for at least 24 h before long-term storage in liquid nitrogen. Frozen cells were rapidly thawed at 37°C and transferred into 10 ml pre-warmed medium. To remove DMSO, cells were sedimented by centrifugation at 200 x g for 10 min, medium was aspirated and 10 ml fresh medium DMEM (+Glu, +P/S) was added. Cells were decollated and transferred into a small flask for further cultivation. Before an experiment could be performed, cells had to be passaged at least twice.

2.2.3.4 Cultivation of Hybridoma Cells

Hybridoma cells and X63/Ag8 cells were grown in RPMI 1640 containing 10 % FCS, 1 % penicillin/streptomycin, 2 % of 1 M Hepes (pH 7.2), and 0.35 % of 1:1000 diluted β -mercapto-ethanol. Occasionally, 10 % of Condimed B1 was added to boost cell viability. Cells were expanded by moving them into roller bottles for production of hybridoma supernatant.

2.2.3.5 Isolation of Primary Hepatocytes

Male B6 mice (7-9 weeks old) were anesthetized by an intraperitoneal injection of 50 μ l – 70 μ l undiluted 1:1 mix Ketamin/Rompun before the surgery. Hanks I and Hanks II solution were placed into a waterbath (42°C) to ensure 37°C solution temperature at the perfusion tube; the flow rate was 8 ml/min, the peristaltic pump was running continuously. The mouse was fixed to a rack within a basin to catch up released blood, the abdomen was opened and fur was folded to the sides. In the peritoneal cavity, the portal vein was kept under light tension with a tweezer and the catheter was flatly inserted into the vein and fixed. To avoid pressure increase within the liver, the vena cava was cut, the liver was perfused with Hanks I solution for 3 min. The mouse was finally sacrificed by cutting the Aorta, the liver was moistened with adhesion medium at all time. Perfusion was changed to Hanks II solution for 5 min and was stopped as soon as the liver was softening and hairlines became visible. Liver capsule was extracted and transferred into pre-warmed adhesion medium (20 ml for 2 livers). Under the sterile hood, the liver capsule was fixed with a pair of broad tweezers at the *ligamentum*, the capsule was opened and gently shaken to release cells into a sterile crystallisation dish. Cells were transferred through a 70 μ m strainer into a 50 ml Falcon tube and added up with adhesion medium to 40 ml volume. Cells were centrifuged down at 37.5 g for 2 min and the supernatant was carefully removed afterwards. Adhesion medium was added carefully in

four 10 ml steps to 40 ml total volume, followed by the previously described centrifugation step. After another resuspension step, cells were counted. Cell viability had to be at least 50 %. About 4×10^6 primary hepatocytes were added to a collagen-coated 10 cm dish (Collagen I coated plates, Nunc, Langensfeld), 1×10^4 cells were added to each well of a collagen-coated 96-well plate. After 4 h, cells had adhered to the plate surfaces and adhesion medium was exchanged with stimulation medium. After 24 h, primary hepatocytes were used either for transduction (s. 2.2.4.1) or AAV 8 library *in vitro* selection (s. 2.2.7.7).

Hanks Buffer (2L)	16 g NaCl 7.1 g Hepes 800 mg KCl 120 mg $\text{Na}_2\text{HPO}_4 \cdot 2 \text{H}_2\text{O}$ 120 mg KH_2PO_4 Adjust pH to 7.4, autoclave
Hanks I Solution	400 ml Hanks buffer 1mM EGTA (complexing of ions) 10 % Glucose
Hanks II Solution	400 ml Hanks buffer Collagenase CLS II (3 mg/ml) 10 mM $\text{CaCl}_2 \cdot 2\text{H}_2\text{O}$ 1 % Glucose
Adhesion Medium	Williams E medium (Sigma-Aldrich, Munich) 10 % FCS 1 % P/S 2 mM Glutamine Insulin (0.01 mg/ml) 100 nM Dexamethason
Culture Medium	Williams E medium (Sigma-Aldrich, Munich) 10 % FCS 1 % P/S 2 mM Glutamine

2.2.3.6 Primary Neonatal Rat Cardiomyocyte Isolation

Cultured primary neonatal rat cardiomyocytes were prepared as previously described (Jacobson *et al.* 1985). For one preparation, 20 – 25 neonatal Sprague-Dawley rats (1-3-day-old) were decapitated and semi-sterilized by a short ethanol bath. Hearts were removed under sterile conditions, immersed in pre-chilled balanced salt solution (1 x Ads buffer) in a

cell culture dish, and dissected into pieces with a scissor. The 1 x Ads buffer was then carefully aspirated and the crude heart pieces were initially treated with collagenase/pancreatin solution (digestion buffer, 1 ml per heart, pre-warmed to 37 °C) in a tissue culture flask under constant shaking at 120 rpm for 30 min in a 37°C water bath. The supernatant was carefully removed from the heart pieces and discarded since it contained mostly non-myocytes, broken cells and red blood cells. Homogenized heart pieces were resuspended in digestion buffer and subjected to the first round of 20 min collagenase/pancreatin digestion in the culture flask under constant agitation at 120 rpm in the 37 °C water bath. The digest 1 (supernatant) was transferred to a 50 ml falcon tube containing 2 ml newborn calf serum (NCS). The remaining heart pieces were processed to the next digestion round under the same condition. The digest 1 mixed with NCS was centrifuged for 5 min at 800 x g and RT. The cell pellet (from digest 1) was resuspended in 4 ml fresh NCS and transferred to a clean 50 ml falcon tube before keeping in a 37 °C and 5 % CO₂ incubator with the cap loosened. After typical 4 rounds of collagenase/pancreatin digestion, pooled cells (from digest 1, 2, 3 and 4) were pelleted by centrifugation for 5 min at 800 x g and RT and resuspended in 4 ml 1x Ads buffer. The cardiomyocytes in the cell suspension were purified by using a discontinuous Percoll gradient (Figure 2-1). 4 ml cell suspension was slowly loaded on top of the Percoll gradient which was freshly made by loading 4 ml top layer in a 15 ml falcon tube, followed by 3 ml bottom layer. The step gradient was centrifuged for 30 min at 2000 x g and RT. The cardiomyocyte enriched fraction sedimenting between two Percoll layers was suck out with a pipette and washed twice in 25 ml 1x Ads buffer by centrifugation for 5 min at 800 x g and RT. The resulting cell pellet was resuspended in 4 ml DMEM-high glucose medium. Cell yield was counted in a hemocytometer under the light microscope. Approximately 4 x 10⁶ primary cardiomyocytes were generated from 20 – 25 individual hearts per preparation.

Collagen-coated 10 cm dishes (Nunc, Langensfeld) were used and cardiomyocytes were allowed to adhere to dishes for 24 h incubation at 37 °C and 5 % CO₂ before DMEM-high glucose media was exchanged by fresh medium. Cells maintained viable in culture for 10 –14 days as long as media was replaced regularly every two days.

10 x Ads Buffer

68 g/l NaCl,
47 g/l HEPES,

13 g/l NaH_2PO_4 ,
 10 g/l, glucose,
 4 g/l KCl, 1 g/l MgSO_4 , pH 7.4

Collagenase/Pancreatin Solution

1 x Ads buffer
 0.5 mg/ml collagenase
 0.6 mg/ml pancreatin

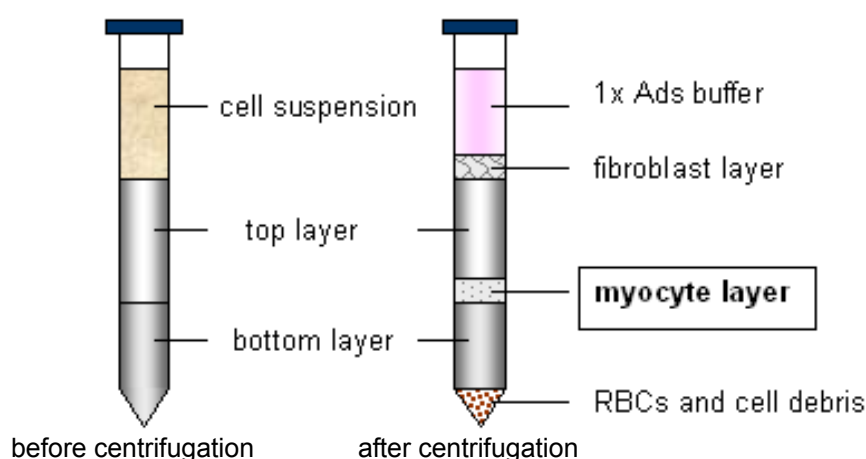


Figure 2-1 Scheme of a discontinuous Percoll gradient for the purification of cardiomyocytes. The positions of the Percoll density layer before centrifugation are shown on the left. After a 30 min centrifugation, the myocyte-enriched layer sedimenting between two Percoll layers was saved.

2.2.3.7 Organotypic Culture of Mouse Liver Tissue Slices

Organotypic culture (OTC) was carried out using methods adapted from previously published protocols (Stoppini *et al.* 1991; Hailer *et al.* 1998). Liver tissue slices were prepared from NMRI mice using a sliding vibratome (VT1000 S - Microtome). After liver extraction from the mouse abdomen, the tissue was placed shortly into 70 % ethanol, dried on a filter paper and adhered onto the specimen disc using histoacryl tissue adhesive. The specimen disc was then inserted into the buffer tray mounted inside the cooling bath (4°C). The liver freshly fixed to the disc was immersed in cooled preparation medium and sectioned to slices of 300 μm thickness under continuous knife feed at the speed of 0.05 mm/s. Obtained slices were transferred to Falcon cell culture inserts (pore size 0.4 μm) in 6-well plates using the cut

Pasteur pipette with fire-polished edges. The drop of extra preparation medium was aspirated afterwards. The slice was fed with 1 ml of culture medium (pre-warmed to 37°C) applied under the insert incorporating polyethylene terephthalate (PET) track-etched membrane. In this condition, media did not cover the membrane of the insert so that the explanted liver slices remained well exposed to the air (Figure 2-2). Diffusion through the membrane was sufficient to insure survival of hepatocytes, if maintained in culture at 37°C with 5 % CO₂. After 24 h, recombinant AAV vectors were added to the medium below the tissue slices. Slices were incubated for 4 days and were immediately prepared for luciferase expression analysis (s. 2.2.4.7).

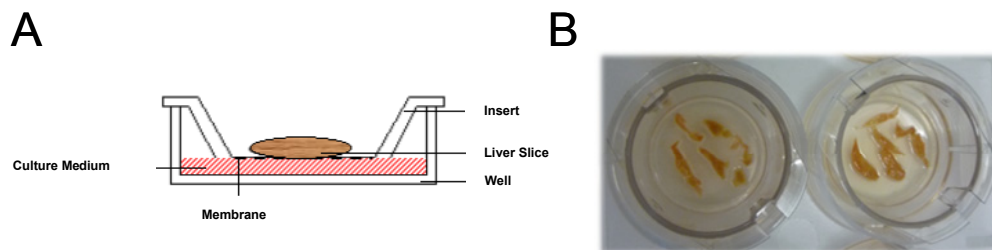


Figure 2-2 Organotypic culture of liver tissue. A) Schematic representation of optimal culture conditions of an OTC, liver slice is placed onto a membrane on top of culture medium. B) Picture taken one day after OTC was started. At least 4-6 organ slices have to be placed onto a single membrane to measure luciferase expression after rAAV vector transduction.

Preparation Medium	95 % MEM, 5 % 2 mM L-glutamine, pH 7.4
Culture Medium	50 % MEM, 25 % HBSS, 25 % NHS, 7.5 % Natriumbicarbonat, 2.5 % HEPES, 1 % 2 mM L-glutamin, 2.4 mg/ml glucose, 50 µg/ml gentamicin, 1 µg/ml insulin, 0.8 µg/ml vitamin C, pH 7.4, sterile filtration
Agarblock Solution	125 mM NaCl, 5 mM KCl, 2 mM MgSO ₄ ·7H ₂ O, 1 mM NaH ₂ PO ₄ , 9 mM glucose, 2 mM CaCl ₂ ·H ₂ O
Agarblock	5 % agar in agarblock solution

2.2.3.8 Transfection of Cells

2.2.3.8.1 Calcium Phosphate (CaPO₄) Transfection

The transfection of human 293T cells was performed by the CaPO₄ method (Naldini *et al.* 1996). One day before transfection, 5×10^6 293T cells were seeded out in 20 ml medium into a 15 cm (\emptyset) culture dish, to ensure 60 – 70 % confluency at the time of transfection. For each 15 cm (\emptyset) dish, 45 – 55 μ g plasmid DNA was resuspended in 1.125 ml sterile Braun H₂O and mixed with 125 μ l of 2.5M CaCl₂. Under constant mixing conditions, 1.25ml of 2 x HBSS was added. The mixture was incubated for 1 min at RT and carefully applied onto the cells. Cells were then incubated for 36 – 48 h at 37°C and 5 % CO₂ before harvesting.

2.2.3.8.2 PolyFect Transfection

One day in advance, 5×10^6 293T cells were seeded out in 20 ml media per 15 cm (\emptyset) culture dish, to ensure 60 – 80 % confluency on the day of transfection. The medium was replaced with fresh medium 2 h before transfection. Per 15 cm (\emptyset) dish, 12 μ g total plasmid DNA was diluted in medium containing no FCS, glutamin, penicillin or streptomycin, to a total volume of 450 μ l. The DNA solution was mixed with 120 μ l of PolyFect (Invitrogen, Karlsruhe) by vortexing for 15 sec. The mixture was incubated for 10 min at RT and mixed with 1ml of fresh media containing 10 % FCS and 1 % penicillin/streptomycin. The transfection complexes were carefully added to the cells. Cells were incubated for 12 – 16 h at 37°C and 5 % CO₂ before replacing the cell culture media. All cells were then incubated for additional 24 – 48 h before harvesting.

2.2.4 Virological Methods

2.2.4.1 Infection and Transduction of Cultured Cells

Previous to cell infection, cell medium was exchanged by fresh medium. The amount of viral particles used in an infection strictly depended on type of experiment and cell type infectivity. For a transduction assay, cells were infected with MOI (multiplicity of infection) of 1000, washed off 6 h after the infection and incubated for 3-4 days before they were harvested for a luciferase gene expression analysis (s. 2.2.4.7). To isolate targeted AAV8 vectors from random AAV8 display peptide libraries *in vitro*, infections were performed on cultured cells with the recombinant vectors at low MOI (MOI 1-100). After 4 h incubation at

37°C and 5 % CO₂, cells were washed with PBS, followed by superinfection with adenovirus type 5 (Ad5) at a specific MOI. The infection was continued until 50 % of a cytopathic effect was observed.

2.2.4.2 AAV Harvest after Transfection

AAV particles were scraped off into medium of the cell dishes 48-62 h after transfection, and transferred into 50 ml Falcon tubes and sedimented by centrifugation for 10 min at 500 x g and RT. The cell pellet was washed in PBS and centrifuged once again. At next, the cell pellet was resuspended in virus lysis buffer (150mM NaCl, 50mM Tris-HCl, pH8.5; 1ml per 10⁶-10⁷ cells). After 3 freeze/thaw cycles (-196°C/37°C), AAV vectors were released from the cell debris into the cell supernatant lysate. Vectors still bound to cellular debris were released into the buffer by a 1 min ultrasound bath (30 W). The cell lysate was treated with Benzonase (50 U/ml) for 30 min at 37°C to remove unpackaged plasmid DNA. The debris was removed from the lysate by an additional 10 min centrifugation step at 4000 x g and 4°C.

2.2.4.3 Large-Scale Production and Purification of AAV Particles

A large-scale AAV vector production was generated by a transfection of 20 15 cm (∅) dishes. Particles were harvested, pooled in 1 Falcon tube and purified rudimentarily from cell debris (s. 2.2.4.2). To increase purity, an iodixanol step gradient was performed (Zolotukhin *et al.* 1999). The lysate (about 20 ml) was loaded in a 40 ml Beckman Quick Seal tube, followed by underlying 7 ml 15 % iodixanol in PBS-MK containing 1 M NaCl, 5 ml 25 % iodixanol in PBS-MK (plus phenol red to achieve a red color), 4 ml 40 % iodixanol in PBS-MK, and 4 ml 60 % iodixanol in PBS-MK (plus phenol red for a yellow color). After a precise balance, the tubes were sealed and ultracentrifuged at 50,000 x g and 4°C for 2 h in a Ti 50.2 rotor. The 40 % iodixanol fraction (about 3 ml) containing mostly full, genome containing particles, was recovered by piercing the side of the tube with a needle and withdrawing the solution without aspirating the 25 % iodixanol phase. For transfections less than 10 x 15 cm (∅), less cell lysate volumes (5 ml) were obtained and loaded onto 12 ml gradients of the Beckman Quick Seal tubes. In this case the gradient consists of a phase with 3 ml 15 % iodixanol in PBS-MK containing 0.75 M NaCl, 2 ml 25 % iodixanol in PBS-MK, 1.5 ml 40 % iodixanol in PBS-MK, and 1.5 ml 60 % iodixanol in PBS-MK. Gradients were centrifuged in a Ti 70.1 rotor

under identical conditions. About 1 ml of the 40 % is aspirated in the smaller purification gradient. In both cases, withdrawn viral vectors are immediately frozen and stored at -20°C until further usage.

PBS-MKPBS plus 1 mM MgCl₂ and 2.5 mM KCL.**2.2.4.4 Titration of AAV Vector Stocks**

Several methods were used to determine viral genome containing particle or capsid titers of AAV vector preparations. Determination of AAV vector titres were performed either by electron micrographs, by DNA dot blot, qRT-PCR or by ELISA.

2.2.4.4.1 Electron Microscopy of AAV Vector Productions (Negative Staining)

In order to judge the quality and determine the amount of AAV particles after purification, negative staining of viral particles was performed. Five µl of a purified virus stock were spotted onto a carbon coated copper grid. After 2 min the liquid was removed by capillary action using Whatman paper and the grid was washed 3 x with PBS. Negative staining of viral particles was achieved by adding 2 % uranyl-acetate for 1 min and air drying the grids. The particles were visualized using a Zeiss EM 10-electron microscope at 80 kV. At least three independent areas of a grid containing a specific serotype were photographed at a magnification of 20 000, particles were counted and the average number of particles determined. The titer was calculated based on a previous determination that 8x10¹² particles/ml equal 4640 particles at a magnification of 20 000 in one EM picture.

2.2.4.4.2 AAV2 Capsid ELISA

The AAV2 capsid titres (capsids/ml) of purified AAV2 vector productions were determined by a commercially available Titration ELISA Kit against AAV2 (Progen, Heidelberg). Vector samples were diluted 1:10 and 1:100 in Wash Buffer before they were added to a capsid-specific A20 (monoclonal antibody specific against AAV2 capsids) coated 96-well-microtiter plate. As a standard, supplied empty AAV2 capsids were serially diluted (start concentration of 1 x 10⁹ – 1 x 10¹⁰ particles/ml) according to manufacturer's protocol. Then, 100 µl of diluted standard and vector samples were added to one well of the microtiter strip. After a 1 h incubation time at 37°C, wells were washed three times with Wash Buffer and incubated for 1 h at 37°C with 100 µl biotinylated A20 (1 µg/ml in Wash Buffer). After repeated

washing, 100 µl/well of streptavidin peroxidase (0.8 µg/ml in Wash Buffer) was incubated for 1 h at 37°C. Three additional washing steps were performed before 100 µl TMB substrate solution (Sigma-Aldrich, Deisenhofen) was added. The resulting color reaction was stopped with 100 µl of 1 M H₂SO₄ per well after 5 min. The color intensity was measured at 450 nm in an ELISA-reader. A titration curve was obtained by plotting the OD reading of the serially diluted standards against their corresponding concentrations. The readings of AAV samples that fell into the linear range were taken and the capsid titers could be determined. Establishing an ELISA for other AAV serotypes will be described in the section 2.2.6.6.

Wash Buffer PBS-T	0.05 % Tween 20 in PBS
TMB Substrate Solution	0.01 % TMB (3,3',5,5'-Tetramethylbenzidine)
	0.1 M Na-Acetate, pH 6.0
	0.003 % Peroxide in dH ₂ O

2.2.4.4.3 DNA Dot-Blot Assay

This method was performed to determine the number of viral genome containing particles. First, 10 – 20 µl of crude lysate viral vector samples or purified viral vectors were incubated with 60 U MNase and 200 µl MNase buffer at 37°C for 3 h to remove not-encapsidated plasmid DNA. The second digestion was performed with 100 µg Proteinase K and 200 µl 2 x Proteinase K Buffer for 3 h at 37°C. DNA was purified from the protein contaminants by pheno-chloroform extraction. 1 vol. of phenol-chloroform-isoamylalcohol was mixed thoroughly with the digested samples by vortexing. The mixture was centrifuged at 16,500 x g for 10 min. The top (aqueous) phase containing the pure DNA was carefully removed and transferred to a new tube. Extracted DNA was then purified by ethanol precipitation (1/10 vol. of 3 M sodium acetate, 40 µg glycogen, and 2 vol. of 100 % ethanol). After o/n storage at -20°C, the samples were centrifuged at 16,500 x g for 10 min. Supernatant was aspirated and the DNA pellet was washed with 70 % ice-cold ethanol and centrifuged again. The DNA pellet was air dried and dissolved in 300 µl sample buffer (0.4 M NaOH, 10 mM EDTA). Aliquots of 270, 27 and 2.7 µl were mixed with sample buffer and filled up to a final volume of 300 µl. To generate a standard curve, pUF2CMV-Luc plasmid DNA harboring the CMV promoter, was serially diluted from 25 ng down to 0.04 ng in sample buffer. Sample and standard DNA were transferred and immobilized to the nylon membrane as described (s. 2.2.2.15). To detect the immobilized genomes, a *rep*-specific probe consisting of a 1477 bp *Sall* restriction fragment

of plasmid pTAV2.0, or a CMV-specific probe consisting of a 620 bp *XhoI-EcoRI* restriction fragment of plasmid pUF2CMV-Luc, was labeled with α - ^{32}P (s. 2.2.2.16) and hybridized to the target DNA immobilized on the membrane. Autoradiography was carried out and the hybridization signal intensity was quantified using a Phosphor-Imager and the ImageQuant 5.1 software. The particle titers were calculated based on the values obtained from the standard samples.

2.2.4.4.4 Quantitative Real-Time PCR

To quantify AAV genome containing particles also in productions with low AAV vector titres, quantitative real-time PCR (qRT-PCR) was adapted from previously described methods (Veldwijk *et al.* 2002). An alkalic lysis was performed to release viral DNA from the AAV particles, 10 μl of purified virions or MNase-treated crude viral vector samples were incubated with 10 μl TE and 20 μl 2M NaOH for 30 min at 56°C. The reaction was neutralized by the addition of 19 μl 2M HCl and 941 μl sterile Braun-H₂O. A negative control containing only sterile Braun-H₂O as well as a positive control with known genomic titre was included. A standard was prepared in a 10-fold serial dilution, ranging from 3.5×10^8 to 3.5×10^1 Vg/ml. Reaction was set up in 20 μl with 1 x *TaqMan* Universal PCR Master Mix, 0.3 μM of relative primer/probe set and 3 μl template in triplicate for the standard, or in duplicate for the sample. Q-RT-PCR was carried out by an ABI PRISM 7900 sequence detection system, the following amplification conditions were used: 2 min at 50°C for the destruction of PCR contaminations by AmpErase, 10 min at 95°C for polymerase activation and initial denaturation, followed by 40 cycles of denaturation at 95°C for 15 sec and annealing/extension at 60°C for 1 min. The data were analyzed using the Sequence Detector version 2.1 software.

2.2.4.4.5 Replicative Titer Determination

Infectious AAV vectors were quantified by determining the amount of replicative particles/ml as previously described (Grimm *et al.* 1998). About 5×10^3 HeLa cells were seeded into each well of a 96-well plate, 24 h before infection. The next day, the medium was exchanged with DMEM containing 2 % FCS. Cells were infected with 10-fold serial dilution (ranging from 1:10 to 1:10¹²) of the AAV samples. After 2 h incubation at 37°C, 5 % CO₂, and 95 % humidity, cells were over-infected with Ad5 with MOI 10 (plaque-forming units (pfu) per cell). About 72 h later, cells were lysed in 100 μl 1.5 M NaOH after three

freezing/thawing cycles at -196°C and 37°C, respectively. The cells were centrifuged at 500 x g for 10 min and 200 µl of the cell lysates containing the replicative AAV particles were pipetted to the nylon membrane in a HybriDot apparatus. After vacuum was applied, the membrane was removed from the HybriDot apparatus, denatured and neutralized as previously described (s. 2.2.2.15). DNA was fixed to the nylon membrane by UV-crosslinking at 1200 Joule in the UV cross-linker. The replicative AAV genomes immobilized on the membrane were detected by a radioactive labeling with a *rep*-specific probe after hybridization analysis (s. 2.2.2.16). Titers of infectious particles were deduced from the highest dilution of each sample which gave a positive hybridization signal.

2.2.4.5 Heparin Binding Analysis of rAAV Vectors

About 1 ml Heparin agarose (Sigma-Aldrich, Deisenhofen) was placed into a glass column and equilibrated with 20 ml PBS-MK. About 5ml PBS-MK containing 1×10^{11} Vg of an AAV vector was pipetted onto the heparin agarose bed. The flow-through was collected in a 15 ml Falcon tube. The heparin agarose bed was washed twice with 5 ml PBS-MK, both wash run-throughs were collected. To elute possible bound vector particles, 5 x 2 ml PBS (+1 M NaCl) was added to the column. Flow-through, wash run-through 1 and 2 as well as first and second elution sample were analysed for AAV vector presence by AAV2 Capsid ELISA (s. 2.2.4.4.3) or DNA Dot-Blot (s. 2.2.2.15).

For the heparinase assay, 1×10^5 HeLa cells were seeded out into each well of a 6-well dish. After 24 h, medium was removed from the cells and washed with 1 x GAG Buffer. Heparinase I (10 mIU) and Heparinase III (1mIU) (Sigma-Aldrich, Deisenhofen) were added to each well, added up to 500 µl with GAG buffer and incubated for 2 h at 37°C. After the incubation time, 1 x GAG Buffer added to each well. Cells were transduced at MOI 1000 (according to viral genome containing particles and harvested 2 days later. Results were determined by a luciferase reporter expression assay.

1 x GAG Buffer

1 x PBS, 0.1 5 BSA, 0.2 % gelatine, 0.1 % glucose

2.2.4.6 AAV Cell Binding and Entry

Cell binding of AAV vectors could have been impeded by peptide insertion into the capsid. It was important to determine the binding ability of mutant vectors to the cells. For the binding assay 1×10^6 HeLa cells were seeded out on 6 cm^2 plates one day in advance. The medium was exchanged with 2 ml FCS-free medium and plates were transferred to 4°C , after 10 min cells were infected with viral vectors (MOI 1000 - MOI 10,000) for 40 min. Every 10 min, plates were shaken to moisture all cells on the plate. After the incubation time, cells were washed twice with cold PBS and were either transferred to 37°C , 5 % CO_2 , with a proper amount of fresh medium for a cell entry analysis or directly scraped into 2 ml PBS for binding analysis. In case of the binding analysis, cells were collected in tubes and centrifuged down at $2000 \times g$, 10 min. Medium was aspirated and pellets were stored at -20°C until the DNA dot blot assay could be performed (s. 2.2.4.4.3). For the entry experiment, cells were kept another 6 h at 37°C , washed twice with PBS and then scraped off into 2 ml medium. After a centrifugation step ($2000 \times g$, 10 min), medium was aspirated from each tube and 200 μl pre-warmed trypsin (0.025 %) was added to each sample. After 5 min, 800 μl DMEM medium was added and the centrifugation step was repeated. Medium was aspirated and pellets were stored at -20°C until further DNA analysis.

2.2.4.7 Luciferase Transgene Expression

To measure the *in vitro* transduction efficiency of viral vectors containing a luciferase reporter transgene, a luciferase expression assay was carried out. A 12-well plate was used, seeded cells should have a 60 % confluency on the day of infection. Next day, cells were infected with an MOI 10 -10000 of the different recombinant AAV vectors. Infected cells were kept at 37°C in 5 % CO_2 and 95 % humidity until harvest after 3-4 days. To harvest the cells, the medium was aspirated, cells were washed with 300 μl PBS and 200 μl 1 x RLB (Promega, Mannheim) was added to each well. The 12-well plates were stored at -80°C until the luciferase expression analysis was assayed. For expression analysis, infected cells and luciferin (Promega, Mannheim) were thawed at RT, 20 μl of the thawed cell lysate was added to a luminometer tube and mixed with 50 μl luciferase assay reagent. Light activities were

measured with a luminometer (Lumat LB9501; Berthold). The emitted photons were measured for 10 seconds to determine the relative light units (RLU) for each well.

For *in vivo* expression analysis, extracted organs of an injected animal were shock frozen in liquid nitrogen and stored at -80°C until further analysis. Before expression analysis could be performed, $1\ \mu\text{l}$ $1 \times \text{RLB}$ was added per mg organ, the organ samples were homogenized and incubated for 10 min at RT. Samples were centrifuged at $10,000 \times g$ for 10 min and the supernatant was transferred into a new tube. Expression analysis with a luminometer was performed as described previously. However, procedure and settings were changed, $50\ \mu\text{l}$ sample plus $100\ \mu\text{l}$ luciferin were used and emitted photons were measured for 20 seconds to determine RLU per organ. Due to differences in protein amounts, it was important to also determine the complete protein amounts in every sample by NanoOrange technology (Invitrogen, Karlsruhe) (s. 2.2.5.2).

2.2.4.8. AAV *In Vivo* Application and Analysis

All animal experiments were carried out in the isolator station of the DKFZ. Under the guidance of M. Friedel, mice were intravenously (iv) injected with 1×10^{11} viral genomes. Normally, 4 mice were injected per mutant vector. One month later, animals were injected with $200\ \mu\text{l}$ of D-luciferin (Synchem, Illinois) and imaged with the IVIS imager system (IVIS 100, Xenogen, Illinois) for 5 min, 10 min after injection.

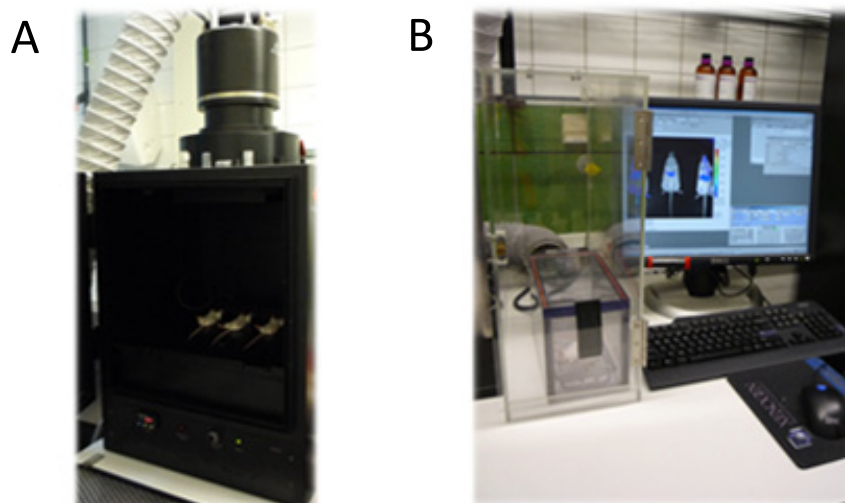


Figure 2-3 IVIS Imaging System. A) Dark chamber with the camera and scanner equipment measuring and calculating luciferase or fluorescence protein expression in organs or tumors while mice are sedated. B) Narcotic chamber to prepare mice for the analysis and imaging software to evaluate protein expression profiles.

2.2.5 Protein Biochemical Methods

2.2.5.1 Bradford Method

Large protein concentrations (Range: 0.5 µg/ml to 1.5 mg/ml) were determined by the DC-Protein Assay-System (BioRad, Munich) based on the Bradford method. For each sample or standard, 25 µl was mixed with 125 µl of reagent A, followed by 1 ml of reagent B and immediate vortexing. Samples were incubated for 15 min before measuring at absorbance 750 nm. Protein concentrations were determined by using a standard curve.

2.2.5.2 NanoOrange[®] Method

If the protein concentration ranged between 100 ng to 10 µg per ml, the NanoOrange[®] Protein Quantitation Kit (N-6666, Invitrogen, Karlsruhe) was used. For 16 samples with three dilution steps as well as a BSA standard, the Working Solution was prepared (2.5 ml Diluent, 22.5 ml H₂O plus 50 µl Reagent). Homogenized mice tissue samples were diluted 1:1000, 1:2000 and 1:4000 in Working Solution and 200 µl of each dilution step was transferred into a well of a V-shaped 96-well plate (Nunc, Langenselbold). The BSA standard was supplied at a concentration of 2 mg/ml, was also diluted in Working Solution to recommended concentrations (10 µg-6 µg-3 µg-1 µg-0 µg per ml) and transferred into the 96-well plate. The plate was heated to 95°C for 10 min and cooled at RT for 20 min before analysis, light protection was needed at all time. Fluorescence was measured using a fluorometer equipped with filters for excitation at about 485 nm and emission at about 590 nm. Subtraction of blank values from that of the samples had to be performed before the standard curve could be generated. At last, protein concentration of each sample was determined.

2.2.5.3 SDS-Page Gel Electrophoresis

First, AAV-2/Ad infected cell extracts or purified viral vector stocks (5×10^9 viral genomes) were analyzed on self-made 15 % polyacrylamide gels in the presence of sodium dodecyl sulfate (SDS-PAGE) according to standard protocol. Later, commercially available NuPAGE[®] Novex[®] Bis-Tris Mini Gels (Invitrogen, Karlsruhe) were used for protein separation. Samples

were added up to 10 µl with H₂O plus additional 10 µl of 2x Protein Sample Buffer. Next, they were heat-treated for 10 min at 99°C. Before samples were loaded onto the gels, the upper (inner) Buffer Chamber was filled with 200 ml 1x NuPAGE[®] SDS Running Buffer, the lower (outer) Buffer Chamber was filled with 600 ml 1x NuPAGE[®] SDS Running Buffer. After the appropriate marker (s. 2.1.10) and samples had been loaded, a constant voltage of 200 V and a current of about 60 mA /gel was applied. After about 1 h, proteins had been separated and the gel could be removed out of its plastic container for Western blot transfer (s. 2.2.5.5).

2 x Protein Sample Buffer

25 % (v/v) 0.5M Tris pH 6.8
20 % (v/v) glycerol
10 % (v/v) β-mercaptoethanol
40 % (v/v) 10 % SDS
0.01 % bromo phenol blue

2.2.5.4 Coomassie-Blue Staining

To visualize proteins in polyacrylamide gels, the gels were stained for at least 10 min in Coomassie blue stain and destained with several changes of destain solution until distinct protein bands were visible. For preservation, gels were dried o/n in cellophane placed into a gel drying aperture (Promega, Heidelberg).

Coomassie Blue Fast Stain

40 % methanol
7 % acetic acid
0.1 % Coomassie-Blue

Destain Solution

20 % methanol
7 % acetic acid

2.2.5.5 Western-Blot-Transfer of Proteins

After protein separation by SDS-PAGE, they were transferred onto a nitrocellulose membrane using the semi-dry procedure. Six sheets of Whatman paper and one nitrocellulose membrane were cut to gel size and moistened in blotting buffer. A sandwich was produced, starting with three pieces of Whatman paper at the anode, followed by the nitrocellulose membrane, the gel and the other three pieces of paper. Air bubbles were

carefully withdrawn from the sandwich. The cathode was then applied and the transfer was carried out at $1\text{mA}/\text{cm}^2$ membrane (75 mA per ready-to-use gel) for 1-1.5 h at 4°C .

The transfer efficiency was checked by Ponceau-S staining of the membrane. The membrane was immersed in Ponceau-S for 10 s and destained with several rinses of PBS. The transferred proteins were visible as red bands. Immunological proceedings for proteins transferred to the membrane were performed as described in section 2.2.6.1.

2.2.6 Antibody Purification and Analysis

2.2.6.1 Immunological Detection after Protein Transfer

First, the membrane was blocked O/N at 4°C in blocking buffer to saturate all unspecific binding sites. The next day, hybridoma supernatant containing the primary antibody of interest (undiluted or diluted 1:10 in blocking buffer) was incubated for 1 h at RT under constant shaking. The membrane was washed 3 times in PBS containing 0.1 % Tween20 and incubated with the corresponding secondary antibody, i.e. a peroxidase-conjugated goat-anti-mouse antibody was diluted 1:5000 in blocking buffer and added to the membrane for 1 h at RT under constant shaking. The membrane was washed again as described above and proteins were visualized by chemiluminescence. Chemiluminescence was performed using the ECL kit (Amersham) according to the manufacturer's guide, the membrane was incubated for 1 min in a 1:1 mix of the provided solutions A and B, then the membrane was dried and placed into a developer cassette for x-ray film exposition. The exposure times varied between different experiments (1-5 min).

Blocking Buffer	6 % skim milk powder 0.1 % Tween 20 in PBS
------------------------	--

2.2.6.2 Antibody Purification

Each monoclonal antibody was purified from hybridoma supernatant by affinity chromatography on protein Sepharose columns (Amersham Pharmacia) as described by the manufacturer's protocol. Hybridoma supernatant was filtered through a $0.45\ \mu\text{m}$ filter and cycled over a protein G column overnight at RT using a peristaltic pump. The column was

then washed with at least 10 column volumes of 20mM phosphate buffer (pH 7.0). IgGs (immunoglobulin G) were eluted with at least 2.5 column volumes of 0.1M glycine (pH 2.7). Fractions were collected in 2 ml tubes and each sample was immediately neutralized with 100µl 1M Tris-HCL (pH 9.0) which previously had been added to the fractionation tubes. Fractions containing IgGs were identified by measuring at 280 nm with a Nanodrop. IgGs containing fractions were pooled and dialysed o/n against PBS (at least 1:500) at 4°C. Pooled fractions were checked once more for the IgG amount (recommended concentration: 1-4 mg/ml) and 0.01 % sodium-azide was added for preservation.

2.2.6.3 Immunofluorescences of Recombinant AAV Vectors

Immunofluorescence analysis was performed to compare AAV2 and AAV8 infection in HeLa cells. HeLa cells (5×10^4 cells per well, 24-wells, Nunc, Langenselbold) were grown on coverslips O/N, medium was exchanged to FCS-free medium and 24-well plates were transferred to 4°C. HeLa cells were infected with MOI 2×10^5 viral genome containing particles. Cells were kept at 4°C for 30 min, were washed and either directly fixed with methanol or transferred for 1 h, 2 h, 4 h or 6 h to 37°C. To fix the cells, they were placed into PBS followed by a 10 min incubation time in ice-cold methanol and another washing step PBS before antibodies were applied. Primary antibodies were added to the fixed cells, normally non-diluted hybridoma supernatant was added, however, in some cases purified antibodies (diluted in PBS + 1 % BSA at various concentrations) were used. The incubation time was carried out for 1-2 h at RT or O/N at 4°C in a humid chamber. The coverslips were washed twice in PBS for at least 10 min before the secondary antibody was added. An Alexa 488 or Alexa 596 conjugated goat α mouse secondary antibody was diluted 1:700 in PBS + 1% BSA and incubated for 1h at RT. After washing the coverslips 3 x in PBS, they were immersed briefly in water and ethanol (100 %) and left in Hoechst staining solution for 5 s before a second wash in water. At last, the coverslips were mounted in mounting medium, (Permafluor, Fisher Scientific, Schwerte). The cells were visualized using a fluorescence microscope and photographed.

2.2.6.4 Antibody Isotyping

The quality control by an Isotyping Kit of a purified antibody production is important for most assays. Therefore, IsoStrips of a Mouse Monoclonal Antibody Isotyping Kit (Roche,

Mannheim) were used according to manufacturer's guide. Antibody samples were diluted to about 1 µg/ml in PBS and 150 µl freshly diluted sample was transferred into a development tube. The sample was incubated for 30 s at RT and then briefly agitated to ensure that the coloured latex was completely resuspended. An isotyping strip was placed with its black end at the bottom into each development tube. Once the positive control bands appeared, the results could be interpreted for antibody class and subclass as well as light-chain composition.

2.2.6.5 Antibody Conjugation

Lynx Rapid Antibody Conjugation Kits from Applied Serotec were chosen to label small quantities of antibodies/proteins at neutral pH, allowing high conjugation efficiency with 100 % antibody recovery. In general, a molar ratio of 1:1 was strongly suggested, i.e. 100 µg antibody to every 100 µg HRP (horse-radish-peroxidase) or biotin was needed in a total volume up to 100 µl. Per 10 µl antibody sample, 1 µl Modifier reagent was added and gently mixed. The mix was pipetted directly onto the LYNX™ lyophilized mix and gently pipetted up and down twice to resuspend. The cap was placed onto the vial and incubated light protected O/N at room temperature. After incubation, 1 µl Quencher reagent for every 10 µl of used antibody was added. After 30 min at RT, conjugated antibody could be used or stored at -20°C.

2.2.6.6 AAV8 ELISA Establishment

The amount of AAV8 capsid of a produced AAV8 vector production was important to the experimental set up and an ELISA against AAV8 with the help of the ADK8 antibody had to be established. Binding of mAbs to AAV serotypes and AAV2 insertion mutants was quantified in an ELISA. The standard AAV8 production consisted of highly purified AAV8 particles. As determined by negative staining (s. 2.2.4.4.1), 4640 counted particles (538 nm x 1950 nm) equal 8×10^{12} particles (Grimm *et al.* 1999). Flexible 96-well microtiter plates (Polysorb, Nunc) were coated with 50 ng ADK8 per well (total volume per well was 100 µl) and stored O/N at 4°C. The microtitre plate was washed twice with PBS before blocking buffer (0.2 % Casein in 0.05 % in PBS-T) was added to each well. It was incubated at 37°C for 1 h. After three more PBS-T washes, the standard (capsids of a production with known capsid titer) and samples containing unknown capsid amounts were added to the wells. A serial dilution

(1:5) for each vector production from 1×10^{10} Vg to 5×10^6 Vg had been performed and was applied. Viral particles were incubated for 1h at 37°C. The wells were washed 3 x with PBS-T before the HRP-conjugated ADK8 (1 µg/ml, diluted in PBS-T) was added. The microtitre plate was kept for another hour at 37°C. After a repeated washing step, 100 µl/well of a TMB substrate solution was added and resulted in a color reaction that was stopped with 50 µl/well 1M H₂SO₄. The color intensity was measured at 450 nm in an ELISA reader (Emax, MWG Biotech).

TMB Substrate Solution	1 mg/ml TMB (3,3',5,5'-Tetramethylbenzidine)
	0.1 M Na-Acetate, pH 6.0
	1:10000 dilution of 30 % H ₂ O ₂

2.2.6.7 Monoclonal Antibody for AAV Vector Characterization

Monoclonal antibody ADK8 had been generated against AAV8 capsids and was used for an entire set of experiments. In presence of monoclonal antibodies, cell binding and entry, endosomal cleavage factors, N-terminal externalization and neutralization was analysed.

2.2.6.7.1 AAV Cell Binding and Entry

Impact of ADK 8 on AAV8 binding was analysed either via DNA Dot Blot (s. 2.2.4.4.3) or IF (s. 2.2.6.3). HeLa cells (8×10^4 cells) were seeded out on coverslides which had been placed into wells of a 24-well plate. One day after cell seeding, medium was exchanged to FCS-free medium and cooled down to 4°C. In the meantime, some rAAV vector samples (MOI 2×10^6 according to viral genomes) were mixed with 0.1 mg antibody and preincubated for at 37°C for 30 min plus additional 10 min at 4°C. Antibody-vector mixes or only vectors were added to the cells for 30 min at 4°C. Cells were fixed and analysed as described in section 2.2.6.3. A DNA Dot Blot was preferred if entry analysis was also needed. In that case, 1×10^6 HepG2 cells were seeded out in 6 cm (Ø) dishes. The next day, medium was also exchanged to FCS-free medium and the cells were left at 4°C for about 10 min before AAV vectors could be applied. Additionally, viral vector particles (MOI 50000) were also incubated with 100 µg antibody at 37°C for 30 min. Samples (vector-antibody mix or vector only) were cooled down to 4°C for 10 min and were then applied onto the cells for 30 min. After a PBS wash, cells

were either transferred to 37°C for an entry analysis or harvested directly. All following steps were performed as described in section 2.2.4.4.3.

2.2.6.7.2 AAV N-terminal Externalization

Heat-shock treatment was performed to assay the externalization capability of AAV N-terminus in presence of ADK8. At first, 4×10^9 viral genomes were preincubated with 4 µg ADK8 at 37°C for 30 min. The sample was split up into 4 PCR tubes and individually heat treated (1st at 37°C, 2nd at 65°C, 3rd at 71°C, 4th at 99°C) for 3 min. For a control, viral genomes were also heat treated without previous antibody addition. Next, all samples were added up to 200 µl with PBS and spotted onto a nitrocellulose membrane for a native dot blot assay. After the vacuum treatment, the membrane was taken out of the dot blot apparatus and treated with an A1 antibody conjugated to HRP (2 µg/ml in Blocking Buffer). The membrane was washed and spots were visualized by chemiluminescence. Chemiluminescence was performed using the ECL kit (Amersham) according to the manufacturer's guide, the membrane was incubated for 1 min in a 1:1 mix of the provided solutions A and B, then the membrane was dried and placed into a developer cassette for x-ray film exposition. The exposure times varied between different experiments (1-5 min).

2.2.6.7.3 Endosomal Cleavage Analysis

To investigate AAV endosomal cleavage patterns in presence of ADK8, 5×10^8 Vg were preincubated with 10 µg ADK8 at 37°C for 30 min. With or without ADK8 preincubation, vectors were treated with 6.5 µg Cathepsin B (resuspended in Solution Buffer) and 2x Reaction Buffer and incubated at 37°C for 8 h. All samples were mixed with 2x Sample Buffer and heated at 99°C for 10 min. Gel electrophoresis and protein transfer were performed as described in 2.2.5.3 and 2.2.5.5. The B1 antibody (1:10 diluted in Blocking Buffer) or polyclonal serum VP51 (1:200 diluted in Blocking Buffer) were used as primary antibodies and Goat α Mouse-HRP or Goat α Rabbit-HRP (both 1:5000 in Blocking Buffer) as secondary antibodies, respectively. Protein bands were visualized by chemiluminescence as described previously (s. 2.2.6.7.2).

Solution Buffer

20 mM Sodium acetate, pH5

1mM EDTA

5 mM L-Cysteine

Reaction Buffer

50 mM Sodium acetate, pH5

3 mM DTT

2.2.6.7.4 Neutralization Analysis

For *in vitro* neutralization, 5×10^3 cells of HeLa, HepG2 or 293T were seeded out in 96-well plates one day in advance. The medium was exchanged with FCS-free medium, AAV vector genomes corresponding to MOI 1000 were incubated with different amounts of antibodies (100 ng to 500 ng) at 37°C for 30 min. Cells were infected with the antibody-virus mix for 6 h. Then, cells were washed and FCS-containing medium was added. After 4 days, cells were harvested and the luciferase expression was measured (s. 2.2.4.7). All experiments were performed in triplicates and repeated three times.

In case of an *in vivo* neutralization, the monoclonal antibody was injected intraperitoneally (ip) into 6-9 weeks old female NMRI mice, 4 h before viral vectors (1×10^{11} viral genome containing) were iv injected. Each group of mice consisted of 4 animals, antibody amounts were 50 µg, 100 µg, 250 µg or 500 µg. Luciferase transgene expression was measured as described in section 2.2.4.7.

2.2.7 AAV8 Library Generation and Screening**2.2.7.1 Generation of AAV8 Library Backbone Plasmids**

To generate a backbone plasmid with a peptide insertion site, *SfiI* binding sites had to be inserted into the AAV8 *cap* gene of p5E18-VD2/8 (s.2.1.7). The *SfiI* binding sites constructed into the sequence pLib588-8, 743 bp in length, was ordered and synthesized from GENEART (Regensburg). The restriction enzymes *XcmI* and *Eco47III* were used to restrict the plasmids and to insert the DNA sequence with the *SfiI* sites into the p5E18-VD2/8 backbone. The generated p5E18-VD2/8+Sfi I was used to insert oligos isolated in AAV2 library selections (Muller *et al.* 2003; Waterkamp *et al.* 2006) and to produce AAV8 based vectors. The *SfiI* digests were performed as described in the end of this section.

The AAV8 library backbone plasmid was generated by a cloning strategy to gain a plasmid containing the stuffer sequence (+ *SfiI* sites) plus ITRs. The *cap* gene with the inserted stuffer sequence was restricted by *EcoRV* and *HindIII*, cloned into pMT187-XX2 (Ying

et al. paper to be published). After ligation had been checked in a sequence analysis, pMT182-XX2/8 was restricted with *Xba*I to to ligate *rep* and *cap* gene (+stuffer) into pSSV9 (received from J. Samulski, Chapel Hill, North Carolina). The pLib588-92+ITRs plasmid was used in the production of the AAV8 peptide display library.

The plasmids were produced in large quantities for the cloning procedure and analysed for amount and degree of contamination before handling (s. 2.2.2.2 and 2.2.2.5). To cleave the 15 bp stuffer within the plasmid, 40 µg plasmid p5E18-VD2/8+SfiI or pLib588-92+ITRs were restricted with 1/10 vol. of *Sfi*I in the presence of 10 x *Sfi*I buffer and 100 µg/ml BSA in an optimal volume. Restriction reaction was carried out for 4 h at 50 °C. The *Sfi*I restricted plasmid was purified using the QIAquick PCR purification columns (s. 2.2.2.9) and eluted with buffer EB (diluted 1:3 in ddH₂O, pH8.5). Concentration of the resulting library backbone plasmid was determined to ensure a functional ligation with an oligo insert of interest (s. 2.2.2.5).

2.2.7.2 Preparation of a Random Insert Sequence

Random oligonucleotide inserts (NNK)₇ were designed to display two different *Bgl*I restriction sites on each end (Muller *et al.* 2003) for directional in-frame cloning into the library backbone plasmid pLib588-92+ITRs. The following degenerated oligonucleotides encoding a random 7- aa peptide insert at aa position 591 in the AAV8 genome were synthesized by MWG Biotech (Ebersberg):

5' -CAGTCGCCAGAGAGGC(NNK)₇GCCCAGGCGGCCGACGAG-3'

(N=A, T, C, or G; K= G or T)

The oligonucleotide insert was first converted into dsDNA using the Sequenase 2.0 kit. To increase the yield of insert, four batches of insert synthesis were carried out, resulting in a sufficient amount of insert for the ligation. For each synthesis reaction, 2 µg of oligonucleotides were incubated with 4 µg AAV library primer (5'-CTCGTCGGCCGCCTGG-3'), 2 µl 5 x sequenase reaction buffer, and ddH₂O in a total amount of 10 µl for 2 min at 65°C. The reaction was slowly cooled down to 40°C and incubated on ice for 2 min. For elongation, 10 µl chilled reaction was incubated with 2 µl diluted sequenase DNA polymerase (pre-diluted in 0.5 vol. of iPPase and 6.5 vol. of glycerol enzyme reaction buffer), 2 µl 10 mM dNTP, 5 µl 0.1M dithiothreitol (DTT), and 31 µl enzyme dilution buffer for 1 h at 37°C. The insert DNA was purified from the enzyme reaction using Qiaquick nucleotide removal

columns (8,000 x g used for elution step) and eluted with buffer EB (diluted 1:3 in ddH₂O, pH8.5). The synthesized insert was then digested with 1/10 vol. of *Bgl*I in the presence of 10 x *Bgl*I buffer and 100 µg/ml BSA for 4 h at 37°C. *Bgl*I restricted insert was purified by Qiaquick nucleotide removal columns and eluted with buffer EB (diluted 1:3 in ddH₂O, pH8.5). DNA concentration of the resulting insert (*Bgl*I restricted) was determined before it was ligated into the library backbone.

2.2.7.3 Ligation of Library Backbone Plasmid and Insert

2.2.7.3.1 Test Ligation

For an optimal ligation, various molar ratios of plasmid versus insert were tested (e.g. 1:10, 1:30, 1:100). About 500 ng backbone plasmid and respective amounts of insert were mixed with ddH₂O to a total vol. of 25 µl and incubated for 2 min at 65°C. The mixture was chilled on ice for 5 – 10 min and incubated with 2 µl of T4 DNA ligase and 3 µl 10 x ligation buffer O/N at 16°C. A re-ligation control without insert was used to determine the background and efficiency. The o/n ligated DNA was purified by ethanol precipitation (s. 2.2.2.3) and resuspended in 25 µl buffer EB (diluted 1:10 in ddH₂O). About 1 µl ligated plasmid was transformed into 20 µl electrocompetent DH5α *E.coli* (s. 2.2.1.5). The transformed bacteria were incubated in 2 ml pre-warmed (37°C) SOC medium for 1 h at 30°C under gentle rotation. An aliquot of 100 µl transformed bacteria culture was diluted 1:10, 1:100 and 1:1000 in H₂O and plated onto ampicillin-containing (100 µg/ml) LB-agar-plates. Plates were kept O/N at 37°C, background and ligation efficiency (per µg ligated plasmid DNA) used was calculated by the amount of colonies on the plates. The calculation was performed according to the protocol (Muller *et al.* 2003) :

No. of colonies x 1 µg/A µg x B µl/100 µl* x dilution factor (1, 10, 100, 1000...)

[A was the amount of plasmid DNA used for the electroporation; B is the total volume of transformed bacteria used for the 1 h culture; *100 µl was the aliquot of diluted transformed bacteria culture.]

2.2.7.3.2 Large Scale Ligation

After determining optimal ligation conditions (1:30 in this case), about 10 – 20 µg library backbone plasmid was mixed with the most suitable amount of insert and was incubated for 2 min at 65°C before the mix was chilled on ice for 5 – 10 min. About 1/10 vol. of T4 DNA ligase and 10 x ligation buffer were added to the chilled plasmid-insert mixture and

incubated O/N at 16°C. The ligated plasmid DNA was purified by ethanol precipitation and resuspended in 200 µl buffer EB (diluted 1:10 in ddH₂O). Before large scale electroporation was started, 1 µl of the ligated library plasmid was transformed separately into 20 µl electrocompetent DH5α *E.coli* to determine the large scale ligation efficiency as previously described (s. 2.2.7.3.1 and s. 2.2.1.5).

Plasmids from the large scale ligation were transformed into electrocompetent DH5α bacteria (ElectroMAX DH5α, Invitrogen, Karlsruhe; or freshly produced s. 2.2.1.3) using the Gene Pulser. For each electroporation, 2 µl plasmid DNA (approximately 100 – 200 ng) and 50 µl electrocompetent cells were applied. About 52 electroporations were carried out for one large scale electroporation. Before transformation, 4 aliquots of mastermix (each containing 26 µl DNA and 650 µl bacteria) were prepared in 4 separate eppendorf tubes on ice for 4 batches transformation. When a batch of 13 electroporations in 26 ml of SOC medium was incubated at 37°C, the next batch of 13 electroporations was carried out subsequently. After 1 h at gentle agitation, a 100 µl aliquot was removed from each transformed batch and the bacteria cultures were diluted 1:10, 1:100 and 1:1000 in H₂O. Diluted cultures were plated on the ampicillin-containing (100 µg/ml) LB-agar-plates and incubated O/N at 37°C (s. 2.2.7.3.1).

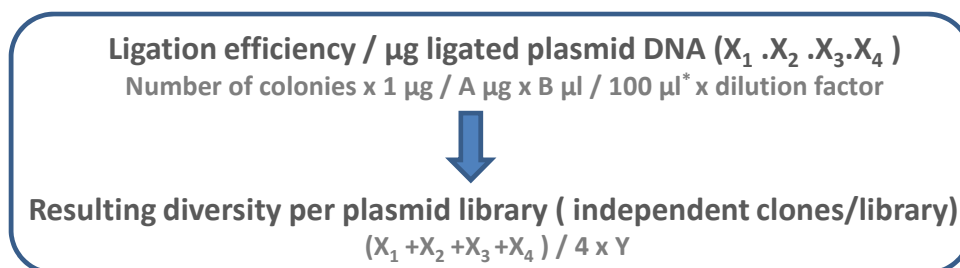


Figure 2-4 Schematic representation for the determination of the diversity of the generated AAV8 plasmid library. Ligation efficiency per µg of ligated plasmid DNA (X_1, X_2, X_3, X_4) was determined by means of colonies on the plates using the formula: No. of colonies x 1 µg/A µg x B µl/100 µl* x dilution factor (1,10,100,1000...). Here, A is the amount of plasmid DNA used in each batch of 13 electroporations, B is the total volume of each batch of transformed bacteria after 1 h culture (26 ml), *100 µl is a representative aliquot of diluted electroporated bacteria culture for plating. 4 batches of electroporations were performed for one large scale electroporation. Y is the total amount of plasmid DNA used in the large scale electroporation.

The colonies, present on the plates, were counted to determine the diversity of the AAV8 plasmid library (s. Fig. 2-4). Each of the four 26 ml bacterial cultures were added up to 500 ml ampicillin (100 µg/ml) containing LB medium and grown for approximately 12 – 18 h at 30°C under agitation at 175 rpm until OD₆₀ reached 2.0. The resulting library plasmids were

harvested from 2 L O/N culture and were purified by the Qiagen DNA Gigaprep kit (s.2.2.2.2). DNA concentration and purity of the AAV8 plasmid library was also determined (s.2.2.2.5). Despite of the calculated, theoretical diversity, the isolated plasmid DNA was also checked for diversity by sequencing. After heat shock transformation of plasmid libraries into CaCl₂ competent *E.coli* DH5α (s.2.2.1.4), 96 randomly picked clones were sequenced to verify the presence of the random insert using the AAV8lib-f primer (5'-CCAGAGACAATGCGGATTACAG-3') by high throughput 96-well plate sequencing (GATC Biotech; Konstanz).

2.2.7.4 Production of the AAV8 Transfer Shuttle Library

To produce the wt-free AAV8 transfer shuttle library, a total amount of 2×10^8 293T cells (20 dishes with 5×10^6 cells had been seeded out) were transfected using polyfect transfection reagents (Invitrogen, Karlsruhe) in an 1:3:7 ratio: 22 µg library plasmid, 66 µg pDGΔVP plasmid (Grimm *et al.* 1998), and 152 µg pRSVVP3cm plasmid, the codon-modified wt-VP3 helper plasmid (Waterkamp *et al.* 2006), respectively. Each polyfect transfection was performed as described in section 2.2.3.8.2. About 48 h after transfection, cells were harvested and centrifuged at 1000 x g for 10 min. Next, cell pellets were resuspended in virus lysis buffer (s. 2.2.4.2) and underwent three freezing/thawing cycles. Cell debris was removed by centrifugation after Benzonase treatment (50 u/ml) and transfer shuttle library was purified by an iodixanol step gradient (s. 2.2.4.3). Genomic titer and replicative titer of the resulting AAV transfer shuttle libraries were determined as described in section 2.2.4.4.

2.2.7.5 Generation of the AAV8 Random Peptide Display Library

Finally, the AAV8 virus library was produced by infecting a total of 1×10^8 293T cells with the library transfer shuttles plus an additional superinfection with Ad5. Per 15 cm (Ø) culture dish, 5.0×10^6 293T cells were seeded out in 20 ml media one day before infection. Cells were infected with the library transfer shuttles at MOI 1 replicative particle per cell. After 4 h incubation at 37°C, cells were superinfected with Ad5 at MOI 10 pfu/cell and incubated at 37°C for 48 – 72 h until at least 50 % cytopathic effect was observed. The AAV8 random display peptide library was harvested from the cells and purified by the iodixanol step gradient. The capsid titer and genomic titer of the resulting AAV8 random display peptide libraries were determined as described in section 2.2.4.4.

2.2.7.6 *In Vitro* Selection by the AAV8 Peptide Display Library

For an optimal *in vitro* selection, 1×10^6 Huh7 cells, 1×10^6 Hepa 1.6 and 2×10^6 primary murine hepatocytes (generation details s. 2.2.3.5), were seeded out in culture dishes one day before infection. At 70 % confluency, cells were infected with the random AAV8 peptide display library at MOI 10,000 viral genomes per cell for the first screening round. After 4 – 6 h incubation at 37°C, cells were washed with PBS, overinfected with Ad5 at 50 pfu/cell (primary rat hepatocytes), 20 pfu/cell (Hepa1.6) or 10 pfu/cell (Huh7) and incubated for 3 – 5 days at 37°C until at least 50 % of cells showed a cytopathic effect. Then, cells were harvested, pelleted by centrifugation at 1000 x g for 10 min and resuspended in 1 ml PBS. A 200 µl aliquot of cell suspension was removed to extract viral DNA (s. 2.2.2.4) for further analysis (s. 2.2.9). The remaining suspension was pelleted by additional centrifugation and resuspended in 0.5 – 1 ml lysis buffer. Replicated AAV particles were harvested from cell lysates after 3 freeze-thaw cycles and viral genomes were determined. For each subsequent selection round, pre-selected viruses recovered from the preceding screening round were added to target cells at reduced MOIs, i.e. for the 4th screening round, Huh7 cells were infected with pre-selected AAV8 library vectors at MOI 1 (according to viral genome containing particles).

2.2.7.7 PCR Amplification and Sequencing of Selected Clones

Isolated viral DNA from harvested cells of selection round 3 and 4 served as templates for PCR amplification (s. 2.2.2.14). For analysis by agarose gel electrophoresis, selected AAV genomic DNA comprising the oligonucleotide library insert region of the *cap* gene was amplified by PCR using the TopoLib8-f – primer [5'-CTGGCATCGCTATGGCAACACAC-3'] and the TopoLib8-r primer [5'-GGATCTGAGGCGGAGGATGTTTC-3'], Taq Polymerase (Invitrogen Karlsruhe) and the corresponding buffer. The PCR product was extracted from the agarose gel with the Qiaquick gel extraction kit (Qiagen, Hilden, s. 2.2.2.8), purified and subcloned into the plasmid pCR2.1 using the TOPO-TA cloning kit (s. 2.2.2.14). The next day, white colonies from the blue/white screening were selected and 32 clones were sent for sequencing for every 3rd and 4th selection round (GATC Biotech, Konstanz) using the M13 primer 5'-AGGAAACAGCTATGACCATG-3'.

2.2.7.9 Generation of Selected AAV8 Vector Mutants

Most prominent oligonucleotides identified in the sequencing results, were selected for insertion into p5E18-VD2/8+Sfi (s. 2.2.7.1). The oligonucleotides encoding the respective peptide were designed and synthesized by MWG Biotech (Ebersberg) according to the *Sfi*I linker (s. 2.1.6.2) to insert the peptides into *Sfi*I digested vector plasmids. To convert oligonucleotides into dsDNA, 2 µg of each forward and reverse oligonucleotide were mixed with 40 µl annealing buffer (10 mM Tris-HCl pH 8.5, 150 mM NaCl) and annealed in one thermo cycle of 5 min at 95°C, 20 min at 76°C and 20 min at 37°C in a PCR thermal cycler. The backbone plasmid, p5E18-VD2/8+Sfi, was digested with *Sfi*I to cut off the 15 bp stuffer as previously described (s. 2.2.7.1). Annealed dsDNA (10 – 20 ng) was ligated into the backbone plasmid p5E18-VD2/8+Sfi (100 ng) in the presence of 1 U T4 DNA ligase, 10 x ligation buffer (Roche, Mannheim) in a final volume of 20 – 30 µl and kept O/N at 12°C. The resulting plasmid provided *rep* gene and selected oligonucleotides modified *cap* gene without ITRs. Plasmids were sent for sequencing (GATC Biotech, Konstanz) to verify the correct oligonucleotide inserts. Positive sequencing results allowed the final production of recombinant AAV8 vectors with the inserted oligonucleotides to further test the functionality AAV8 library screening *in vitro* and *in vivo*.

2.2.8 Statistical Data Analysis

Statistical analysis was obtained by unpaired Student's t-test. Presented values were mean values of at least three independent measurements plus the corresponding standard deviation. Values $p < 0.05$ were defined to be significant.

3. RESULTS

3.1 In Vitro Analysis of rAAV8 in Comparison to rAAV2

3.1.1 Homology between AAV8 and AAV2 Capsids

Studies concerning the AAV serotype 8 have revealed significantly stronger liver transduction efficiency compared to other serotypes *in vivo* (Wang *et al.* 2005) but a strongly reduced transduction *in vitro* (Grimm *et al.* 2008). The reported crystal structure of the AAV8 capsid at 2.6 Å resolution elucidated an overall topology similar to the well described AAV2 capsid (Nam *et al.* 2007). Interestingly, protrusions on the capsid surface which are known to control transduction efficiency for AAV2 are structurally different between AAV8 and AAV2.

To understand the basis of the superior *in vivo* performance of AAV8, a more detailed analysis of its amino acid sequence as well as of its secondary structure and capsid surface became necessary. The AAV8 capsid protein sequences were analysed in direct comparison to AAV2 by ClustalW. A performed homology study of both serotypes verified that for 738 aa of the *cap* gene, an 83 % match between AAV2 and AAV8 was present (Fig. 3-1 A). Despite of the identical residues, indicated with *, many conserved substitutions (:) as well as semi-conserved substitutions (•) were observed. Several regions with large discrepancies were identified in the homology analysis between AAV2 and AAV8 (blue letters). Interestingly, the secondary structure analysis pointed out, that seven of the larger non-conserved regions could be structurally relevant, as they were located within loop IV of the AAV8 capsid secondary structure (Fig. 3-1 A, highlighted in grey boxes with blue capital letters; Fig. 3-1 B, grey squares in loop IV). This indicates that the amino acid residues in loop IV are also potentially responsible for the AAV8 transduction efficiency.

Furthermore, computational modelling of the AAV2 and AAV8 capsid illustrated that regional distinctions between both capsids are present on the capsid outer surface (Fig. 3-2). The used colour-scheme presented a shift from blue to red colour the more the amino acids were externalized. Whereas the overall topology of the capsids showed a similar structure, a view on one of the capsid trimers elucidated differences. As previously mentioned, loop IV region contributes mostly to the formation of the spikes around the 3-fold symmetry axes.

Compared to the AAV2 protrusions, the AAV8 spikes are more flattened (Fig. 3-2, encircled region in the side view of one of the capsid trimers) and the amino acids contributing to the five-fold pore formation are more arched upward for AAV8 (Fig. 3-2, grey boxes). These findings revealed that even with an 83 % homology between the AAV2 and AAV8 capsid, only some non-conserved aa can contribute to major structural and functional differences. A more stringent analysis of important AAV8 capsid domains in comparison to the AAV2 capsid was requisite.

A

AAV8	MAADGYLPDWLEDNLSEGIREWALKPGAPKPKANQQKQDDGRGLVLPGYKYLGPENGLD	60
AAV2	MAADGYLPDWLEDTLSEGIQWKLKPGPPPKPAERHKDDSRGLVLPGYKYLGPENGLD	60
	*****.*****:** ***. * ** . : : : ** . *****	
AAV8	KGEPVNAADAAALEHDKAYDQQLQAGDNPYLRYNHADAEFQERLQEDTSFGGNLGRAVFQ	120
AAV2	KGEPVNEADAAALEHDKAYDRQLDSGDNPYLKYNHADAEFQERLKEDTSFGGNLGRAVFQ	120
	***** *****. : * : ***** . ***** . *****	
AAV8	AKKRVLEPLGLVEEGAKTAPGKKRPVEPSPQRS PDSSTGIGKKGQQPARKRLNFGQTGDS	180
AAV2	AKKRVLEPLGLVEEPVKTAPGKKRPVEHSPVE - PDSSSGTGKAGQQPARKRLNFGQTGDA	179
	***** . ***** ** . ***** * ** *****	
AAV8	ESVPDPQPLGEPFAAPSGVGPNTMAAGGGAPMADNNEGADGVGSSSGNWHCDSTWLGDRV	240
AAV2	DSVPDPQPLGQPPAAPSGLGTNTMATGSGAPMADNNEGADGVGNSSGNWHCDSTWMDRV	239
	: ***** : ***** : * . ***** : ***** : *****	
AAV8	ITTSTRTWALPTYNNHLYKQISNGTSGGATNDNTYFGYSTPWGYFDNRFHCHFSPRDWQ	300
AAV2	ITTSTRTWALPTYNNHLYKQIS--SQSGASNDNHYFGYSTPWGYFDNRFHCHFSPRDWQ	297
	***** : . ** : ** * *****	
AAV8	RLINNNWGFPRKRLSFKLFNIQVKEVTQNEGTKTIANNLSTIQVFTDSEYQLPYVLGSA	360
AAV2	RLINNNWGFPRKRLNFKLFNIQVKEVTQNDGTTTIANNLSTVQVFTDSEYQLPYVLGSA	357
	***** . ***** : ** . ***** : *****	
AAV8	HQGCLPPFPADVFMIPQYGYLTLNNGSQAVGRSSFYCLEYFPSQMLRTGNNFQFTYTFED	420
AAV2	HQGCLPPFPADVFMVPOYGYLTLNNGSQAVGRSSFYCLEYFPSQMLRTGNNFTFSYTFED	417
	***** : ***** * : *****	
AAV8	VPFHSSYAHSQSLDRLMNPLIDQYLYLSRTQTGGTANTQTLQFSQGGPNTMANQAKNW	480
AAV2	VPFHSSYAHSQSLDRLMNPLIDQYLYLSRTNTPSGTTTQSRQFSQAGASDIRDQSRNW	477
	***** : . ** : . * ** . * . : : : **	
AAV8	LPGPCYRQQRVSTTTGQNNNSNFAWTAGTKYHLNGRNSLANPGIAMATHKDDEERFFPSN	540
AAV2	LPGPCYRQQRVSKTSADNNNSEYSWTGATKYHLNGRDSLVPNGPAMASHKDDEEKFFPQS	537
	***** . * : . : ***** : : ** . ***** : ** . * ** * : ***** : ** . .	
AAV8	GILIFGKQNA R NAD YSDVMLTSEEEIKTTNPVATEEYGI V A N L Q Q N T A P Q I G T V N S	600
AAV2	GVLIFGKQGS E K I N V D I E K V M I T D E E E I R T T N P V A T E Q Y G S V S I N L Q R G N R C A A T A V N T	597
	* : ***** . : : * . * . ** : * . ***** : ***** : ** * : * : * . . ** :	
AAV8	QGALPGMVWQNRDVYLQGPWIWAKIPHTDGNFHPSPLMGGFGLKHPPPQILIKNTVPADP	660
AAV2	QGVLPGMVWQDRDVYLQGPWIWAKIPHTDGHFHPSPLMGGFGLKHPPPQILIKNTVPANP	657
	** . ***** . ***** : ***** : ***** : *****	
AAV8	PTTFNQSKLNSFITQYSTGQVSVEIEWELQKENSKRWNPEIQYTSNYKSTSVDFAVNTE	720
AAV2	STTFSAAKFASFITQYSTGQVSVEIEWELQKENSKRWNPEIQYTSNYKSVNVDFTVDTN	717
	. *** . : * : ***** ***** ** . *** : * : *	
AAV8	GVYSEPRPIGTRYLTRNL	738
AAV2	GVYSEPRPIGTRYLTRNL	735

B

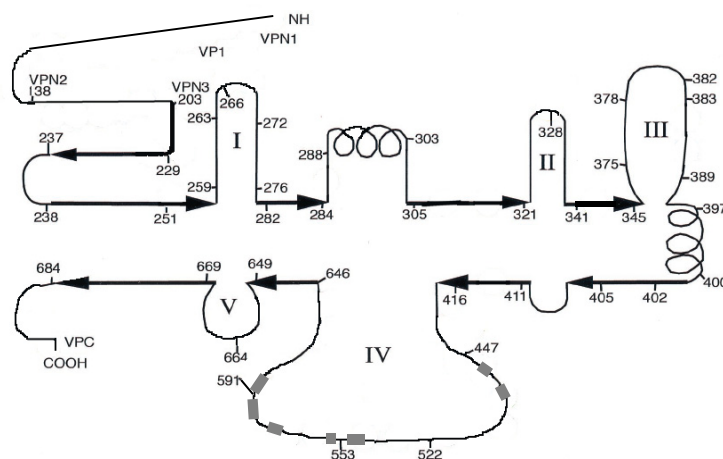


Figure 3-1 Homology study between AAV2 and AAV8 based on primary sequence and secondary structure. A) Amino acid sequence alignment of VP1 was performed between AAV2 and AAV8. ClustalW based sequence alignment assayed several regions with non-conserved aa (blue capital letters), a number of identical residues (*), conserved substitutions (:), and semi-conserved substitutions (.). Aligned were 738 aa with a homology score of 83%. Highlighted in grey boxes are these regional differences which could be structurally relevant. B) The secondary structure of the AAV2 capsid (modified from Wu *et al.* 2000) identified that seven of the non-homologous regions between AAV2 and AAV8 were positioned in loop IV (grey bars).

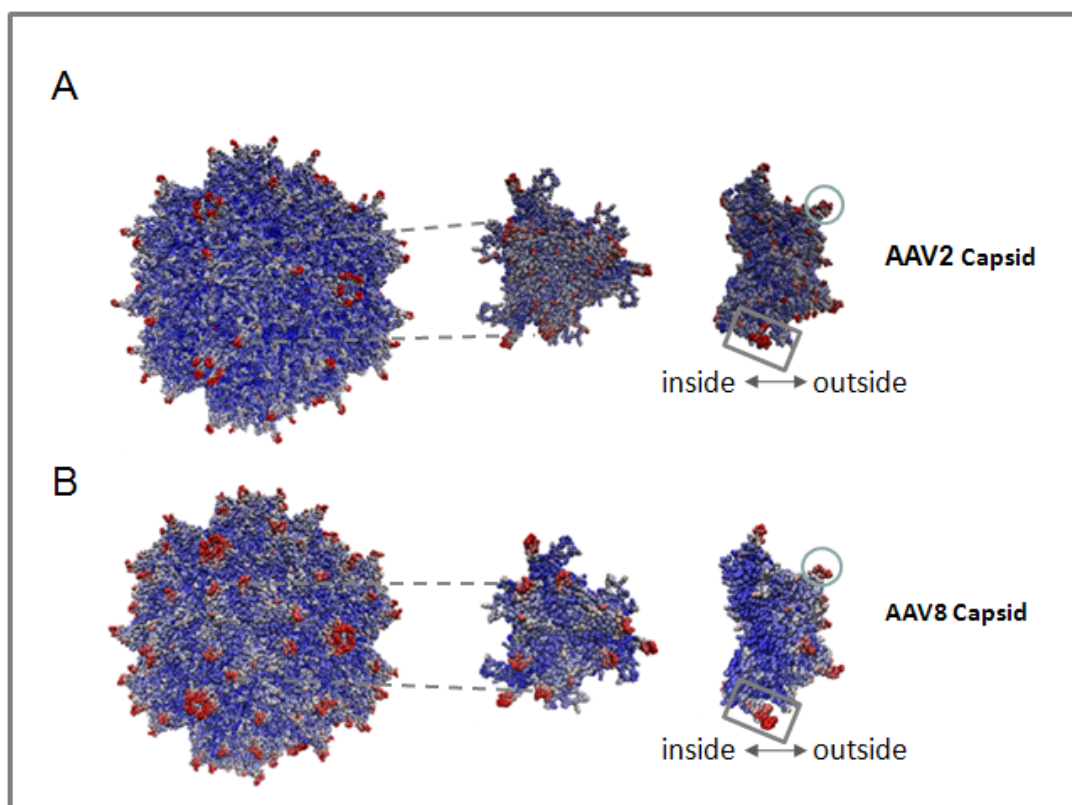


Figure 3-2 Capsid topology of AAV8 and AAV2. By computational modelling, a blue-to-red color scheme was used to demonstrate the degree of externalization of the aa, dark blue indicates a position within the capsid backbone, dark red colorization indicates a position strongly externalized. A) Complete AAV2 capsid, as well as front and side view from one of the AAV2 capsid trimers, are presented. In case of the side view, outer and inner capsid surface are indicated. Encircled is one of the spikes externalized from the capsid and one set of aa contributing to the five-fold pore formation are marked by a grey box. B) Complete AAV8 capsid, as well as front and side view from one of the AAV8 capsid trimers are depicted. In case of the side view, outer and inner capsid surface are indicated. Encircled is one of the spikes externalized from the capsid and one set of aa contributing to the five-fold pore formation are marked by a grey box.

3.1.2 Transduction Efficiencies of rAAV8 and rAAV2 in Different Cell Lines or Primary Cells

As previously described, AAV8 *in vivo* performance cannot be exhibited in *in vitro* experiments. Published results demonstrated that after cell line infection, the amount of green fluorescent protein –expressing cells were at least 10-fold higher for AAV2 than for AAV8 (Grimm *et al.* 2008).

To ensure that the vector productions of AAV2 and AAV8 transduce cells as published and to see whether a change in transduction profile of AAV8 can be achieved, several candidate cell lines or primary cells were transduced in a transgene expression assay. The transgene had been packaged into the AAV capsids, containing a luciferase gene driven by a CMV promoter. Correspondingly, the readout was based upon luciferase expression, relative light units per well (table 3-1). Obtained results ascertained that rAAV8 transduced all cell lines much less than AAV2. In fact, transduction efficiency of newly isolated primary cells was relatively high for rAAV2 compared to rAAV8 (about 100 fold). Vector productions could be used to further investigate differences between AAV2 and AAV8.

Tabel 3-1 *In vitro* transduction rates of rAAV2 and AAV8 in several cell lines of different origin

Human Cell Line	Origin	rAAV2 (RLU / Well) ^{a, b}	rAAV8 (RLU / Well) ^{a, b}
K562	Blood	1.45E+02 ± 7.89E+01	5.25E+01 ± 2.26E+01
CCRF-CM	Blood	1.99E+02 ± 1.15E+02	3.67E+01 ± 5.58E+01
Hela	Cervix	7.57E+03 ± 1.12E+03	5.94E+02 ± 1.10E+02
Caco2	Colon	1.32E+04 ± 4.39E+02	8.40E+02 ± 1.21E+02
KM12	Colon	6.10E+04 ± 2.67E+03	4.63E+02 ± 1.01E+02
Huh7	Liver	1.25E+05 ± 2.38E+04	1.09E+03 ± 7.33E+01
HepG2	Liver	1.46E+05 ± 1.17E+04	2.60E+03 ± 3.15E+02
MCF-7	Breast	2.85E+04 ± 1.93E+03	9.01E+02 ± 5.66E+01
Hs 578T	Mammary Gland	5.30E+05 ± 2.16E+04	2.07E+03 ± 1.05E+02
293T	Kidney	1.02E+06 ± 1.04E+05	8.44E+03 ± 8.80E+02
HT1080	Skin	2.00E+03 ± 1.84E+02	1.36E+03 ± 5.16E+02
Non-Human Primate Cells			
COS7	Kidney	1.02E+05 ± 1.12E+04	3.21E+03 ± 1.47E+02
Rodent			
C2C12	Skeletal Muscle	5.60E+03 ± 3.94E+02	5.02E+02 ± 2.42E+01
C2C12 differentiated	Skeletal Muscle	5.93E+03 ± 8.33E+01	4.19E+02 ± 6.61E+01
H9C2	Cardiac Muscle	2.25E+04 ± 7.20E+02	3.46E+03 ± 5.58E+02
M5V	Heart	2.52E+03 ± 4.01E+02	5.78E+01 ± 3.59E+01
Hepa1.6	Liver	1.56E+03 ± 2.23E+02	4.12E+02 ± 1.11E+02
Primary Cardiomyocytes		1.04E+05 ± 1.78E+03	1.35E+02 ± 7.78E+01
Primary Hepatocytes		5.45E+04 ± 3.12E+03	9.43E+02 ± 3.12E+01

^a Mean values and ± standard deviations are results from at least three independent experiments and two independent virus productions.

^b For reproduction, multiplicity of infection (MOI) was conducted according to viral genome containing particles, capsid ELISA against AAV8 had not been established yet. MOI 1000 was used in all transduction experiments, cells were harvested 4 days after transduction.

3.1.3 Heparan Sulphate Proteoglycan Binding of rAAV2 and rAAV8

The primary receptor binding site HSPG has been determined for AAV2 (Kern *et al.* 2003; Opie *et al.* 2003). As a first differentiation criterion we compared binding of AAV8 and AAV2 to Heparin-agarose, a substitute for heparan sulphate proteoglycan.

To validate previous findings and to further investigate the importance of heparin binding, binding properties of AAV2 and AAV8 were analysed by a Heparin-agarose column (Fig.3-3 A). A performed DNA dot blot analysis revealed that rAAV8 capsids were already detected in the flow-through as well as in the wash steps. It indicated that compared to rAAV2, heparin binding for rAAV8 is barely present and unstable. AAV2 capsids could be eluted well with the elution buffer and were strongly detectable by DNA dot blot analysis. Interestingly, the elution sample showed that little binding to heparin was also visible for rAAV8, but clearly much less than for rAAV2. Additionally, heparinase treatment of HeLa cells induced a strong decrease of rAAV2 mediated gene transduction, but not in case of rAAV8. In fact, heparinase treatment even increased cell transduction of rAAV8. Taken together, the results demonstrate that heparin binding is not a key factor to rAAV8 gene transduction but may play a secondary role in AAV8 infection. Removal of HSPG on the cell surface increased rAAV8 transduction efficiency *in vitro*, nevertheless, even with heparinase treatment rAAV8 does not transduce HeLa cells as strongly as AAV2.

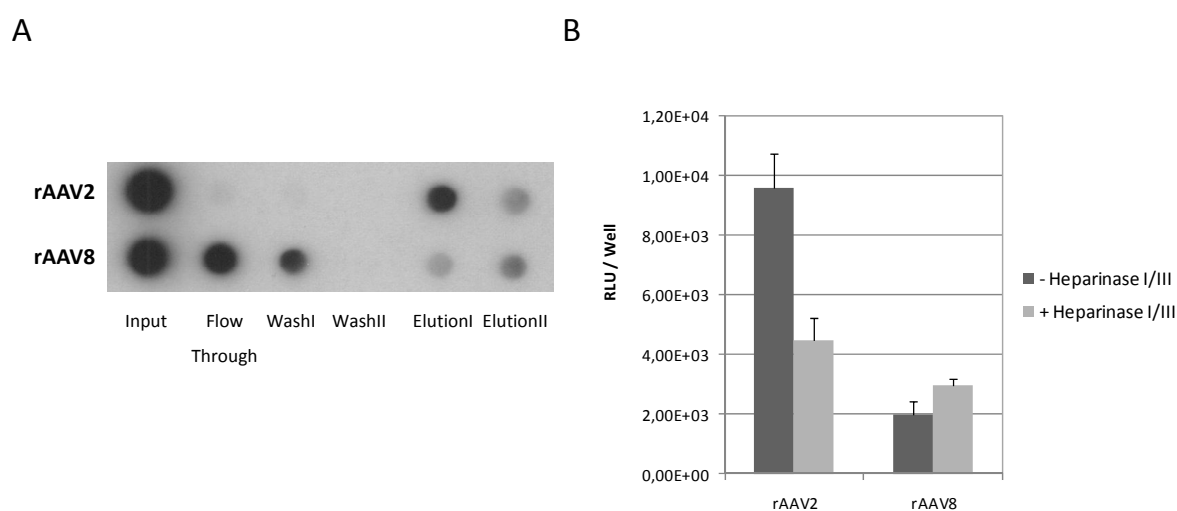


Figure 3-3 HSPG-Binding of AAV2 and AAV8. A) Heparin binding columns were used to analyse heparin binding; 1×10^{11} viral genome containing particles of rAAV2 and rAAV8 were added to each heparin agarose bed. After flow-through collection, columns were washed twice with PBS, capsids were eluted with PBS containing 1M sodium chloride. Viral DNA was isolated and analysed by a DNA dot blot. To detect and quantify immobilized genomes, a CMV-specific fragment was used as a probe and radioactively labeled with α - ^{32}P . B) Heparinase treatment of HeLa cells prior to virus application was implemented. Two hours after preincubation, cells were transduced with MOI 1000, and harvested 2 days later. Relative light units per well were determined in a luciferase reporter assay. Mean values were results from two independent experiments, infection was performed in triplicates.

3.1.4 Differences in Infection Pathways between AAV2 and AAV8

Yeast-two hybrid screens as well as high-throughput protein-interaction screens revealed more than 70 interaction partners shared between AAV8 and AAV2 (Akache *et al.* 2007; Murphy *et al.* 2008a). Cathepsin B and L were identified as uncoating factors of both serotypes and CDK2/cyclin A resulted in reduced transduction for both serotypes. The 37/67-kilodalton laminin receptor was also identified as a secondary receptor for AAV2 and AAV8 (Akache *et al.* 2006). A biophysical study on particle stability and genome uncoating of both serotypes revealed a slightly greater thermostability for AAV8 (Murphy *et al.* 2008a).

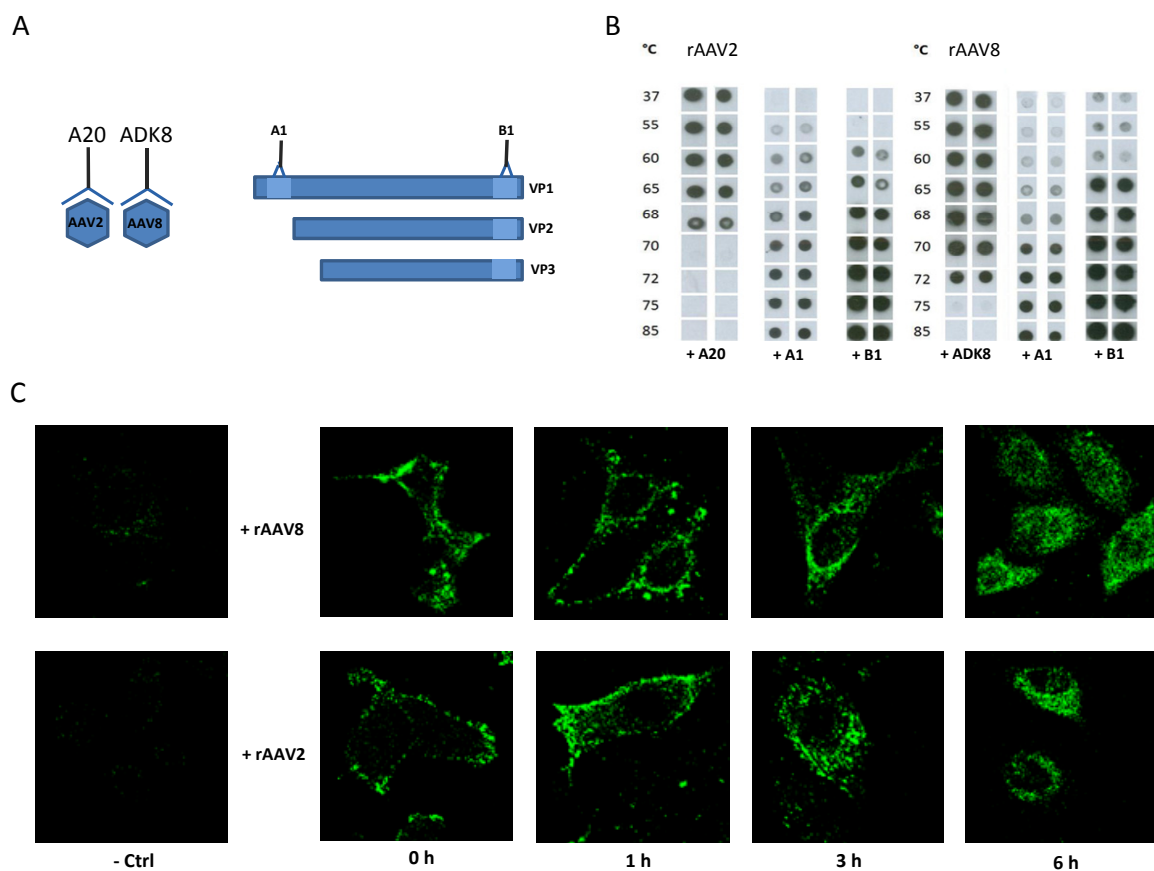


Figure 3-4 Differences in infection pathways for AAV2 compared to AAV8. A) Illustration of binding sites of applied monoclonal antibodies (mAB). Antibodies A20 and ADK8 react only with intact capsids. Antibodies A1 and B1 monoclonal antibodies recognize the N-terminus and the C-terminus of the VP proteins, respectively. B) Native dot blot assay of rAAV2 and rAAV8 capsids after heat treatment (temperature ranged from 37°C - 85°C). Under non-denaturing conditions, capsids were applied onto the nitrocellulose membrane with the indicated monoclonal antibodies. The experiment was repeated twice. C) The infection pathways of rAAV2 and rAAV8 were visualized by indirect immunofluorescence using mAB ADK8 (for AAV8 capsids) or A20 (for AAV2 capsids) in two independent experiments. HeLa cells were infected with MOI 2×10^5 of viral genome (vg) containing particles, and fixed with ice-cold methanol 0 h, 1 h, 3 h and 6 h later. Negative control images were taken from uninfected cells. Cells were visualized by fluorescence microscopy.

To gain more insights into differences between AAV2 and AAV8 infection pathways, heat-treated capsids were analysed by a native dot blot assay for capsid stability and VP1 N-terminal externalization. The latter is an essential step in the infection process. As depicted in figure 3-4 A, four different monoclonal antibodies were chosen for the assay: A20 and ADK8 for measuring the integrity of rAAV2 and rAAV8 capsids; A1 for detection of the VP1 N-terminus and B1 for detecting the C-terminus of all VP proteins, which indicates capsid opening and genome release (Bleker *et al.* 2005). The results of the native dot blot demonstrated that a higher capsid stability for rAAV8 capsids. Capsids were still recognized by ADK8 at 72°C, whereas detection of rAAV2 capsids was lost at 70°C. However, while B1 started to recognize rAAV2 VP proteins at 60°C, rAAV8 VP proteins were already detectable at 37°C, strongly detectable at 65°C. Genome uncoating seems to be a faster process for AAV8, as the C-terminus of the VP proteins are presented already at very low temperatures, even though intact capsids are still present. The detection of the VP1 N-termini by A1 showed that the AAV8 capsid N-terminus may be earlier externalized contributing to a faster release from the LE than for AAV2 capsids.

Virus uptake into Hela cells was analysed by indirect immunofluorescences. Hela cells were fixed at different time points (0 h, 1 h, 3 h, 6 h) of the rAAV2 or rAAV8 infection with MOI 2×10^5 of viral genome (vg) containing particles and viral capsids were detected by capsid specific antibodies, A20 (for AAV2 capsids) and ADK8 (for AAV8 capsids). The pictures taken by fluorescence microscopy suggested that processing throughout the cell advanced more rapidly for rAAV8 than for rAAV2. Perinuclear localization was already present after 3 h for rAAV8, after 6 h for rAAV2. Moreover, after 6 h, the pattern of rAAV8 particles did not show any perinuclear localization anymore but seemed to have entered the nucleus. The complete set of data gave evidence for a higher stability of AAV8 capsids compared to AAV2 capsids. Furthermore it could be demonstrated *in vitro* that AAV8 is processed much faster in the infection pathway to the nucleus than AAV2, though it does not explain why AAV8 *in vitro* transduction efficiency is strongly reduced compared to AAV2.

3.1.4 Investigating Poor *In Vitro* Performance of AAV8

As mentioned above, AAV8 transduces cells less efficient than AAV2 *in vitro*. Not all factors involved in the superior *in vivo* transduction efficiency, can be mimicked in an *in vitro* situation. Transcytosis, a process by which proteins overcome barrier epithelia, was

identified to play a role for AAV5 in lung epithelia cells (Di Pasquale *et al.* 2006). Studies revealed that transcytosis is a transduction independent process which is serotype and cell-type specific and its inhibition by temperature or chemical inhibitors dramatically increased tissue transduction. Other studies on adenovirus serotype 5 (Ad5) demonstrated that serum, in particular coagulation factor (F) X dramatically improved *in vitro* transduction of liver cells (Waddington *et al.* 2008).

To determine whether serum or purified serum factors could also improve transduction of AAV8 *in vitro*, murine serum and human F X was added to medium of the cells prior to infection. Serum addition up to 10 % even reduced transduction efficiencies of rAAV2 and rAAV8 (fig. 3-5 A). A 50 % serum addition reduced transduction of rAAV2 about 5-fold compared to without additional serum.

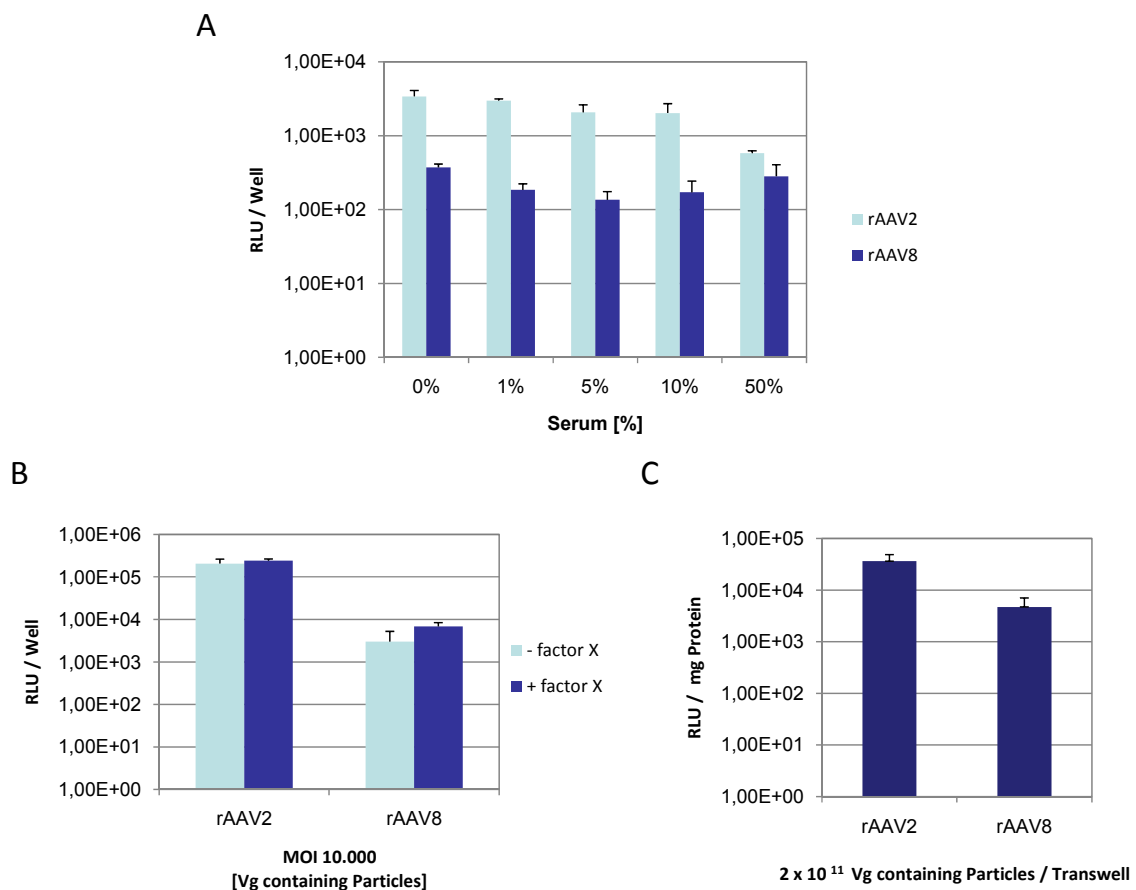


Figure 3-5 Attempted improvement of AAV8 mediated *in vitro* transduction efficiency. A) Murine serum was added to the medium of HeLa cells in different percentages before infection. After 30 min, cells were transduced with MOI 1000 of vg containing rAAV8 or rAAV2 particles. Three days after transduction, cells were harvested and luciferase expression was measured. Relative light units per well in relation to serum portion was analysed. B) Prior to HepG2 cell infection with MOI 10,000 of vg containing particles, human factor X (1 IU) was added to wells. Harvest and transgene expression analysis were assayed four days later. C) Liver sections were cut with the vibratom and placed onto transwells. About 2×10^{11} vg containing particles were added to each transwell. Liver sections were homogenized 4 days after infection and luciferase reporter expression per mg protein was determined. All experiments were carried out in quadruples and repeated twice.

Transduction efficiency of rAAV8 at 50 % serum addition was similar to transduction levels determined without serum addition. However, after 50 % serum addition cells were not in best shape three days after infection, meaning that too high serum concentrations in medium could have contributed to lower transduction levels. The addition of purified human F X to well transducible HepG2 cells did not have a strong impact on transduction of rAAV8 (Fig.3-5 B). A slight increase (less than 2- fold) in transduction could be measured, but still in much lower level than cell transduction present for rAAV2.

To assay whether an *ex vivo* environment could contribute to a better transduction efficiency of AAV8, liver sections were cut with a vibratom and cultured. Luciferase transgene expression revealed that rAAV8 could not transduce liver sections as well as rAAV2, even though transduction differences were less than 10-fold (Fig. 3-5 C). Consequently, not one factor could be identified which strongly improved AAV8 transduction efficiency *in vitro*. Possibly, multiple factors and the *in vivo* environment act synergistic and contribute together to the high AAV8 transduction efficiency *in vivo*.

3.2 In Vivo Performance of rAAV Vectors and rAAV derived Capsid Mutants

3.2.1 In Vivo Analysis of rAAV2 and rAAV8

Recombinant AAV vectors have come forward as an important tool for gene delivery in animal models and more recently in clinical trials (Warrington *et al.* 2006; Mueller *et al.* 2008a; Mueller *et al.* 2008b). Even though other serotypes than AAV2 show a more efficient gene delivery profile and their usage will likely increase, most elapsed studies have been performed with recombinant AAV2 vectors (Brantly *et al.* 2009). A general drawback to the usage of AAV vectors is the quality control of vector productions and the inability to normalize vector doses administered from different investigators to animals and humans. In the field of Ad5 research, adenoviral reference material was successfully generated to normalize titers and doses of Ad5 vectors (Hutchins *et al.* 2000). Thus, an AAV2 reference standard was also generated to normalize laboratory-specific internal reference standards and to test vector titers accordingly (Lock M *et al.* submitted).

Being part of the AAV2 reference standard working group, we had the chance to directly evaluate our own vector productions according to the international reference

standard of AAV2. Therefore, vector titers and purity of rAAV2 and rAAV8 vector productions were compared to the available rAAV2 reference standard. An ELISA demonstrated that 8×10^{11} capsids were present in the rAAV2 production, whereas rAAV8 particles could not be detected by the A20 ELISA (Fig. 3-6 A). The degree of purity was evaluated by an SDS PAGE gel stained with Sypro Ruby (Fig. 3-6 B). Both productions had been purified to a lesser extent than the highly pure reference standard due to the fact that only one iodixanol-step gradient had been used for purification. According to the ImageJ software, the degree of purity was 73 % for the rAAV2 production and 83 % for rAAV8 production compared to the 100 % pure reference standard. VP proteins of the rAAV2 and rAAV8 production had the correct size when compared to the AAV2 reference standard VP proteins. According to reports in the literature, both productions purified by one iodixanol step-gradient were pure enough for *in vivo* experiments.

For the mice experiments, 1×10^{11} vg containing particles of rAAV2 and rAAV8 vectors were intravenously (iv) injected into mice and analysed 1 month later. Fifteen minutes after D-luciferin was intraperitoneally injected into each mouse, *in vivo* imaging software (IVIS) images were taken and showed in case of the rAAV2 vector injections a widely disseminated pattern in all injected animals, with some localized detection in liver and masseter. Luciferase expression was 10- to 100-fold lower than for injections with rAAV8. Mice injected with rAAV8 vectors, showed 15 min after D-luciferin injections in the IVIS imaging also rAAV8 vector detection throughout the whole mouse body with highest detection signals in liver tissue. Interestingly, those mice were also imaged one year after injection and AAV vectors were still traceable. The rAAV2 vector injected mice showed luciferase expression of vectors in heart, masseter and muscle tissue, whereas in case of the rAAV8 vector injected mice, showed vector detection in the entire mouse system, especially in heart liver and muscle tissue. In another animal experiment, 6 mice were injected with viral vectors, and sacrificed. For heart, liver, muscle, lung, spleen, kidney and muscle tissue, luciferase expression per mg protein was measured (Fig 3-6 D). As described previously, rAAV8 vector transgene expression was present in all organs, especially in heart and liver, whereas 10-fold less rAAV2 vectors were determined in heart, liver, lung and muscle, and even 100-fold less in spleen and kidney. The obtained results clearly underlined that our produced vectors had been pure enough and could be used to reproduce published results on accomplished mice experiments.

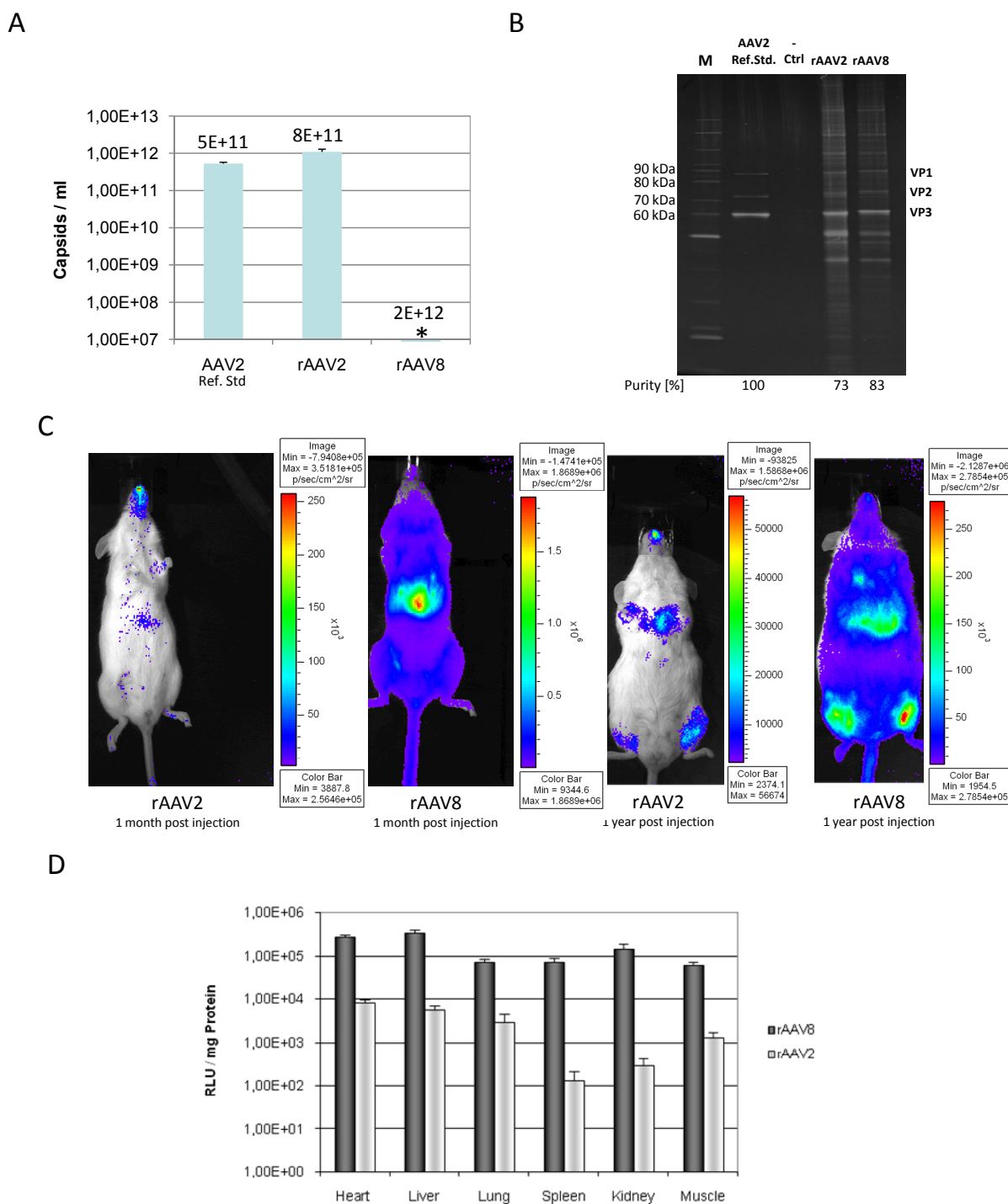


Figure 3-6 Vector production quality control prior to *in vivo* analysis of rAAV2 and rAAV8. A) A20 capsid ELISA was performed for rAAV2 and rAAV8 vector productions in correlation to the AAV2 reference standard (Lock M *et al.* submitted). Each production was analysed in triplicates in four independent experiments. Vg containing particles are indicated above the bars. * indicates rAAV8 capsids below detection levels. B) Vector samples run on SDS PAGE gels under reducing conditions and stained with Sypro Ruby. In comparison to the AAV2 reference standard samples of the rAAV2 and rAAV8 vectors were analysed. VP proteins of the AAV2 reference standard were 100 % pure. According to pixel density measurements by ImageJ software, the rAAV2 vector production had a 73 % purity and the rAAV8 vector production had an 83 % purity as indicated below the gel. C) IVIS imaging pictures of mice were taken 15 min after ip D-luciferin injection. Animals were imaged 1 month and 1 year post vector injections, 1×10^{11} vg containing particles of rAAV2 and rAAV8 vectors had been injected into each mouse. D) Luciferase transgene expression (RLU / mg protein) was measured in heart, liver, lung, spleen, kidney and muscle of dissected mice, one month after vector injection ($n = 2 \times 3$ mice of two independent vector productions). About 1×10^{11} vg containing particles had been iv injected into each mouse.

3.3.2 Vector Analysis of Mutants Comprising Large AAV2 Domains in AAV8 Capsids

Even though AAV2 and AAV8 share an 82% capsid amino acid sequence homology, the VP protein sequences responsible for their unequal *in vivo* gene transduction efficiency have not been elucidated yet. A first comparative study between AAV2 and AAV8 demonstrated that within the VP1 encoding sequence, the loop domain IV, especially its subloops 1 and 4, play a critical role for mouse liver gene transduction efficiency (Shen *et al.* 2007). To validate and further investigate these findings, several domain swaps were performed. Five different VP domains were transferred from AAV2 to AAV8 to generate chimeric AAV packaging helpers (Fig. 3-7 A). Domain swaps (DS) were designed and conducted to either preserve loop IV (basepairs 3542 to 4231) of the AAV8 capsid (DS I) or to exchange it completely to AAV2 (DS IV). In the additional DS mutant vectors, parts of the AAV8 loop IV were kept in combination with further VP proteins of AAV8 after the AAV2 capsid domain exchanges. DS capsid mutants containing CMV driven luciferase transgene vector genomes were not packaging-deficient, VP proteins were present in the typical stoichiometric pattern (Fig. 3-7 B). DS mutant vectors could be produced in sufficient amounts to *iv* inject 1×10^{11} vg containing particles into NMRI mice to analyse the *in vivo* transgene expression.

One month after injection, animals were imaged (Fig. 3-7 C). IVIS imaging ascertained that luciferase expression was drastically reduced for all DS mutant vectors compared to rAAV8 transgene expression, DS I vector dependent transgene expression was mainly present in the liver, but for other DS mutants very scattered signals could only be detected. After the animals had been sacrificed, transgene expression of the DS capsid mutants were analysed for six selected tissue types and compared to rAAV8 and rAAV2 (Fig.3-7 D). All DS mutant vectors did show a strongly reduced transduction efficiency compared to rAAV8. Interestingly, the *in vivo* performance of several investigated DS mutant vectors was even lower than that of AAV2, especially in liver, lung and muscle tissue indicating that AAV2 and AAV8 VP protein domains influence each other. The DS IV mutant vector, containing a complete swap of loop IV of AAV2 to AAV8, demonstrated by far the lowest transduction efficiencies confirming results published already by another group (Shen *et al.* 2007). When parts of the AAV8 loop IV domain were still present after the AAV2 domain insertion (DS II, III and V), highly transducible organs such as heart, liver and muscle, showed better transduction efficiency compared to DS IV. These differences could not be observed in lung, spleen and kidney because of low transgene expression levels at the detection limit.

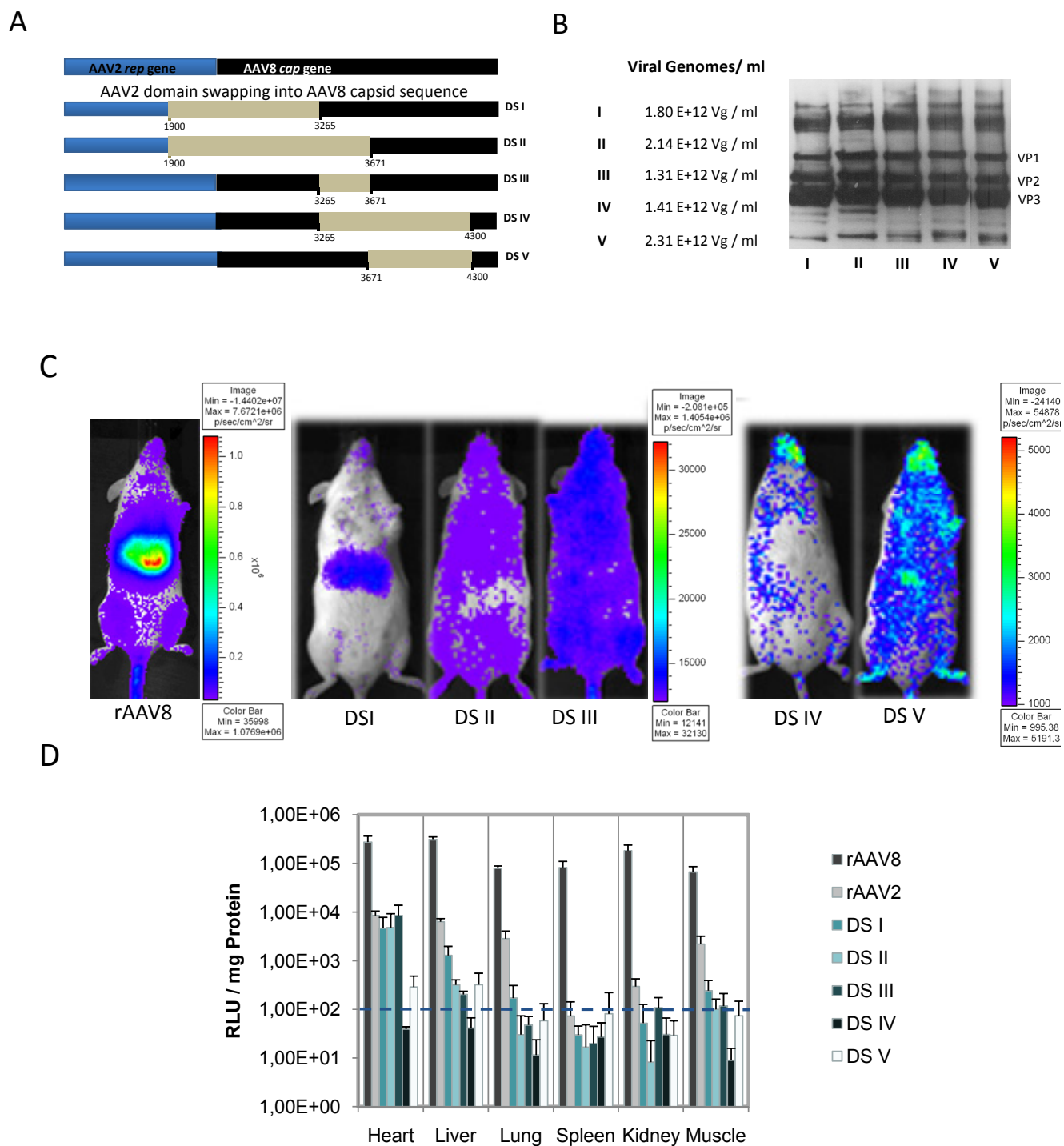


Figure 3-7 AAV2 capsid domain insertions into the AAV8 capsid and DS vector *in vivo* analysis. A) A schematic overview of the cloning strategy of AAV2 domains cloned into helper plasmid P5E18-VD2/8 of AAV8. Domain swap I – V were generated by restriction digests (light grey bars) of the nucleic acid sequences. Below each DS swap, numbers indicate the sites of restriction within the nucleic acid sequence B) Vg containing particles titers of DS vector productions were determined by qRT-PCR and VP proteins were validated by Western Blot. C) IVIS Imaging of mice which had been intravenously injected with 1×10^{11} Vg of DS vectors one month earlier. Transgene expression was measured for 5 min, 10 min after ip injection of D-luciferin. D) Transgene expression analysis of heart, liver, lung, spleen, kidney and muscle tissue of mice injected with DS capsid vectors. Six groups of NMRI mice, 5 mice per DS vector, plus 1 group of 3 mice for rAAV8 vectors were i.v. injected and dissected 1 month after injection. Luciferase transgene expression per mg protein was quantified.

3.3.3 Seven Regions of Non-conserved AA between AAV2 and AAV8

As mentioned above, loop IV domain is a region known to be involved in the fate of AAV serotype tissue tropism (Wu *et al.* 2000; Nam *et al.* 2007; Shen *et al.* 2007). Based upon the domain swap results, we decided to analyse the DS IV swap in more detail. Sequence analysis of the domain exchanged from AAV8 to AAV2 in the packaging helper indicated that seven of the amino acid sequence regions containing non-conserved amino acid residues, which possibly contribute to structural differences between AAV2 and AAV8 capsid, were situated within DS IV (Fig. 3-8). Consequently, the strongly reduced transgene expression *in vivo* obtained with DS IV vectors was caused by exchanging the entire series of important aa residues from AAV8 to AAV2.

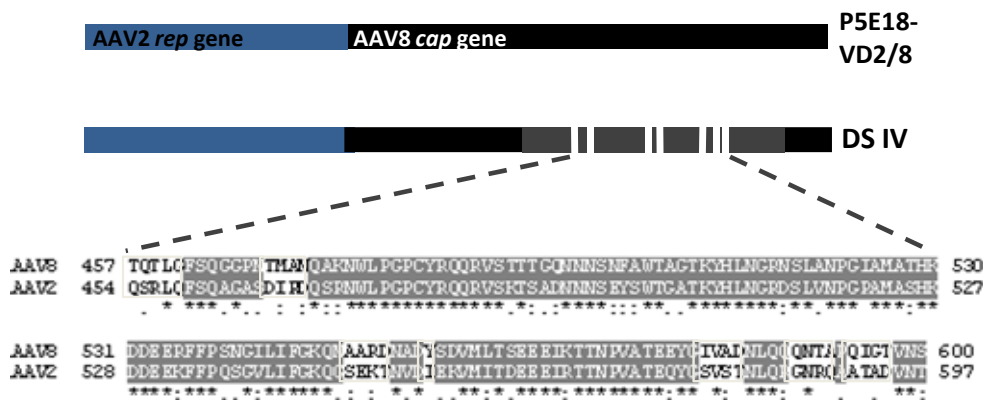


Figure 3-8 DS IV VP1 sequence exchanged all critical regions of non-conserved amino acids from AAV8 to AAV2. A) An excerpt of the amino acid sequence alignment between AAV2 and AAV8 indicating seven of the non-conserved regions within swap DS IV (white boxes with black capital letters). Sequence alignment indicates identical residues (*), conserved substitutions (:), and semi-conserved substitutions (.).

To evaluate the importance of each non-conserved region for AAV2 and AAV8, regions had to be separately investigated. At first, the non-conserved aa residues of the seven regions were modeled into the AAV8 capsid trimer (Fig. 3-9). In fact, visual molecular dynamics (VMD) modeling of an AAV8 capsid trimer clarified the allocations of these seven non-conserved regions. Region 1 was identified at the top of the spike region and region 3 and 4 were present on the outer capsid surface, but outside of the spike region. Instead, region 2 was located within the capsid shell structure but at the basis of the spike protrusions. Amino acids of the non-conserved region 6 were localized at the inner spike

shoulder, whereas region 5 and 7 were shown to be at the dimple of the spikes. Based upon that data, single aa residue mutant vector were produced and further analysed.

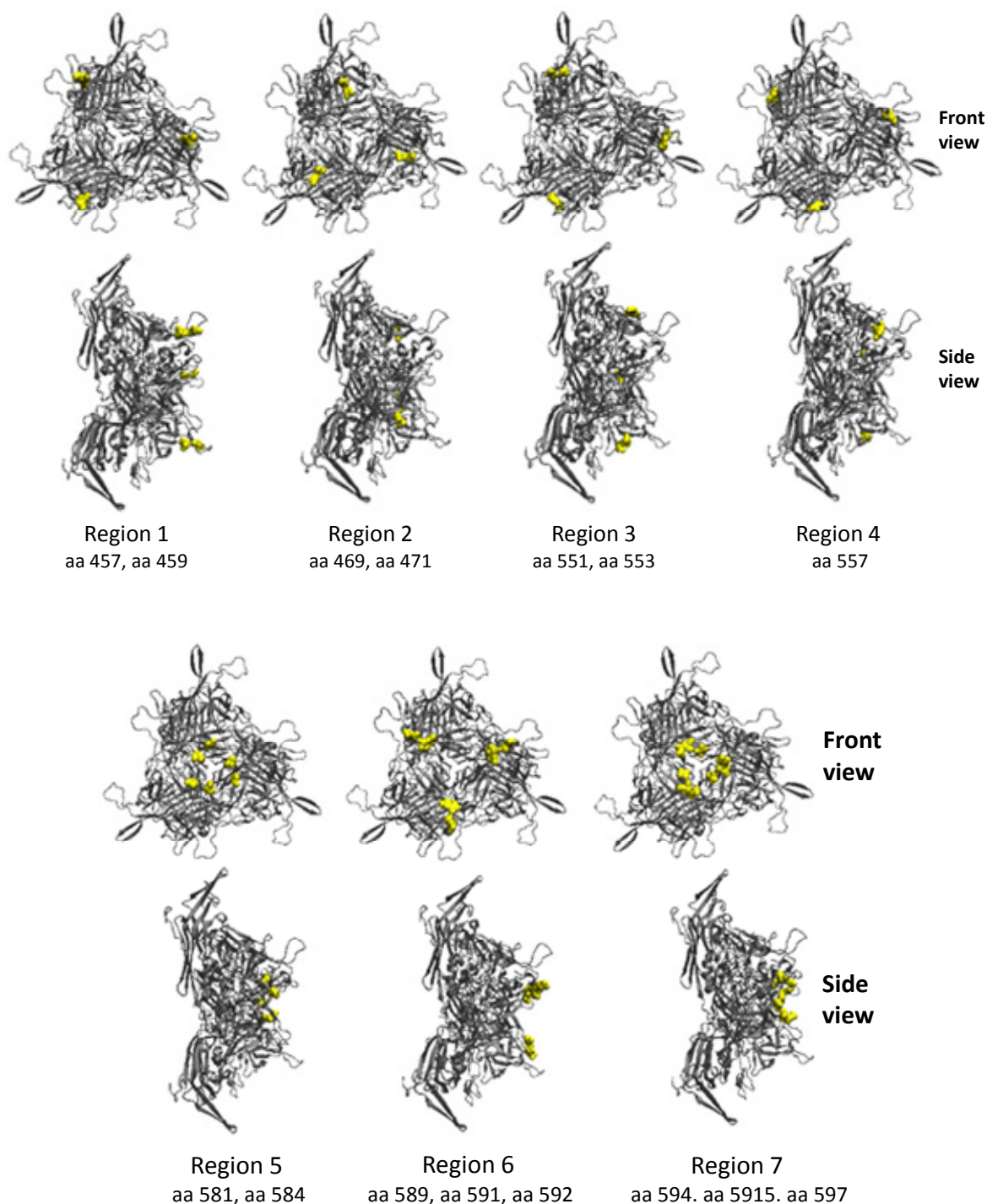


Figure 3-9 VMD modeling of the seven non-conserved regions into the AAV8 trimer. For computational analysis, the trimer was displayed in the 'newcartoon' style and was colorized in grey. Amino acid residues different between AAV8 and AAV2 were highlighted in yellow and displayed in a surf style. The trimer was modeled according to the coordinates of the AAV8 structure (Protein data bank Accession No. 2QAO).

3.3.4 Single AA Exchanges of Non-Conserved Residues from AAV2 into AAV8

Loss of functional interactions between different domains of assembled AAV capsids or to host cell factors may be the consequence of large domain exchanges between AAV2 and AAV8 (Xie *et al.* 2002; Nam *et al.* 2007; Shen *et al.* 2007). Therefore, instead of exchanging complete VP protein domains, only single amino acid residues were exchanged from AAV2 into AAV8. Figure 3-10 A shows the capsid amino acid sequence of AAV8 (aa 400-650) with the seven substitutions depicted in black boxes and as capitalized, red letters. Subsequently, modified packaging helper plasmids were used to generate chimeric vectors. Mutant vectors could be produced in sufficient amounts for iv injections into NMRI mice (Fig.3-10 B and C).

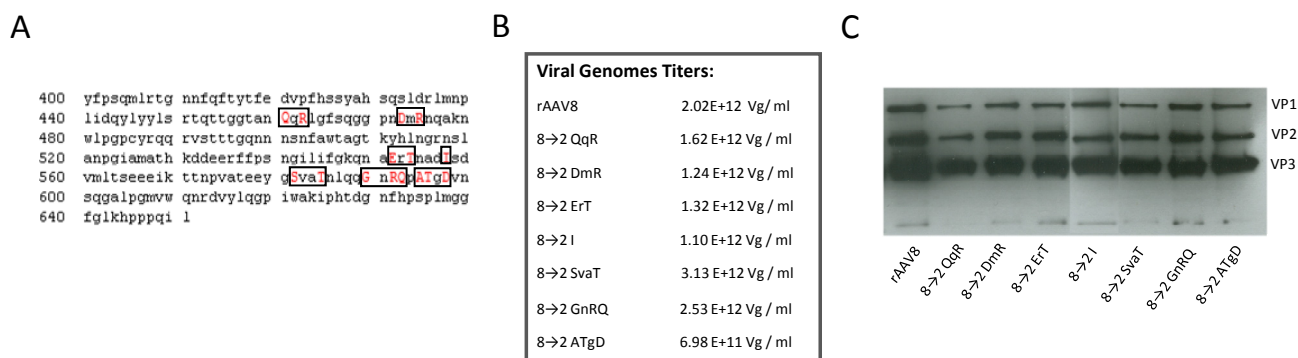
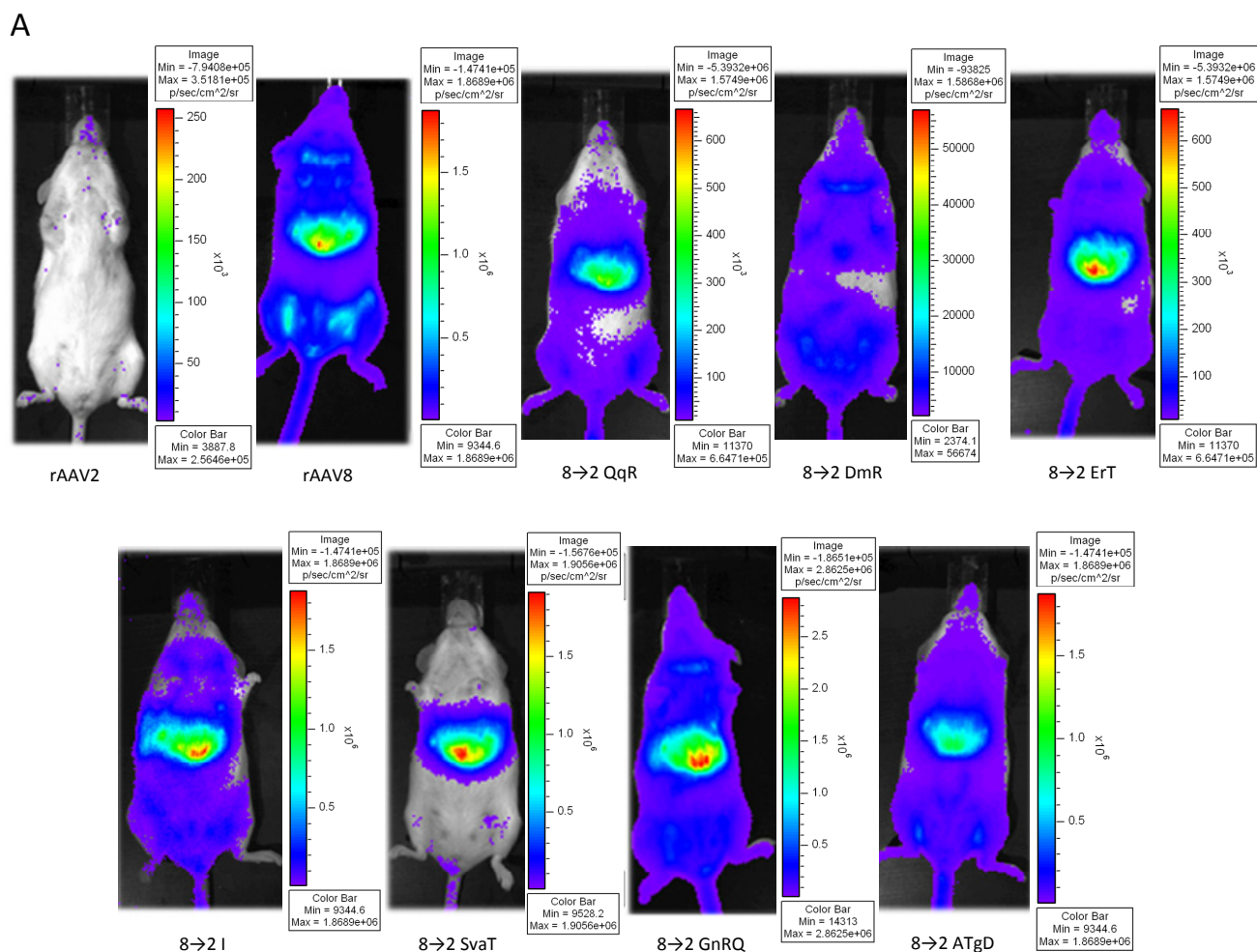


Figure 3-10 Single aa exchanges from AAV2 into AAV8 for mutant vector generation. A) Excerpt of the AAV8 based amino acid sequence (AA 400-650); the seven non-conserved regions between AAV2 and AAV8 are marked by black boxes. Generated point mutations of amino acids converted from AAV8 into AAV2 are indicated by capitalized, red letters. B) The seven mutant vector productions were generated and vg containing particle titers per ml were determined by qRT-PCR. C) Western blot analysis was performed for all productions; B1 antibody recognized all VP proteins of denatured capsids, VP protein sizes and stoichiometry between VP1, VP2 and VP3 could be demonstrated.

One month after mutant vectors had been intravenously injected, mice were imaged and subsequently sacrificed. Imaging already revealed that vector dissemination throughout the mice had changed for most single aa exchanged mutant vectors compared to rAAV8 i.v. injected animals (Fig. 3-11 A). One mutant vector, 8→2 DmR, had completely lost any preferential tissue targeting. Transgene expression was strongly reduced and widely dispersed in the mouse. Mutant vector 8→2 QqR and 8→2 ATgD appeared to cause less efficient transgene expression in the liver than rAAV8 vectors. Vector 8→2 I had not changed

the expression pattern compared to rAAV8, whereas 8→2 SvaT showed a more specific but as efficient transduction to the liver. Interestingly, vector 8→2 GnRQ demonstrated even more efficient transgene expression to the liver compared to rAAV8. The transgene expression profiles were also analysed for each mutant vector in six different tissue types, in comparison to rAAV8 and rAAV2 (Fig. 3-11 B). The results gave a more detailed picture of the transgene expression patterns than IVIS imaging. Most surprisingly, the chimera 8→2 GnRQ, a mutant which had a partial reconstituted heparin binding motif, induced an increase (10-fold) in transduction efficiency of heart and liver compared to rAAV8. Transduction of lung, spleen and muscle tissue was equivalent to rAAV8, indicating that increased transgene expression was restricted to heart and liver. Similarly, the very closely by mutant 8→2 SvaT also transduced heart and liver tissue very efficient, but transduction of other tissue types was reduced compared to wt AAV8. Those observations suggest that modification of the AAV8 capsid in these positions has an impact on gene transduction specificity or relatively preferred transduction of some tissues. Another remarkable result was that the exchange of two aa residues of AAV8 exchanged with those aa of AAV2, 8→2 DmR, resulted in a mutant capsid vector which transduced all selected tissue types very similar to AAV2.



B

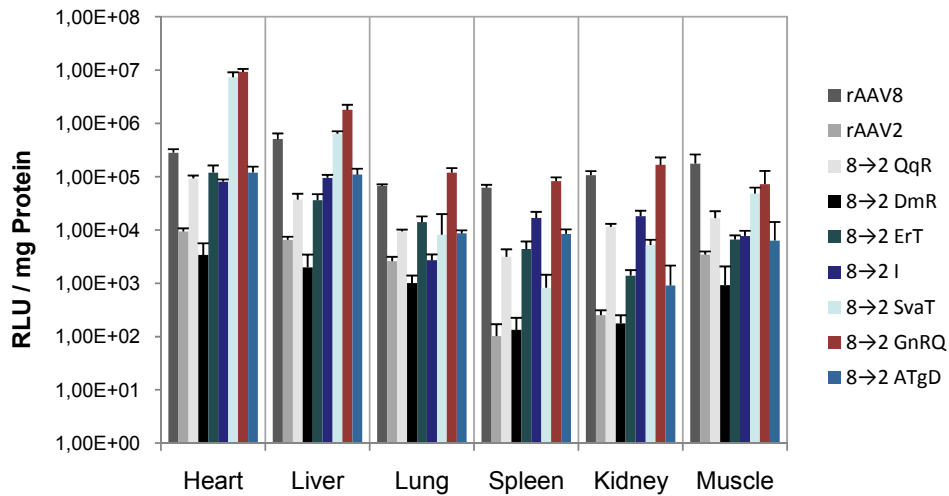


Figure 3-11 Reporter gene expression mutant vectors with single aa residues exchanged from AAV2 into AAV8 after systemic application. A) IVIS Imaging of mice i.v. injected with 1×10^{11} vg containing particles of produced mutant vectors in comparison to rAAV2 and rAAV8 vectors. Images was taken 15 min after D-luciferin i.p. injection. B) Reporter gene expression of AAV8 capsid mutants in comparison to rAAV2 and rAAV8. Seven groups of mice were i.v. injected with 1×10^{11} vg containing particles of each mutant vector, mice experiments were performed twice with two independent vector productions ($n = 6$). Two groups of 4 mice were either injected with 1×10^{11} vg containing particles of rAAV2 or rAAV8 ($n = 4$). Animals were sacrificed 1 month after injection, luciferase transgene expression per mg protein was determined for heart, liver, lung, spleen, kidney and muscle tissue.

The other vector mutants (8→2 QqR, 8→2 Ert, 8→2 I and 8→2 ATgD) induced a “non-tissue-specific” reduction of transgene expression in all tissues analysed.

Substitutions at the inner shoulder of the 3-fold spikes (8→2 GnRQ and 8→2 SvaT) - equivalent to the HSPG binding site of AAV2 – had an effect on transduction efficiency and on tissue specificity and selectivity. Mutations of aa on the outside of the spikes (8→2 Ert and 8→2 I) and on the very top (8→2 QqR) just reduced transduction efficiency to intermediate levels between rAAV8 and rAAV2 levels, suggesting that these sites act in concert with other AAV8 regions for efficient gene transduction. Replacement of 8→2 DmR, located within the capsid shell and not on the surface reduced transgene expression in all tissues to the level of rAAV2 vectors indicating a similar intracellular processing to rAAV2.

3.3.5 Adequate Substitutions of Non-Conserved Residues of AAV2 by those of AAV8

Due to the fact that single amino acid exchanges from AAV2 into AAV8 already had a strong impact on transduction efficiency, reverse single amino acid residue swaps, from AAV8 into

AAV2 were also generated. Figure 3-12 A outlines the capsid amino acid sequence of AAV2 (aa 400-650) plus the AAV8 based substitutions which were chosen. As before, exchanges were generated by site-directed mutagenesis indicated by black boxes and capitalized, red letters. Mutant vectors could also be produced in sufficient quantities for animal experiments. The VP protein expression pattern had been analysed by SDS PAGE protein gels and Western blotting (Fig.3-12 B and C).

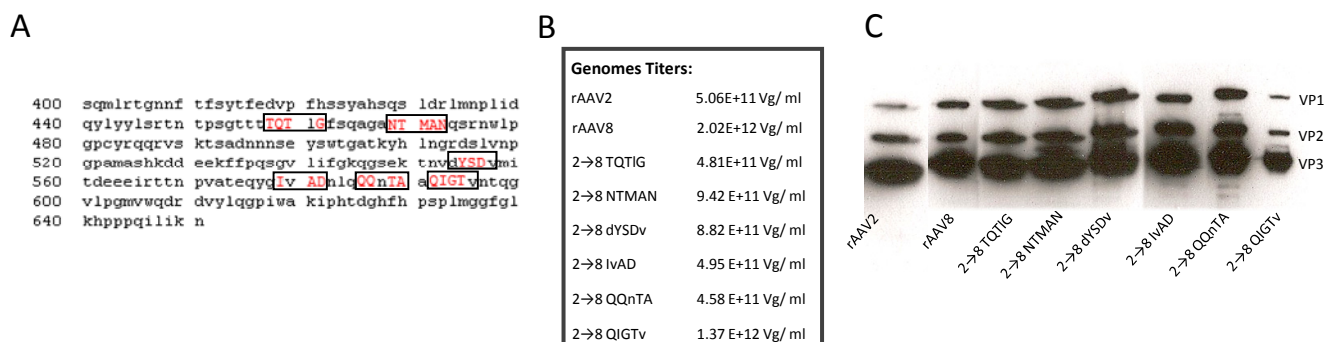
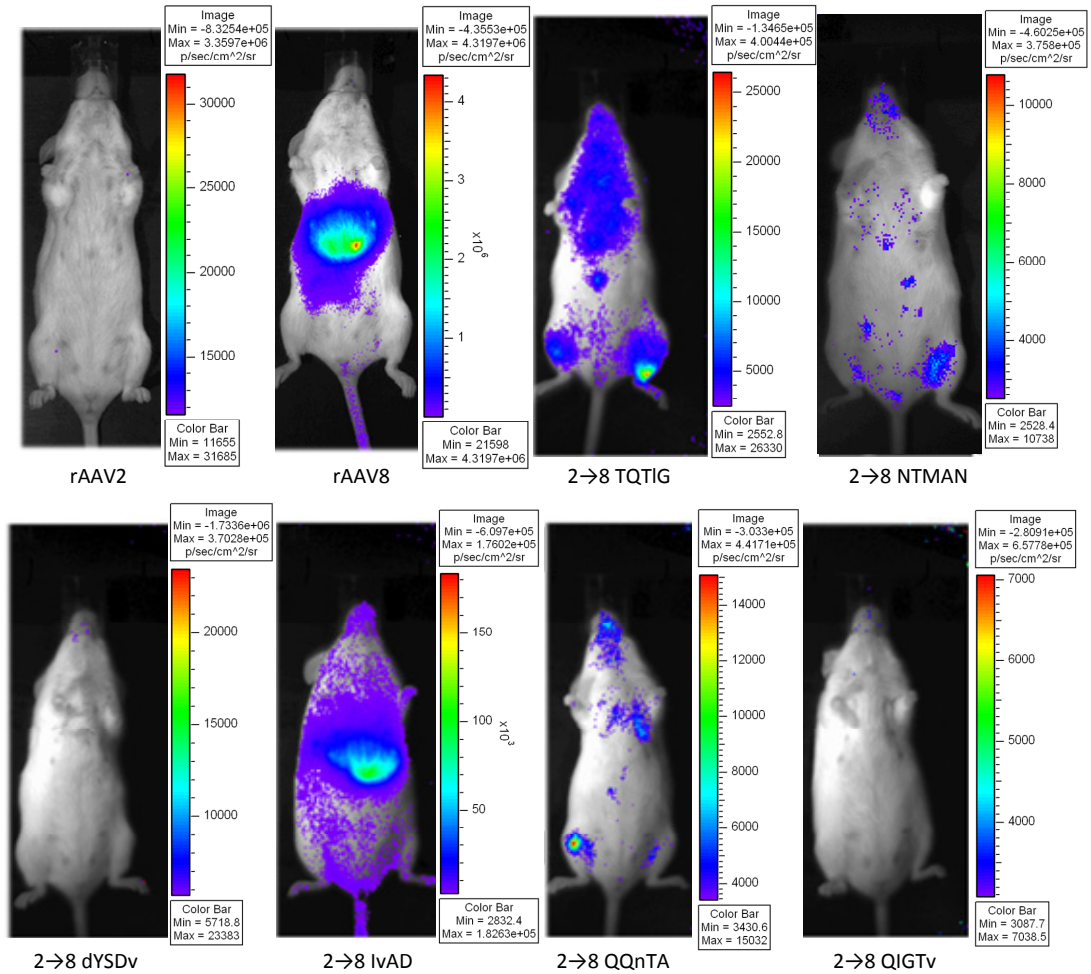


Figure 3-12 Substitutions of non-conserved aa of AAV2 by those of AAV8. A) An excerpt of the AAV2 based amino acid sequence (AA 400-650); six of the non-conserved regions between AAV2 and AAV8 are marked by black boxes, exact aa residue substitutions from AAV8 into AAV2 are with capitalized, red letters. B) The six reverse mutant vector productions were generated and vg containing particles per ml were determined by qRT-PCR. C) Western blot analysis was performed for all productions; B1 antibody recognized all VP proteins of denatured capsids, VP protein sizes and stoichiometry between VP1, VP2 and VP3 were determined.

A special focus of this experiment was the question, whether any of the reverse mutants could bring forth a rAAV2 vector with superior *in vivo* transduction efficiencies of AAV8. As seen in the images, only reverse mutant vector 2→8 IvAD fulfilled that expectation at least partially (Fig. 3-13 A). This was also evident from the reporter gene activity in different tissues (Fig. 3-13 B), although reporter gene expression similar to the expression with rAAV8 vectors was only detectable in heart tissue. Strikingly, the previously generated mutant vector 8→2 SvaT had a similar effect (Fig.3-11 C). It indicates that mutations in this region of both capsids – AAV8 and AAV2- had a positive effect on transgene expression in heart tissue. A second interesting observation was that the destruction of the AAV2 heparan sulfate proteoglycan binding motif decreased transduction into liver and lung tissue but not in heart, spleen kidney and skeletal muscle. This confirms earlier observations that mutations of the HPSG-binding motif did not prevent heart transduction but effectively reduced liver transduction (Kern *et al.* 2003).

A



B

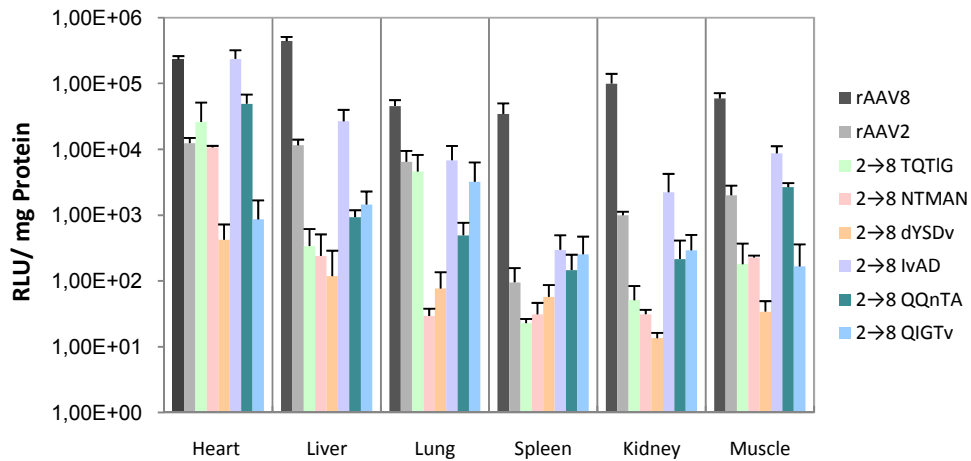


Figure 3-13 *In vivo* reporter gene expression analysis of reverse mutant vectors with single aa residues exchanged from AAV8 into AAV2. A) IVIS Imaging of mice i.v. injected with 1×10^{11} vg containing particles of mutant vectors in comparison to rAAV2 vectors and rAAV8 vectors. Images were taken 15 min after D-luciferin i.p. injection. B) Reporter expression analysis of AAV8 capsid mutants in comparison to rAAV2 and rAAV8. Six groups of mice were i.v. injected with 1×10^{11} vg containing particles of each mutant vector ($n = 5$). 1×10^{11} vg containing particles had been i.v. injected with rAAV2 or rAAV8 ($n = 4$). Animals were sacrificed 1 month after injection, luciferase transgene expression per mg protein was determined for heart, liver, lung, spleen, kidney and muscle tissue.

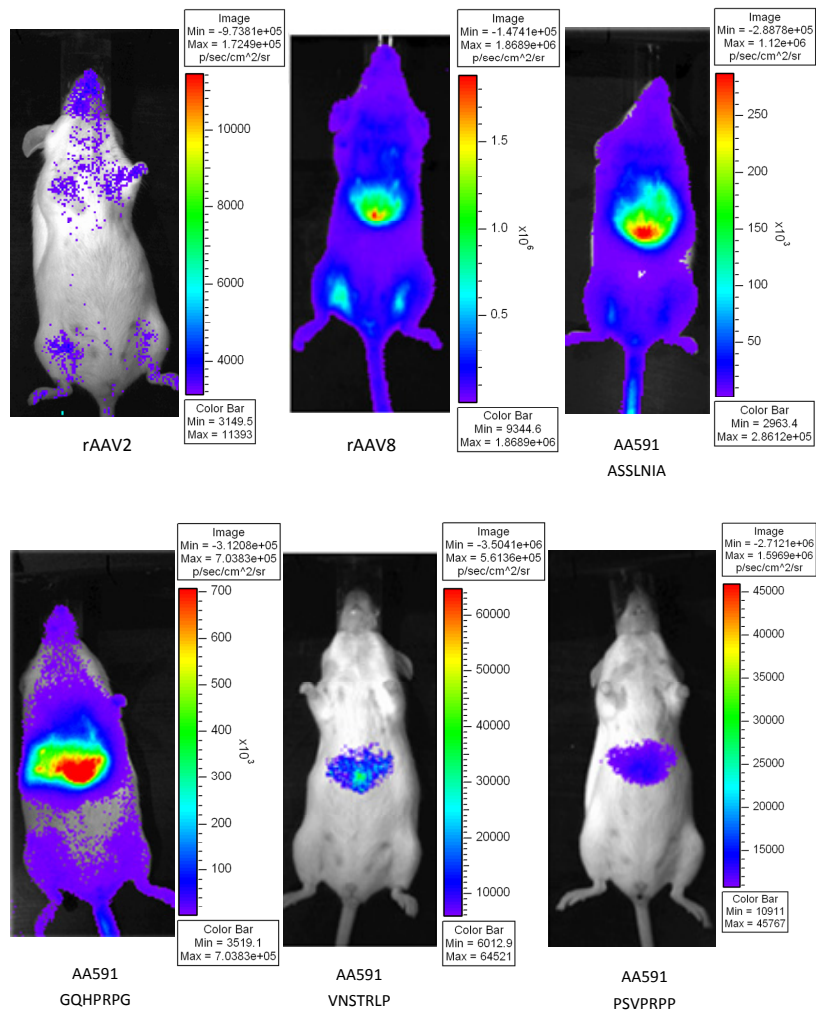
A third expectation was not fulfilled, namely the conversion of region 2 of AAV2 to AAV8 (located in the capsid shell; not at the capsid surface) did not restore general transduction efficiency, e.g. by improving intracellular processing. The other mutants had all a negative effect on transduction of most tissues indicating that several domains or aa sequences interact in a given AAV serotype and are required for optimal functioning of the rAAV vector.

3.3.6 Validation of a Peptide Insertion Site within the AAV8 Scaffold

In analogy to the AAV2 based random peptide display (Muller *et al.* 2003; Perabo *et al.* 2003; Waterkamp *et al.* 2006), a peptide insertion site for an AAV8 peptide display library was designed at the homologous position in the threefold spikes (Fig. 3-14 A). The insertion site had been positioned according to Muller *et al.*, (2003) and in addition to the *Sfi*I restriction sites, modifications were constructed according to the previous single mutant vector analysis. In fact, corresponding to mutant vector 8→2 GnRQ whose exchanges to AAV2 had strongly increased transduction efficiency, those AAV2 specific aa residues (G, R, Q and A) were exchanged at the site of insertion.

For vector production, a functional insertion site was cloned into the packaging helper plasmid p5E18-VD2/8 (Fig. 3-14 B). Without an oligonucleotide insertion coding for a peptide sequence, the modified helper plasmid could not generate functional AAV8 capsids (data not shown). By inserting oligonucleotides coding for four peptide sequences from previously derived AAV2 library selections (Yu *et al.* 2009; Ying *et al.* 2010), AAV8 based chimeric vectors (AAV8-VNS, AAV8-ASS, AAV8-PSV, AAV8-GQH) were generated into which < CMV driven *luciferase* gene was packaged (Fig. 3-14 C). IVIS images of mice which had been iv injected with peptide displaying AAV8 vectors 1 month earlier, did demonstrate a change in mutant vector dissemination in the mouse compared to rAAV8 and rAAV2 vector gene expression (Fig.3-15 A). Two motifs (ASSLNIA, GQHPRPG) demonstrated similar transduction efficiencies compared to rAAV8 vectors. On the other hand, *in vivo* selected AAV2 library derived motifs (PSVPRPP, VNSTRLP) showed a strong reduction of transduction efficiency. Reporter gene expression in different tissues, 1 month after iv administered vectors (1×10^{11} vg containing particles) ascertained that insertion of two peptide sequences, ASSLNIA and GQHPRPG, evoked a change in transduction profile compared to rAAV8 (Fig. 3-15 B).

A



B

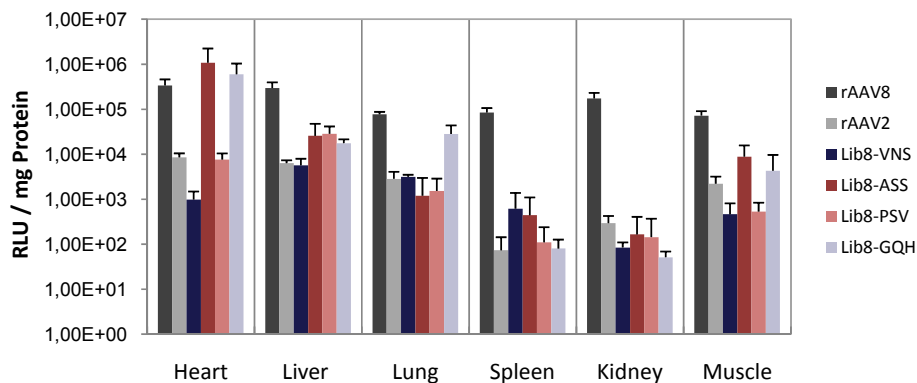


Figure 3-15 Tissue retargeting of AAV8 vectors by peptide sequence insertions into the 3-fold spike region of AAV8 capsids. A) IVIS imaging of mice, 1 month after iv injection with four different peptide displaying mutant vectors in comparison to rAAV2 and rAAV8. B) Gene expression analysis of the four peptide displaying AAV8 capsid mutants and rAAV2 and rAAV8. Wt AAV vectors had been iv injected into 3 animals each. Four groups of 3 mice were i.v. injected with 1×10^{11} vg containing particles. Mice experiments with peptide displaying mutant vectors were performed twice with two independent vector productions ($n = 6$). Animals were dissected 1 month after injection. Luciferase transgene expression per mg protein was determined for heart, liver, lung, spleen, kidney and muscle tissue.

Whereas transduction efficiency was even slightly increased in heart tissue, it was reduced in spleen, kidney, lung (moderately for GQHPRPG), and to a lower extent also in liver and muscle tissue. The results showed that the insertion of peptide sequences at that site can influence AAV8 tissue targeting and does not negatively impact capsid formation. Consequently, the insertion of a random peptide display library into the AAV8 capsid amino acid sequence at the estimated insertion site (aa 591) would make sense.

3.4 Development of a Random AAV8 Peptide Display Library

The production of a functional random peptide display library is a difficult task. As described for the AAV2 based random peptide display library, possible insertion sites were identified by mutational studies (Girod *et al.* 1999; Wu *et al.* 2000; Kern *et al.* 2003; Opie *et al.* 2003) and the AAV2 atomic structure determination by X-ray crystallography (Xie *et al.* 2002; Xie *et al.* 2003). Accordingly, the position of arginine 588 (R588), which is known to be involved in heparin binding (Kern *et al.* 2003; Opie *et al.* 2003) was a perfect candidate-site for the insertion of a random oligonucleotide into the AAV2 viral capsid. The site was suitable for peptide insertions and was exposed on the outer capsid surface. Therefore, successful AAV2 random peptide library screenings could be performed (Muller *et al.* 2003; Perabo *et al.* 2003; Waterkamp *et al.* 2006; Michelfelder *et al.* 2007; Michelfelder *et al.* 2009). Analogous to the functional insertion site in the AAV2 capsid, an insertion site was designed for the AAV8 scaffold. As presented in the previous chapter, the insertion site could be used for oligo insertion and retargeting was accomplished. For the production of the AAV8 random peptide display library, the strategy of Muller *et al.*, (2003) was used. In a first step, the plasmid library was produced by inserting randomized oligonucleotide sequences encoding 7-aa peptides into the insertion site of the AAV8 *cap* gene. Next, the so-called AAV library transfer shuttles carrying chimeric capsids composed of wt AAV2 and AAV8 library-derived capsid subunits was generated, followed by the final AAV8 random peptide display library production by infecting 293T cells at a low MOI (Müller *et al.*, 2003; Waterkamp *et al.*, 2006). Subsequently, the AAV8 random peptide display library could be used to screen for hepatotropic clones in *in vitro* selections on different hepatic cells.

3.4.1 Generation and Characterization of the Plasmid Library

An AAV8 plasmid library was produced by the insertion of 7 random oligonucleotide codons (NNK)₇ into the AAV8 library backbone (s. 2.2.7.3). Prior to the large-scale ligation, test ligations were performed using 500 ng backbone plasmid plus the adequate amounts of the insert in several molar ratios (plasmid to insert: 1:15, 1:30 or 1:100). Library backbone without the insert was used as a negative control to determine the amount of religation. The results of the test-ligation are presented in table 3-1, ligation efficiency and percentage of religation were calculated for all molar ratios and best conditions were present at the molar ratio 1:15 between plasmid and insert. The ligation efficiency was 6.25×10^6 , with only 1.57 % religation. Accordingly, the large-scale ligation could be produced. Ligated plasmids were transformed into electro-competent DH5 α bacteria, 52 electroporations were performed for the plasmid library generation (s. 2.2.7.3.2).

Table 3-1 Ligation efficiency

AAV8 Plasmid Library Test Ligation	Ligation Efficiency ¹			Percentage of Religation ²		
Molar Ratio Library : Insert	1 : 15 [350 ng : 40 ng]	1 : 30 [350 ng : 80 ng]	1 : 100 [350 ng : 40 ng]	1 : 15	1 : 30	1 : 100
(NNK) ₇ Insertion	6.25E+06	1.73E+06	1.82E+06	1.57 %	5.11 %	4.69 %

¹Colony forming units (CFU) $\times 1 \mu\text{g}/\text{A} \mu\text{g} \times \text{B} \mu\text{l}/100 \mu\text{l}^* \times$ dilution factor was calculated to determine the ligation efficiency per μg of ligated plasmid DNA. **A** is the amount of plasmid DNA used in the electroporation protocol (20 ng). **B** is the total volume of transformed bacteria after 1 h cultivation (1ml). *100 μl of the bacterial culture was plated (undiluted or diluted 1:10 in H₂O).

²Percentage of religation was determined for each molar ratio. Acceptable religation values have to be $< 2.0 \%$.

One hour after pre-shaking at 37°C, the bacterial culture (100 ml) was subdivided onto four flasks containing 475 ml and grown O/N under constant shaking conditions at 30°C. After 16 h, the plasmid library was purified by the Qiagen DNA Gigaprep kit (s. 2.2.2.2). To determine the diversity of the produced plasmid library, a sample from each flask was taken prior to the O/N shaking at 30°C, and plated (undiluted, 1:10, 1:100 and 1:1000 diluted). In table 3-2, the plasmid library diversity for each bacterial culture was determined and the resulting diversity was 4.1×10^7 , 30-fold below the theoretical diversity value 1.28×10^9 .

Table 3-2 Diversity determination of the AAV8 plasmid library

AAV8 Plasmid Library Large-Scale Electroporation	Number of Colonies				Resulting Diversity [*]	
	Dilution Factor	-	1:10	1:100	1:1000	1:100
X_1	nd.	nd.	280	35	2.7E+07	² Theoretical Diversity: 1.28E+09
X_2	nd.	nd.	250	15	2.4E+07	
X_3	nd.	nd.	440	30	4.2E+07	
X_4	nd.	nd.	740	45	7.0E+07	

*Resulting diversity of the plasmid library was determined as presented in figure 2-4. ²Theoretical diversity of the (NNK)₇ plasmid library was determined as (20)⁷, 20 is the total possibilities of encoded amino acids excluding the only possible stop codon TAG of the triple nucleotide NNK. If colonies could not be counted by eye, they were indicated with nd., not able to determine colony numbers.

(Calculation Example: 280 CFU x (1 µg/ 0.26 µg [13 x 20 ng electroporated]) x (25000 µl [4 x 25 ml culture after 1 h pre-shaking] /100 µl) x 100 [dilution factor] = 2.692 x 10⁷ diversity)

3.4.2 Analysis of the AA Frequency Distribution in the Generated Plasmid Library

To verify the presence of random oligonucleotide inserts, 96 clones were picked randomly from the agar plates used to determine the diversity of the plasmid library. Clones were sent for sequencing, 89 clones had positive sequencing results. DNA sequencing showed that oligonucleotides had been successfully cloned into the plasmid library backbone and the sequencing results revealed a high diversity of peptides. The aa residue and stop-codon frequency in the sequenced (NNK)₇ oligonucleotides was calculated and compared to the theoretical distribution of aa in the (NNK)₇ plasmid library (Fig. 3-16). The aa frequencies were mostly similar to the theoretical values. However, four aa residues strongly deviated from their theoretical frequencies. Phenyl-alanine (F) should have been at 2.5 % but had a frequency of 8 %. Proline (P) had a theoretical appearance of 6 % but was actually only at about 2.5 %, whereas valine (V) and tryptophan (W) should have had a frequency of 6 % and 2.5 %, but showed frequencies of 10 % and 8 %, respectively. Nonetheless, these results were good enough for a transfer shuttle library generation.

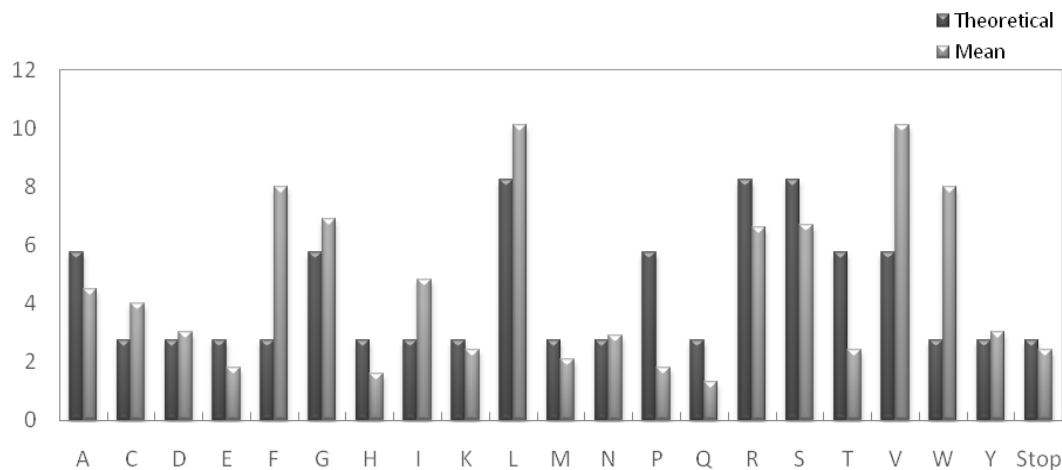


Figure 3-16 Frequencies of all aa residues in the generated AAV8 plasmid library. In comparison to the theoretical distribution (Theoretical) of the aa residues in an (NNK)₇ oligonucleotide based plasmid library, the actual frequencies of aa and stop-codons according to the sequences of 89 randomly picked and sequenced clones are illustrated (Mean).

3.4.3 Transfer Shuttle Library Generation

As described in Y. Ying (Ying 2007), the insertion of peptides with seven aa in length into the AAV2 library plasmid caused the most vg containing particle formations in a transfer shuttle library production. After insertions of larger (12, 19 or 26 aa) or smaller (5) peptides, the production of vg containing particles was decreased. Therefore, the generated AAV8 transfer shuttle library was analysed in comparison to the corresponding AAV2 transfer shuttle library (Fig. 3-17). The presented results showed that the AAV8 transfer shuttle library was as functional as the AAV2 transfer shuttle library. For vg containing particles, replicative units and particle infectivity same sampled values could be obtained, thus the produced AAV8 transfer shuttle library was identified to be fully functional. This was an important validation because the produced chimeric capsids were partially composed of wt AAV2 and

AAV8 library-derived capsid subunits. An *in vitro* transduction of 293T cells to produce the final AAV8 random peptide display library could be approached.

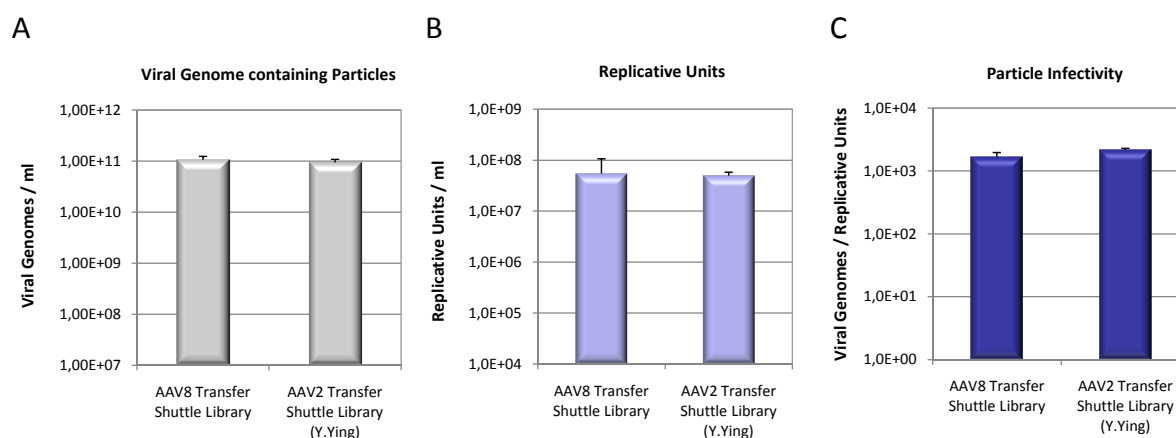


Figure 3-17 Generation of the transfer shuttle library after (NNK)₇ peptide insertions into the AAV8 library backbone. A) The yields of genome-containing transfer shuttle particles were determined with a *rep* probe by qRT-PCR. B) Replicative units of particles were determined by a replicative assay and corresponding DNA labeling by a ³²P radioactively labeled probe. C) Transfer shuttle library particle infectivity was quantified by vg containing particles per replicative units. Titration assays for the AAV8 based library production was carried out independently three times to determine mean values and standard deviations. All data were compared to results of the AAV2 transfer shuttle library performed by Y. Ying (Ying 2007).

3.4.4 *In Vitro* Selection and Identification of Liver Targeting Vectors from the AAV8 Display Peptide Library

After the AAV8 random peptide display library had been produced in sufficient amounts (8×10^{12} vg containing particles/ml), it was used for an *in vitro* screening approach. *In vitro* selections were performed to assay whether targeted vectors could be enriched (Fig. 3-18). Target cells were infected with the AAV8 library. The virions which could not enter the cells were removed by washing cells with PBS 4 h after infection, next, cells were superinfected with Ad5 to amplify the internalized AAV8 library clones. Replicated AAV particles were recovered from the cell lysate. AAV vg titer was determined by qRT-PCR and the particles were added to cells with a reduced MOI for another selection round. From the cell lysate, DNA was extracted and the region containing the oligonucleotide inserts of the selected AAV particles was amplified by PCR, subcloned and sequenced (s. 2.2.7.7). Three different kinds of target cells were chosen for the *in vitro* selection. To select for hepatotropic targeted vectors, murine hepatocytes Hepa 1.6, human hepatocytes Huh7 and primary mouse hepatocytes were used. All three cell types had in common that AAV8 cell transduction was

inefficient. Prior to the selection, the infectivity of Ad5 was tested for all three cell lines to ensure that adeno-dependent helper functions were able to support AAV vector replication.

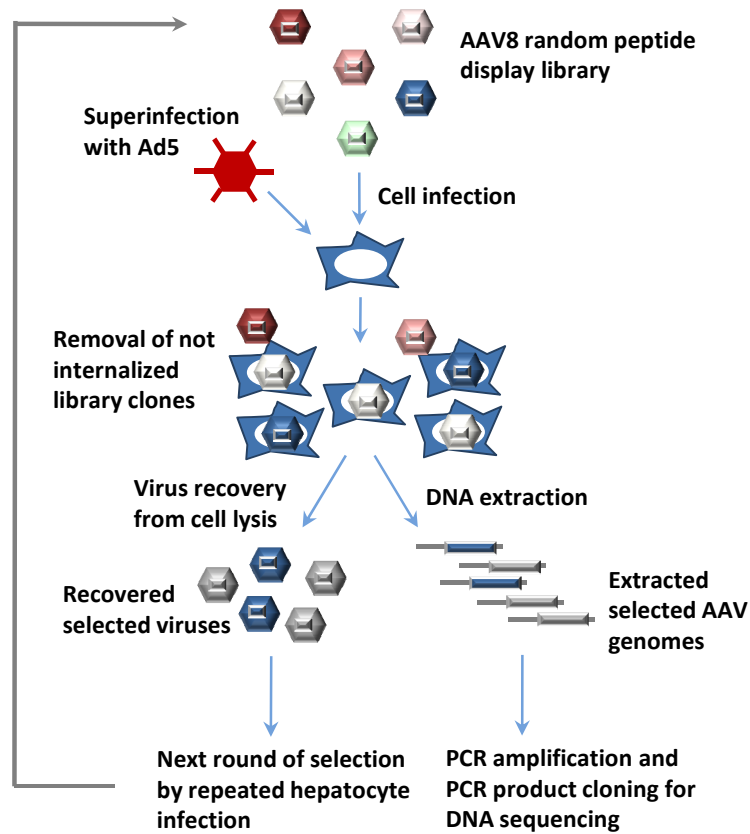


Figure 3-18 Schematic representation of the *in vitro* selection of targeted vectors from an AAV8 random peptide display library. See text for details.

It turned out that Hepa 1.6 and Huh7 cells had to be superinfected with MOI 10, whereas MOI 10,000 was needed for the superinfection of primary murine hepatocytes. As illustrated in table 3-3, four selection rounds were performed. MOI of vg containing particles was serially decreased to improve selection for targeted vectors. Generally, none of the three selections showed optimal selection results, especially for primary hepatocytes and Hepa 1.6, the yield was rather low compared to the vector input. On the other hand, in case of Huh7, the yield was very high for all selection rounds.

Nonetheless, DNA was extracted from the third and fourth selection round, oligonucleotide inserts were PCR-amplified, subcloned and send for sequencing.

Table 3-3 *In vitro* selections with the AAV8 random peptide display library

Cell Type ¹	Selection Round ²	MOI ³	Input ⁴	Yield ⁵
Primary Hepatocytes	Round 1	1,0E+04	1,00E+10	5,40E+10
	Round 2	5,0E+02	5,00E+08	1,20E+07
	Round 3	50	5,00E+07	4,00E+07
	Round 4	5	5,00E+06	9,23E+06
Hepa 1.6	Round 1	1,0E+04	1,00E+10	1,00E+10
	Round 2	5,0E+03	5,00E+09	2,00E+08
	Round 3	5	5,00E+06	2,90E+06
	Round 4	1	1,00E+06	2,30E+06
Huh7	Round 1	1,0E+03	1,00E+09	1,60E+12
	Round 2	1,0E+02	1,00E+08	4,20E+12
	Round 3	10	1,00E+07	1,66E+12
	Round 4	1	1,00E+06	4,40E+12

¹The selections on three different target cells with the AAV8 library displaying random peptide 7 aa in length.

²Four selection rounds were performed for the different target cells.

³ MOI (vg containing particles per cell) of the AAV8 library vectors used for each selection round. MOI was reduced with every following selection round.

⁴ Input was determined as the total amounts of vg containing particles added to the target cells (MOI x total cell amount).

⁵ Yield was the amount of AAV vectors recovered from the respective selection round. Titers were determined by qRT-PCR.

3.4.4.1 Characterization of Targeting Peptides Recovered from the *In Vitro* Selections

Sequence analysis of the PCR-amplified DNA extracts (s. 2.2.7.8) revealed that the recovered peptide inserts strongly differed from peptides of previous *in vitro* selections performed with the AAV2 random peptide display library on heart tissue cells. In all three selections, peptide sequences were identified which were enriched with all 4 selection rounds (Fig. 3-19). Interestingly, the selections could show that of all recovered clones, distinct aa residues were present in high abundance. In case of the *in vitro* selection on Huh7 cells, the peptide module RSS, RSR or RSV were repeatedly identified as the 5th to 7th aa of the peptide sequence. The aa residue F was highly prevalent in the 1st and 4th position and all isolated peptide inserts were G and R rich. As highlighted in grey in fig. 3-19 A, the peptide sequences SSRGLGK (21.7 %) and SEVARCR (60.9 %) were the most prominent peptides identified after the 4th selection in the screen. In the *in vitro* selection on Hepa 1.6 cells, two peptide sequences were also enriched with the 4th selection round, SSRGLGK and VGLVLRs were

present in 28.6 % of the clones (Fig. 3-19 B). The peptide module SV was present in the last aa residues of two peptide sequences and the inserts were generally rich in S, L and I. The 3rd selection had been performed with primary murine hepatocytes and most recovered peptide sequences contained the aa residues G, I and L (Fig. 3-19 C). The majority of peptide inserts recovered had the peptide sequences SEGLKNL (18.5 %) and WFAAKLA (14.8 %). Some peptide sequences were recovered from two independent screens, e.g. SSRGLGK had been recovered in the screen on Hepa 1.6 cells and Huh7 cells, VGLVLRV was identified in the 4th selection round of Hepa 1.6 cells and from the primary murine hepatocytes and WFAAKLA was determined in the 3rd selection round of Hepa 1.6 cells and had been enriched in the primary murine hepatocyte selection. Whether the isolated, most abundant peptide sequences really were hepatotropic, they had to be displayed on the AAV8 capsid surface and analysed *in vivo*.

A

CellType (NNK) ₇	Peptide Sequence	Selection Round 3	Selection Round 4
Huh7	RSYMLE	21.7 % (5x)	13% (3x)
	RGKRRSS	8.7 % (2x)	-
	GGKRRSS	8.7 % (2x)	4.3 % (1x)
	ENWFASV	4.3 % (1x)	-
	ENWFRSV	4.3 % (1x)	-
	TGKRRSS	4.3 % (1x)	-
	SGKPRSR	4.3 % (1x)	-
	AGKRRSS	4.3 % (1x)	-
	FAWELSV	4.3 % (1x)	-
	ENWEGSV	4.3 % (1x)	-
	TLSRVMF	4.3 % (1x)	-
	KDRPSLM	4.3 % (1x)	-
	SSRGLGK	21.7 % (5x)	21.7 % (5x)
	SEVARCR	-	60.9 % (14x)
ENWFRSV	-	4.3 % (1x)	
ENWFSSV	-	4.3 % (1x)	

B

CellType (NNK) ₇	Peptide Sequence	Selection Round 3	Selection Round 4
Hepa 1.6	KPTKRLW	35.7 % (5x)	14.3 % (2x)
	WFAAKLA	21.4 % (3x)	-
	QLWTLVS	7.1 % (1x)	-
	WLKAHVS	7.1 % (1x)	-
	SLDNSFR	7.1 % (1x)	-
	SSRGLGK	7.1 % (1x)	28.6 % (4x)
	ASLRSGC	7.1 % (1x)	-
	RSISALF	7.1 % (1x)	-
	VGLVLRV	-	28.6 % (4x)
	DFSTSGE	-	14.3 % (2x)
	GVYIPVN	-	7.1 % (1x)
	GLISNVF	-	7.1 % (1x)

C

Cell Type	(NNK) ₇ Peptide Sequence	Selection Round 3	Selection Round 4
Primary Hepatocytes	GFASGRV	3.7 % (1x)	-
	RNGGLKS	3.7 % (1x)	-
	AGNSRC	3.7 % (1x)	-
	SEGLKNL	3.7 % (1x)	18.5 % (5x)
	GLDNFR	3.7 % (1x)	-
	GAHPSYY	3.7 % (1x)	-
	DVEVYFN	3.7 % (1x)	-
	DSGFWFA	3.7 % (1x)	-
	KPTKRLW	3.7 % (1x)	-
	VGLVLR	3.7 % (1x)	-
	CRILVGR	3.7 % (1x)	-
	SSLGLTC	3.7 % (1x)	-
	KGFVEFA	3.7 % (1x)	-
	WFAAKLA	-	14.8 % (4x)
	LWARGER	-	3.7 % (1x)
	SLDNLFR	-	3.7 % (1x)
	CSRANLC	-	3.7 % (1x)
	YKGLASA	-	3.7 % (1x)
	VLFVSVV	-	3.7 % (1x)
	IQAVGKM	-	3.7 % (1x)
CRILVGR	-	3.7 % (1x)	
GEMVIRR	-	3.7 % (1x)	
LREPGGR	-	3.7 % (1x)	
VLFQRVV	-	7.4 % (2x)	
LGCALFI	-	3.7 % (1x)	

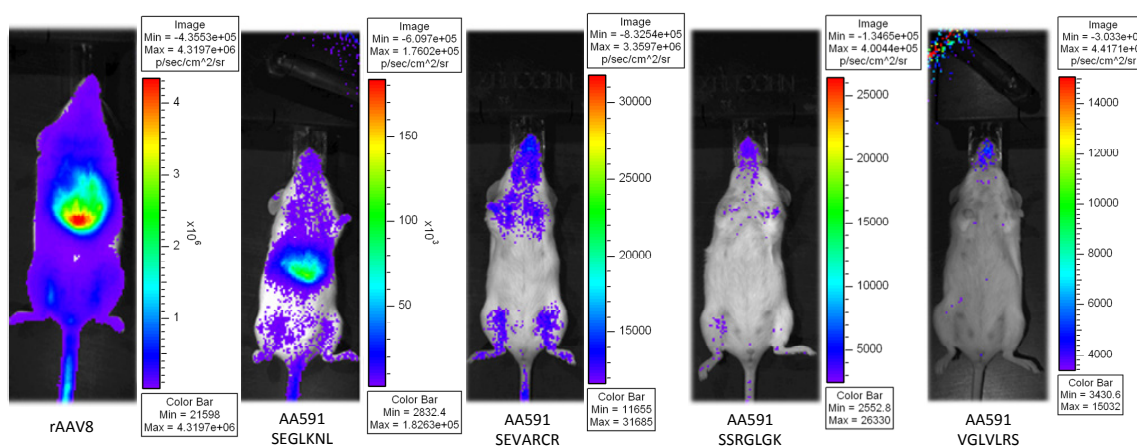
Figure 3-19 Peptide sequences isolated from DNA extracts of the 3rd and 4th selection round with the AAV8 random peptide display library on Huh7 cells, Hepa 1.6 cells and primary murine hepatocytes. Peptide sequences (one letter code) obtained from the DNA extracts of the different selection rounds are presented. Recovery rate (%) was calculated according to the total amount of peptide sequences recovered, actual numbers of recoveries are indicated in brackets. Most frequent aa residues are highlighted by colored boxes, most prominent peptide sequences of all three different selections are highlighted in grey. Empty columns (-) indicate that the particular peptide sequence was not present in that selection round. A) Peptide sequences recovered from the 3rd and 4th selection on Huh7 cells. B) Peptide sequences recovered from the 3rd and 4th selection on Hepa 1.6 cells. C) Peptide sequences recovered from the 3rd and 4th selection on primary murine hepatocytes.

3.4.5 Generation of Vectors Displaying AAV8 Library Selected Peptides

The four most enriched peptide sequences isolated from selections on different hepatocytes were selected as candidate peptides to analyze their capabilities of hepatotropic targeting. The oligonucleotides coding for peptides SSRGLGK, SEVARCR, SEGLKNL and VGLVLR were inserted into the *Sfi*I insertion site of the modified helper plasmid p5E18-VD2/8+*Sfi*I in order to produce recombinant vectors displaying the respective peptide sequences (Fig. 3-20 A). HEK293T cells were transfected as illustrated in figure 3-20 B. Viral vectors displaying the different peptides, 7 aa residues in length, could be produced sufficient quantities for gene transduction analysis.

Analysis of transgene expression in several tissues gained more insight into chimeric vector induced changes in transduction efficiency (Fig. 3-21 B). Compared to rAAV8, the vector displaying the peptide SEGLKNL revealed 3-fold transgene expression in the liver, but caused a dramatic reduction in other organs close to the border of detection level. Especially in heart tissue and also in muscle tissue was some gene expression detectable for other vectors displaying peptide sequences SEVARCR, SSRGLGK and VGLVLRs. However, in liver, lung and kidney tissue, transduction efficiency was strongly reduced (> 100-fold). In conclusion, the *in vitro* selection gave rise to a peptide sequence SEGLKNL which did not increase transduction efficiency of rAAV8 in liver tissue but significantly detargeted rAAV8 from several non-hepatic tissue types.

A



B

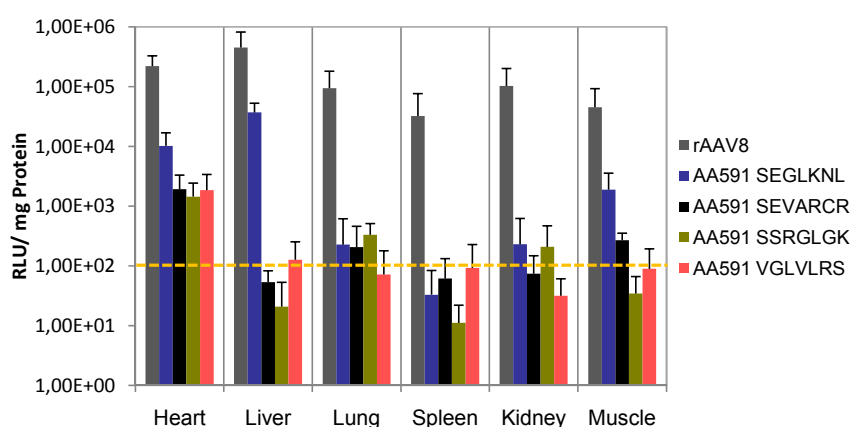


Figure 3-21 *In vivo* analysis of the *in vitro* selected peptide sequences derived by an AAV8 random peptide display library.

A) IVIS images of mice analysed 1 month after i.v. injection with rAAV8 or with one of the four peptide-displaying AAV8 capsid mutants, injection contained 1×10^{11} vg containing particles. Images were taken 15 min after i.p. D-luciferin injection. B) *In vivo* analysis of four peptide-displaying AAV8 capsid mutants in comparison to rAAV8 ($n = 3$). Peptide displaying vectors were iv injected into mice with 1×10^{11} vg containing particles. Mice experiments with peptide displaying vectors were repeated with a second set of vector productions ($n = 6$). Animals were dissected 1 month after injection. Luciferase transgene expression per mg protein was determined for heart, liver, lung, spleen, kidney and muscle tissue. The yellow dashed line indicates the border of detection at 100 RLU / mg protein.

3.5 AAV8 dependent Cell Binding and Post-Entry Processing

3.5.1 Comparison of Genome Transfer and Transgene Expression in Different Tissues

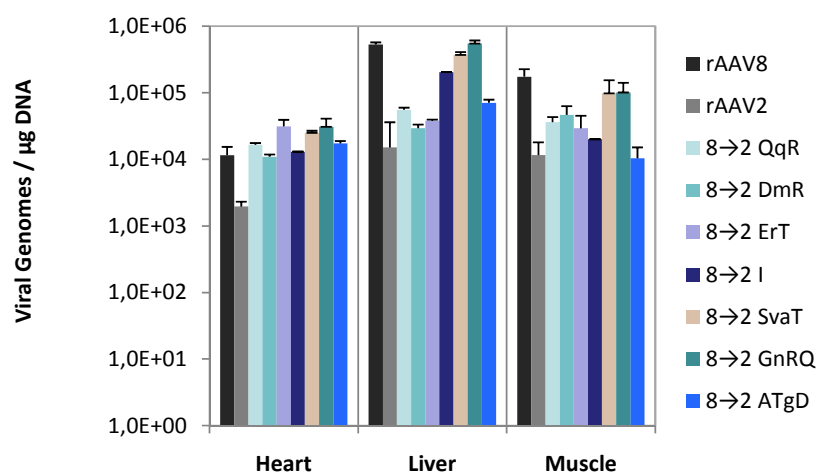
Several attempts have been made to characterize the importance of uncoating for rAAV vector particles (Thomas *et al.* 2004; Akache *et al.* 2007; Murphy *et al.* 2008a). The heat treatment assays were very speculative for the interpretation of uncoating efficiency *in vivo* (Murphy *et al.* 2008a). However, the coimmunoprecipitation of capsid specific antibodies with rAAV vector genomes from isolated nuclei showed a more efficient rAAV8 transport to the nucleus than for rAAV2 vectors. Additionally, more biological activity (measured by the amounts of detected hFIX protein) of nuclear localized AAV vg in liver tissue also suggested a more rapid uncoating for rAAV8 vectors (Thomas *et al.* 2004). Nonetheless, a comparison between wt AAV vectors only and a focus on liver tissue could not contribute to a general characterization of uncoating for rAAV vectors.

Instead, we decided to quantify vector genome uptake in heart, liver and muscle tissue for rAAV2 vectors, rAAV8 vectors but also for capsid mutant vectors which had been generated by aa substitutions from the AAV2 protein sequence into the AAV8 capsid (Fig 3-22 A). In general, the amount of viral genomes per μg DNA was similar in heart, liver and muscle tissue. However the amount of rAAV8 vg compared to rAAV2 vg was about 10-fold higher in heart and muscle tissue and even higher in liver tissue. All analysed mutant vectors showed similar vg amounts in heart tissue, homolog to rAAV8 vg amounts. But quantities of vg varied in liver and muscle tissue for the mutant vectors. Interestingly, for mutants 8 \rightarrow 2 QqR, 8 \rightarrow 2 DmR, 8 \rightarrow 2 ErT and 8 \rightarrow 2 ATgD similar vg amounts were detected compared to rAAV2 vectors and the amount of vg present in mutants 8 \rightarrow 2 SvaT and 8 \rightarrow 2 GnRQ were homolog to rAAV8 vector quantities.

Next, the obtained data were related to transgene expression of the different rAAV vectors and a ratio was determined indicating efficiency of uncoating (Fig. 3-22 B). Three different aspects were observed. According to the ratios, rAAV2 showed less uncoating than rAAV8 in all organs, especially in liver tissue (more than 50-fold). Mutants 8 \rightarrow 2 SvaT and 8 \rightarrow 2 GnRQ showed much higher uncoating in heart tissue than rAAV8 but not in muscle tissue. In liver tissue, uncoating was strongly increased for mutant 8 \rightarrow 2 GnRQ compared to rAAV8. Mutant 8 \rightarrow 2 DmR whose exchanges were situated within the capsid shell showed less uncoating

than even rAAV2 in heart and muscle tissue and uncoating similar to rAAV2 in liver tissue. Uncoating efficiency was different for the three tissue types. Whereas, in heart tissue, the highest uncoating values were detected, uncoating in muscle and liver tissue was less efficient. Uncoating efficiency does not only depend on the analysed AAV serotype but also on the analysed tissue type.

A



B

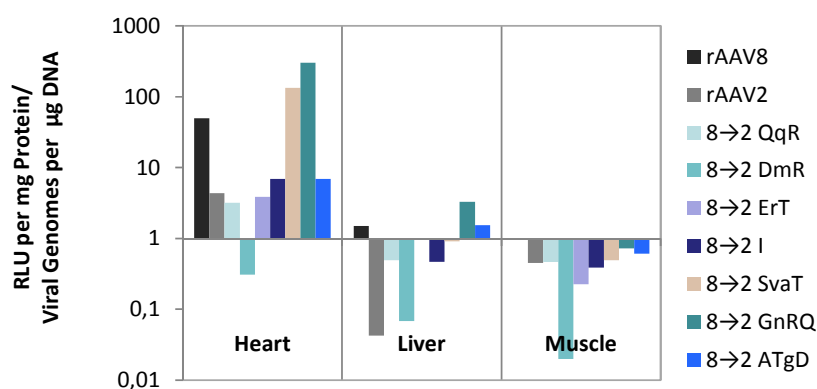


Figure 3-22 Correlation between transfer of viral genomes and transgene expression in heart, liver and muscle tissue. A) Viral genome uptake in heart, liver and muscle tissue was determined by qRT-PCR for rAAV8, rAAV2 and capsid mutants which had been generated by aa substitutions from the AAV2 protein sequence into the AAV8 capsid. Organs of six animals, which had been iv injected with 1×10^{11} vg containing particles, were analysed in the experiment, results were correlated to $1 \mu\text{g}$ total mouse DNA. Total DNA was determined with a probe specific for GAPDH. B) Ratios were calculated by analyzing gene expression (RLU/ mg protein) per viral genomes (viral genomes / $\mu\text{g DNA}$) for heart, liver and muscle tissue.

3.5.2 Characterization of an AAV8 Capsid Specific Monoclonal Antibody ADK8

In the field of AAV research, many monoclonal antibodies, such as B1, A1, A69 or A20, have been well studied and characterized in the past (Wistuba *et al.* 1995; Wobus *et al.* 2000; Kuck *et al.* 2007). The collection of generated monoclonal antibodies has been increasing rapidly and contributed to a detailed analysis of AAV2 capsid (Grimm *et al.* 1999; Kern *et al.* 2003), the best studied serotype. The generation of monoclonal antibody with AAV8 capsid specificity (ADK8) was the basis for studies on the AAV8 capsid.

At first, it was validated whether the derived monoclonal antibody ADK8 was really specific for AAV8 capsids. In a native dot-blot assay, it could be determined that ADK8 only recognizes AAV8 particles (Table 3-23 A). Whereas B1 recognized all the denature capsids of AAV1 – AAV9, despite of AAV4 (rAAV7 vectors were not available), a weak recognition of AAV3 capsids was present in immune-fluorescence studies and in a native dot blot.

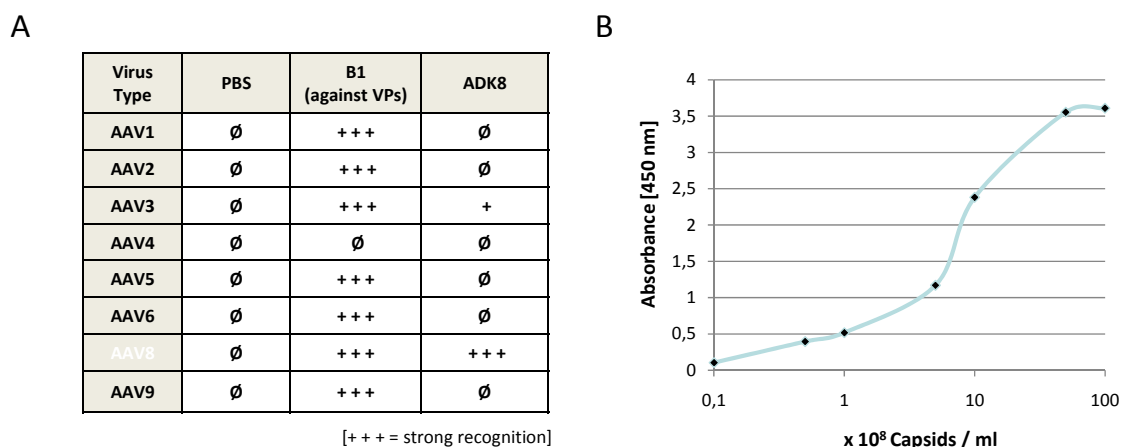


Figure 3-23 Capsid detection of the monoclonal antibody ADK8. A) Specific binding properties of ADK8 are illustrated by demonstrating its specificity for AAV8 capsids in comparison to B1, a monoclonal antibody which recognizes all indicated C-termini despite of the AAV4 C-terminus. B) An example of a titration curve of the produced AAV8 standard. Absorbance was measured in correlation to capsids, the detection was limited to 1×10^7 capsids/ ml.

A mouse isotyping kit (Roche, Bensberg) revealed that the derived monoclonal antibody was an IgG 2a antibody. For antibody purification from hybridoma culture, a Sepharose A column was used and sufficient quantities of ADK8 antibody could be purified (about 20 mg). For the AAV8 capsid standard, rAAV8 vectors were produced and purified adequately to calculate the capsid amounts by negative staining (s. 2.2.6.6). An ELISA against AAV8 capsids could be established subsequent to the determination of a standard titration curve (Fig. 3-23 B).

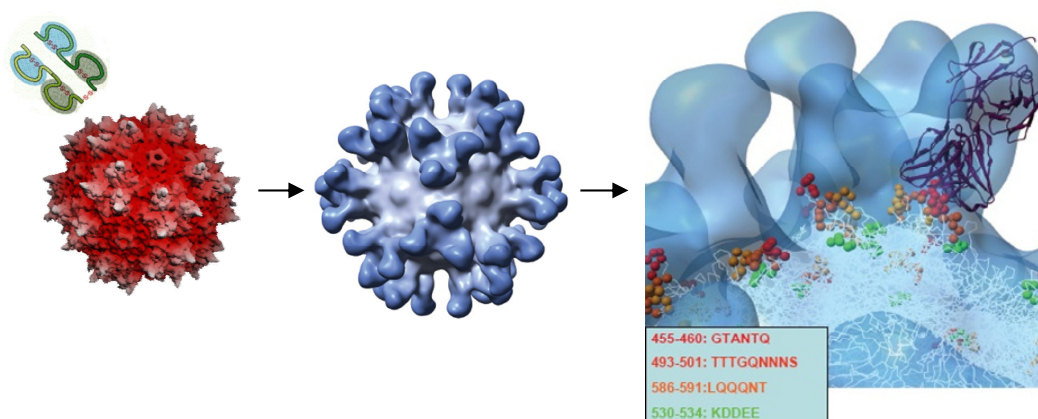


Figure 3-24 ADK8 footprint analysis. AAV8 capsids and ADK8 Fab fragments were combined, and Fab fragments bind to the capsid surface. The AAV8-ADK8 Fab complexes were analysed by cryo-electron microscopy. Complexed particles contributed to a preliminary ADK8 footprint on the AAV8 capsid surface could be generated. Possible binding epitopes on the capsid could be identified. Enlarged, on the right hand side red, orange, yellow and green ball shape structures indicate the four possible binding epitopes. The aa present in each epitope are marked with the same color as their structures. The peptide sequence and aa position are shown in a box (light-blue) below the footprint. One Fab fragment is illustrated in a blue ribbon structure bound to the four potential epitopes on the capsid.

Next, an ADK8 footprint analysis was performed by M. Agbandje-McKenna to properly characterize the binding epitope of ADK8. ADK8 Fab fragments were bound to AAV8 particles and an AAV8-ADK8 complex image was reconstituted from pictures taken at a resolution of 21 Å. A preliminary footprint indicated four possible binding epitopes (Fig. 3-24). In particular one possible epitope was interesting to us, as LQQQNT (aa 586-591) was overlapping with the peptide sequence of capsid mutant 8→2 GnRQ. All four possible epitopes were analysed in a homology study between AAV2 and AAV8. With the exception to KDDEE, whose potential epitope was common to AAV8 and AAV2, all other possible epitopes were non-homologues between AAV2 and AAV8 (Fig. 3-25 A). VMD modeling revealed that the three remaining potential epitopes were all present externalized on the capsid either on top or on the outer surface of the 3-fold spike region (Fig.3-25 B). Accordingly, 3 capsid mutants were generated by substitutions of AAV2 aa residues into the AAV8 protein sequences: 8→2 GTTTQS (aa 455-460 of the AAV8 VP protein sequence), 8→2 KTSAD (aa 493-497 of the AAV8 VP protein sequence) and 8→2 LQRGNR (aa 586-591 of the AAV8 VP protein sequence).

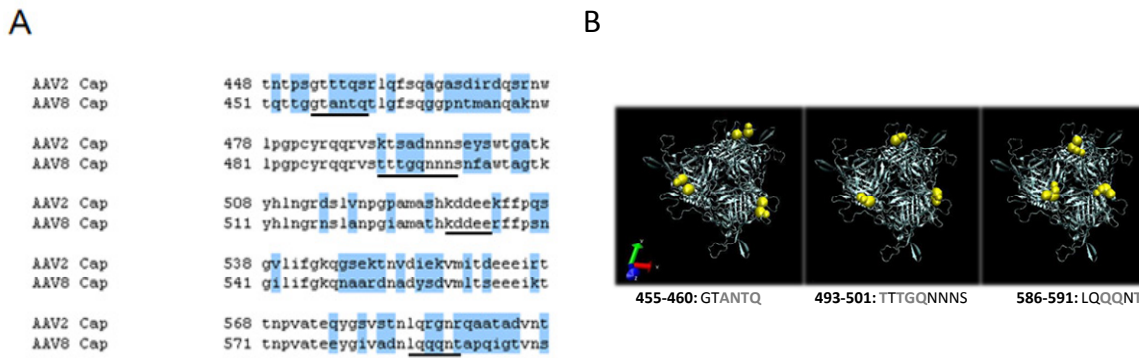


Figure 3-25 ADK8 binding epitopes. A) A homology alignment of AAV2 and AAV8 VP3 demonstrates that several amino acid (aa) are different (letters, highlighted in light-blue). Underlined aa are the possible epitope binding sites of ADK8 (GTANTQ, TTTGQNNNS, KDDEE, LQQQNT). Binding site KDDEE was omitted as AAV2 and AAV8 share the same aa sequence. B) VMD modelling of an icosahedral 3-fold region was performed; α -helices and β -sheets are shown in grey ribbon shape. Yellow balls indicate the position of the putative binding epitopes of AAV8. The grey colored aa (below the figure) were exchanged to identify the binding epitope of ADK8.

Additionally, two reverse mutant vectors from chapter 3.3.5 were also included in the analysis (rAAV2 \rightarrow rAAV8 457TQTLG461 and rAAV2 \rightarrow rAAV8 585QQNTA589), as the first and third possible binding epitope of the AAV8 capsid was mostly present in the AAV2 capsid. The results of a qRT-PCR analysis indicated that all mutants but rAAV8 \rightarrow rAAV2 586LQRGNR591 showed normal packaging and capsid assembly (Fig. 3-26 A). For the latter, about 20-fold less vg containing particles per ml were identified. However, all mutant vectors did show the correct VP protein stoichiometry in the Western blotting (Fig. 3-26 B).

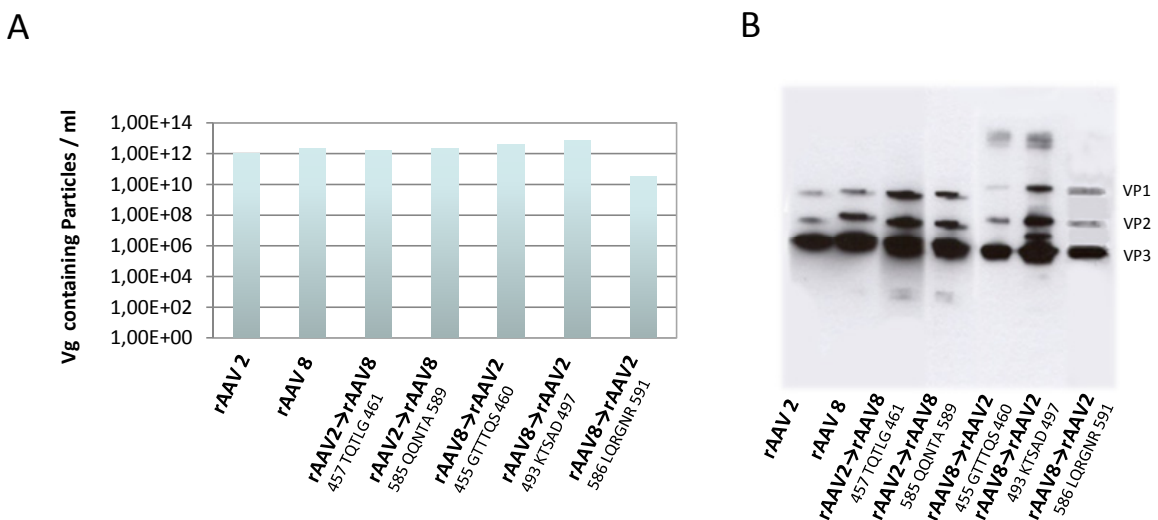


Figure 3-26 Generated vector mutants for the investigation of epitope binding. A) For quantification of generated epitope mutant vectors rAAV8 \rightarrow rAAV2 455GTTTQS460, rAAV8 \rightarrow rAAV2 493KTSAD497 and rAAV8 \rightarrow rAAV2 586LQRGNR591, as well as reverse mutant vectors rAAV2 \rightarrow rAAV8 457TQTLG461 and rAAV2 \rightarrow rAAV8 585QQNTA589 in comparison to rAAV2 and rAAV8 vectors, a qRT-PCR was performed. Titers of vg containing particles could be measured for all produced vectors. Production of vg containing particles was repeated twice for each generated epitope vector mutant. B) In a Western blot analysis, VP proteins were analysed by the monoclonal antibody B1. VP1, 2 and 3 were detected for all mutant vectors.

Therefore, all generated mutants were used to further investigate the binding properties of ADK8. These results permitted an ADK8 ELISA to test the mutant vectors for their recognition by ADK8. For the ADK8 ELISA, 1×10^{10} vg containing particles were immobilized on microtiter plates and analyzed whether mutant capsids reacted with the ADK8 antibody.

At first, the DS mutants were analysed in an ADK8 ELISA. Whereas DS I, DS II and DS III could be detected by the ADK8 antibody, DS IV and DS V mutant capsids could not be recognized, suggesting that the overlapping region between DS IV and DS V, which had been swapped to AAV2, was the region of the ADK8 binding epitope (Fig. 3-27 A). Additionally, the ADK8 ELISA showed less recognition for some of the detectable DS mutants, especially the DSI mutant capsid showed reduced ADK8 capsid detection (5-fold less). The overall capsid structure may be impacted by large domain exchanges contributing indirectly to a less efficient ADK8 binding.

The ADK8 ELISA performed with the epitope mutant vectors showed that two mutant vectors, rAAV8→rAAV2 455GTTTQS460 and rAAV8→rAAV2 493KTSAD497 were detected indistinguishable from rAAV8 (Fig. 3-27 B). In contrast those mutants, the third mutant vector, rAAV8→rAAV2 586LQNRGNR591, could not be detected with the ADK8 ELISA. This indicated that the binding site 586-591 LQQQNT is required for ADK8 binding to the AAV8 capsid surface. Additionally, the reverse mutant 2→8 585QQNTA589 which contained the possible binding epitope of AAV8 in the AAV2 capsid was the only detectable mutant by the ADK8 antibody (Fig.3-27 C).

Insertion of a seven aa peptide sequence into the AAV8 capsid at position of aa 591, prevented binding of ADK8 to AAV8 capsid (Fig. 3-27 D). Due to the fact that the insertion was situated within the identified ADK8 binding epitope LQQQNT, capsids displaying peptides at the insertion site aa 591 could not be detected by the ADK8 antibody anymore.

Taken together, the experiments could demonstrate that of all possible binding sites, the position 586-591 LQQQNT is directly involved in ADK8 binding to AAV8.

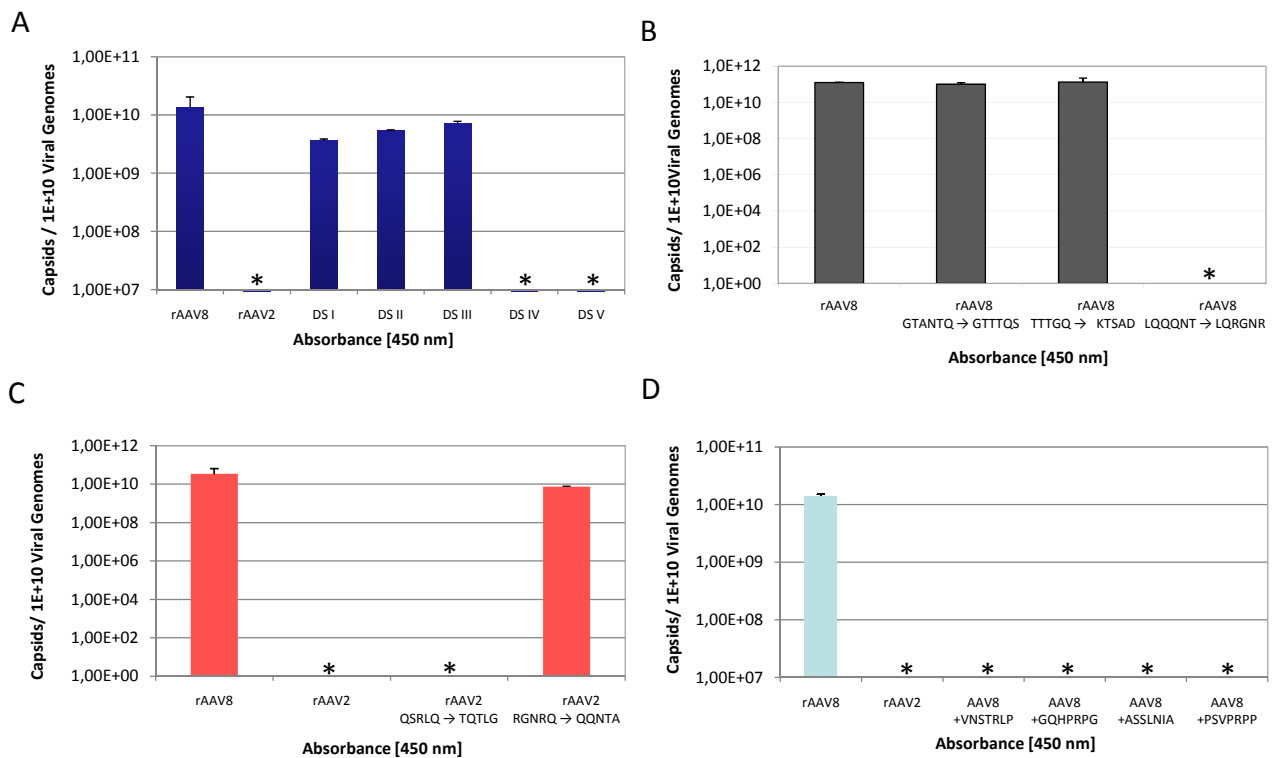


Figure 3-27 Determination of the ADK8 binding epitope by an AAV8 capsid ELISA A) ADK8 ELISA of domain swap mutants (DS I-V). Vectors of rAAV2 and rAAV8 served as positive and negative controls, respectively. B) ADK8 ELISA of epitope vector mutants rAAV8→rAAV2 455GTTTQS460, rAAV8→rAAV2 493KTSAD497 and rAAV8→rAAV2 586LQNRGNR591. Vectors of rAAV8 served as positive a control. C) ADK8 ELISA of reverse vector mutants rAAV2→rAAV8 457TQTLG461 and rAAV2→rAAV8 585QQNTA589. Vectors of rAAV8 and rAAV2 served as positive and negative controls, respectively. D) ADK8 ELISA of vectors displaying different peptide sequences on the AAV8 capsid at position of aa 591: +VNSTRLP, +GQHPRPG, +ASSLNIA and +PSVPRPP. Vectors of rAAV8 and rAAV2 served as positive and negative controls, respectively. Symbol (*) indicates no detection of capsids, even though 10¹⁰ vg were applied per well. All assays were carried out in three independent experiments.

3.5.3 Monoclonal Antibody ADK8 Neutralization of AAV8 Capsids

Because the ADK8 antibody binds to an AAV8 epitope involved in efficiency and tissue selectivity of gene transduction, we were interested whether the antibody could also neutralize AAV8 infection.

First, we analysed if ADK8 inhibits gene transduction *in vitro*. Three of the produced rAAV vectors were selected for the assay, rAAV2, rAAV8 and mutant rAAV2→rAAV8 585QQNTA589 which contained the ADK8 binding epitope in the AAV2 capsid. They were preincubated either without, with 250 ng or 500 ng the ADK8 antibody. As a control the assay was also performed with the A20 antibody which is known to neutralize AAV2 capsid

gene expression (Wobus *et al.* 2000). HepG2 cells were infected with the different antibody-vector mixes and incubated for 6 h. Vector mixes were washed off and cells were incubated for another 48 h before cells were harvested and analysed for luciferase reporter expression. Figure 3-28 demonstrates that ADK8 was able to reduce gene transduction of AAV8 as well as of mutant rAAV2→ rAAV8 585QQNTA589 by more than 50-fold. As expected, ADK8 did not neutralize rAAV2 vectors. Capsids preincubated with A20 neutralized rAAV2 vector and not rAAV8 vector mediated gene transduction, transduction of the AAV2 capsid mutant vector containing the ADK8 binding epitope also showed some neutralization by A20 antibody.

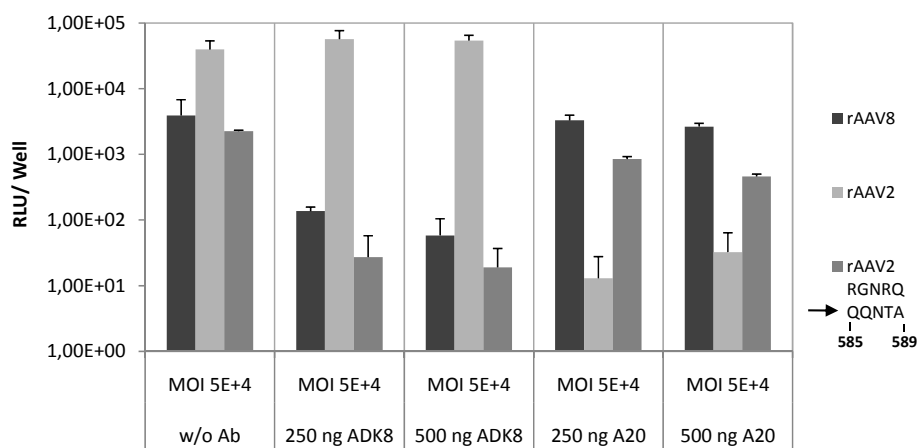


Figure 3-28 Neutralization of AAV8 *in vitro* gene transduction by ADK8. HepG2 cells were either transduced with rAAV2, rAAV8 or reverse mutant vector rAAV2→rAAV8 585QQNTA589. Prior to HepG2 cell infection (MOI 5×10^4 of vg containing particles), viral vectors were preincubated with different amounts (250 ng and 500 ng) of antibody ADK8 or A20 for 30 min at 37°C. After 6 h, viral vector-antibody mix was washed off and cells were harvested two days after infection for the

To investigate *in vivo* neutralization of AAV8 gene transduction by the ADK8 antibody, four groups of 4 mice were used for the animal experiments. As a control, mice were injected with rAAV8 without any antibodies. The other 3 groups were ip injected with ADK8 (50 μ g and 250 μ g) or as a negative control with ADK4, a monoclonal antibody specific for AAV4 capsids (250 μ g). Four hours later mice were iv injected with rAAV8 vectors (1×10^{11} vg containing particles). After 2 weeks, mice were imaged with the IVIS imaging system (Fig. 3-29 A). The images could show that 50 μ g ADK8 antibody had completely neutralized rAAV8 vector dependent gene transduction. To ensure fully functional rAAV8 vectors, mice had

been iv injected with rAAV8 vectors only. A typical transgene expression pattern induced by rAAV8 vector transduction was obtained. Furthermore, ADK4 antibody could not neutralization rAAV8 vector transgene expression. The ADK8 mediated neutralization could also be confirmed by the transgene expression analysis in liver and heart tissues of the dissected mice (Fig. 3-29 B). As already observed in the IVIS imaging, luciferase reporter expression was reduced more than 100-fold in liver and heart after the 50 µg ADK8 ip injection. With the ip injection of 250 µg ADK8 antibody, RLU were even below the detection limit. Intraperitoneal injection of ADK4 prior to the i.v. injection with 1×10^{11} vg containing particles of rAAV8 did not have any impact on transgene expression compared to rAAV8 without antibody injection.

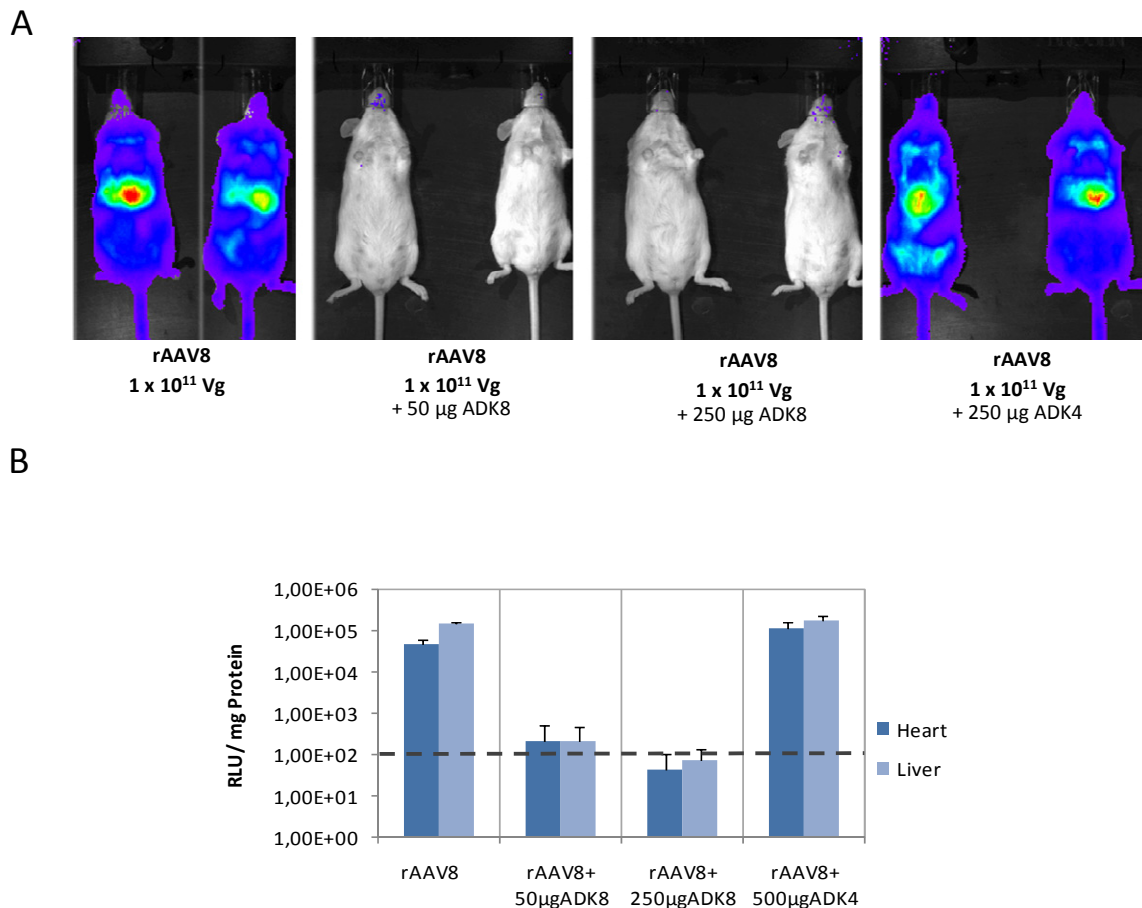


Figure 3-29 Neutralization of AAV8 *In vivo* gene transduction by ADK8. Four hours after ip injection of ADK8 (50 µg and 250 µg) or ADK4 (250 µg only), mice were iv injected with 1×10^{11} vg containing particles. Two weeks after injection, mice were injected with D-luciferin, imaged for 5 min, 10 min after D-luciferin injection. C) After mice had been sacrificed, transgene expression per mg protein was determined in heart and liver tissues. transgene expression per mg protein was determined. Dashed line (grey) indicates the detection limit of the luciferase reporter assay.

3.5.4 Analysis of ADK8 Neutralization

The data so far do not discriminate whether ADK8 already prevents AAV8 capsids from cell binding or inhibits AAV8 gene transduction at a post entry step. As illustrated in figure 3-30, the antibody could cause neutralization at 5 possible sites: Cell binding could be intercepted (I), endocytosis could be prevented (II), cleavage factors could be inhibited from cleaving the capsids in a specific pattern (III), the N-terminal domain might not be externalized anymore preventing endosomal release (IV), DNA release inside the nucleus could be blocked by ADK8 (V).

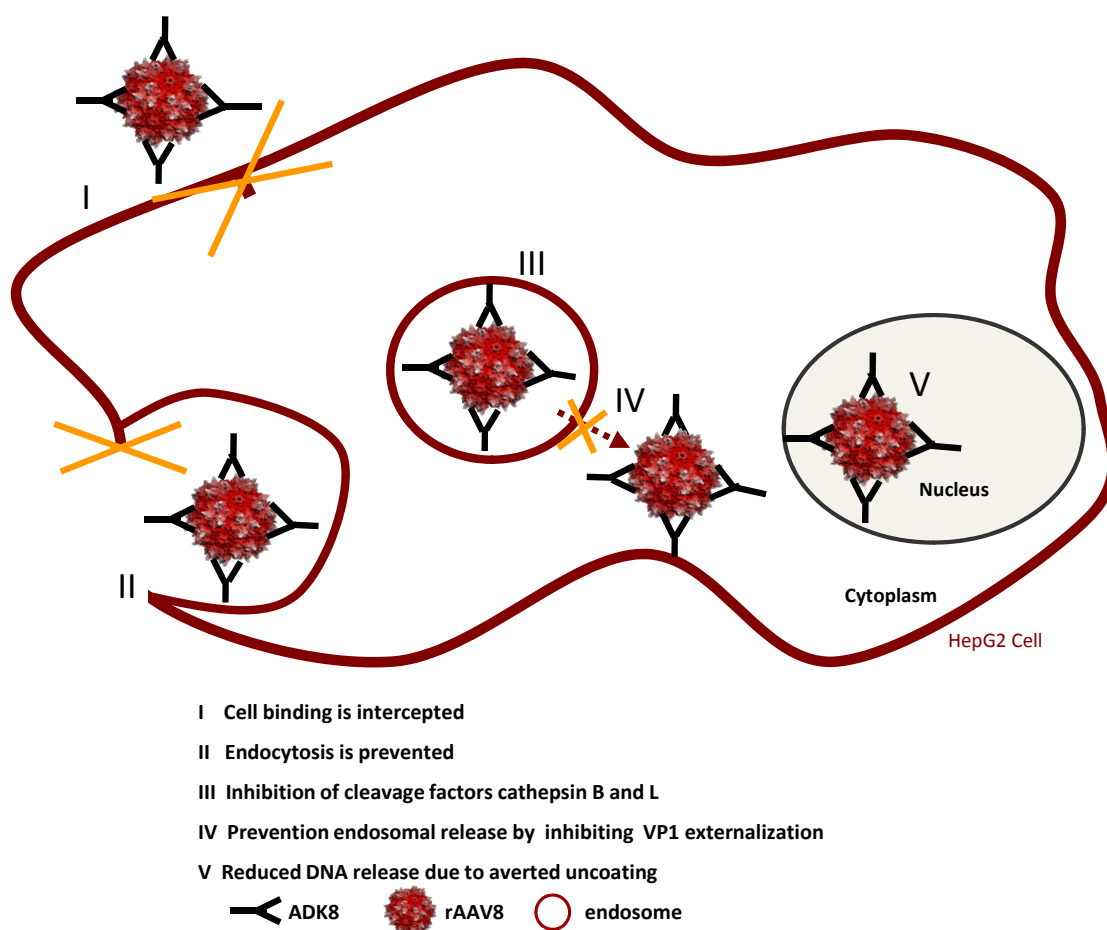


Figure 3-30 Possible sites of blocking AAV8 gene transduction by ADK8. Five different sites are illustrated in a HepG2 cell; blocks are indicated by yellow lines. Binding to ADK8 could prevent rAAV8 vectors from cell binding, could stop rAAV8 particles from endocytosis, could inhibit endosomal cleavage factors cathepsin B and L from pre-cleaving the AAV8 capsid or could prevent rAAV8 vectors to release the DNA in the nucleus.

To test each of these steps, several experiments were conducted. Cell binding of AAV8 in presence of ADK8 was analysed by indirect immunofluorescence technique and DNA dot blot analysis. It had been described that monoclonal antibodies such as C37B or C24B prevent AAV2 binding to cells (Wobus *et al.* 2000). Figure 3-31 A indicates that this is not the case for ADK8. Neither in presence of ADK8 nor in presence of an antibody which did not bind to AAV8 (IVA7), could a reduction in rAAV8 vector binding to HeLa cells be observed. The results were validated by DNA dot blot analysis (Fig. 3-31 B). Additionally, rAAV2 vectors were preincubated with C37B and it could be shown that the amount of rAAV2 vectors bound to the cells was reduced. However, for rAAV8 vectors, reduced cell binding in presence of ADK8 could not be determined, even amounts of 500 ng ADK8 did not decrease rAAV8 binding to the cell. Instead, the addition of the AAV4 capsid specific antibody ADK4 even improved rAAV8 vector binding to the HepG2 cells.

Whether the ADK8 antibody prevented endocytosis of rAAV8 vectors was studied by a temperature shift from 4°C to 37°C of infected cells. Next, cells were harvested and cell pellets were incubated in 0.05 % trypsin to deplete defective or not endocytosed particles from cell surfaces. For the rAAV8 vector and the rAAV2 vector mutant containing the ADK8 binding epitope less vg amounts corresponding to the amount of endocytosed vectors, were detected but not for rAAV2 vectors. In presence of ADK8, detected vector genomes were even more reduced but only in a very small extent. In presence of ADK8, endocytotic vesicles form less efficiently but the antibody does not completely block entry of AAV8 particles into the cells.

Published data had suggest that cathepsin-mediated cleavage could prime AAV capsids for subsequent nuclear uncoating (Akache *et al.* 2007). A treatment with one of the identified uncoating factors cathepsin B was performed to see if ADK8 binding could prevent AAV capsid cleavage (Fig 3-31 C). At first, viral vectors were preincubated or not with ADK8 for 30 min at 37°C, followed by the addition of cathepsin B - or not - for another 30 min incubation period. Western blot analysis was performed and it could be demonstrated that cathepsin B treatment caused a loss of signal detection for VP1 and VP2 and less detection of VP3 (Fig.3-31 D). In presence of ADK8, cathepsin B did not function as efficiently, more VP1 and VP2 could be recovered. However, a complete block of cleavage could not be observed, some bands corresponding to cleaved VP proteins reappeared. Surprisingly, this result was also obtained with AAV2 and the reverse AAV2 vector mutant. The results suggest

that the inhibition of cathepsin B cleavage was not due to specific binding of ADK8 to the AAV8 capsid epitope.

To analyse the possible inhibition of the N-terminal externalization by ADK8, a native dot blot combined with a temperature treatment was performed. *In vitro*, the exposure of the VP1 N-terminus can be triggered by heat-treatment of the vector particles which can be detected by the A1 antibody. The A1 antibody is known to bind a defined epitope close to the PLA2 domain on the N-terminus of VP1 (Wobus *et al.* 2000). Figure 3-31 D showed that after particle incubation for 5 min at 37°C, A1 antibody could not detect any externalized N-termini. But after 5 min at 65°C, rAAV2 and reverse mutant rAAV2 particles N-termini could be detected by the A1 antibody. In case of the rAAV8 vector, 5 min incubation at 71°C was needed to detect the N-termini with the A1 antibody.

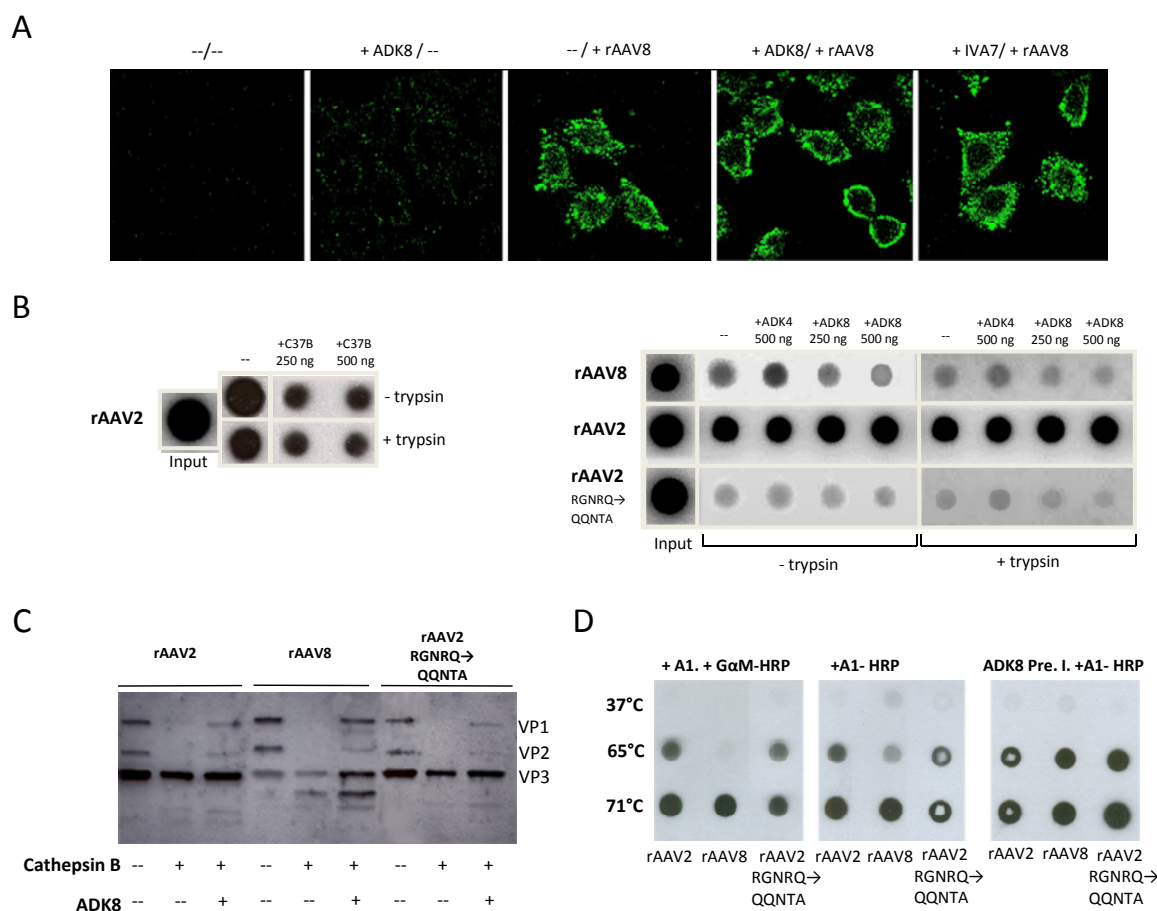


Figure 3-31 Analysis of possible steps in AAV8 gene transfer neutralization by ADK8 antibodies.
See details on the next page

A) AAV8 cells binding in presence of ADK8 was visualized by indirect immunofluorescences. At 4°C only, HeLa cells were infected with rAAV8 (MOI of 1×10^6 vg containing particles) which had either been preincubated with or without ADK8 (0.1 mg). Cells were fixed with ice-cold methanol. As a negative control, only ADK8 was added to the cells or nothing was added. As a positive control, rAAV8 infected HeLa cells were analysed without ADK8 preincubation or after rAAV8 preincubation with a non-binding antibody IVA7. After fixation, ADK8 hybridoma supernatant was added, followed by a G α M-A488 treatment. Images were taken with a widefield fluorescence microscope. B) DNA dot blot analysis was carried out after HepG2 cells had been infected with rAAV8, rAAV2 and reverse mutant vector rAAV2 (585RGNRQ \rightarrow QQNTA589). Displayed on the left hand side, the inhibition control is illustrated. The rAAV2 vectors were preincubated with C37B (250 ng and 500 ng) for 30 min prior to cell infection and kept at 4°C or shifted to 37°C for 2 h before trypsinization. As seen on the right hand side, the vg containing particles (MOI of 5×10^4 vg containing particles) were preincubated with ADK8 or ADK4 (250ng and 500 ng) for 30 min or particles were not incubated with antibodies. Subsequently, cells were infected with the vector-antibody mix for 30 min at 4°C. Cells were either directly harvested or kept at 37°C for 2 h before harvest and trypsin treatment. For all samples, DNA was extracted and hybridized using a 32 P labeled DNA fragment of CMV promoter region. Input indicates the complete viral load without cell infection. The dot blot was repeated 3 times. C) For a capsid cleavage assay, rAAV2, rAAV8 and reverse mutant rAAV2 (585RGNRQ \rightarrow QQNTA589) were preincubated with ADK8 (500 ng), followed by a Cathepsin B treatment. Western blot analysis was performed and polyclonal rabbit serum VP51 was used as a primary antibody, followed by a treatment with the secondary antibody G α R-HRP. Depicted as (-) and (+) are the additions of cathepsin B and ADK8. VP1, VP2 and VP3 indicate the 3 capsid proteins. D) In a native dot blot assay, vg containing particles (1×10^9) were incubated with or without ADK8 (1 μ g per sample) for 30 min at 37°C. Thereafter, they were kept at either 37°C, 65°C or 71°C for 5 min. Particles or particle-antibody mixes were spotted onto a nitrocellulose membrane and reacted with A1 hybridoma supernatant or purified A1 antibodies directly coupled to horse radish peroxidase (HRP). Antibody preincubation is illustrated as ADK8 Pre. I. + A1-HRP.

Next, rAAV vectors were preincubated with ADK8 prior to the three different temperature treatments. For detection of vector particles prebound to antibodies, the purified A1 antibody directly coupled to horseradish peroxidase (HRP) was used. The A1-HRP antibody detected rAAV vectors just like the A1 antibodies derived from hybridoma culture, but A1-HRP did not have any crossreactivity with the ADK8 antibody from the preincubation step. After preincubation with ADK8, no differences in detection could be identified for rAAV2 vectors and the reverse mutant vector. Surprisingly, for rAAV8 vectors, the N-termini were already detectable with the A1-HRP antibody at 65°C. Therefore, the data suggested that the ADK8 antibody does not block N-terminal externalization and does not prevent endosomal release of the rAAV8 vectors.

The last experiment was carried out to determine whether DNA release could be inhibited by the addition of ADK8 antibodies. DNA release can be triggered *in vitro* by heating vector particles to temperatures between 63°C-70°C (Bleker *et al.* 2005). After antibody preincubation (100 ng of ADK8 or A20 per 1×10^9 vg containing particles), viral vector samples were subjected to heat treatments for 5 min. Then, Mnase treatment was performed to digest released DNA, which was followed by Proteinase K treatment and

further steps to extract vg. Genome detection was possible by immobilizing purified genomes to a GeneScreen membrane. Subsequently, the viral genomes were hybridized using a ^{32}P labelled DNA fragment of the CMV promoter region. Autoradiography was carried out and the hybridization signal intensities were captured on exposed films (fig. 3-32). Less AAV2 genomes were already detected at 60°C, whereas less vg of the rAAV8 was determined at 62°C. After A20 preincubation, the DNA release from rAAV2 vectors was inhibited, but not after ADK8 preincubation. Compared to the detection of rAAV2 vectors, the signal intensity was strongly increased for rAAV8 vectors due to the presence of A20 or ADK8 antibodies. However, A20 preincubation of rAAV8 vectors could not inhibit DNA release after heat treatments higher than 65°C. Instead, the preincubation of rAAV8 particles with ADK8 antibodies suggested less release of DNA at higher temperatures than 65°C. However, due to the still small differences in DNA release between with ADK8 and A20 preincubated rAAV8 vectors after heat treatment at 67°C, higher temperature treatments should have still been performed. According to the obtained results, a blockage of DNA release from the AAV8 capsid can be suggested but for validation, the experiment has to be repeated with higher heat treatments.

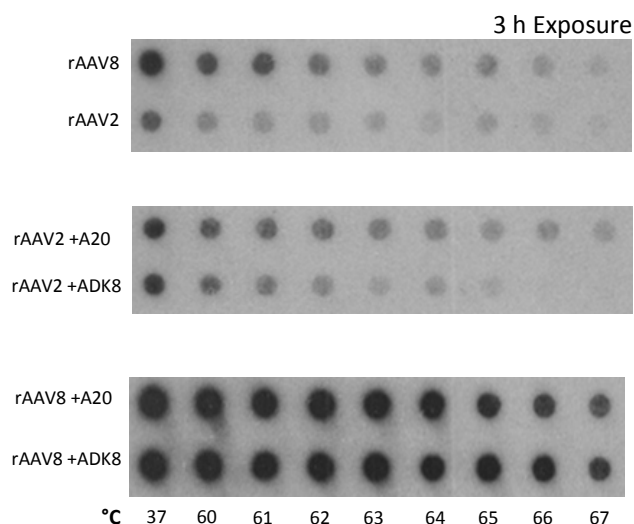


Figure 3-32 The nucleus as a possible position for ADK8 neutralization of AAV8 capsids. Particles of rAAV2 and rAAV8 were preincubated with ADK8 or A20 for 30 min at 37°C and subjected to different heat-treatments (37 °C and 60-67°C). DNA was extracted and analysed with a DNA dot blot assay and a radioactive labeling by a P32 radioactive probe. Displayed are viral genomes of rAAV2 and rAAV8 particles with or without antibody addition which could be recovered in the assay after 9 different temperature-treatments. Indicated with °C are the temperatures, AAV particles were exposed to. Time of exposure was 3 hours.

Taken together, these results indicate that ADK8 does not influence AAV8 binding to the cell and only has a slight impact on endocytosis. An inhibition of the endosomal uncoating factor cathepsin B by ADK8 could not be demonstrated. Furthermore no direct or indirect influence on the N-terminal externalization and endosomal particle release could be demonstrated. Most likely, the ADK8 antibody blocks the release of DNA from the AAV8 capsid. Unfortunately, the presented results were not clear enough and the experiment has to be repeated with higher temperature treatments of the rAAV8 particles to draw a final conclusion.

4. Discussion

The concern for safety and efficiency of gene transfer by viral vectors has been discussed and reviewed repeatedly (Berns *et al.* 1995; Verma *et al.* 1997; Somia *et al.* 2000; Buning *et al.* 2003; Perabo *et al.* 2006; Buning *et al.* 2008; Guy *et al.* 2009; Huang *et al.* 2009). Nonetheless, recent successful trials on the treatment of ocular diseases and inherited immune deficiencies with AAV serotypes are particularly encouraging (Herzog *et al.* 2010). Together with the discovery of novel naturally occurring AAV isolates (Gao *et al.* 2004), efforts have been triggered to understand and manipulate this 'simple' parvovirus for many gene therapy applications. As immune responses and specific targeting remain major obstacles to molecular medicine with AAV vectors, newly recovered AAV serotypes were mainly analyzed for their capability to evade immune host response and for their potential in efficient and specific tissue targeting (Gao *et al.* 2002; Vandenberghe *et al.* 2007).

The main task of this thesis was to characterize AAV8, a serotype which was isolated 2002 and showed a superior *in vivo* transduction to heart, liver and muscle tissue (Gao *et al.* 2002; Nakai *et al.* 2005; Wang *et al.* 2005). Interestingly, AAV2 and AAV8 share an 83 % homology in their VP1 aa sequences, but show differences in capsid structure and intracellular processing. Furthermore, both serotypes strongly differ in their *in vitro* and *in vivo* performance. Therefore, it was decided to study AAV8 in a direct correlation to AAV2, the most researched serotype, to gain more insights into the molecular basis of AAV8's exceptional transduction efficiency *in vivo*.

4.1 Comparison of rAAV8 and rAAV2 Vectors *In Vitro*

The first part of the work focused on data acquisition and comparisons between AAV2 and AAV8 based on their VP1 protein sequences, secondary and tertiary structure. As mentioned before, comparing 738 aa between AAV2 and AAV8 by Clustal 2.0.12, an 83 % homology score was confirmed and several non-conserved aa residue sequence regions were detected. Seven non-homologous regions were identified within loop IV of the AAV2 based secondary structure. This was of interest because, loop IV mainly contributes to the spike formation on the capsid outer surface, concluding that if there are major discrepancies between AAV2 and

AAV8, these regions could be a cause for structural differences (Shen *et al.* 2007). Tertiary structures of the AAV2 and AAV8 capsids had shown differences on the capsid outer surfaces (Xie *et al.* 2002; Nam *et al.* 2007). But our computational modeling of the AAV8 capsid showed that spikes appeared more flattened and that the proteins comprising the 5-fold pore were more externalized. Both, the 5-fold pore as well as the spikes highly impact capsid functionality. In case of the 5-fold pore, it has been postulated that the pore formation is important for DNA packaging. Genome-bound Rep proteins seem to interact at the 5-fold symmetry axes and initiate genome packaging (Bleker *et al.* 2006), the more externalized proteins at the channel structure of the 5-fold symmetry axes could improve Rep/capsid interactions and would explain the generally higher amount of packaged genomes for AAV8 after one iodixanol step gradient. The more flattened spike regions might be due to the fact that the AAV8 primary receptor site is not located on the tip of the protrusion. In fact, it has been shown for other DNA viruses such as MVM and CPV, that aa residues in the twofold depression at the sialic acid receptor binding domain are important to the viral tropism (Tresnan *et al.* 1995; Lopez-Bueno *et al.* 2006; Lopez-Bueno *et al.* 2008). Sialic acid itself could act as a possible cellular interaction site, a fact which was also been suggested for AAV1 (Wu *et al.* 2006b; Schmidt *et al.* 2008). One possible approach to determine sialic acid binding could be the complexation with (apo-)transferrin, a structural homologue for sialic acid (Wu *et al.* 2006b). Despite of the locus of the primary receptor site on the AAV8 capsid, spike flattening would also speak for a more flexible virus. According to the VP1 protein sequence of AAV8, I determined that 17 % of the aa residues different to AAV2 consisted of high amounts of glycine (G), proline (P) and tyrosine (Y). Less amounts of these proteins were determined in the VP1 sequences of AAV2. These aa are known to induce flexibility to protein formations like viral capsids, as demonstrated for the human rhinovirus (Wang *et al.* 2005). In that case, the VP proteins were not only rich in G and P, but in a hydrogen exchange and protein enzymatic fragmentation approach, the interface at the 5-fold symmetry axes was defined to be highly flexible and dynamic, they even speculate an active role of the interface in uncoating of human rhinovirus HRV14. But not only DNA viruses have been described as being flexible, in fact small RNA viruses as well as plant viruses were analysed by a large variety of physical methods and an overwhelming evidence for viral capsid flexibility and its key role in the infection process could be detected (Witz *et al.* 2001).

A set of different biophysical studies and *in vitro* assays were performed to characterize the vector productions and compare AAV8 and AAV2 functions (Table 4-1). According to the correlation with the international standard of AAV2, productions of AAV2 and AAV8 used in this study did not have highest purity but were suitable for the *in vitro* and *in vivo* studies to compare AAV8 to AAV2. We confirmed a greater thermostability for AAV8 capsids than for AAV2 (Murphy *et al.* 2008a).

Table 4-1 Overview of the parameters used for comparison of AAV2 and AAV8

83% Homology between the VP1 protein sequences*	Capsid ELISA ¹⁾	Viral Genome containing Particles ¹⁾	Antibody Detection after Temperature Treatment ²⁾	Intracellular trafficking ³⁾	<i>In Vitro</i> Performance ⁴⁾	<i>In Vivo</i> Performance ⁵⁾	Receptors ⁶⁾
	5 x 10 ¹² capsids/ml	5 x 10 ¹¹ vg/ml	+ B1 + A1 + A20 ≥ 60°C ≥ 55°C ≤ 68°C	Perinuclear accumulation after 6 h	excellent	poor Heart. Liver. Muscle	HSPG Integrin α _v β 5 Human FGFR-1 HGF Laminin receptor
	4 x 10 ¹² capsids/ml	1 x 10 ¹² vg/ml	+ B1 + A1 + ADK8 ≥ 37°C ≥ 37°C ≤ 72°C	Perinuclear accumulation after 3 h	poor 10-100 fold less transduction than for AAV2	Superior 10-100 fold better than AAV2 to Heart. Liver. Muscle	Laminin receptor

* Experiments were based on the 83% homology between VP1 protein sequences of AAV2 and AAV8

¹⁾ Capsid ELISA and vg containing particles were determined with the same vector productions, purifications were performed by 1 Iodixanol step gradient.

²⁾ Native dot blot analysis, B1 was used to detect VP proteins, A1 was for VP1 N-terminus detection and A20/ADK8 detected formed capsids only.

³⁾ Results of the DNA dot blot and the trafficking pathways of AAV2 and AAV8 by indirect immunofluorescences.

⁴⁾ *In vitro* cell transduction assay by reporter luciferase expression in many different cell types.

⁵⁾ *In vivo* analysis after 1 x 10¹¹ vg were i.v. injected into mice and analysed 1 month later.

⁶⁾ All identified receptors are indicated but only HSPG binding was analysed as the primary receptor of AAV2

Additionally, we were also able to show that heat-treated particles which were detected by A1 binding to the N-terminal domain was very different between AAV2 and AAV8. At 37°C, the VP1 N-terminal domain of AAV8 capsids could already be detected by A1, instead A1 began to recognize the N-terminus of AAV2 capsid at 55°C, suggesting that the AAV8 VP1 N-terminus is externalized much faster which could lead to a faster particle release into the cytoplasm. Immunofluorescence analysis of AAV2 and AAV8 capsids revealed that AAV8 accumulates more rapidly in the perinuclear region of the cell, about 3 h after infection. Other groups described that major differences are due to a more rapid uncoating and more efficient annealing to double stranded DNA genomes (Thomas *et al.* 2004; Murphy *et al.* 2008a) but our findings could show that externalization of VP1 N-termini, PLA activation and intracellular trafficking may contribute to a more efficient

transduction capability of AAV8. Regardless, more efficient transduction efficiency could only be demonstrated *in vivo* so far.

In vitro studies should be the easier and more rapid approach to compare AAV8 and AAV2 but due to the unusual weak transduction efficiency of AAV8 *in vitro* and a well functional *in vitro* transduction of AAV2, the obtained results are inconsistent with the *in vivo* transduction results. We tested a series of factors (mouse serum, hFX, heparinase treatment, *ex vivo* liver sections) which could have impacted *in vitro* transduction but we came to the conclusion that not a single factor but many factors would need to be present to increase AAV8 *in vitro* transduction. Furthermore, it has become obvious that not everything of an *in vivo* system can be mimicked *in vitro*. It has been verified that viral shells significantly increase their hydrodynamic diameter in size (≥ 15 nm) following the adsorption of serum proteins in the blood circulation, the mechanism could be ablated by surface coating (Schipper *et al.* 2009). In fact, a recent publication demonstrated that a copolymer coating of AAV8 allowed specific retargeting via the epidermal growth factor receptor (Carlisle *et al.* 2008). A different hydrodynamic diameter of AAV2 and AAV8 could contribute to the poor *in vitro* performance of AAV8.

But there are also other viruses which do not infect cultured cells. In case of hepadnaviruses, early mechanisms of virus-cell interactions remained poorly understood until DMSO-treated HepG2 cells increased transduction efficiency >200-fold (Paran *et al.* 2001). Literature search revealed that weak *in vitro* performance often even contributed to misinterpretation. The regulator protein Nef was mistakenly labeled a negative regulator factor of HIV due to its little affect on retroviral spread in cultured cells (Niederman *et al.* 1989; Reiss *et al.* 1989). However, *in vivo* experiments in macaques showed that Nef is a multi-functional protein that plays a pivotal role in viral persistence and pathogenesis (Baba *et al.* 1995; Arien *et al.* 2008). Knowing this, it was a pure coincidence that AAV8 was not discarded as a non-functional AAV isolate.

4.2 *In Vivo* Analysis of Domain and Single Residue Exchanges between AAV2 and AAV8

To understand the structural basis for different *in vivo* gene transduction efficiencies of AAV8 and AAV2, we exchange domains and single amino acids between the two vectors and compared their performance after iv application.

Domain exchanges between AAV1 and AAV2 capsid contributed to defining the major region responsible for muscular tropism (Hauck *et al.* 2004) and domain swaps between AAV2 and AAV8 pointed towards loop IV and its subloop 1 and 4 to play a critical role for mouse liver transduction efficiency (Shen *et al.* 2007).

These results coincide with our findings, we also determined that loop IV and its subloops play an important role in transduction efficiency but in both cases, the major drawbacks to a swapping approach also became obvious. Domain exchanges implicated that the transfer of several aa sequence differences from one viral capsid to the other may cause involvement in different steps of gene transfer such as receptor binding and post-entry processing which might be part of different functional elements of the capsids.

Therefore, we decided to minimize the number of residues changed by swaps to single amino acid exchanges. Within loop IV, seven regions of non-identical amino acids between AAV8 and AAV2 had been identified and were chosen to be exchanged from AAV8 to AAV2 and vice versa. The detailed analysis of differences of AAV8 and AAV2 capsids within loop IV by single residue exchanges intended to answer two questions: (1) What is the structural basis for the better performance of rAAV8 compared to rAAV2 *in vivo* and (2) can we identify a peptide insertion site in the AAV8 capsid which retains the high performance of AAV8 but but can influence the tropism.

To answer the first question, all generated mutants with aa residue exchanges on the outer border of the loop showed a reduction of transduction efficiency. The same result was obtained with mutant 8→2 ATgD whose aa substitution to the AAV2 peptide sequence was situated in the dimple of the threefold spikes. This result demonstrated that structural components can impact the different transduction efficiencies of rAAV8 and rAAV2. Noticeable applies to the generated mutants was the substitution of mutant 8→2 DmR whose amino acid exchanges were located within the capsid shell (Fig. 4-1 A) and not on the outer capsid surface. In that case a general reduction of the AAV8 transduction efficiency

was reduced to levels of rAAV2 transduction. Due to the localization of the mutation within the capsid shell, it was assumed that the disturbance of a proper transduction was rather due to the intrinsic nature of the capsid, such as a change in conformation during uncoating, than a dysfunctional interaction with the host cell. This would mean that this particular difference in the protein sequence between AAV8 and AAV2 could affect post-entry processing. The presented ratio analysis between genome uptake and gene expression strongly confirmed this theory (s. Chapter 5.4). Two additional mutants with peptide sequences exchanged from AAV2 into the AAV8 capsid did not reduce transduction efficiency of rAAV8.

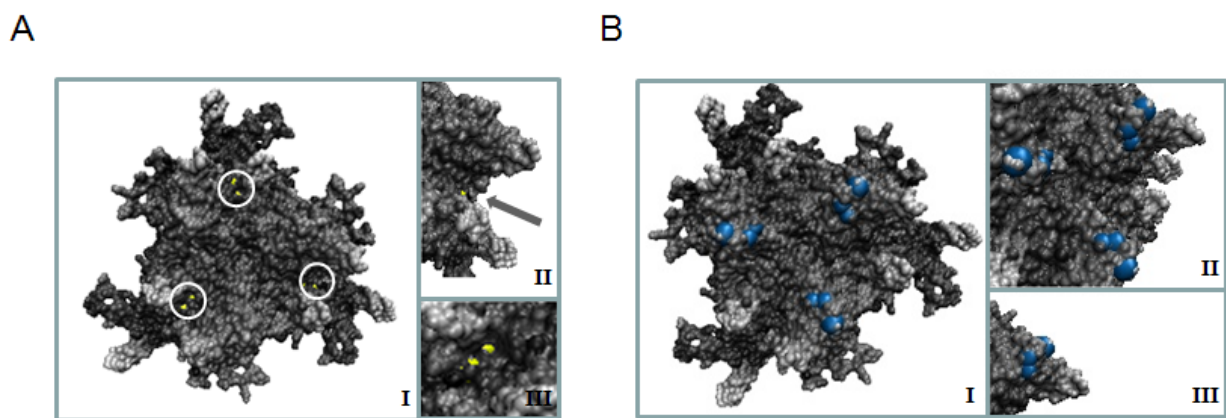


Figure 4-1 Computational modelling of an AAV8 capsid trimer with highlighted aa substitutions that dramatically impact AAV8 transduction. A) The swap of 2 aa residues of vector mutant 8→2 DmR are modelled into the AAV8 trimer (surf style shape) and marked in yellow and highlighted by white circles (I). A side view shows the protrusion with the substitutions situated in the cavity of the 3-fold spike region (grey arrow indicates the exact localization of the substitutions (II) and a close-up image of the 2 amino acids within the dimple (III). B) The swap of the 3 aa residues of vector mutant 8→2 GnRQ are modelled into the AAV8 trimer (surf style shape) and marked in blue (I). Close-up images of the trimer are either turned 30° counter clockwise and illustrate all three positions of the aa substitutions within the trimer (II) or at the inner shoulder of the 3-fold spike region (III).

Whereas mutant 8→2 GnRQ generally increased transduction efficiency, the mutant 8→2 SvaT additionally had an impact on the rAAV8 vector tropism by increasing targeting to heart and liver tissue but not to other organs (Fig. 3-11). Both mutants contain exchanges located at the inner shoulder of the 3-fold spike region, homologous to the heparin binding site of AAV2. In fact, for mutant 8→2 GnRQ, heparin binding was partially reconstituted and could contribute to its high transduction efficiency (Fig. 4-1 B).

HSPG binding plus primary receptor binding are known to act synergistic for the *in vivo* transduction efficiency of AAV8. Coreceptors of AAV2 such as $\alpha\text{V}\beta\text{5}$ integrin have been shown to cooperatively bind HSPG for cellular entry of AAV2 (Summerford *et al.* 1999) and mutations in the NGR motif, the highly conserved interaction domain, reduced transduction

efficiency by an order of magnitude relative to that of wt AAV2 transduction *in vivo* and *in vitro* (Summerford *et al.* 1999; Asokan *et al.* 2006). A last consideration should be mentioned at this point, partial HSPG reconstitution might also be a drawback to the benefits of the newly generated mutant vector because heparin binding was identified to cause T cell activation against AAV2 capsids (Vandenberghe *et al.* 2006). Correspondingly, T cell activation might also be induced by mutant 8→2 GnRQ capsids.

In order to answer the second question -whether a site for peptide insertion could be identified for the AAV8 capsid, the inner shoulder of the 3-fold spike region presented itself as a perfect candidate for a peptide insertions site. Especially the mutant 8→2 SvaT had demonstrated that transduction efficiency of AAV8 was retained even though a change in tissue tropism could also be identified.

The capsid characterization by 8→2 mutant vectors had revealed many interesting details on AAV8. Thus, reverse mutants were also generated which contained aa substitutions from AAV8 within the AAV2 VP protein sequence. However, compared to the mutants with AAV2 peptide sequences inserted into AAV8 capsid which had generally reduced AAV8 gene transduction efficiency, none of the reverse mutants could increase rAAV2 gene transduction efficiency to the level of rAAV8 vectors. This result also supports the opinion that not a single difference between the AAV2 and the AAV8 peptide sequences is responsible for the different transduction efficiencies of both serotypes. In fact, it seems that a cooperation of several sequence differences in loop IV contributes to the improved gene transfer efficiency of rAAV8. Surprisingly, the introduction of the AAV8 peptide sequence into the AAV2 capsid in the region of the inner shoulder of the 3-fold spike could also increase gene transduction of AAV2. Once again, it was demonstrated that this region of the capsid tolerates changes in the peptide sequence which can be associated with an increase in transduction efficiency and a partially change in transduction selectivity (Fig. 3-13). However, it does not explain the functional basis of the differences between the gene transduction activities of rAAV2 and rAAV8. To gain more insights into this question, combinations of the different single aa mutants would have to be analysed, above all it would be too much to be part of a single dissertation.

As suggested the inner shoulder at the 3-fold spike region was used to construct a peptide insertion site into the AAV8 scaffold. At first, the peptide insertion site had to be tested for its functionality. Interestingly, peptide sequence insertions from previous AAV2

library selections could retarget AAV8 capsid vectors but with a different gene transduction profile, e.g. the muscle targeting peptide ASSLNIA increased transduction efficiency of muscle tissue for AAV2 (Yu *et al.* 2009) but inserted into the AAV8 capsid, the peptide sequence induced AAV8 particle retargeting to heart tissue. The functionality of the insertion site could be approved. Retargeting was induced by an insertion peptide. However, whether retargeting was directly due to cell binding or indirectly caused by post-entry processing could not be identified.

4.3 Selection of Targeted rAAV8 Vectors from the AAV8 Peptide Display Library

The AAV8 random peptide display library was also generated by the insertion of the (NNK)₇ oligonucleotides into the packaging plasmid which was responsible for the AAV8 capsid formation. Displaying random peptide sequences, we decided to perform *in vitro* selections to recover targeted rAAV8 vectors. Looking back, a selection on hepatocytes was perhaps not the best choice, as most naturally occurring AAV serotypes exhibit ubiquitous tendency to sequester in the liver (Zincarelli *et al.* 2008; Wang *et al.* 2010) and because previous AAV2 library selections focused on liver detargeting (Waterkamp *et al.* 2006; Michelfelder *et al.* 2009). However, AAV8 liver targeting is hardly specific, previous data had clearly demonstrated that the AAV8 serotype showed also transduction to organs such as spleen, kidney or lung tissue. An AAV8 random peptide display library selection could help to recover peptides which detarget from all other organs than liver tissue. As presented in the result section, many different peptide sequences were isolated which strongly differed from previous screens with AAV2 libraries. In the hepatocyte screen, motifs such as NDV or NSV were not observed. Both motifs have been identified as potential ligand motifs for venous and arterial endothelial cells (Muller *et al.* 2003; Vandenberghe *et al.* 2006; Waterkamp *et al.* 2006) and their presence in the screen for hepatotropic peptide sequences would have only questioned the quality of the screen. Additionally, no peptide sequence similarities were present in comparison to screens on leukemia cells (Perabo *et al.* 2003), lung carcinoma cell lines (Calu6) or prostate carcinoma cell lines (PC3) (Waterkamp *et al.* 2006). In particularly the Huh7 screen revealed serine (S) and arginine (R) rich motifs such as SSRR. The isolation of R in combination with P, as seen in AAV2 screens from Y. Ying (Ying 2007),

was not detectable. Whether the hydrophilic aa residue R is highly prevalent to reconstitute cell binding or whether it is critical for post-entry processing remains unclear. Interestingly, in Hepa1.6 selection rounds, less SR rich motifs could be recovered and even less in primary hepatocytes. Instead, in Hepa1.6 and in primary hepatocytes the majority of peptides isolated were non-polar aa residues G, L, V or A, especially at the 1st to 4th position of peptide inserts.

Vectors with an overall positive net charge are prone to confer HSPG binding (Perabo *et al.* 2006). Table 4-2 shows an assortment of the selected peptide sequences and it can be seen that most recovered inserts have a positive net charge. It was hypothesized that the increased amount of R residues could have improved HSPG binding after all, but it seems that Huh7 cells, Hepa1.6 cells and primary hepatocytes vary in the amount of HSPG expressed on the cell surfaces. The Huh7 cells could be more permissive for vectors displaying peptides with R residues than primary hepatocytes or Hepa1.6 cells. Notably, all selections recovered many peptide sequences with many serines. Whether serine residues generally impact vector retargeting could not be determined.

Table 4-2 Collection and characterization of enriched peptide sequences

Huh7 selected peptides	Net charge	Hepa 1.6 selected peptides	Net charge	Primary hepatocyte selected peptides	Net charge
RGKRRSS	+	WFAAKLA	+	RNGGLKS	+
GGKRRSS	+	KPTKRLW	+	GFASGRV	+
TGKRRSS	+	SLDNSFR	+	WFAAKLA	+
SGKPRSR	+	SSRGLGK	+	VGLVLR	+
AGKRRSS	+	ASLRSGC	+	AGNSRC	+
SSRGLGK	+	VGLVLR	+	SLDNLFR	
SEVARCR	+	RSISALF	+	SEGLKNL	
FNWFRSV	+	GVYIPVN		DVGVFYFN	-
RSYFMLE		GLISNVF		LGCALFI	
FNWFSSV		QLWTLVS		KGFVEFA	
FNWFASV		DFSTSGE	-	SSLGLTC	

Peptide sequences recovered from the selections with Huh7 cells, Hepa1.6 cells and primary hepatocytes. Shown are most frequent peptides and their encompassed net charge. Basic amino acids are illustrated in blue, acidic amino acids are indicated in red. Bolt capitalized letter present those peptides used for further *in vivo* applications. Yellow letters mark possible phosphorylation sites.

After the insertion of four of the most enriched oligonucleotides into the packaging plasmid and after producing the peptide displaying AAV8 vectors, one peptide sequence was recovered, SEGLKLN, which induced tissue detargeting. It was one of the peptides which had a neutral net charge, with only one S at position 1 of the sequence. *In vivo* analysis demonstrated that this peptide induced complete detargeting from other tissue types than liver and heart. Transduction efficiency to liver and heart was however decreased compared to wt AAV8 transduction. Other analysed peptide sequences reduced transduction mostly below the detection limit. An alternative insertion site should be considered to produce an AAV8 random peptide display library which could more efficiently improve the selection for targeted rAAV8 vectors. Additionally, an *in vivo* selection might have recovered more efficient rAAV8 targeted vectors. Directly Reengineering rAAV vectors according to receptor footprints could also contribute to a generation of synthetic AAV variants with improved properties for clinical applications (Asokan *et al.* 2010). The combination of the random-peptide display approach with the family shuffling strategy (Grimm *et al.* 2008; Koerber *et al.* 2008; Gray *et al.* 2010) might also improve the synthetic AAV vector generation with retargeting to a specific tissue type.

4.4 Uncoating – A Critical Step of Post Entry-Processing

The process of uncoating has been demonstrated to play a key role for gene transduction of AAV serotypes (Thomas *et al.* 2004; Murphy *et al.* 2008a). It was hypothesized that major differences between AAV2 and AAV8 are due to more efficient genome release of AAV8 contributing to a more rapid annealing of double-strands (Thomas *et al.* 2004). An important asset to understanding the basis of uncoating was the identification of cysteine proteases which showed different degradation patterns of AAV2 and AAV8 capsids (Akache *et al.* 2007). The pre-digested capsids could contribute to the faster uncoating rate of AAV8 vector genomes in the nucleus. Other groups speculated that heat-induced genome uncoating was intrinsically related to capsid stability (Murphy *et al.* 2008a). Even though, non-physiological conditions could not truly reflect the *in vivo* process of rAAV vectors. Therefore an assay was developed to measure the contribution of post entry processing in an *in vivo* situation. The generated mutant vectors had shown to influence AAV8 gene transduction efficiency after

single aa residue had been exchanged from AAV2 into the AAV8 capsid. Therefore, these mutants were used in our approach to analyse uncoating. To do this, the amount of vector genomes present in heart, liver and muscle tissue were measured and related to transgene expression (s. Fig. 3-22). The ratio between vector genom uptake into a tissue for transgene expression should indicate the efficiency of post entry processing. The measured ratios revealed major differences between wt AAV8 and wt AAV2. According to the ratios, post entry processing including uncoating seemed to be more effective for AAV8 than for AAV2. In liver tissue the difference was almost 50-fold. Two vector mutants (8→2 GnRQ and 8→2 SvaT) even excelled wtAAV8 uncoating, especially 8→2 GnRQ (70-fold higher). Generally, heart tissue demonstrated the best viral genome uncoating rates compared to liver or muscle tissue. Due to the fact that it has been demonstrated that AAV vectors naturally end up in the liver for hepatic clearance (Di Paolo *et al.* 2009; Wang *et al.* 2010), it is actually possible that only a portion of the total vectors in this tissue is responsible for transgene expression. It would be interesting to see whether vector genomes from AAV9 capsids are also more rapidly uncoated in heart tissue than in other tissue types (Sarkar *et al.* 2006; Bish *et al.* 2008).

4.5 Monoclonal Antibody ADK8 Uncovers New AAV8 Capsid Features

A large collection of monoclonal antibodies has been generated and many of these antibodies contributed to a detailed analysis of AAV2 (Wistuba *et al.* 1995; Grimm *et al.* 1999; Wobus *et al.* 2000; Kern *et al.* 2003; Kuck *et al.* 2007). By making use of an AAV8 capsid specific antibody, we attempted to uncover more details on the basis of the AAV8 serotype. The footprint mapping and the corresponding mutant vectors had demonstrated that the ADK8 binding epitope was situated on the inner shoulder of the spikes surrounding the 3-fold symmetry axis. Peptide sequences inserted into the capsid at that region completely destroyed the ADK8 recognition of the AAV8 capsid confirming the ADK8 binding site. Neutralization of AAV8 derived transgene expression *in vitro* and *in vivo* by the ADK8 antibody, showed that the antibody does not inhibit binding or uptake of rAAV8 vectors but post-entry processing.

Characterization of other viruses by monoclonal antibody application could be accomplished. For example, maturation intermediates of the HIV1 virus have been intensely

studied by monoclonal antibodies and helped to gain more insights into the intracellular trafficking of HIV particles (Otteken *et al.* 1996). In the field of AAV research, the monoclonal antibody A20 showed that it neutralizes AAV2 particles following receptor attachment by binding to an epitope formed during AAV2 capsid assembly (Wobus *et al.* 2000). Other monoclonal antibodies such as C37B, which was also used as a positive control in our studies, directly inhibits AAV2 cell binding. Our work could show that the antibody ADK8 impedes AAV8 infection at a post entry step and not by inhibiting cell binding. This is remarkable, since mutagenesis of the antibody binding epitope affected AAV8 tissue tropism (Fig. 3-11 and 3-12). Furthermore, the insertion of peptide sequences at that position of the capsid changed transgene expression pattern in different mouse tissues after iv vector delivery. This points either to an indirect effect on another position on the capsid which might be directly involved in cell binding / binding to cellular receptors or that the different transgene expression pattern is due to different post entry processing in cells of different tissues. Genome transfer data (Fig. 3-22) clearly indicated a reduction of genome transfer to heart, liver and skeletal muscle tissue after mutations of other sites than QNTA (the ADK8 epitope sequence) and no effect after conversion of QNTA to GNRQ. This argues for an indirect effect of the modification of QNTA sequence motif on another capsid site which interacts with a putative cellular receptor. On the other site, calculation of gene expression/gene transfer ratios clearly indicated also an influence of the mutation of this domain to GNRQ during post entry processing. This is in agreement with the neutralization activity of the ADK8 antibody. So far, however, it is not clear at which post entry infection step the antibody exerts its inhibiting function. There is a slight effect on vector genome uptake and there might be an effect on genome release. The latter has still to be confirmed. Analysis of the mechanism of the infection neutralization is hampered by the fact that it has to be performed in vitro or in cell culture which only partially reflects the exceptional gene transduction ability of rAAV8 vectors *in vivo*.

4.6 Final Conclusion

We could show that the AAV8 serotype possesses a stable but also flexible capsid structure. Comparison of the AAV8 and AAV2 capsid revealed major differences at the pores of the 5-fold symmetry axes and on the spike regions. Both features could contribute to a faster trafficking to the nucleus and a more rapid uncoating mechanism. Vector mutants helped to determine capsid regions of importance to the higher gene transfer efficiency of the AAV8 capsid *in vivo*. An insertion site into the capsid was detected for peptide sequence display that can be used to retarget AAV8 vectors. Nonetheless, we came to the conclusion that the insertion site is probably not located on the primary receptor binding site of AAV8 and could therefore induce retargeting indirectly on a post-entry level. AAV8 library selections recovered a peptide sequence with hepatotropic targeting and detargeting from other tissue types in the mouse after iv vector application. Uncoating was determined to be one of the most important reasons for superior transduction of AAV8 *in vivo* which could be shown by the ratio of gene expression to gene transfer. The AAV8 serotype is a promising candidate for somatic gene therapy applications in which efficient liver or muscle gene transfer is required.

5. References

- Afione, S. A., C. K. Conrad, et al. (1996). "In vivo model of adeno-associated virus vector persistence and rescue." *J Virol* **70**(5): 3235-41.
- Akache, B., D. Grimm, et al. (2006). "The 37/67-kilodalton laminin receptor is a receptor for adeno-associated virus serotypes 8, 2, 3, and 9." *J Virol* **80**(19): 9831-6.
- Akache, B., D. Grimm, et al. (2007). "A two-hybrid screen identifies cathepsins B and L as uncoating factors for adeno-associated virus 2 and 8." *Mol Ther* **15**(2): 330-9.
- Allocca, M., C. Mussolino, et al. (2007). "Novel adeno-associated virus serotypes efficiently transduce murine photoreceptors." *J Virol* **81**(20): 11372-80.
- Anand, V., B. Duffy, et al. (2002). "A deviant immune response to viral proteins and transgene product is generated on subretinal administration of adenovirus and adeno-associated virus." *Mol Ther* **5**(2): 125-32.
- Arien, K. K. and B. Verhasselt (2008). "HIV Nef: role in pathogenesis and viral fitness." *Curr HIV Res* **6**(3): 200-8.
- Arnold, G. S., A. K. Sasser, et al. (2006). "Metabolic biotinylation provides a unique platform for the purification and targeting of multiple AAV vector serotypes." *Mol Ther* **14**(1): 97-106.
- Arruda, V. R., H. H. Stedman, et al. (2005). "Regional intravascular delivery of AAV-2-F.IX to skeletal muscle achieves long-term correction of hemophilia B in a large animal model." *Blood* **105**(9): 3458-64.
- Asokan, A., J. C. Conway, et al. (2010). "Reengineering a receptor footprint of adeno-associated virus enables selective and systemic gene transfer to muscle." *Nat Biotechnol* **28**(1): 79-82.
- Asokan, A., J. B. Hamra, et al. (2006). "Adeno-associated virus type 2 contains an integrin alpha5beta1 binding domain essential for viral cell entry." *J Virol* **80**(18): 8961-9.
- Atchison, R. W., B. C. Casto, et al. (1965). "Adenovirus-Associated Defective Virus Particles." *Science* **149**: 754-6.
- Auricchio, A. (2003). "Pseudotyped AAV vectors for constitutive and regulated gene expression in the eye." *Vision Res* **43**(8): 913-8.
- Auricchio, A., G. Kobinger, et al. (2001). "Exchange of surface proteins impacts on viral vector cellular specificity and transduction characteristics: the retina as a model." *Hum Mol Genet* **10**(26): 3075-81.
- Baba, T. W., Y. S. Jeong, et al. (1995). "Pathogenicity of live, attenuated SIV after mucosal infection of neonatal macaques." *Science* **267**(5205): 1820-5.
- Balague, C., M. Kalla, et al. (1997). "Adeno-associated virus Rep78 protein and terminal repeats enhance integration of DNA sequences into the cellular genome." *J Virol* **71**(4): 3299-306.
- Bantel-Schaal, U., H. Delius, et al. (1999). "Human adeno-associated virus type 5 is only distantly related to other known primate helper-dependent parvoviruses." *J Virol* **73**(2): 939-47.
- Bantel-Schaal, U., B. Hub, et al. (2002). "Endocytosis of adeno-associated virus type 5 leads to accumulation of virus particles in the Golgi compartment." *J Virol* **76**(5): 2340-9.
- Bartlett, J. S., J. Kleinschmidt, et al. (1999). "Targeted adeno-associated virus vector transduction of nonpermissive cells mediated by a bispecific F(ab'gamma)2 antibody." *Nat Biotechnol* **17**(2): 181-6.
- Bartlett, J. S., R. Wilcher, et al. (2000). "Infectious entry pathway of adeno-associated virus and adeno-associated virus vectors." *J Virol* **74**(6): 2777-85.
- Bearer, E. L. (2003). "Overview of image analysis, image importing, and image processing using freeware." *Curr Protoc Mol Biol* **Chapter 14**: Unit 14 15.

- Becerra, S. P., F. Koczot, et al. (1988). "Synthesis of adeno-associated virus structural proteins requires both alternative mRNA splicing and alternative initiations from a single transcript." *J Virol* **62**(8): 2745-54.
- Bell, P., L. Wang, et al. (2005). "No evidence for tumorigenesis of AAV vectors in a large-scale study in mice." *Mol Ther* **12**(2): 299-306.
- Bello, A., K. Tran, et al. (2009). "Isolation and evaluation of novel adeno-associated virus sequences from porcine tissues." *Gene Ther*.
- Berns, K. I. and C. Giraud (1995). "Adenovirus and adeno-associated virus as vectors for gene therapy." *Ann N Y Acad Sci* **772**: 95-104.
- Berns, K. I., T. C. Pinkerton, et al. (1975). "Detection of adeno-associated virus (AAV)-specific nucleotide sequences in DNA isolated from latently infected Detroit 6 cells." *Virology* **68**(2): 556-60.
- Bevington, J. M., P. G. Needham, et al. (2007). "Adeno-associated virus interactions with B23/Nucleophosmin: identification of sub-nucleolar virion regions." *Virology* **357**(1): 102-13.
- Birnboim, H. C. and J. Doly (1979). "A rapid alkaline extraction procedure for screening recombinant plasmid DNA." *Nucleic Acids Res* **7**(6): 1513-23.
- Bish, L. T., K. Morine, et al. (2008). "Adeno-associated virus (AAV) serotype 9 provides global cardiac gene transfer superior to AAV1, AAV6, AAV7, and AAV8 in the mouse and rat." *Hum Gene Ther* **19**(12): 1359-68.
- Blackburn, S. D., R. A. Steadman, et al. (2006). "Attachment of adeno-associated virus type 3H to fibroblast growth factor receptor 1." *Arch Virol* **151**(3): 617-23.
- Blankinship, M. J., P. Gregorevic, et al. (2004). "Efficient transduction of skeletal muscle using vectors based on adeno-associated virus serotype 6." *Mol Ther* **10**(4): 671-8.
- Bleker, S., M. Pawlita, et al. (2006). "Impact of capsid conformation and Rep-capsid interactions on adeno-associated virus type 2 genome packaging." *J Virol* **80**(2): 810-20.
- Bleker, S., F. Sonntag, et al. (2005). "Mutational analysis of narrow pores at the fivefold symmetry axes of adeno-associated virus type 2 capsids reveals a dual role in genome packaging and activation of phospholipase A2 activity." *J Virol* **79**(4): 2528-40.
- Boucas, J., K. Lux, et al. (2009). "Engineering adeno-associated virus serotype 2-based targeting vectors using a new insertion site-position 453-and single point mutations." *J Gene Med*.
- Brantly, M. L., J. D. Chulay, et al. (2009). "Sustained transgene expression despite T lymphocyte responses in a clinical trial of rAAV1-AAT gene therapy." *Proc Natl Acad Sci U S A* **106**(38): 16363-8.
- Buller, R. M., J. E. Janik, et al. (1981). "Herpes simplex virus types 1 and 2 completely help adenovirus-associated virus replication." *J Virol* **40**(1): 241-7.
- Buning, H., S. A. Nicklin, et al. (2003). "AAV-based gene transfer." *Curr Opin Mol Ther* **5**(4): 367-75.
- Buning, H., L. Perabo, et al. (2008). "Recent developments in adeno-associated virus vector technology." *J Gene Med* **10**(7): 717-33.
- Buning, H., M. U. Ried, et al. (2003). "Receptor targeting of adeno-associated virus vectors." *Gene Ther* **10**(14): 1142-51.
- Calcedo, R., L. H. Vandenberghe, et al. (2009). "Worldwide epidemiology of neutralizing antibodies to adeno-associated viruses." *J Infect Dis* **199**(3): 381-90.
- Carlisle, R. C., R. Benjamin, et al. (2008). "Coating of adeno-associated virus with reactive polymers can ablate virus tropism, enable retargeting and provide resistance to neutralising antisera." *J Gene Med* **10**(4): 400-11.
- Carter, B. J. (2005). "Adeno-associated virus vectors in clinical trials." *Hum Gene Ther* **16**(5): 541-50.

-
- Caspar, D. L. and A. Klug (1962). "Physical principles in the construction of regular viruses." Cold Spring Harb Symp Quant Biol **27**: 1-24.
- Cassinotti, P., M. Weitzand, et al. (1988). "Organization of the adeno-associated virus (AAV) capsid gene: mapping of a minor spliced mRNA coding for virus capsid protein." Virology **167**(1): 176-84.
- Chao, H., P. E. Monahan, et al. (2001). "Sustained and complete phenotype correction of hemophilia B mice following intramuscular injection of AAV1 serotype vectors." Mol Ther **4**(3): 217-22.
- Chejanovsky, N. and B. J. Carter (1989). "Mutagenesis of an AUG codon in the adeno-associated virus rep gene: effects on viral DNA replication." Virology **173**(1): 120-8.
- Chenuaud, P., T. Larcher, et al. (2004). "Autoimmune anemia in macaques following erythropoietin gene therapy." Blood **103**(9): 3303-4.
- Chiorini, J. A., F. Kim, et al. (1999). "Cloning and characterization of adeno-associated virus type 5." J Virol **73**(2): 1309-19.
- Chiorini, J. A., L. Yang, et al. (1997). "Cloning of adeno-associated virus type 4 (AAV4) and generation of recombinant AAV4 particles." J Virol **71**(9): 6823-33.
- Chirmule, N., K. Propert, et al. (1999). "Immune responses to adenovirus and adeno-associated virus in humans." Gene Ther **6**(9): 1574-83.
- Chirmule, N., W. Xiao, et al. (2000). "Humoral immunity to adeno-associated virus type 2 vectors following administration to murine and nonhuman primate muscle." J Virol **74**(5): 2420-5.
- Clark, K. R., F. Voulgaropoulou, et al. (1996). "A stable cell line carrying adenovirus-inducible rep and cap genes allows for infectivity titration of adeno-associated virus vectors." Gene Ther **3**(12): 1124-32.
- Collaco, R. F., V. Kalman-Maltese, et al. (2003). "A biochemical characterization of the adeno-associated virus Rep40 helicase." J Biol Chem **278**(36): 34011-7.
- Conlon, T. J., T. Cossette, et al. (2005). "Efficient Hepatic Delivery and Expression from a Recombinant Adeno-associated Virus 8 Pseudotyped alpha1-Antitrypsin Vector." Mol Ther.
- Cotmore, S. F., M. D'Abramo A, Jr., et al. (1999). "Controlled conformational transitions in the MVM virion expose the VP1 N-terminus and viral genome without particle disassembly." Virology **254**(1): 169-81.
- Davidoff, A. M., J. T. Gray, et al. (2005). "Comparison of the ability of adeno-associated viral vectors pseudotyped with serotype 2, 5, and 8 capsid proteins to mediate efficient transduction of the liver in murine and nonhuman primate models." Mol Ther **11**(6): 875-88.
- Davidoff, A. M., C. Y. Ng, et al. (2004). "Purification of recombinant adeno-associated virus type 8 vectors by ion exchange chromatography generates clinical grade vector stock." J Virol Methods **121**(2): 209-15.
- Davidson, B. L., C. S. Stein, et al. (2000). "Recombinant adeno-associated virus type 2, 4, and 5 vectors: transduction of variant cell types and regions in the mammalian central nervous system." Proc Natl Acad Sci U S A **97**(7): 3428-32.
- Daya, S. and K. I. Berns (2008). "Gene therapy using adeno-associated virus vectors." Clin Microbiol Rev **21**(4): 583-93.
- Daya, S., N. Cortez, et al. (2009). "AAV site-specific integration is mediated by proteins of the non-homologous end joining pathway." J Virol.
- Di Paolo, N. C. and D. M. Shayakhmetov (2009). "Adenovirus de-targeting from the liver." Curr Opin Mol Ther **11**(5): 523-31.
- Di Pasquale, G. and J. A. Chiorini (2006). "AAV transcytosis through barrier epithelia and endothelium." Mol Ther **13**(3): 506-16.

- Ding, W., L. Zhang, et al. (2005). "Intracellular trafficking of adeno-associated viral vectors." Gene Ther **12**(11): 873-80.
- Ding, W., L. N. Zhang, et al. (2006). "rAAV2 traffics through both the late and the recycling endosomes in a dose-dependent fashion." Mol Ther **13**(4): 671-82.
- DiPrimio, N., A. Asokan, et al. (2008). "Surface loop dynamics in adeno-associated virus capsid assembly." J Virol **82**(11): 5178-89.
- Dong, J. Y., P. D. Fan, et al. (1996). "Quantitative analysis of the packaging capacity of recombinant adeno-associated virus." Hum Gene Ther **7**(17): 2101-12.
- Donsante, A., D. G. Miller, et al. (2007). "AAV vector integration sites in mouse hepatocellular carcinoma." Science **317**(5837): 477.
- Douar, A. M., K. Poulard, et al. (2001). "Intracellular trafficking of adeno-associated virus vectors: routing to the late endosomal compartment and proteasome degradation." J Virol **75**(4): 1824-33.
- Duan, D., Q. Li, et al. (1999). "Dynamin is required for recombinant adeno-associated virus type 2 infection." J Virol **73**(12): 10371-6.
- Duan, D., P. Sharma, et al. (1998). "Circular intermediates of recombinant adeno-associated virus have defined structural characteristics responsible for long-term episomal persistence in muscle tissue." J Virol **72**(11): 8568-77.
- Duan, D., Y. Yue, et al. (2000). "A new dual-vector approach to enhance recombinant adeno-associated virus-mediated gene expression through intermolecular cis activation." Nat Med **6**(5): 595-8.
- Duan, D., Y. Yue, et al. (2000). "Endosomal processing limits gene transfer to polarized airway epithelia by adeno-associated virus." J Clin Invest **105**(11): 1573-87.
- Erles, K., P. Sebokova, et al. (1999). "Update on the prevalence of serum antibodies (IgG and IgM) to adeno-associated virus (AAV)." J Med Virol **59**(3): 406-11.
- Farr, G. A., L. G. Zhang, et al. (2005). "Parvoviral virions deploy a capsid-tethered lipolytic enzyme to breach the endosomal membrane during cell entry." Proc Natl Acad Sci U S A **102**(47): 17148-53.
- Feng, D., J. Chen, et al. (2006). "A 16bp Rep binding element is sufficient for mediating Rep-dependent integration into AAVS1." J Mol Biol **358**(1): 38-45.
- Ferrari, F. K., T. Samulski, et al. (1996). "Second-strand synthesis is a rate-limiting step for efficient transduction by recombinant adeno-associated virus vectors." J Virol **70**(5): 3227-34.
- Fisher, K. J., K. Jooss, et al. (1997). "Recombinant adeno-associated virus for muscle directed gene therapy." Nat Med **3**(3): 306-12.
- Flotte, T., B. Carter, et al. (1996). "A phase I study of an adeno-associated virus-CFTR gene vector in adult CF patients with mild lung disease." Hum Gene Ther **7**(9): 1145-59.
- Flotte, T. R. (2000). "Size does matter: overcoming the adeno-associated virus packaging limit." Respir Res **1**(1): 16-8.
- Flotte, T. R., X. Barraza-Ortiz, et al. (1995). "An improved system for packaging recombinant adeno-associated virus vectors capable of in vivo transduction." Gene Ther **2**(1): 29-37.
- Flotte, T. R., P. L. Zeitlin, et al. (2003). "Phase I trial of intranasal and endobronchial administration of a recombinant adeno-associated virus serotype 2 (rAAV2)-CFTR vector in adult cystic fibrosis patients: a two-part clinical study." Hum Gene Ther **14**(11): 1079-88.
- Gao, G., M. R. Alvira, et al. (2003). "Adeno-associated viruses undergo substantial evolution in primates during natural infections." Proc Natl Acad Sci U S A **100**(10): 6081-6.
- Gao, G., Y. Lu, et al. (2006). "Biology of AAV serotype vectors in liver-directed gene transfer to nonhuman primates." Mol Ther **13**(1): 77-87.

-
- Gao, G., L. H. Vandenberghe, et al. (2004). "Clades of Adeno-associated viruses are widely disseminated in human tissues." J Virol **78**(12): 6381-8.
- Gao, G., L. H. Vandenberghe, et al. (2005). "New recombinant serotypes of AAV vectors." Curr Gene Ther **5**(3): 285-97.
- Gao, G., X. Zhou, et al. (2003). "High throughput creation of recombinant adenovirus vectors by direct cloning, green-white selection and I-Sce I-mediated rescue of circular adenovirus plasmids in 293 cells." Gene Ther **10**(22): 1926-30.
- Gao, G. P., M. R. Alvira, et al. (2002). "Novel adeno-associated viruses from rhesus monkeys as vectors for human gene therapy." Proc Natl Acad Sci U S A **99**(18): 11854-9.
- Ghosh, A., M. Allamarvdasht, et al. (2006). "Long-term correction of murine glycogen storage disease type Ia by recombinant adeno-associated virus-1-mediated gene transfer." Gene Ther **13**(4): 321-9.
- Ghosh, A., Y. Yue, et al. (2006). "Viral serotype and the transgene sequence influence overlapping adeno-associated viral (AAV) vector-mediated gene transfer in skeletal muscle." J Gene Med **8**(3): 298-305.
- Girod, A., M. Ried, et al. (1999). "Genetic capsid modifications allow efficient re-targeting of adeno-associated virus type 2." Nat Med **5**(12): 1438.
- Girod, A., C. E. Wobus, et al. (2002). "The VP1 capsid protein of adeno-associated virus type 2 is carrying a phospholipase A2 domain required for virus infectivity." J Gen Virol **83**(Pt 5): 973-8.
- Goncalves, M. A. (2005). "Adeno-associated virus: from defective virus to effective vector." Virol J **2**(1): 43.
- Gray, S. J., B. L. Blake, et al. (2010). "Directed evolution of a novel adeno-associated virus (AAV) vector that crosses the seizure-compromised blood-brain barrier (BBB)." Mol Ther **18**(3): 570-8.
- Green, M. R. and R. G. Roeder (1980). "Definition of a novel promoter for the major adenovirus-associated virus mRNA." Cell **22**(1 Pt 1): 231-42.
- Grieger, J. C., S. Snowdy, et al. (2006). "Separate basic region motifs within the adeno-associated virus capsid proteins are essential for infectivity and assembly." J Virol **80**(11): 5199-210.
- Grifman, M., M. Trepel, et al. (2001). "Incorporation of tumor-targeting peptides into recombinant adeno-associated virus capsids." Mol Ther **3**(6): 964-75.
- Grimm, D. and M. A. Kay (2003). "From virus evolution to vector revolution: use of naturally occurring serotypes of adeno-associated virus (AAV) as novel vectors for human gene therapy." Curr Gene Ther **3**(4): 281-304.
- Grimm, D., A. Kern, et al. (1999). "Titration of AAV-2 particles via a novel capsid ELISA: packaging of genomes can limit production of recombinant AAV-2." Gene Ther **6**(7): 1322-30.
- Grimm, D., A. Kern, et al. (1998). Novel tools for production and purification of recombinant adenoassociated virus vectors. Hum Gene Ther. **9**: 2745-60.
- Grimm, D., J. S. Lee, et al. (2008). "In vitro and in vivo gene therapy vector evolution via multispecies interbreeding and retargeting of adeno-associated viruses." J Virol **82**(12): 5887-911.
- Guy, J., X. Qi, et al. (2009). "Efficiency and safety of AAV-mediated gene delivery of the human ND4 complex I subunit in the mouse visual system." Invest Ophthalmol Vis Sci **50**(9): 4205-14.
- Hailer, N. P., F. L. Heppner, et al. (1998). "Astrocytic factors deactivate antigen presenting cells that invade the central nervous system." Brain Pathol **8**(3): 459-74.
- Halbert, C. L., J. M. Allen, et al. (2001). "Adeno-associated virus type 6 (AAV6) vectors mediate efficient transduction of airway epithelial cells in mouse lungs compared to that of AAV2 vectors." J Virol **75**(14): 6615-24.

- Halbert, C. L., E. A. Rutledge, et al. (2000). "Repeat transduction in the mouse lung by using adeno-associated virus vectors with different serotypes." *J Virol* **74**(3): 1524-32.
- Halbert, C. L., T. A. Standaert, et al. (1998). "Successful readministration of adeno-associated virus vectors to the mouse lung requires transient immunosuppression during the initial exposure." *J Virol* **72**(12): 9795-805.
- Handa, A., S. Muramatsu, et al. (2000). "Adeno-associated virus (AAV)-3-based vectors transduce haematopoietic cells not susceptible to transduction with AAV-2-based vectors." *J Gen Virol* **81**(Pt 8): 2077-84.
- Hansen, J., K. Qing, et al. (2001). "Adeno-associated virus type 2-mediated gene transfer: altered endocytic processing enhances transduction efficiency in murine fibroblasts." *J Virol* **75**(9): 4080-90.
- Hansen, J., K. Qing, et al. (2001). "Infection of purified nuclei by adeno-associated virus 2." *Mol Ther* **4**(4): 289-96.
- Harbison, C. E., J. A. Chiorini, et al. (2008). "The parvovirus capsid odyssey: from the cell surface to the nucleus." *Trends Microbiol* **16**(5): 208-14.
- Hauck, B. and W. Xiao (2003). "Characterization of tissue tropism determinants of adeno-associated virus type 1." *J Virol* **77**(4): 2768-74.
- Hauck, B., R. R. Xu, et al. (2006). "Efficient AAV1-AAV2 hybrid vector for gene therapy of hemophilia." *Hum Gene Ther* **17**(1): 46-54.
- Hauck, B., W. Zhao, et al. (2004). "Intracellular viral processing, not single-stranded DNA accumulation, is crucial for recombinant adeno-associated virus transduction." *J Virol* **78**(24): 13678-86.
- Hermonat, P. L., M. A. Labow, et al. (1984). "Genetics of adeno-associated virus: isolation and preliminary characterization of adeno-associated virus type 2 mutants." *J Virol* **51**(2): 329-39.
- Hermonat, P. L. and N. Muzyczka (1984). "Use of adeno-associated virus as a mammalian DNA cloning vector: transduction of neomycin resistance into mammalian tissue culture cells." *Proc Natl Acad Sci U S A* **81**(20): 6466-70.
- Herzog, R. W., O. Cao, et al. (2010). "Two decades of clinical gene therapy--success is finally mounting." *Discov Med* **9**(45): 105-11.
- Hoggan, M. D., N. R. Blacklow, et al. (1966). "Studies of small DNA viruses found in various adenovirus preparations: physical, biological, and immunological characteristics." *Proc Natl Acad Sci U S A* **55**(6): 1467-74.
- Huang, X. and Y. Yang (2009). "Innate Immune Recognition of Viruses and Viral Vectors." *Hum Gene Ther*.
- Humphrey, W., A. Dalke, et al. (1996). "VMD: visual molecular dynamics." *J Mol Graph* **14**(1): 33-8, 27-8.
- Hunter, L. A. and R. J. Samulski (1992). "Colocalization of adeno-associated virus Rep and capsid proteins in the nuclei of infected cells." *J Virol* **66**(1): 317-24.
- Hutchins, B., N. Sajjadi, et al. (2000). "Working toward an adenoviral vector testing standard." *Mol Ther* **2**(6): 532-4.
- Im, D. S. and N. Muzyczka (1992). "Partial purification of adeno-associated virus Rep78, Rep52, and Rep40 and their biochemical characterization." *J Virol* **66**(2): 1119-28.
- Inagaki, K., C. Piao, et al. (2008). "Frequency and spectrum of genomic integration of recombinant adeno-associated virus serotype 8 vector in neonatal mouse liver." *J Virol* **82**(19): 9513-24.
- Jacobson, S. L., M. Banfalvi, et al. (1985). "Long-term primary cultures of adult human and rat cardiomyocytes." *Basic Res Cardiol* **80 Suppl 1**: 79-82.
- James, J. A., C. R. Escalante, et al. (2003). "Crystal structure of the SF3 helicase from adeno-associated virus type 2." *Structure* **11**(8): 1025-35.

-
- Jiang, H., D. Lillicrap, et al. (2006). "Multiyear therapeutic benefit of AAV serotypes 2, 6, and 8 delivering factor VIII to hemophilia A mice and dogs." *Blood* **108**(1): 107-15.
- Jiang, H., G. F. Pierce, et al. (2006). "Evidence of multiyear factor IX expression by AAV-mediated gene transfer to skeletal muscle in an individual with severe hemophilia B." *Mol Ther* **14**(3): 452-5.
- Johnson, F. B., H. L. Ozer, et al. (1971). "Structural proteins of adenovirus-associated virus type 3." *J Virol* **8**(6): 860-63.
- Kaludov, N., K. E. Brown, et al. (2001). "Adeno-associated virus serotype 4 (AAV4) and AAV5 both require sialic acid binding for hemagglutination and efficient transduction but differ in sialic acid linkage specificity." *J Virol* **75**(15): 6884-93.
- Kashiwakura, Y., K. Tamayose, et al. (2005). "Hepatocyte growth factor receptor is a coreceptor for adeno-associated virus type 2 infection." *J Virol* **79**(1): 609-14.
- Kawamoto, S., Q. Shi, et al. (2005). "Widespread and early myocardial gene expression by adeno-associated virus vector type 6 with a beta-actin hybrid promoter." *Mol Ther* **11**(6): 980-5.
- Kay, M. A. (2007). "AAV vectors and tumorigenicity." *Nat Biotechnol* **25**(10): 1111-3.
- Kern, A., K. Schmidt, et al. (2003). "Identification of a heparin-binding motif on adeno-associated virus type 2 capsids." *J Virol* **77**(20): 11072-81.
- Kilham, L. and L. J. Olivier (1959). "A latent virus of rats isolated in tissue culture." *Virology* **7**(4): 428-37.
- King, J. A., R. Dubielzig, et al. (2001). "DNA helicase-mediated packaging of adeno-associated virus type 2 genomes into preformed capsids." *EMBO J* **20**(12): 3282-91.
- Koerber, J. T., J. H. Jang, et al. (2008). "DNA shuffling of adeno-associated virus yields functionally diverse viral progeny." *Mol Ther* **16**(10): 1703-9.
- Kotin, R. M. (1994). "Prospects for the use of adeno-associated virus as a vector for human gene therapy." *Hum Gene Ther* **5**(7): 793-801.
- Kotin, R. M., M. Siniscalco, et al. (1990). "Site-specific integration by adeno-associated virus." *Proc Natl Acad Sci U S A* **87**(6): 2211-5.
- Kronenberg, S., B. Bottcher, et al. (2005). "A conformational change in the adeno-associated virus type 2 capsid leads to the exposure of hidden VP1 N termini." *J Virol* **79**(9): 5296-303.
- Kronenberg, S., J. A. Kleinschmidt, et al. (2001). "Electron cryo-microscopy and image reconstruction of adeno-associated virus type 2 empty capsids." *EMBO Rep* **2**(11): 997-1002.
- Kuck, D., A. Kern, et al. (2007). "Development of AAV serotype-specific ELISAs using novel monoclonal antibodies." *J Virol Methods* **140**(1-2): 17-24.
- Lai, Y., D. Li, et al. (2008). "Design of trans-splicing adeno-associated viral vectors for Duchenne muscular dystrophy gene therapy." *Methods Mol Biol* **433**: 259-75.
- Laughlin, C. A., C. B. Cardellicchio, et al. (1986). "Latent infection of KB cells with adeno-associated virus type 2." *J Virol* **60**(2): 515-24.
- Laughlin, C. A., N. Jones, et al. (1982). "Effect of deletions in adenovirus early region 1 genes upon replication of adeno-associated virus." *J Virol* **41**(3): 868-76.
- Laughlin, C. A., M. W. Myers, et al. (1979). "Defective-interfering particles of the human parvovirus adeno-associated virus." *Virology* **94**(1): 162-74.
- Leberherz, C., G. Gao, et al. (2004). "Gene therapy with novel adeno-associated virus vectors substantially diminishes atherosclerosis in a murine model of familial hypercholesterolemia." *J Gene Med* **6**(6): 663-72.
- Li, H., S. L. Murphy, et al. (2007). "Pre-existing AAV capsid-specific CD8+ T cells are unable to eliminate AAV-transduced hepatocytes." *Mol Ther* **15**(4): 792-800.
- Liu, X., M. Luo, et al. (2005). "Spliceosome-mediated RNA trans-splicing with recombinant adeno-associated virus partially restores cystic fibrosis transmembrane conductance regulator

- function to polarized human cystic fibrosis airway epithelial cells." Hum Gene Ther **16**(9): 1116-23.
- Liu, Y., T. Okada, et al. (2005). "Specific and efficient transduction of Cochlear inner hair cells with recombinant adeno-associated virus type 3 vector." Mol Ther **12**(4): 725-33.
- Lochrie, M. A., G. P. Tatsuno, et al. (2006). "Mutations on the external surfaces of adeno-associated virus type 2 capsids that affect transduction and neutralization." J Virol **80**(2): 821-34.
- Lock M, S. M., Alberto Auricchio, Eduard Ayuso, E. Jeffrey Beecham,, M. F. B.-T. Véronique Blouin-Tavel, Mahuya Bose, Barry Byrne, Tina, et al. (submitted). "Characterization of a Recombinant Adeno-Associated Virus Type 2 Reference Standard Material." Hum Gene Ther
- Loiler, S. A., T. J. Conlon, et al. (2003). "Targeting recombinant adeno-associated virus vectors to enhance gene transfer to pancreatic islets and liver." Gene Ther **10**(18): 1551-8.
- Lopez-Bueno, A., M. P. Rubio, et al. (2006). "Host-selected amino acid changes at the sialic acid binding pocket of the parvovirus capsid modulate cell binding affinity and determine virulence." J Virol **80**(3): 1563-73.
- Lopez-Bueno, A., J. C. Segovia, et al. (2008). "Evolution to pathogenicity of the parvovirus minute virus of mice in immunodeficient mice involves genetic heterogeneity at the capsid domain that determines tropism." J Virol **82**(3): 1195-203.
- Louboutin, J. P., L. Wang, et al. (2005). "Gene transfer into skeletal muscle using novel AAV serotypes." J Gene Med **7**(4): 442-51.
- Lowenstein, P. R. (2004). "Input virion proteins: cryptic targets of antivector immune responses in preimmunized subjects." Mol Ther **9**(6): 771-4.
- Lusby, E., R. Bohenzky, et al. (1981). "Inverted terminal repetition in adeno-associated virus DNA: independence of the orientation at either end of the genome." J Virol **37**(3): 1083-6.
- Lusby, E., K. H. Fife, et al. (1980). "Nucleotide sequence of the inverted terminal repetition in adeno-associated virus DNA." J Virol **34**(2): 402-9.
- Lux, K., N. Goerlitz, et al. (2005). "Green fluorescent protein-tagged adeno-associated virus particles allow the study of cytosolic and nuclear trafficking." J Virol **79**(18): 11776-87.
- Ma, H. I., P. Guo, et al. (2002). "Suppression of intracranial human glioma growth after intramuscular administration of an adeno-associated viral vector expressing angiostatin." Cancer Res **62**(3): 756-63.
- Ma, H. I., S. Z. Lin, et al. (2002). "Intratumoral gene therapy of malignant brain tumor in a rat model with angiostatin delivered by adeno-associated viral (AAV) vector." Gene Ther **9**(1): 2-11.
- Malecki, M., P. Swoboda, et al. (2009). "Recombinant adeno-associated virus derived vectors (rAAV2) efficiently transduce ovarian and hepatocellular carcinoma cells--implications for cancer gene therapy." Acta Pol Pharm **66**(1): 93-9.
- Manning, W. C., S. Zhou, et al. (1998). "Transient immunosuppression allows transgene expression following readministration of adeno-associated viral vectors." Hum Gene Ther **9**(4): 477-85.
- Manno, C. S., A. J. Chew, et al. (2003). "AAV-mediated factor IX gene transfer to skeletal muscle in patients with severe hemophilia B." Blood **101**(8): 2963-72.
- Manno, C. S., G. F. Pierce, et al. (2006). "Successful transduction of liver in hemophilia by AAV-Factor IX and limitations imposed by the host immune response." Nat Med **12**(3): 342-7.
- Mastakov, M. Y., K. Baer, et al. (2002). "Immunological aspects of recombinant adeno-associated virus delivery to the mammalian brain." J Virol **76**(16): 8446-54.
- Mayor, H. D. and R. M. Jamison (1966). "Morphology of small viral particles and subviral components." Prog Med Virol **8**: 183-213.

-
- McCarty, D. M., H. Fu, et al. (2003). "Adeno-associated virus terminal repeat (TR) mutant generates self-complementary vectors to overcome the rate-limiting step to transduction in vivo." *Gene Ther* **10**(26): 2112-8.
- McCarty, D. M., J. H. Ryan, et al. (1994). "Interaction of the adeno-associated virus Rep protein with a sequence within the A palindrome of the viral terminal repeat." *J Virol* **68**(8): 4998-5006.
- McLaughlin, S. K., P. Collis, et al. (1988). "Adeno-associated virus general transduction vectors: analysis of proviral structures." *J Virol* **62**(6): 1963-73.
- McPherson, R. A., L. J. Rosenthal, et al. (1985). "Human cytomegalovirus completely helps adeno-associated virus replication." *Virology* **147**(1): 217-22.
- Mendelson, E., J. P. Trempe, et al. (1986). "Identification of the trans-acting Rep proteins of adeno-associated virus by antibodies to a synthetic oligopeptide." *J Virol* **60**(3): 823-32.
- Michelfelder, S., J. Kohlschutter, et al. (2009). "Successful expansion but not complete restriction of tropism of adeno-associated virus by in vivo biopanning of random virus display Peptide libraries." *PLoS One* **4**(4): e5122.
- Michelfelder, S., M. K. Lee, et al. (2007). "Vectors selected from adeno-associated viral display peptide libraries for leukemia cell-targeted cytotoxic gene therapy." *Exp Hematol* **35**(12): 1766-76.
- Morgenstern, B., K. Frech, et al. (1998). "DIALIGN: finding local similarities by multiple sequence alignment." *Bioinformatics* **14**(3): 290-4.
- Mori, S., L. Wang, et al. (2004). "Two novel adeno-associated viruses from cynomolgus monkey: pseudotyping characterization of capsid protein." *Virology* **330**(2): 375-83.
- Moskalenko, M., L. Chen, et al. (2000). "Epitope mapping of human anti-adeno-associated virus type 2 neutralizing antibodies: implications for gene therapy and virus structure." *J Virol* **74**(4): 1761-6.
- Mueller, C. and T. R. Flotte (2008a). "Clinical gene therapy using recombinant adeno-associated virus vectors." *Gene Ther* **15**(11): 858-63.
- Mueller, C. and T. R. Flotte (2008b). "Gene therapy for cystic fibrosis." *Clin Rev Allergy Immunol* **35**(3): 164-78.
- Muller, O. J., F. Kaul, et al. (2003). "Random peptide libraries displayed on adeno-associated virus to select for targeted gene therapy vectors." *Nat Biotechnol* **21**(9): 1040-6.
- Mullis, K. B. and F. A. Faloona (1987). "Specific synthesis of DNA in vitro via a polymerase-catalyzed chain reaction." *Methods Enzymol* **155**: 335-50.
- Murphy, S. L., A. Bhagwat, et al. (2008a). "High-throughput screening and biophysical interrogation of hepatotropic AAV." *Mol Ther* **16**(12): 1960-7.
- Murphy, S. L., H. Li, et al. (2008b). "Prolonged susceptibility to antibody-mediated neutralization for adeno-associated vectors targeted to the liver." *Mol Ther* **16**(1): 138-45.
- Myers, M. W., C. A. Laughlin, et al. (1980). "Adenovirus helper function for growth of adeno-associated virus: effect of temperature-sensitive mutations in adenovirus early gene region 2." *J Virol* **35**(1): 65-75.
- Nahreini, P., S. H. Larsen, et al. (1992). "Cloning and integration of DNA fragments in human cells via the inverted terminal repeats of the adeno-associated virus 2 genome." *Gene* **119**(2): 265-72.
- Nakai, H., S. Fuess, et al. (2005). "Unrestricted hepatocyte transduction with adeno-associated virus serotype 8 vectors in mice." *J Virol* **79**(1): 214-24.
- Nakai, H., C. E. Thomas, et al. (2002). "A limited number of transducible hepatocytes restricts a wide-range linear vector dose response in recombinant adeno-associated virus-mediated liver transduction." *J Virol* **76**(22): 11343-9.
- Nakai, H., X. Wu, et al. (2005). "Large-scale molecular characterization of adeno-associated virus vector integration in mouse liver." *J Virol* **79**(6): 3606-14.

- Naldini, L., U. Blomer, et al. (1996). "Efficient transfer, integration, and sustained long-term expression of the transgene in adult rat brains injected with a lentiviral vector." Proc Natl Acad Sci U S A **93**(21): 11382-8.
- Nam, H. J., M. D. Lane, et al. (2007). "Structure of adeno-associated virus serotype 8, a gene therapy vector." J Virol **81**(22): 12260-71.
- Nathwani, A. C., J. T. Gray, et al. (2006). "Self-complementary adeno-associated virus vectors containing a novel liver-specific human factor IX expression cassette enable highly efficient transduction of murine and nonhuman primate liver." Blood **107**(7): 2653-61.
- Natkunarahaj, M., P. Trittibach, et al. (2008). "Assessment of ocular transduction using single-stranded and self-complementary recombinant adeno-associated virus serotype 2/8." Gene Ther **15**(6): 463-7.
- Niederman, T. M., B. J. Thielan, et al. (1989). "Human immunodeficiency virus type 1 negative factor is a transcriptional silencer." Proc Natl Acad Sci U S A **86**(4): 1128-32.
- O'Donnell, J., K. A. Taylor, et al. (2009). "Adeno-associated virus-2 and its primary cellular receptor--Cryo-EM structure of a heparin complex." Virology **385**(2): 434-43.
- Ogston, P., K. Raj, et al. (2000). "Productive replication of adeno-associated virus can occur in human papillomavirus type 16 (HPV-16) episome-containing keratinocytes and is augmented by the HPV-16 E2 protein." J Virol **74**(8): 3494-504.
- Opie, S. R., K. H. Warrington, Jr., et al. (2003). "Identification of amino acid residues in the capsid proteins of adeno-associated virus type 2 that contribute to heparan sulfate proteoglycan binding." J Virol **77**(12): 6995-7006.
- Otteken, A., P. L. Earl, et al. (1996). "Folding, assembly, and intracellular trafficking of the human immunodeficiency virus type 1 envelope glycoprotein analyzed with monoclonal antibodies recognizing maturational intermediates." J Virol **70**(6): 3407-15.
- Owens, R. A., J. P. Trempe, et al. (1991). "Adeno-associated virus rep proteins produced in insect and mammalian expression systems: wild-type and dominant-negative mutant proteins bind to the viral replication origin." Virology **184**(1): 14-22.
- Pajusola, K., M. Gruchala, et al. (2002). "Cell-type-specific characteristics modulate the transduction efficiency of adeno-associated virus type 2 and restrain infection of endothelial cells." J Virol **76**(22): 11530-40.
- Paran, N., B. Geiger, et al. (2001). "HBV infection of cell culture: evidence for multivalent and cooperative attachment." Embo J **20**(16): 4443-53.
- Passini, M. A., D. J. Watson, et al. (2003). "Intraventricular brain injection of adeno-associated virus type 1 (AAV1) in neonatal mice results in complementary patterns of neuronal transduction to AAV2 and total long-term correction of storage lesions in the brains of beta-glucuronidase-deficient mice." J Virol **77**(12): 7034-40.
- Pekrun, K., R. Shibata, et al. (2002). "Evolution of a human immunodeficiency virus type 1 variant with enhanced replication in pig-tailed macaque cells by DNA shuffling." J Virol **76**(6): 2924-35.
- Perabo, L., H. Buning, et al. (2003). "In vitro selection of viral vectors with modified tropism: the adeno-associated virus display." Mol Ther **8**(1): 151-7.
- Perabo, L., J. Endell, et al. (2006). "Combinatorial engineering of a gene therapy vector: directed evolution of adeno-associated virus." J Gene Med **8**(2): 155-62.
- Perabo, L., D. Goldnau, et al. (2006). "Heparan sulfate proteoglycan binding properties of adeno-associated virus retargeting mutants and consequences for their in vivo tropism." J Virol **80**(14): 7265-9.
- Pereira, D. J., D. M. McCarty, et al. (1997). "The adeno-associated virus (AAV) Rep protein acts as both a repressor and an activator to regulate AAV transcription during a productive infection." J Virol **71**(2): 1079-88.

-
- Ponnazhagan, S., G. Mahendra, et al. (2002). "Conjugate-based targeting of recombinant adeno-associated virus type 2 vectors by using avidin-linked ligands." *J Virol* **76**(24): 12900-7.
- Powell, S. K., M. A. Kaloss, et al. (2000). "Breeding of retroviruses by DNA shuffling for improved stability and processing yields." *Nat Biotechnol* **18**(12): 1279-82.
- Qazilbash, M. H., X. Xiao, et al. (1997). "Cancer gene therapy using a novel adeno-associated virus vector expressing human wild-type p53." *Gene Ther* **4**(7): 675-82.
- Qing, K., C. Mah, et al. (1999). "Human fibroblast growth factor receptor 1 is a co-receptor for infection by adeno-associated virus 2." *Nat Med* **5**(1): 71-7.
- Rabinowitz, J. E., D. E. Bowles, et al. (2004). "Cross-dressing the virion: the transcapsidation of adeno-associated virus serotypes functionally defines subgroups." *J Virol* **78**(9): 4421-32.
- Rabinowitz, J. E., F. Rolling, et al. (2002). "Cross-packaging of a single adeno-associated virus (AAV) type 2 vector genome into multiple AAV serotypes enables transduction with broad specificity." *J Virol* **76**(2): 791-801.
- Rabinowitz, J. E. and J. Samulski (1998). "Adeno-associated virus expression systems for gene transfer." *Curr Opin Biotechnol* **9**(5): 470-5.
- Rabinowitz, J. E., W. Xiao, et al. (1999). "Insertional mutagenesis of AAV2 capsid and the production of recombinant virus." *Virology* **265**(2): 274-85.
- Reich, S. J., A. Auricchio, et al. (2003). "Efficient trans-splicing in the retina expands the utility of adeno-associated virus as a vector for gene therapy." *Hum Gene Ther* **14**(1): 37-44.
- Reiss, P., A. de Ronde, et al. (1989). "Antibody response to the viral negative factor (nef) in HIV-1 infection: a correlate of levels of HIV-1 expression." *Aids* **3**(4): 227-33.
- Ren, C., S. Kumar, et al. (2005). "Genomic stability of self-complementary adeno-associated virus 2 during early stages of transduction in mouse muscle in vivo." *Hum Gene Ther* **16**(9): 1047-57.
- Richardson, W. D. and H. Westphal (1981). "A cascade of adenovirus early functions is required for expression of adeno-associated virus." *Cell* **27**(1 Pt 2): 133-41.
- Rivera, V. M., G. P. Gao, et al. (2005). "Long-term pharmacologically regulated expression of erythropoietin in primates following AAV-mediated gene transfer." *Blood* **105**(4): 1424-30.
- Rose, J. A., J. V. Maizel, Jr., et al. (1971). "Structural proteins of adenovirus-associated viruses." *J Virol* **8**(5): 766-70.
- Ruffing, M., H. Heid, et al. (1994). "Mutations in the carboxy terminus of adeno-associated virus 2 capsid proteins affect viral infectivity: lack of an RGD integrin-binding motif." *J Gen Virol* **75** (Pt 12): 3385-92.
- Ruffing, M., H. Zentgraf, et al. (1992). "Assembly of viruslike particles by recombinant structural proteins of adeno-associated virus type 2 in insect cells." *J Virol* **66**(12): 6922-30.
- Rutledge, E. A., C. L. Halbert, et al. (1998). "Infectious clones and vectors derived from adeno-associated virus (AAV) serotypes other than AAV type 2." *J Virol* **72**(1): 309-19.
- Ryan, J. H., S. Zolotukhin, et al. (1996). "Sequence requirements for binding of Rep68 to the adeno-associated virus terminal repeats." *J Virol* **70**(3): 1542-53.
- Samulski, R. J., L. S. Chang, et al. (1989). "Helper-free stocks of recombinant adeno-associated viruses: normal integration does not require viral gene expression." *J Virol* **63**(9): 3822-8.
- Samulski, R. J., A. Srivastava, et al. (1983). "Rescue of adeno-associated virus from recombinant plasmids: gene correction within the terminal repeats of AAV." *Cell* **33**(1): 135-43.
- Samulski, R. J., X. Zhu, et al. (1991). "Targeted integration of adeno-associated virus (AAV) into human chromosome 19." *Embo J* **10**(12): 3941-50.
- Sandalon, Z., E. M. Bruckheimer, et al. (2007). "Long-term suppression of experimental arthritis following intramuscular administration of a pseudotyped AAV2/1-TNFR:Fc Vector." *Mol Ther* **15**(2): 264-9.

- Sanger, F., S. Nicklen, et al. (1977). "DNA sequencing with chain-terminating inhibitors." Proc Natl Acad Sci U S A **74**(12): 5463-7.
- Sanlioglu, S., P. K. Benson, et al. (2000). "Endocytosis and nuclear trafficking of adeno-associated virus type 2 are controlled by rac1 and phosphatidylinositol-3 kinase activation." J Virol **74**(19): 9184-96.
- Sarkar, R., M. Mucci, et al. (2006). "Long-term efficacy of adeno-associated virus serotypes 8 and 9 in hemophilia a dogs and mice." Hum Gene Ther **17**(4): 427-39.
- Sarkar, R., R. Tetreault, et al. (2004). "Total correction of hemophilia A mice with canine FVIII using an AAV 8 serotype." Blood **103**(4): 1253-60.
- Sayle, R. A. and E. J. Milner-White (1995). "RASMOL: biomolecular graphics for all." Trends Biochem Sci **20**(9): 374.
- Scallan, C. D., H. Jiang, et al. (2006). "Human immunoglobulin inhibits liver transduction by AAV vectors at low AAV2 neutralizing titers in SCID mice." Blood **107**(5): 1810-7.
- Schipper, M. L., G. Iyer, et al. (2009). "Particle size, surface coating, and PEGylation influence the biodistribution of quantum dots in living mice." Small **5**(1): 126-34.
- Schlehofer, J. R., M. Ehrbar, et al. (1986). "Vaccinia virus, herpes simplex virus, and carcinogens induce DNA amplification in a human cell line and support replication of a helpervirus dependent parvovirus." Virology **152**(1): 110-7.
- Schmidt, M., A. Voutetakis, et al. (2008). Adeno-associated virus type 12 (AAV12): a novel AAV serotype with sialic acid- and heparan sulfate proteoglycan-independent transduction activity. J Virol. **82**: 1399-406.
- Schnepf, B. C., R. L. Jensen, et al. (2005). "Characterization of adeno-associated virus genomes isolated from human tissues." J Virol **79**(23): 14793-803.
- Seiler, M. P., A. D. Miller, et al. (2006). "Adeno-associated virus types 5 and 6 use distinct receptors for cell entry." Hum Gene Ther **17**(1): 10-9.
- Seisenberger, G., M. U. Ried, et al. (2001). "Real-time single-molecule imaging of the infection pathway of an adeno-associated virus." Science **294**(5548): 1929-32.
- Shen, X., T. Storm, et al. (2007). "Characterization of the relationship of AAV capsid domain swapping to liver transduction efficiency." Mol Ther **15**(11): 1955-62.
- Shi, W., G. S. Arnold, et al. (2001). "Insertional mutagenesis of the adeno-associated virus type 2 (AAV2) capsid gene and generation of AAV2 vectors targeted to alternative cell-surface receptors." Hum Gene Ther **12**(14): 1697-711.
- Shi, W. and J. S. Bartlett (2003). "RGD inclusion in VP3 provides adeno-associated virus type 2 (AAV2)-based vectors with a heparan sulfate-independent cell entry mechanism." Mol Ther **7**(4): 515-25.
- Shi, X., G. Fang, et al. (2006). "Insertional mutagenesis at positions 520 and 584 of adeno-associated virus type 2 (AAV2) capsid gene and generation of AAV2 vectors with eliminated heparin- binding ability and introduced novel tropism." Hum Gene Ther **17**(3): 353-61.
- Siegl, G., R. C. Bates, et al. (1985). "Characteristics and taxonomy of Parvoviridae." Intervirology **23**(2): 61-73.
- Smith, R. H. and R. M. Kotin (1998). "The Rep52 gene product of adeno-associated virus is a DNA helicase with 3'-to-5' polarity." J Virol **72**(6): 4874-81.
- Snyder, R. O., D. S. Im, et al. (1990). "Evidence for covalent attachment of the adeno-associated virus (AAV) rep protein to the ends of the AAV genome." J Virol **64**(12): 6204-13.
- Somia, N. and I. M. Verma (2000). "Gene therapy: trials and tribulations." Nat Rev Genet **1**(2): 91-9.
- Sonntag, F., S. Bleker, et al. (2006). "Adeno-associated virus type 2 capsids with externalized VP1/VP2 trafficking domains are generated prior to passage through the cytoplasm and are maintained until uncoating occurs in the nucleus." J Virol **80**(22): 11040-54.

-
- Sonntag, F., K. Schmidt, et al. (2010). "A viral assembly factor promotes AAV2 capsid formation in the nucleolus." Proc Natl Acad Sci U S A (in press).
- Soong, N. W., L. Nomura, et al. (2000). "Molecular breeding of viruses." Nat Genet **25**(4): 436-9.
- Srivastava, A., E. W. Lusby, et al. (1983). "Nucleotide sequence and organization of the adeno-associated virus 2 genome." J Virol **45**(2): 555-64.
- Stachler, M. D. and J. S. Bartlett (2006). "Mosaic vectors comprised of modified AAV1 capsid proteins for efficient vector purification and targeting to vascular endothelial cells." Gene Ther **13**(11): 926-31.
- Stoppini, L., P. A. Buchs, et al. (1991). "A simple method for organotypic cultures of nervous tissue." J Neurosci Methods **37**(2): 173-82.
- Suikkanen, S., M. Antila, et al. (2003). "Release of canine parvovirus from endocytic vesicles." Virology **316**(2): 267-80.
- Summerford, C., J. S. Bartlett, et al. (1999). "AlphaVbeta5 integrin: a co-receptor for adeno-associated virus type 2 infection." Nat Med **5**(1): 78-82.
- Summerford, C. and R. J. Samulski (1998). "Membrane-associated heparan sulfate proteoglycan is a receptor for adeno-associated virus type 2 virions." J Virol **72**(2): 1438-45.
- Sun, L., J. Li, et al. (2000). "Overcoming adeno-associated virus vector size limitation through viral DNA heterodimerization." Nat Med **6**(5): 599-602.
- Tan, I., C. H. Ng, et al. (2001). "Phosphorylation of a novel myosin binding subunit of protein phosphatase 1 reveals a conserved mechanism in the regulation of actin cytoskeleton." J Biol Chem **276**(24): 21209-16.
- Thomas, C. E., T. A. Storm, et al. (2004). "Rapid uncoating of vector genomes is the key to efficient liver transduction with pseudotyped adeno-associated virus vectors." J Virol **78**(6): 3110-22.
- Thomson, B. J., F. W. Weindler, et al. (1994). "Human herpesvirus 6 (HHV-6) is a helper virus for adeno-associated virus type 2 (AAV-2) and the AAV-2 rep gene homologue in HHV-6 can mediate AAV-2 DNA replication and regulate gene expression." Virology **204**(1): 304-11.
- Tratschin, J. D., I. L. Miller, et al. (1984). "Genetic analysis of adeno-associated virus: properties of deletion mutants constructed in vitro and evidence for an adeno-associated virus replication function." J Virol **51**(3): 611-9.
- Tratschin, J. D., I. L. Miller, et al. (1985). "Adeno-associated virus vector for high-frequency integration, expression, and rescue of genes in mammalian cells." Mol Cell Biol **5**(11): 3251-60.
- Tratschin, J. D., J. Tal, et al. (1986). "Negative and positive regulation in trans of gene expression from adeno-associated virus vectors in mammalian cells by a viral rep gene product." Mol Cell Biol **6**(8): 2884-94.
- Tratschin, J. D., M. H. West, et al. (1984). "A human parvovirus, adeno-associated virus, as a eucaryotic vector: transient expression and encapsidation of the procaryotic gene for chloramphenicol acetyltransferase." Mol Cell Biol **4**(10): 2072-81.
- Trempe, J. P. and B. J. Carter (1988). "Alternate mRNA splicing is required for synthesis of adeno-associated virus VP1 capsid protein." J Virol **62**(9): 3356-63.
- Trempe, J. P., E. Mendelson, et al. (1987). "Characterization of adeno-associated virus rep proteins in human cells by antibodies raised against rep expressed in Escherichia coli." Virology **161**(1): 18-28.
- Tresnan, D. B., L. Southard, et al. (1995). "Analysis of the cell and erythrocyte binding activities of the dimple and canyon regions of the canine parvovirus capsid." Virology **211**(1): 123-32.
- Vandenberghe, L. H., L. Wang, et al. (2006). "Heparin binding directs activation of T cells against adeno-associated virus serotype 2 capsid." Nat Med **12**(8): 967-71.
- Vandenberghe, L. H. and J. M. Wilson (2007). "AAV as an immunogen." Curr Gene Ther **7**(5): 325-33.

- Veldwijk, M. R., J. Topaly, et al. (2002). "Development and optimization of a real-time quantitative PCR-based method for the titration of AAV-2 vector stocks." Mol Ther **6**(2): 272-8.
- Verma, I. M. and N. Somia (1997). "Gene therapy -- promises, problems and prospects." Nature **389**(6648): 239-42.
- Waddington, S. N., J. H. McVey, et al. (2008). "Adenovirus serotype 5 hexon mediates liver gene transfer." Cell **132**(3): 397-409.
- Wang, L., R. Calcedo, et al. (2005). "Sustained correction of disease in naive and AAV2-pretreated hemophilia B dogs: AAV2/8-mediated, liver-directed gene therapy." Blood **105**(8): 3079-86.
- Wang, L., J. Figueredo, et al. (2007). "Cross-presentation of adeno-associated virus serotype 2 capsids activates cytotoxic T cells but does not render hepatocytes effective cytolytic targets." Hum Gene Ther **18**(3): 185-94.
- Wang, L. and D. L. Smith (2005). "Capsid structure and dynamics of a human rhinovirus probed by hydrogen exchange mass spectrometry." Protein Sci **14**(6): 1661-72.
- Wang, L., H. Wang, et al. (2010). "Systematic evaluation of AAV vectors for liver directed gene transfer in murine models." Mol Ther **18**(1): 118-25.
- Wang, X. S., K. Qing, et al. (1997). "Adeno-associated virus type 2 DNA replication in vivo: mutation analyses of the D sequence in viral inverted terminal repeats." J Virol **71**(4): 3077-82.
- Wang, Z., H. I. Ma, et al. (2003). "Rapid and highly efficient transduction by double-stranded adeno-associated virus vectors in vitro and in vivo." Gene Ther **10**(26): 2105-11.
- Wang, Z., T. Zhu, et al. (2005). "Adeno-associated virus serotype 8 efficiently delivers genes to muscle and heart." Nat Biotechnol **23**(3): 321-8.
- Ward, P. and C. E. Walsh (2009). "Chimeric AAV Cap sequences alter gene transduction." Virology **386**(2): 237-48.
- Warrington, K. H., Jr., O. S. Gorbatyuk, et al. (2004). "Adeno-associated virus type 2 VP2 capsid protein is nonessential and can tolerate large peptide insertions at its N terminus." J Virol **78**(12): 6595-609.
- Warrington, K. H., Jr. and R. W. Herzog (2006). "Treatment of human disease by adeno-associated viral gene transfer." Hum Genet **119**(6): 571-603.
- Waterkamp, D. A., O. J. Muller, et al. (2006). "Isolation of targeted AAV2 vectors from novel virus display libraries." J Gene Med **8**(11): 1307-19.
- Weber, M., J. Rabinowitz, et al. (2003). "Recombinant adeno-associated virus serotype 4 mediates unique and exclusive long-term transduction of retinal pigmented epithelium in rat, dog, and nonhuman primate after subretinal delivery." Mol Ther **7**(6): 774-81.
- White, S. J., S. A. Nicklin, et al. (2004). "Targeted gene delivery to vascular tissue in vivo by tropism-modified adeno-associated virus vectors." Circulation **109**(4): 513-9.
- Wistuba, A., A. Kern, et al. (1997). "Subcellular compartmentalization of adeno-associated virus type 2 assembly." J Virol **71**(2): 1341-52.
- Wistuba, A., S. Weger, et al. (1995). "Intermediates of adeno-associated virus type 2 assembly: identification of soluble complexes containing Rep and Cap proteins." J Virol **69**(9): 5311-9.
- Witz, J. and F. Brown (2001). "Structural dynamics, an intrinsic property of viral capsids." Arch Virol **146**(12): 2263-74.
- Wobus, C. E., B. Hügler-Dorr, et al. (2000). "Monoclonal antibodies against the adeno-associated virus type 2 (AAV-2) capsid: epitope mapping and identification of capsid domains involved in AAV-2-cell interaction and neutralization of AAV-2 infection." J Virol **74**(19): 9281-93.

-
- Wonderling, R. S., S. R. Kyostio, et al. (1995). "A maltose-binding protein/adeno-associated virus Rep68 fusion protein has DNA-RNA helicase and ATPase activities." *J Virol* **69**(6): 3542-8.
- Work, L. M., H. Buning, et al. (2006). "Vascular bed-targeted in vivo gene delivery using tropism-modified adeno-associated viruses." *Mol Ther* **13**(4): 683-93.
- Wu, J., W. Zhao, et al. (2007). "Self-complementary recombinant adeno-associated viral vectors: packaging capacity and the role of rep proteins in vector purity." *Hum Gene Ther* **18**(2): 171-82.
- Wu, P., W. Xiao, et al. (2000). "Mutational analysis of the adeno-associated virus type 2 (AAV2) capsid gene and construction of AAV2 vectors with altered tropism." *J Virol* **74**(18): 8635-47.
- Wu, Z., A. Asokan, et al. (2006a). "Adeno-associated virus serotypes: vector toolkit for human gene therapy." *Mol Ther* **14**(3): 316-27.
- Wu, Z., E. Miller, et al. (2006b). "Alpha2,3 and alpha2,6 N-linked sialic acids facilitate efficient binding and transduction by adeno-associated virus types 1 and 6." *J Virol* **80**(18): 9093-103.
- Wu, Z., J. Sun, et al. (2008). "Optimization of self-complementary AAV vectors for liver-directed expression results in sustained correction of hemophilia B at low vector dose." *Mol Ther* **16**(2): 280-9.
- Xiao, W., N. Chirmule, et al. (1999). "Gene therapy vectors based on adeno-associated virus type 1." *J Virol* **73**(5): 3994-4003.
- Xiao, W., K. H. Warrington, Jr., et al. (2002). "Adenovirus-facilitated nuclear translocation of adeno-associated virus type 2." *J Virol* **76**(22): 11505-17.
- Xiao, X., J. Li, et al. (1996). "Efficient long-term gene transfer into muscle tissue of immunocompetent mice by adeno-associated virus vector." *J Virol* **70**(11): 8098-108.
- Xie, Q., W. Bu, et al. (2002). "The atomic structure of adeno-associated virus (AAV-2), a vector for human gene therapy." *Proc Natl Acad Sci U S A* **99**(16): 10405-10.
- Xie, Q., T. Somasundaram, et al. (2003). "Structure determination of adeno-associated virus 2: three complete virus particles per asymmetric unit." *Acta Crystallogr D Biol Crystallogr* **59**(Pt 6): 959-70.
- Xu, D., D. McCarty, et al. (2005). "Delivery of MDR1 small interfering RNA by self-complementary recombinant adeno-associated virus vector." *Mol Ther* **11**(4): 523-30.
- Yakobson, B., T. A. Hrynko, et al. (1989). "Replication of adeno-associated virus in cells irradiated with UV light at 254 nm." *J Virol* **63**(3): 1023-30.
- Yakobson, B., T. Koch, et al. (1987). "Replication of adeno-associated virus in synchronized cells without the addition of a helper virus." *J Virol* **61**(4): 972-81.
- Yalkinoglu, A. O., R. Heilbronn, et al. (1988). "DNA amplification of adeno-associated virus as a response to cellular genotoxic stress." *Cancer Res* **48**(11): 3123-9.
- Yan, Z., R. Zak, et al. (2002). "Ubiquitination of both adeno-associated virus type 2 and 5 capsid proteins affects the transduction efficiency of recombinant vectors." *J Virol* **76**(5): 2043-53.
- Yan, Z., Y. Zhang, et al. (2000). "Trans-splicing vectors expand the utility of adeno-associated virus for gene therapy." *Proc Natl Acad Sci U S A* **97**(12): 6716-21.
- Yang, G. S., M. Schmidt, et al. (2002). "Virus-mediated transduction of murine retina with adeno-associated virus: effects of viral capsid and genome size." *J Virol* **76**(15): 7651-60.
- Yang, L., J. Jiang, et al. (2009). "A myocardium tropic adeno-associated virus (AAV) evolved by DNA shuffling and in vivo selection." *Proc Natl Acad Sci U S A* **106**(10): 3946-51.
- Yang, Q., M. Mamounas, et al. (1998). "Development of novel cell surface CD34-targeted recombinant adeno-associated virus vectors for gene therapy." *Hum Gene Ther* **9**(13): 1929-37.

- Ying, Y. (2007). "Improvement and application of random adeno-associated virus type 2 (AAV2) display peptide libraries for selection of targeted gene transfer AAV2 vectors." Thesis.
- Ying, Y., O. Muller, et al. (2010). In vivo selection on heart tissue by an AAV2 derived random peptide display library. Gene Ther (in press)
- Yu, C. Y., Z. Yuan, et al. (2009). "A muscle-targeting peptide displayed on AAV2 improves muscle tropism on systemic delivery." Gene Ther **16**(8): 953-62.
- Zabner, J., M. Seiler, et al. (2000). "Adeno-associated virus type 5 (AAV5) but not AAV2 binds to the apical surfaces of airway epithelia and facilitates gene transfer." J Virol **74**(8): 3852-8.
- Zadori, Z., J. Szelei, et al. (2001). "A viral phospholipase A2 is required for parvovirus infectivity." Dev Cell **1**(2): 291-302.
- Zaiss, A. K., Q. Liu, et al. (2002). "Differential activation of innate immune responses by adenovirus and adeno-associated virus vectors." J Virol **76**(9): 4580-90.
- Zhang, J. F., C. Hu, et al. (1996). "Gene therapy with an adeno-associated virus carrying an interferon gene results in tumor growth suppression and regression." Cancer Gene Ther **3**(1): 31-8.
- Zhong, L., L. Chen, et al. (2004). "Self-complementary adeno-associated virus 2 (AAV)-T cell protein tyrosine phosphatase vectors as helper viruses to improve transduction efficiency of conventional single-stranded AAV vectors in vitro and in vivo." Mol Ther **10**(5): 950-7.
- Zhou, X., I. Zolotukhin, et al. (1999). "Biochemical characterization of adeno-associated virus rep68 DNA helicase and ATPase activities." J Virol **73**(2): 1580-90.
- Zhu, T., L. Zhou, et al. (2005). "Sustained whole-body functional rescue in congestive heart failure and muscular dystrophy hamsters by systemic gene transfer." Circulation **112**(17): 2650-9.
- Zincarelli, C., S. Soltys, et al. (2008). "Analysis of AAV serotypes 1-9 mediated gene expression and tropism in mice after systemic injection." Mol Ther **16**(6): 1073-80.
- Zolotukhin, S., B. J. Byrne, et al. (1999). "Recombinant adeno-associated virus purification using novel methods improves infectious titer and yield." Gene Ther **6**(6): 973-85.
- Zoltick, P. W. and J. M. Wilson (2000). "A quantitative nonimmunogenic transgene product for evaluating vectors in nonhuman primates." Mol Ther **2**(6): 657-9.

Acknowledgement

At first, I would like to thank apl. Prof. Dr. Jürgen Kleinschmidt for making me part of his group and for giving me the chance to work on a very interesting topic. His constant support and willingness for scientific discussions at any time helped me to become a better scientist. I will never forget his dedication to sciences. I am thankful for his critical reviewing of my thesis prior to submission. Along the line, I would like to thank Prof. Lutz Gissmann for being my second evaluator of the dissertation. Furthermore, I would like to thank apl. Prof. Dr. Gabriele Petersen and PD Dr. Anne Regnier-Vigouroux for agreeing to be part of my evaluation committee.

A special thanks goes to PD Dr. Oliver Müller for designing the plasmid to generate the AAV8 random peptide library and for being positive and enthusiastic about my results. Additionally, I am indebted to him for supporting my work financially in the last six months of my practical time in the lab. I would like to thank all members of the Department Infection and Cancer, and especially my former lab 2.219 for the good working atmosphere. I am grateful to Karl Varadi for always being helpful, especially with VectorNTI and library questions; Britta Gerlach for teaching me all steps of the vector production, Petra Zeisberger and Kristin Schmidt for their attentive assistance and nice discussions; Matthias Naumer for helping me with questions about the library productions. Most of all I would like to thank Dr. Florian Sonntag and Dr. Karen Nieto who always helped me, no matter how stupid the problem was and for being my friends. I would like to thank Anna Sacher who was a big support to me and who always had time for discussions and trouble shootings and thanks to Anne Fassel for being just the great person she is. A "thank you" also goes to my new group, Dirk Grimm and his team for giving me such a warm welcome. The last people I would like to thank is the AG Hoppe-Seyler for letting me be part of the "coffee circle" and Thomas Holz for being the most helpful computer specialist at the DKFZ.

Thanks to everyone for helping me to get the thesis submitted. I finish it with a quote of one of my favorite book authors who somehow knows how life of a PhD student can be.....

Ever try. Ever fail. No matter. Try again. Fail again. Fail better.

- Samuel Beckett

Zu guter Letzt' möchte ich mich an dieser Stelle bei meinem Mann Nik Raupp bedanken, der es nicht immer einfach mit mir hatte, aber mich nichtsdestotrotz immer unterstützte und für mich der Fels in der Brandung war. Ich danke meinen Eltern Prof. Ulrich Stegelmann und Sabine Stegelmann sowie meinem Bruder Michael Stegelmann für die liebevolle Unterstützung zu jeder Zeit. Widmen möchte ich diese Arbeit meinen beiden Großmüttern, Gerda Stegelmann und Gisela Balzer, die mich leider viel zu früh verlassen haben.